LBL-7027
UC-66
TID-4500-R66

INVITATIONAL WELL-TESTING SYMPOSIUM

PROCEEDINGS

October 19-21, 1977
Berkeley, California

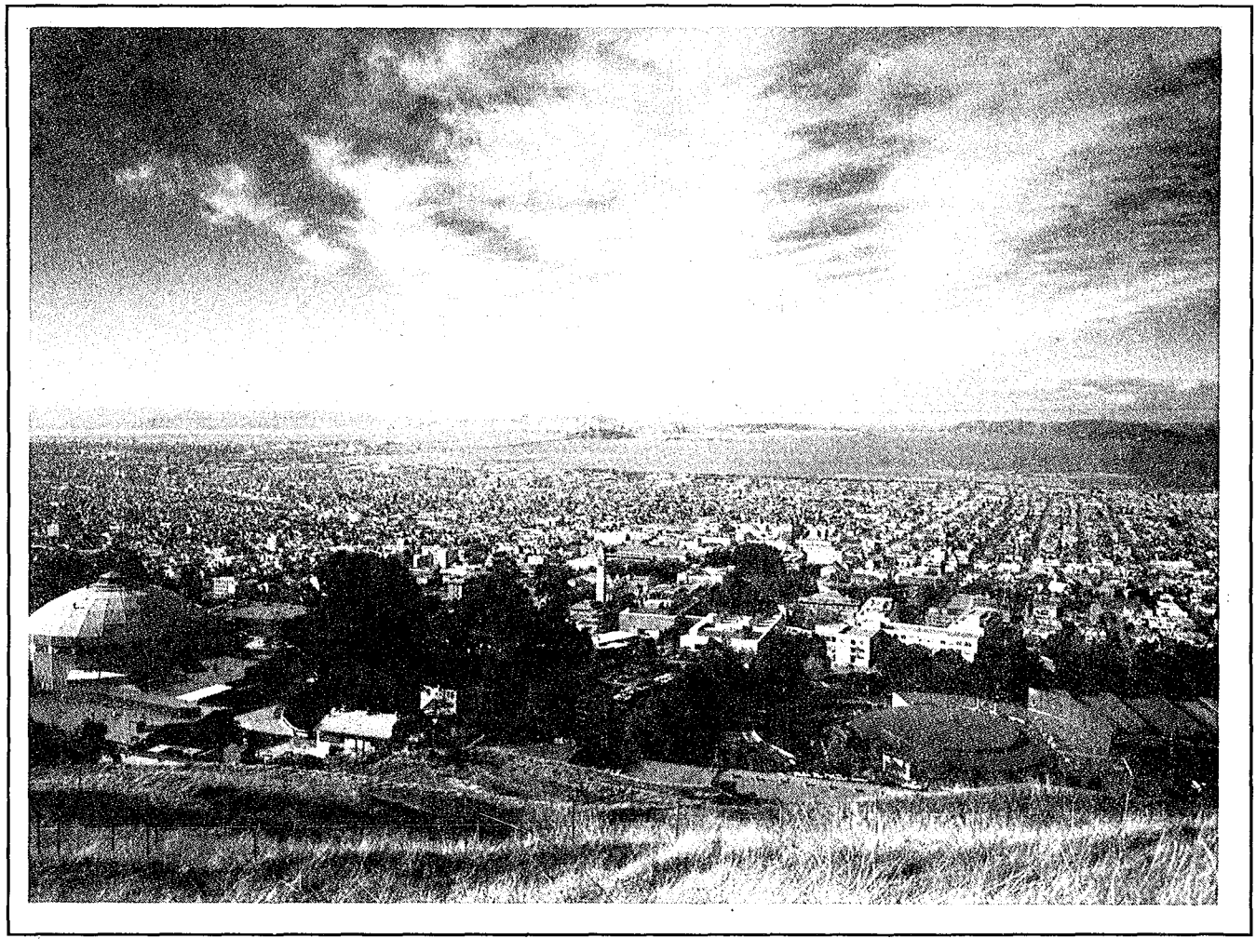

Sponsored by

U.S. Department of Energy
Division of Geothermal Energy

Through the

Earth Sciences Division
Lawrence Berkeley Laboratory
University of California

March 1977

CONTENTS

PREFACE

During the last ten years, the techniques and equipment of well testing have undergone a phenomenal development. The symposium was held to evaluate the state of the art in general, and its application to geothermal systems in particular. The symposium was supported by the Geothermal Energy Division of the United States Department of Energy.

Lawrence Berkeley Laboratory has been testing geothermal wells for about three years, and has recently begun testing hard rocks of extremely low permeability as possible sites for storing high-level nuclear wastes. Well testing is potentially a tool of utmost importance in solving many challenging new problems. In the spring of 1977, R. C. Schroeder of the Reservoir Engineering Group at Lawrence Berkeley Laboratory conceived the spirit and purpose of the symposium to be held to assess the state of the art of well testing, with a view to advancing the science to meet these new challenges.

The Earth Sciences Division accordingly selected a symposium organizing committee, under the chairmanship of Professor P. A. Witherspoon. Members were J. H. Howard, M. J. Lippmann, T. N. Narasimhan, R. C. Schroeder, W. J. Schwarz, and C. F. Tsang. The symposium and the proceedings were coordinated by W. J. Schwarz.

The symposium provided the 150 invited participants a forum in which to exchange ideas and present new information on instrumentation, technique development, and well-test analysis. The emphasis was on reviewing existing capabilities, identifying current limitations, and generating new ideas for extending well-test capabilities.

The participants were well-testing experts from the oil and gas industries, and from the fields of geothermal energy and ground water hydrology. In addition to identifying areas which need additional research and development, the symposium sought to unify the ideas and methods of these three disciplines, where possible.

Abstracts and papers from outside the Lawrence Berkeley Laboratory were obtained from the authors and are being reproduced without any changes. Lawrence Berkeley Laboratory papers were reviewed by the Earth Sciences Division's Publications Committee and by the Technical Information Department.

PROGRAM

SESSION I - 8:30 am to 12:00 noon, Wednesday, October 19, 1977

Introduction

R. C. Schroeder - Chairman
Lawrence Berkeley Laboratory (LBL)

Welcome

E. K. Hyde
Deputy Director
Lawrence Berkeley Laboratory

Keynote Address -- Well Testing, A Recapitulation of Its Development

P. A. Witherspoon
Head
Earth Sciences Division, LBL

Petroleum Engineering Well Test Analysis -- State of the Art

H. J. Ramey, Jr.
Stanford University

Aquifer Tests -- The State of the Art in Hydrology

E. P. Weeks
U. S. Geological Survey

Technology and Needs for Drilling and Well Testing Instrumentation

W. J. McDonald
Maurer Engineering Inc.

SESSION II - 1:30 pm to 5:00 pm, Wednesday, October 19, 1977

Session Introduction -- Instrumentation

G. B. Miller - Chairman
Occidental Research Corporation

Oil and Gas Instrumentation

W. E. Kenyon
Schlumberger-Doll Research Center

Continuous Bottom-Hole Pressures are Measured by Non-Electric System

T. J. Ashby
Sperry-Sun

High Temperature Instrumentation

A. F. Veneruso
Sandia Laboratories

Downhole Hydrology Laboratory

W. L. Still and L. A. Rubin
ENSCO, Inc.

SESSION III - 8:30 am to 12:00 noon, Thursday, October 20, 1977

Session Introduction -- Field Applications

R. Ershaghi - Chairman
University of Southern California

Well Testing Analysis: A Guide to Practical Oil and Gas Field Decisions

W. C. Miller
Shell Oil

Field Studies of Dispersion in a Shallow Sandy Aquifer

J. F. Pickens and J. A. Cherry
University of Waterloo, Canada

Application of Well Testing to Liquid-Dominated Geothermal Systems

T. N. Narasimhan
Earth Sciences Division, LBL

Testing and Sampling Procedures for a
Geopressured Well

M. H. Dorfman and W. E. Boyd
University of Texas, Austin

SESSION IV - 1:30 pm to 5:00 pm, Thursday, October 20, 1977

Session Introduction -- Analysis and Interpretation

H. K. van Poollen - Chairman
H. K. van Poollen & Associates, Inc.

Analysis and Interpretation of Oil, Gas,
and Geothermal Well Tests

W. E. Brigham
Stanford University

Interpretation of Tracer Tests by Means of Type Curves --
Application to Uniform and Radial Flow

J. P. Sauty
Bureau de Recherches Geologiques et Minieres, France

Role of Parameter Identifications in the Design
and Analysis of Pumping Tests

S. P. Neuman
University of Arizona, Tucson

Variable Rate Multiple Well Testing Analysis

D. G. McEdwards and C. F. Tsang
Earth Sciences Division, LBL

SESSION V - 7:00 pm, Thursday, October 20, 1977

U. S. Department of Energy - Geothermal Plans

W. J. Schwarz - Chairman
Earth Sciences Division, LBL

Department of Energy's Role in Furthering the Development of Geothermal Energy

A. C. Wilbur
Department of Energy, San Francisco Operations Office

SESSION VI - 8:30 am to 12:00 noon, Friday, October 21, 1977

Session Introduction -- Special Problems

J. H. Howard - Chairman
Earth Sciences Division, LBL

Transient Flow in Tight Fractures

J. S. Wang
Earth Sciences Division, LBL

Pressure Behavior of Wells Intercepting Fractures

R. Raghavan
University of Tulsa

Application and Interpretation of Drill Stem Test

M. F. Anderson
Halliburton Services

Well Testing Practice and Analysis in Fissured Aquifers

A. C. Gringarten
Bureau de Recherches Geologiques et Minieres, France

Panel Discussion - Summary and Recommendations

M. H. Dorfman
G. B. Miller
R. Raghavan
R. C. Schroeder
W. C. Walton

INTRODUCTION

T. N. Narasimhan
Earth Sciences Division
Lawrence Berkeley Laboratory

As it is generally understood, well testing consists in correlating well flows with pressure or water level changes and drawing inferences about the ability of a reservoir to transmit and store fluids. Ever since the pioneering investigations of Forchheimer, Slichter, and Thiem at the turn of the century, well testing has established itself as an invaluable tool for estimating field parameters of groundwater, petroleum, gas, and, more recently, geothermal reservoirs. Its preeminence in this regard stems from the fact that well testing is the only method that provides in situ information about the reservoir on a scale meaningful for long term exploitation of the resource.

Despite the fundamental unity in the principles of well testing, the art of well testing has developed along two parallel lines--hydrogeology, following the lead of C. V. Theis; and petroleum engineering, following the early contributions of William Hurst and others. Being concerned mainly with open or semi-open, shallow systems, the hydrogeologists generally have been more interested in interference-type of well testing. Petroleum engineers, on the other hand, traditionally have been challenged by the problem of exploiting closed reservoirs by means of deep, expensive wells. As a consequence, a major portion of their well-testing efforts has been directed towards productivity, build-up, and other tests on the production well. Unfortunately, there was a certain lack of free communication of ideas between the two disciplines, leading--among other things--to the duplication of some studies, a multiplicity of nomenclature, and the use of different systems of units. In the recent past, there have been several attempts to bridge this gap in communication.

New developments will profoundly enlarge the scope of well testing. Thanks to the phenomenal development in electronic technology, data can be automatically measured and recorded with an accuracy and rapidity that was impossible only a few years ago. In the search for alternate forms of energy, well testing has been extended to geothermal reservoirs. The hostile environment within geothermal wells and the phenomenon of energy transport are fresh challenges. More recently, attempts to identify virtually impermeable subsurface horizons to isolate radioactive wastes have raised such questions as: How impermeable is impermeable? How can a well test be performed on an impermeable system?

The Invitational Well Testing Symposium, organized by the Lawrence Berkeley Laboratory, was attended by 152 participants. The twenty or so technical presentations were followed by a brief panel discussion. In his keynote address, Paul Witherspoon briefly traced the history of well testing by chronologically recalling the significant contributions from hydrogeology and petroleum literatures. This presentation, embellished by many lively comments from Henry Ramey, set the pace for the entire conference.

The presentation made during the symposium can be broadly classified into five categories: reviews; instrumentation; field applications; theory and techniques; and drilling and related activities.

There were three review papers. Henry Ramey surveyed the status of transient well testing in petroleum engineering, with special emphasis on the producing well. E. P. Weeks comprehensively reviewed the up-to-date literature on the state of the art of well testing in hydrogeology. A detailed study of the various theories available for studying near-well fractures was presented by R. Raghavan.

The importance of well-test instrumentation was the focus of four papers. William Kenyon drew attention to such recent trends in oil and gas instrumentation as dielectric logging, x-ray spectroscopy, and repeat formation testing. Ted Ashby described a pressure transmission system for measuring downhole pressures under hostile conditions. Anthony Veneruso summarized recent work on the development of a high temperature instrument technology for making downhole measurements at 275°C and 7,000 psi. William Still presented the concept of a downhole laboratory for measuring water movement in extremely dry and impermeable rocks over a period of a few years.

Theoretical and technical aspects were the subject of five papers. William Brigham discussed the problems to be considered in semi-log plots and briefly indicated the type of well-testing problems relevant to geothermal systems. Papers by William Miller, Chin Fu Tsang and Shlomo Neuman discussed the inverse problem. Miller described the application of the inverse procedure through the use of a numerical model, while Tsang described a computer assisted curve matching procedure for multiple-well test analysis. Neuman discussed the importance of personal judgment in choosing the best solution from those suggested by an analysis of well-field data using parameter identification techniques. Joseph Wang described the theoretical basis for testing fractures of extremely small apertures using packer tests.

Three of the presentations discussed drilling and drilling-related activities. William McDonald reviewed instruments and techniques used in well logging, well development, drill-stem tests, directional surveys, and strain measurements. Merlin Anderson discussed availability packers and other types of equipment that have greatly enhanced the value of drill-stem tests. Myron Dorfman discussed the drilling, sampling, and testing procedures relevant to the 15,000- to 20,000-foot-deep geopressured wells soon to be drilled in the Gulf Coast of Texas.

Field application of well testing was the subject of four papers. Two of these pertained to the estimation of parameters related to hydrodynamic dispersion and the hydraulic conductivity of groundwater systems: John Pickens described the field data collected with radioactive and non-radioactive tracers using multi-level point sampling devices. Jean Pierre Sauty described the use of type curves in identifying dispersion parameters for systems with uniform or radial flow. T. N. Narasimhan summarized field experiences in testing liquid-dominated geothermal systems. Alain Gringarten described a method of analyzing fractured aquifers with the help of the concepts of equivalent anisotropy and an equivalent single fracture.

The concluding panel, moderated by Jack Howard, included William Brigham, Myron Dorfman, George Miller, Ron Schroeder, William Walton, and Edward Weeks. Points made during this discussion included: the possibility that geothermal systems may be "leaky"; the importance of vertical permeability in geothermal systems; the need for the use of tracers in well tests; the utility of computer aided applications; the importance of blending geology and geophysics with hydraulics; and the problem of water chemistry related to well testing. In closing, Jack Howard posed some questions to ponder: Why do we test a well? How reliable are the data? Was the information worth it?

The panel members as well as many of the participants strongly felt that the symposium should be scheduled again, about a year from now.

Well Testing, A Recapitulation of Its Development

P. A. Witherspoon

Lawrence Berkeley Laboratory
University of California
Berkeley, California 94720

For over a hundred years now hydrogeologists, civil engineers and petroleum engineers have employed well testing as an important tool for evaluating the fluid flow parameters of subsurface reservoirs. The earliest analytical work related to the technique of well testing should probably be attributed to Dupuit (1848) and Forchheimer (1901) who studied the flow of water in unconfined systems. In the U.S., Slichter (1902, 1905) of the United States Geological Survey pioneered field investigations on the movement of groundwater. The work of Thiem (1906) on the steady radial flow of water to a well in a circular reservoir of finite radius is generally quoted in hydrogeology literature as the earliest work on well testing. Except for Slichter's work, these investigations mainly concentrated on the steady-state flow of water and this emphasis on steady flow persisted up to the early 1930's.

A major landmark in the history of the science of well-testing was the general recognition during the early 1930's of the importance of the phenomenon of non-steady flow. As is well known, non-steady flow is characterized by the consideration of the release of water from storage in the porous medium. The science of modern well test analysis can be considered to have been born with the consideration of non-steady flow.

The importance of non-steady flow was recognized more or less contemporaneously in hydrogeology by Theis (1935) and in petroleum engineering by Hurst (1934) and Muskat (1934). The work of Theis is widely known in hydrogeology and the analytical solution for nonsteady radial flow to a line source is known as the Theis equation. In the petroleum literature, Hurst has referred to his analytical solution as the *G* function, but more often petroleum engineers refer to this as the *line source* or *exponential integral* solution. However, due to a lack of free communication of ideas between hydrogeologists and petroleum engineers (which has persisted until recently), Theis' work was generally unknown in petroleum engineering while most hydrogeologists were unaware of the early work of Hurst and Muscat. As a result, there have existed arguments as to who should be rightly given the credit for the introduction of the non-steady, line-source radial flow solution. It is pertinent to point out here that the aforesaid solution was known in the heat condition literature prior to the 1930's.

The Theis solution (or the *G* function or the *exponential integral* as it is variously called) is an improper integral and cannot be directly applied to well test data. To overcome this, Theis proposed the ingenious technique of *type-curve* matching. As an alternative, Jacob (1940) suggested an asympototic solution (the semi-log plot). Together, the type-curve matching technique and the semi-log method persist to this day as the backbone of well-test interpretation.

An important review of methods for determining the permeability of porous materials was published by Wenzel (1942) and this included, for the first time, a comprehensive bibliography of both petroleum and hydrogeology literature. Wenzel reviewed the applicability of well test techniques and also published type-curves for the first time.

The late 1940's and the early 1950's saw important contributions from van Everdingen and Hurst departed from the traditional, abstract, line source and considered the role of a finite diameter well with well-bore storage; Hantush and Jacob initiated the study of multiple *leaky* aquifer systems which focused attention on the importance of the caprocks or aquitards on reservoir physics.

Due to the fact that oil reservoirs are generally closed systems and the fact that the performance of individual oilwells is of considerable importance in the economics of oil production, Horner (1951) and Miller, Dyes, and Hutchison (1950) developed techniques for interpreting pressure build-up analysis by many workers have extended build up analysis to evaluate bore-hole damage, presence or absence of fractures, well-bore storage effects and commingling of aquifers.

By the early 1960's the modern well test analysis literature had become so voluminous that the Society of Petroleum Engineers commissioned a special monograph on the subject. The result was the work of Matthews and Russell (1967).

In discussing the development of well testing mention should be made of the contributions from the mid-1960's to the present from Henry Ramey of Stanford University, his students and associates. The Stanford group has directed a great deal of their attention to the analysis of production well data and have developed a variety of diagnostic type-curve techniques for interpreting effects of well bore storage (after flow), discrete fractures, skin or well bore damage, non-darcian flow and commingling of producing horizons.

The early 70's has witnessed a phenomenal breakthrough in the development of sensitive, automatic data gathering and recording devices. This has provided a fresh impetus and challenge to develop new techniques of analysis and interpretation greatly increasing the utility of well tests. Recognizing this and the many contributions that have been made since the monograph of Mathews and Russell, the SPE commissioned a second monograph on well testing by Earlougher (1977).

At present there is no reason to believe that the development has come to an end. Quite the contrary. With the availability of new improved data gathering equipment and fast computing devices, well testing is in a position to take on fresh challenges. In this regard, we may consider two examples. The first is the extension of well testing to non-isothermal conditions, which are characterized by the dependence of viscosity and hence hydraulic conductivity on temperature and the presence of two phases in the well or in the reservoir. The second challenge is the problem of testing rocks (fractures) of extremely low permeability. The hydraulic assessment of such formations is of upmost importance in attempting to store radioactive wastes underground. Among the questions to be considered in testing wells in such rocks, one may mention the duration of the test, the influence of borehole diameter on the parameters calculated and the apertures of the fracture encountered.

It is obvious from what has been presented above that the technology of well testing is continuing to develop and holds much promise to continue in the future to serve as an invaluable tool for earth scientists working on a wide variety of field problems.

References

Dupuit, J., *Etudes Theoretiques et Practiques sur le Movement des Eaux Courantes*, Paris, 275 pages, (1848).

Earlougher, R.C., *Advances in Well Test Analysis*, Society of Petroleum Engineers, Monograph 5, Dallas (1977).

Forchheimer, P., *Wasserbewegung durch Boden*, Zeitschrift Ver. Deutscher Ing., V. 45, pages 1736-1741 and 1781-1788, Berlin (1901).

Hantush, M.S., and Jacob, C.E., *Nonsteady Radial Flow in an Infinite Leaky Aquifer*, Transactions, American Geophysical Union,V. 36. p. 95 (1955).

Horner, D.R., *Pressure Build-Up in Well*, Transactions, Third World Pet. Congress, The Hague, Sec. II, pages 503-523 (1951).

Hurst, W., *Unsteady Flow of Fluids in Oil Reservoirs*, Physics, V. 5, pages 20-30, (1934).

Matthews, C.S., Russell,D.G., *Pressure Buildup and Flow Tests in Wells* , Society of Petroleum Engineers, Monograph 1, Dallas (1967).

Miller, C.C., Dyes, A.B., and Hutchinson, C.A., *The Estimation of Permeability and Reservoir Pressure from Bottom Hole Pressure Build-Up Characteristics*, Transactions, AIME, V. 189, pages 81-104 (1950).

Muscat, M., *The Flow of Compressible Fluids Through Porous Media and Some Problems in Heat Conduction*, Physics, V. 5., pages 71-94 (1934).

Slichter, C.S., *The Motions of Underground Waters*, U.S. Geological Survey Water Supply Paper 67, 106 pages, Washington (1902).

Slichter, C.S., *Field Measurements of the Rate of Movement of Underground Waters*, U.S. Geological Survey Water Supply Paper 140, 122 pages, Washington, (1905).

Theim, G., Hydrologische Methoden, 56 pages, J.M. Gebhardt, Leipzig.

Theis, C.V., *The Relation Between the Lowering of the Peizometric Surface and the Rate and Duration of Discharge of a Well Using Ground-Water Storage*, American Geophysical Union, Transactions, pages 519-524, (1935).

PETROLEUM ENGINEERING WELL TEST ANALYSIS--STATE OF THE ART

Henry J. Ramey, Jr.
Stanford University, Petroleum Engineering Department
Stanford, California

Summary

It is hard to find a subject in oil production which epitomizes the development of petroleum technology better than well-test analysis. One of the earliest endeavors of petroleum technologists was testing wells for a variety of purposes. What was wrong with poorly performing wells? Was it possible to forecast large production rate performance from tests made at low producing rates? Was it possible to forecast long-term behavior from short-duration well tests? What kind of well stimulation should be done, if any? What would be the result?

Development of this technology began almost with the drilling of the Drake well, intensified during the early 1900s, and reached a modern level of sophistication by 1950.

In the next decade, more than 200 papers on this subject appeared. By early 1960, the consensus was that all important work on fundamentals had been completed. This sort of conclusion has occurred in other petroleum specialties at one time or another. The state of this art was so well developed and so important that the Society of Petroleum Engineers selected it for the first topic in a new monograph series. The monograph, "Pressure Buildup and Flow Tests in Wells," by Matthews and Russell[1], was published in 1967, and a second topic "Advances in Well Test Analysis" was presented by R.C.Earlougher, Jr., in 1977[2].

A new school of thought began to develop in the early 1960s. What could be done with test data for tests that had not been run long enough for conventional analysis methods? Were there methods which could guarantee that the proper portion of the data had been analyzed?

These second-generation studies were aimed at problems considered too complex for useful analysis. Naturally, the final analysis was simple, and important results began to appear by the early 1970s. These included development of pulse testing and interference testing, modern log-log type curve analysis for producing wells, and real gas potential type applications for non-linear problems.

There are many parallels between developments in well test analysis, other branches of petroleum technology, and business science. The elements are generally: (1) a well-established technology, (2) an exploding electronics technology producing computers, ultra-sensitive sensors, and pertinent software, and (3) an exploding technology not fully appreciated by the industry.

The result is a period between development and wide acceptance of new technology. The new technology appears impossible or magical to practitioners of the established technology. The time period between concept and industry-wide acceptance is about 15 years. An important objective of current activities is to reduce this time lag to optimize the impact of well test analysis on meeting national energy production objectives.

Objectives of Well Testing

The technology of well test analysis has developed in a number of distinctly separated petroleum technologies. (This paper is concerned with the status of petroleum technology, and will not cite similar developments in hydrology thoroughly.) Considering these in a chronological sense, the specialties involved are geological engineering, drilling engineering, production engineering, and reservoir engineering.

During the drilling of an exploratory well, there is considerable overlap between the functions of the well site geologist, a geological engineer, and the drilling engineer. Well test analysis is generally involved in the interpretation of pressure transient records taken during drill stem testing either through casing or in an open hole. In the open hole drill stem test, the decision as to whether or not it is worthwhile to run pipe and plan a permanent completion involves an assimilation of information from well logs and pressure transient tests. It is important to identify nearby drainage limits or a decline in reservoir pressure.

In the case of drill stem tests run through perforations in a number of interesting intervals identified from wire-line logs, the main problem is which of many opportunities appears to provide a reasonable well completion opportunity. During this phase of the testing, drilling and reservoir objectives are often contradictory. Extensive periods of testing in a given production interval may lead to difficult drilling problems, and will obviously lead to increased costs due to rig time while waiting on a completion of well test objectives. The net result is a compromise based upon drilling objectives and reservoir evaluation objectives. Reservoir engineering objectives of these tests generally involve determination of eventual delivery rates, should the interval prove to be economically productive, and the eventual development of field-wide production.

Once a completion is effected, the production engineer takes charge. Development drilling, hopefully, will continue for some time. The production engineer has the main problem of analyzing well behavior and determining whether or not some remedial work or a different completion practice is required to obtain optimum production from existing wells. The problems involve answering questions such as: (1) is poor performance due to a low

driving force moving fluids into the well [low formation pressure], (2) due to low formation permeability, and (3) due to a damaged well bore condition? If poor performance is due to a damaged well bore, what kind of well stimulation is required to overcome this problem? Well stimulation is a major interest of the production engineer.

The reservoir engineer is involved in the long-term behavior of the well and the reservoir. Important questions he must answer are: what is the optimum plan of development of the reservoir; how many wells and what sort of pattern of wells will be required for the optimum development of the reservoir; what sort of oil recovery techniques will be involved throughout the producing life of the reservoir; and what will be the ultimate recovery of fluid from the reservoir throughout its producing life under various economic scenarios involving a variety of oil recovery mechanisms? Well test analysis often provides the first estimates of formation conductivity, storage, and important producing mechanisms.

In general, well tests provide something for nearly every technologist involved in petroleum production. In this respect, there is much overlap between the different fields of technology in oil production.

Conventional Well Test Methods

Well test analysis technology involves the interpretation of pressure-time information obtained following a specific production schedule of a well or wells in an oil or gas reservoir. Interpretation must involve an understanding of pressure-time solutions of transient flow problems for multi-phase flow of fluids through multi-dimensional porous mediums.

Conventional well test analysis methods began in 1950 with the pioneering studies by Horner[3] and Miller-Dyes-Hutchinson.[4] The following summarizes the results of those studies.

Horner, and Miller-Dyes-Hutchinson - (1950-1951)

The Horner[3] and Miller-Dyes-Hutchinson[4] methods concern pressure buildup analysis. In this kind of well testing, a well is produced at a constant rate q, for a period of time (t), and then shut-in. Pressures are measured during the shut-in period as a function of the shut-in time following the producing period.

Two kinds of pressure buildup graphs were proposed. Horner suggested that the buildup pressures should be graphed as a function of the logarithm of the time ratio involving the producing time plus the shut-in time divided by the shut-in time (previously shown by C. V. Theis[6] in 1935). Miller-Dyes-Hutchinson suggested that the shut-in pressure should be graphed versus the logarithm of the shut-in time only. In both cases, it was suggested that a straight line should result, and that the slope of the straight line should be inversely related to the effective permeability of the formation to the flowing phase. The relationship was:

$$k = 162.6 \frac{qB\mu}{mh} \qquad (1)$$

The units involved are: k in millidarcys, q in stock tank barrels/day, B in reservoir volumes per standard volume, viscosity in centipoise, formation thickness in feet, and m, the straight line slope of the graph, in psi per log cycle.

The obvious problem is that two different graphs are involved, and often, the methods yield different answers. A report by Ramey and Cobb[5] (1971) indicated that the Horner pressure buildup graph is usually the most reliable for wells in closed drainage shapes. An example of the Horner pressure buildup graph is given in Fig. 1. Pressures measured after shut-in of a well result in an almost perfectly straight semi-logarithmic line.

The Horner time ratio also has the interesting characteristic that an infinite shut-in time would correspond to a time ratio of unity. Thus, the graph provides an interesting manner for extrapolating the buildup pressures to an infinitely long shut-in time. This can be seen on Fig. 1 by observing the extension of the straight line drawn through the buildup pressures to a time ratio of unity as indicated by the pressure p*. Horner was the first to show how to correct this "false" pressure to the mean pressure, $\bar{p}$, for closed drainage shapes.

By 1953, Hurst[7] and Van Everdingen[8] showed that although pressure data generally did form a semi-logarithmic straight line, the lines appeared to be displaced from the ideal solutions which existed at that time. Both investigators proposed the use of a new concept, the skin effect, for the behavior of wells. The skin effect idea is shown in Fig. 2. It was proposed that the drilling process could result in a "skin," or a zone of damage on the surface of the producing formation. This would amount to a zone of reduced permeability immediately adjacent to the sand face. Figure 2 shows a rough graph of pressure versus radial distance away from the well illustrating this idea. The restriction of permeability on the sand face would cause a large pressure drop immediately adjacent to the sand face. The skin effect (as originally conceived) was a dimensionless number directly proportional to the pressure drop across the damaged permeability adjacent to the sand face.

$$S = 1.15 \left[\frac{p_{1\ hr} - p_{wf}}{m} - \log_{10} \frac{k}{\phi \mu c_t r_w^2} + 3.23 \right] \qquad (2)$$

The dimensionless skin effect is not easy to visualize. For this reason the pressure drop across the skin region may be computed and used to determine the flow efficiency of the well. Pressure drop across the skin may be found from:

$$\Delta p_s = 0.87\ ms \qquad (3)$$

Once the pressure drop across the skin effect is determined, the flow efficiency of a well may be computed from Eq. 4:

$$FE = \frac{PI_{act}}{PI_{theo}} = \frac{\bar{p} - p_{wf} - \Delta p_s}{\bar{p} - p_{wf}}$$

$$\simeq \frac{p^* - p_{wf} - \Delta p_s}{p^* - p_{wf}} \qquad (4)$$

Equation 4 defines the flow efficiency of a well as the ratio of the actual productivity index to the theoretical productivity index. The Productivity index is defined as the flow rate per unit pressure drop. Because the flow rates cancel in Eq. 4, the flow efficiency becomes a ratio of pressure differences. The expression on the right in Eq. 4 indicates that the extrapolated, false pressure, p*, of Horner may be used to replace the volumetric average pressure $\bar{p}$.

The relationship between the volumetric average pressure $\bar{p}$ and p* was presented by Horner as indicated in Fig. 3, by Miller-Dyes-Hutchinson and Perrine[9] in Fig. 4, later by Pitzer[10] in Fig. 5, and finally by Matthews-Brons-Hazebroek[11] in 1954.

The relationship between the pressure p* and pressure $\bar{p}$ is given by Eq. 5:

$$\frac{p^* - \bar{p}}{(\frac{0.87m}{2})} = p_{D_{MBH}} \qquad (5)$$

The main elements important to well test analysis are given in the preceding five equations. Equation 1 presents a formulation for the effective conductivity or permeability of the rock to the flowing phase. Equations 2, 3, and 4 concern the skin effect or the well condition. Equation 5 concerns the mean pressure and the drainage volume of the well, and thus the driving force available to move the fluids from the formation into the wellbore.

The Real Life Problems

Figure 6 shows many known effects which cause changes in the shape of pressure buildup curves. Fracturing or wellbore damage or well fillup affect the early-time shapes of a pressure buildup graph. The drainage boundary or interference caused by production or injection from adjacent wells affect the long-time shape of a pressure buildup graph. Unfortunately the sequence of shapes of the curves caused by either wellbore effects or the long-time drainage effects is often the same. Thus, it may not be obvious which portion of the buildup graph is seen if a complete history is not available. This then leads to the following real life problems.

(1) Where is the correct straight line, if there is one in the data available?

(2) Which type of pressure buildup curve graphing should be used? (Horner or Miller-Dyes-Hutchinson)

(3) Can the short-time pressure buildup data obtained before the conventional semi-log straight line be used?

(4) How can a proper well test be designed to be certain that useful information is obtained? What production rate should be used? How long should the well be shut-in?

Modern Methods

The answers to the preceding questions are frequently available through a well test analysis technique called log-log type curve matching. In this procedure a mathematical solution for the transient flow problem is graphed on a piece of log-log coordinate paper (an example is shown on Fig. 7). The solution graphed on Fig. 7 is the answer to the problem posed by measuring pressure drops in a shut-in well caused by the production of an adjacent well some distance away. This is called an interference test.

It is possible to compare the entire field data history with a simple analytic solution by using the unique characteristics of log-log graphing. It is also possible to do many additional things. It can be shown that interference data will become semi-log straight for values of the abscissa on Fig. 7 of five or greater. It is possible to compare field data directly with a type curve and identify the start of a correct semi-log straight line. It is also possible to see important things about the existence of drainage boundaries in the pressure transient data. The solution graphed on Fig. 7 is for a well appearing in an infinitely large system. As long as field data follow the solution, it is a reasonable conclusion that no drainage boundaries are evident.

The possibility of using log-log type curves for solution of problems other than interference testing is obviously interesting. An important question is whether other problems of interest have unique "fingerprints" on log-log graphs that can be seen and identified easily.

Behavior of Wells with Fractures

Figure 8 presents a schematic view of a well with a vertical fracture in a closed drainage volume. It is commonly accepted that results of hydraulic fracturing are vertical fractures. Since the invention of hydraulic fracturing in 1955, there have been over 500,000 wells fractured. A log-log type curve for a vertically-fractured well is presented in Fig. 9 (see Gringarten, et al.[12]). Figures 9 and 7 are quite different. In the early-time data there is a straight line that has a slope of one-half. This behavior is unique and is indicative of the presence of linear flow into a fracture.

This slope may be seen on a log-log graph, but it is not evident on conventional well test semi-log graphs. By regraphing the data on Fig. 9 on semi-log coordinates, it is possible to identify the start of a correct semi-log straight line which may be used to obtain permeability with Eq. 1. The start of the semi-log straight line data is indicated on Fig. 9 at a dimensionless time of approximately three or four. Thus, a log-log type curve for a fractured well can be used to identify the start of the correct semi-log straight line.

In some cases for gas wells, high gas compressibility often leads to long initial periods (hundreds of hours) prior to the start of the semi-log straight line. In this case log-log type curve matching may be necessary. Currently, many new studies concerning the behavior of finite fracture conductivity problems are appearing at professional society meetings.

The log-log type curve method in Fig. 9 suggests the answers to many important problems which have plagued production engineers for years. For example, it is not unusual during water injection to reach injection pressures high enough to fracture formations. Operators of waterfloods may be faced with the perplexing question of whether or not a formation was inadvertently fractured. Log-log graphing of pressure transient data for the injection well should answer this question. Another problem may concern fracture orientation. Figure 10 presents a log-log type curve for a horizontal fracture. Figures 9 and 10 are different.

Storage and Skin Effect Type Curves

If a well is damaged, it is necessary to consider the effect of the storage of fluids within the wellbore on the performance of a well. If a valve is opened at the surface and fluid allowed to produce, fluid expands from the casing-tubing annulus and perhaps a liquid level will begin to fall in the annulus. For some portion of the early producing times, the fluid production originates from expansion of fluids in the wellbore. Eventually fluid will pass through the sand face into the wellbore at the same rate as the surface producing rate. This wellbore storage effect leads to a delay in pressure behavior that must be considered in well test analysis. For example, a well 1,000 feet deep will normally have about 50 barrels of storage space within the wellbore. If a well is produced at a rate of 25 barrels per day, it would be necessary to produce for two days to pump the storage space dry, if no fluid entered through the sand face. Time delays caused by wellbore storage may be a matter of many hours in practical cases. A log-log type curve which considers this effect is shown on Fig. 11.

Figure 11 has a complex appearance, but contains only a few essential features. For short times, all cases shown on Fig. 11 follow a line of unit slope. When pressure data follow the unit slope, all fluid production comes from expansion of fluid in the wellbore. There is little flow through the sand face. On the other hand, at long times, pressures approach the flat lines shown along the top of Fig. 11 and identified by the zero storage numbers. When data reach these flat lines, as indicated by the heavy dot in the center of the figure, the semi-log straight line begins to form and a conventional analysis becomes possible. The start of the correct semi-log straight line may be found approximately one and one-half log cycles after the data depart from the initial unit slope straight line. This is indicated by the arrow across the top of Fig. 11.

Current Trends

Interpretation of pressures measured in a well (either producing or shut-in) has provided the main problem considered in the petroleum literature. The large compressibility of gas and oil made interference testing between wells a lengthy testing procedure. In the last five years, high-precision pressure gauges[16] have become available, and interference testing has become important. Furthermore, the need for a more complete description of reservoirs for planning enhanced oil recovery has led to detailed well-by-well interference testing. Accounts of current practice may be found in Strobel, et al.[14], and Kamal and Brigham[15].

Summary

Modern interpretation methods involving use of all well test data from the moment a valve setting is changed on a well, through very long duration tests, offers great power in data interpretation. However, well tests are not always practical, and many important problems remain. One important case which frequently makes well testing difficult or impossible is the thick-sand problem. When the formation is thick, the straight line slope on conventional well test graphs may be too small to measure. In order to obtain measurable straight line slopes, it might be necessary to take the entire field producing rate from one well. Thus, it is necessary to design a well test to be certain that useful information can be obtained.

Among the important problems which are not yet susceptible to complete analysis by modern methods are the layered system problems, certain types of fractured systems and bottom water coning problems, and gas cap problems. Work is underway on these problems, however, and it is likely that useful solutions will be found in the near future. In regard to the thick-sand problem, one possible solution is measurement of pressures with extreme precision. Fortunately, new pressure measuring devices of very high precision are becoming available. These gauges are sufficiently accurate to measure gravitational effect on formation pressure caused by the moon passing the surface of the earth. It now appears that this earth-tide effect may be of practical use in estimation of the porosity of formations. It is clear that many new solutions will be found which may be graphed on log-log coordinates and used to interpret the complex modern problems that occur in well test analysis.

Acknowledgement

This study was completed under contract No. ERDA-LBL 167-3500 at Stanford University.

Nomenclature and Units

All symbols used in this study are standard Society of Petroleum Engineering symbols. The English system of engineering units is used in equations in the text. See references 1 and 2 for detail.

References

1. Matthews, C.S., and Russell, D.G.: Pressure Build-Up and Flow Tests in Wells, Soc. Pet. Eng. Monograph Series, Vol. 1, SPE Dallas (1967), 4.

2. Earlougher, R.C., Jr.: Advances in Well Test Analysis, Soc. Pet. Eng. Monograph Series, Dallas, 1977.

3. Horner, D.R.: "Pressure Build-Up in Wells," Proc., Third World Pet. Cong., E.J. Brill, Leiden (1951), II, 503-521.

4. Miller, C.C., Dyes, A.B., and Hutchinson, C.A., Jr.: "Estimation of Permeability and Reservoir Pressure from Bottom-Hole Pressure Build-Up Characteristics," Trans., AIME (1950), 189, 91-104.

5. Ramey, Henry J., Jr., and Cobb, W.M.: "A General Pressure Build-Up Theory for a Well in a Closed Drainage Area," J. Pet. Tech. (Dec. 1971), 1493.

6. Theis, C.V.: "The Relationship between the Lowering of the Piezometric Surface and the Rate and Duration of Discharge Using Ground-Water Storage," Trans., AGU (1935), 519.

7. Hurst, W.: "Establishment of the Skin Effect and Its Impediment to Fluid Flow in a Wellbore," Pet. Eng. (Oct. 1953), 25, B-6.

8. Van Everdingen, A.F.: "The Skin Effect and Its Influence on the Productive Capacity of a Well," Trans., AIME (1953), 198, 171-176.

9. Perrine, R.L.: "Analysis of Pressure Build-Up Curves," Drill. and Prod. Prac., API (1956), 482.

10. Pitzer, S.C., Rice, J.D., and Thomas, C.E.: "A Comparison of Theoretical Pressure Buildup Curves with Field Curves Obtained from Bottom Hole Shut-in Tests," Trans., AIME (1959), 416.

11. Matthews, C.S., Brons, F., and Hazebroek, P.: "A Method for Determination of Average Pressure in a Bounded Reservoir," Trans., AIME (1954), 201, 182-191.

12. Gringarten, A.C., Ramey, H.J., Jr., and Raghavan, R.: "Applied Pressure Analysis for Fractured Wells," J. Pet. Tech. (July 1975), 887-892.

13. Ramey, H.J., Jr., Kumar, A., and Gulati, M.S.: Gas Well Test Analysis under Water-Drive Conditions, AGA, Arlington, Va., 1973.

14. Strobel, C.J., Gulati, M.S., and Ramey, H.J., Jr.: "Reservoir Limit Tests in a Naturally Fractured Reservoir--A Field Case Study Using Type Curves," J. Pet. Tech. (Sept. 1976), 1097.

15. Kamal, M., and Brigham, W.E.: "Pulse-Testing Response for Unequal Pulse and Shut-in Periods," Soc. Pet. Eng. J. (Oct. 1975), 399.

16. Miller, G.B., Seeds, R.W.S., and Shira, H.W.: "A New, Surface-Recording, Down-Hole Pressure Gage," paper SPE 4125, 47th Annual Fall Meeting, SPE of AIME, San Antonio, Texas, Oct. 8-11, 1972.

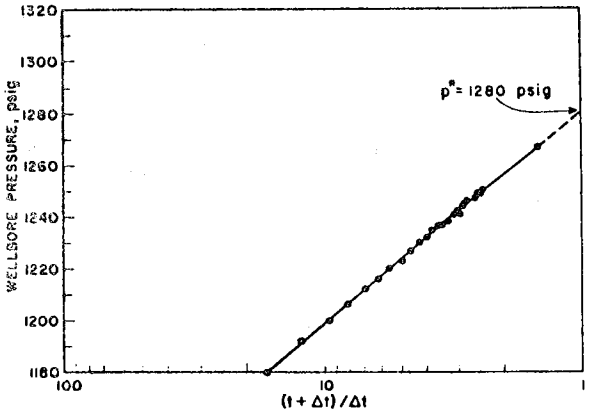

Fig. 1. Pressure buildup in a nearly ideal reservoir.

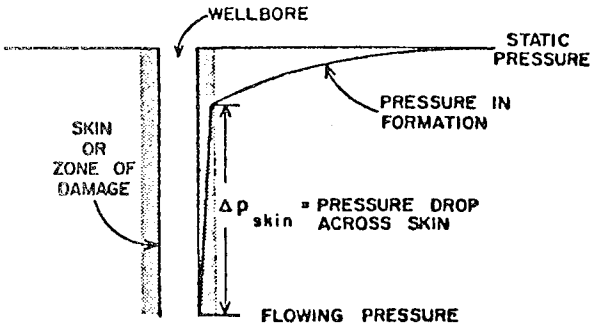

Fig. 2. Pressure distribution in a reservoir with a skin.

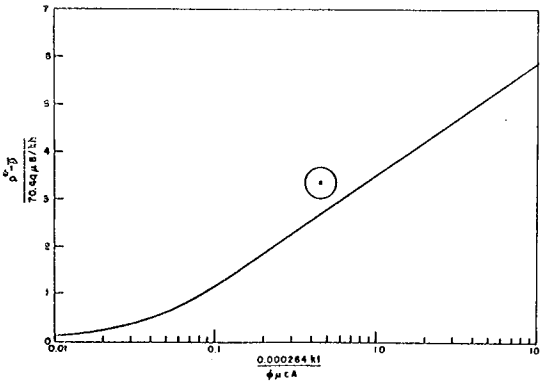

Fig. 3. Pressure function for one well in center of cylindrical reservoir.

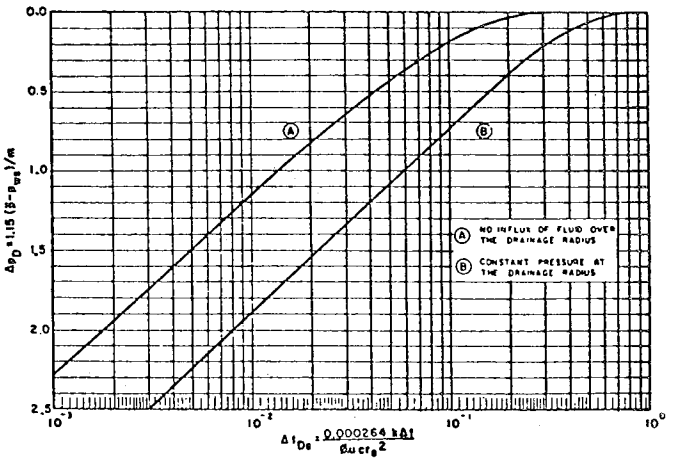

Fig. 4. Theoretical pressure buildup curves. From Miller, Dyes, and Hutchinson, and Perrine.

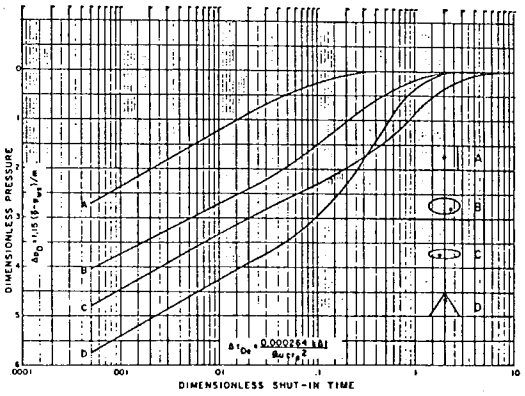

Fig. 5. Theoretical pressure buildup curves. After Pitzer.

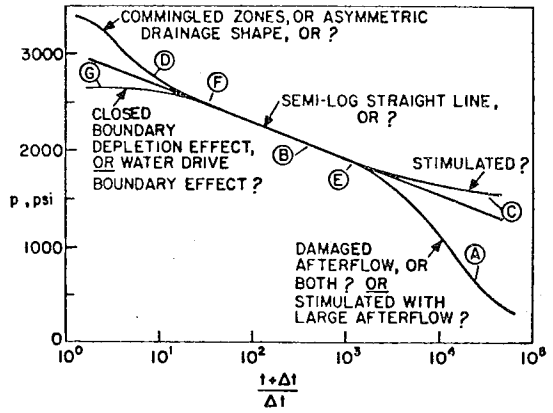

Fig. 6. Buildup factors.

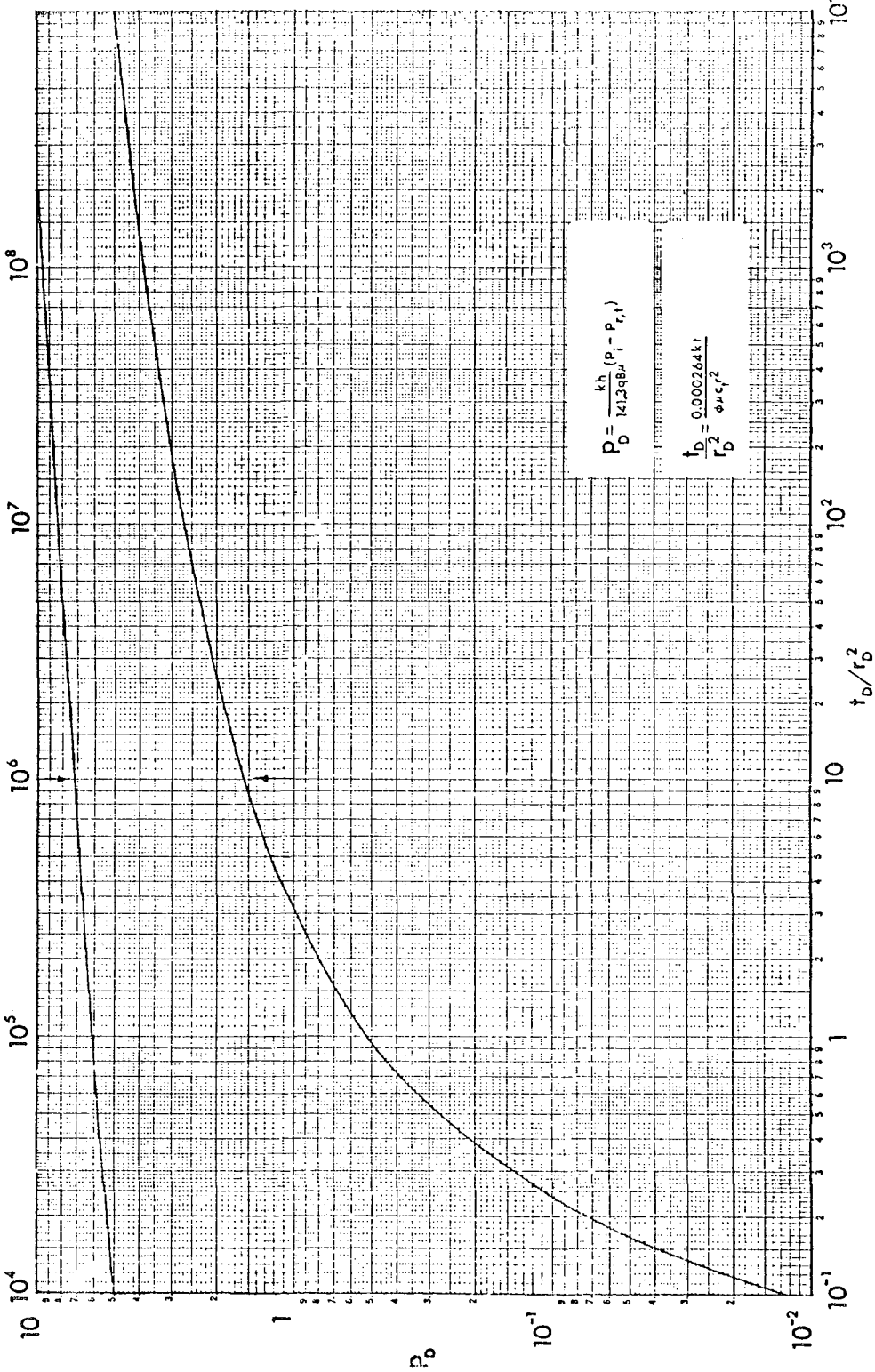

Fig. 7. Line source solution.

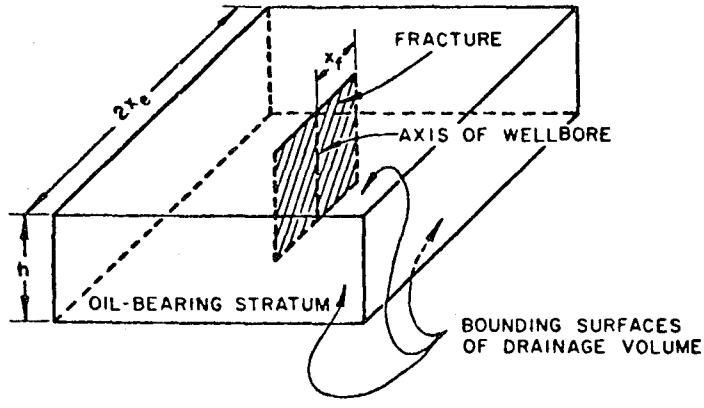

Fig. 8. Schematic view of fractured well and accompanying reservoir drainage volume.

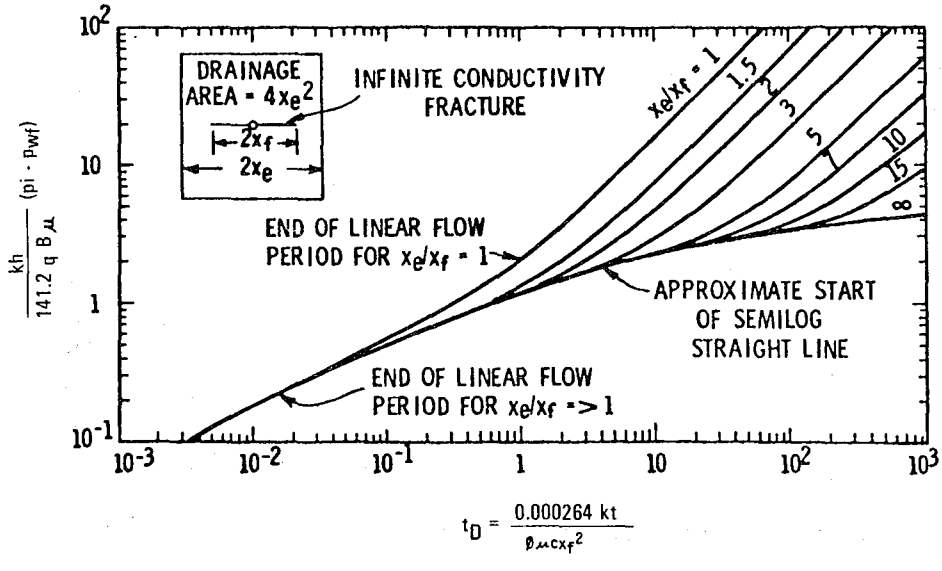

Fig. 9. Type curve for vertically fractured well.

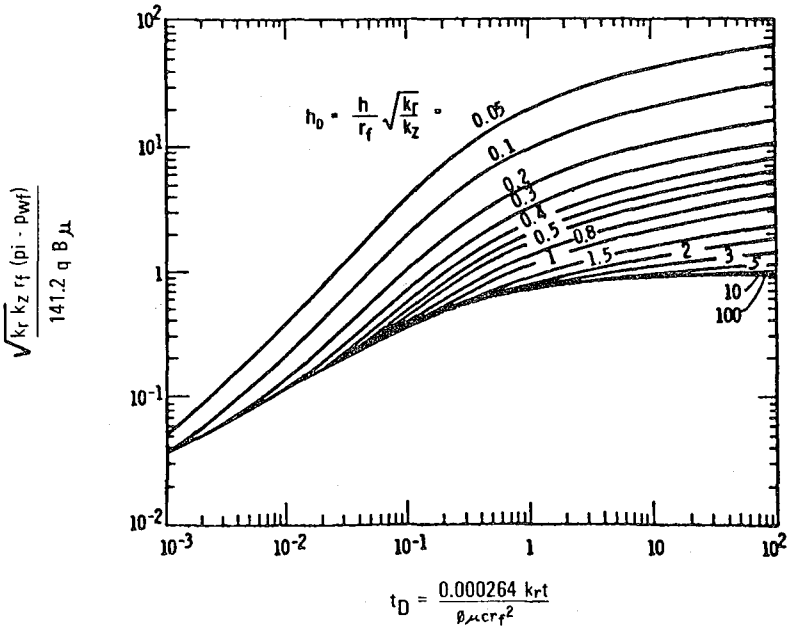

Fig. 10. Type curve for horizontal fracture.

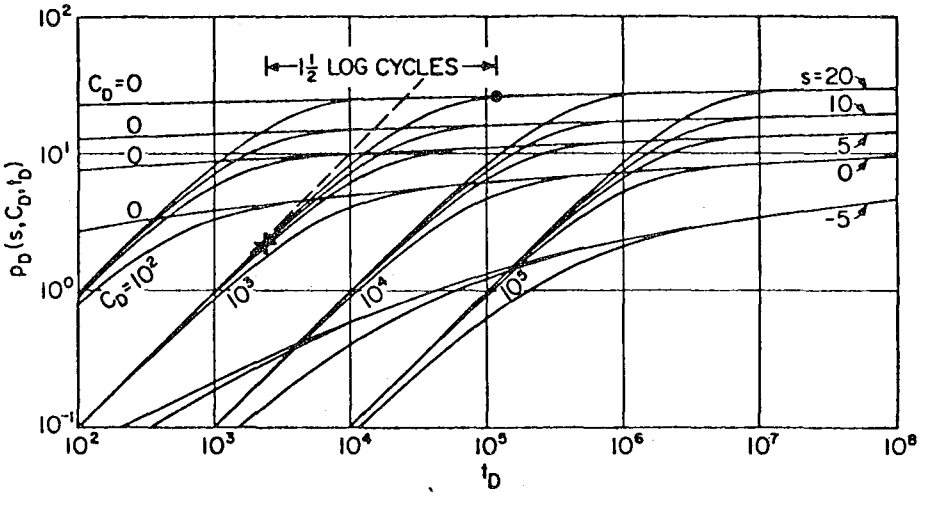

Fig. 11. Well bore storage and skin effect.

AQUIFER TESTS - THE STATE OF THE ART IN HYDROLOGY

By E. P. Weeks
U. S. Geological Survey
Lubbock, Texas

ABSTRACT

Numerous developments have been made in the theory and design of aquifer tests since C. V. Theis published his famous paper in 1935, and it is now possible to analyze data obtained under geohydrologic conditions that depart in a number of ways from those assumed in his development. Concerning the aquifer itself, several theories have been developed and applied to describe and analyze flow in leaky aquifers, in aquifers which are anisotropic with respect to distribution of hydraulic conductivity between different horizontal directions, and in unconfined aquifers. Well characteristics can be dealt with by equations now available for analyzing flow toward production wells that partially penetrate the aquifer, that have significant storage in the well bore, or that exhibit significant well losses. In regard to the type of discharge or head control imposed at the production well, equations are available for analyzing the effects of various types of changes in discharge with time, for effects of constant drawdown, and for effects of an instantaneous change in head (the "slug" test).

The equations developed for various aquifer and well conditions provide tools for analyzing data from many different geohydrologic situations. However, many of the aquifer-test solutions result in curves of similar shape, and therefore, are not unique to only one flow system. Consequently, careful site evaluation and aquifer-test design are essential to ensure the success of planned aquifer tests. Pretest prediction of aquifer response, based upon best estimates of the properties of the aquifer and confining bed and upon the hydrologist's analysis of the geohydrologic setting is highly desirable in designing an aquifer test. Such a prediction will enhance the probability that the test is run long enough and the observation wells are spaced such that proper and adequate drawdown data are available for analysis and definition of the flow system.

INTRODUCTION

Stallman (1971) defines an aquifer test as a controlled field experiment made to determine the hydraulic properties of water-bearing and associated rocks. Such a definition is both useful and accurate. However, in view of the symposium title and the general interest of its participants, the scope of this paper is limited to a discussion of tests involving radial symmetry, those aquifer test situations for which analytical equations are available, and equations or methods dealing with transient flow. Test situations for which no analytical equations are available are mentioned only briefly and solution by numerical modeling is suggested. Knowledge and familiarity with the use of the Theis (1935) equation is assumed.

By way of acknowledgment, this paper is an outgrowth of an effort to update and revise, for another purpose, the publication by Stallman (1971) and hence draws heavily upon his earlier work.

AVAILABLE ANALYTICAL SOLUTIONS

Most of the publications describing advances in aquifer test theory since Theis (1935) have presented equations that avoid one or more of the assumptions of the Theis equation. Consequently, they can be categorized with respect to the Theis equation assumptions as listed below. For clarity, these assumptions are divided into three categories. The first category deals with assumptions regarding the aquifer and its boundaries, the second with assumptions regarding characteristics of the production well, and the third with the nature of the stress applied at the control or production well. Some analyses deal with variations for assumptions in more than one category and are discussed under the section deemed most relevant.

The Theis equation solution involves the following categorized assumptions:

1. Aquifer: a. infinite in areal extent; b. confined above and below by impermeable beds; c. homogeneous, isotropic, and of uniform thickness; d. remains filled with water, and e. releases water from storage instantaneously with a decline in head.
2. Production well: a. completely penetrates the aquifer; b. infinitesimal diameter; c. produces water without head loss in the well bore; and d. flow to the well per unit length open to the aquifer is uniform.
3. Stress applied at the well: a. discharge is constant, starting at some initial time t=0.

Other assumptions involved in use of the Theis equations, such as the validity of Darcy's Law, that flow is laminar, that the fluid is homogeneous and completely saturates the medium, and that the medium is physically and chemically stable, are in general implicit in the analytical solutions described below as well.

Aquifer Conditions

Historically, the first of the assumptions regarding the aquifer to be overcome is that concerning its infinite areal extent. Generally, tests on aquifers of limited areal extent are analyzed by the application of image-well theory, as described, for example, by Ferris and others (1962). Based upon theory, Stallman (1963) presented type curves to analyze tests on semiinfinite

aquifers bounded by a linear fully penetrating stream or by a linear contact with impermeable rock. Moreover, if the boundary configuration of the tested aquifer is more complicated, but can be idealized as a series of line segments, type curves can be tailormade by application of image-well theory to the appropriate infinite-aquifer response functions.

Bixel and others (1963) present equations that describe drawdowns due to pumping from an aquifer linearly bounded by an aquifer of different hydraulic properties. Use of image-well theory is limited in this case to steady-state conditions or to the unlikely situation in which the ratios of transmissivity to storage, or hydraulic diffusivities, of the two adjoining aquifers are the same. For other situations, the equations are quite complicated, and any actual field application of their theory to analyze aquifer-test data is unknown to this author.

Hantush (1965) presents an equation that describes drawdowns in an aquifer bounded by a fully-penetrating stream separated from the aquifer by a thin layer of low permeability. He did not numerically evaluate the function, however, and the equation has not been applied. Instead, standard practice in the analysis of tests made in such geohydrologic situations has been to determine an "effective distance" to the stream boundary (Kazmann, 1946; Rorabaugh, 1956; Hantush, 1959a). In using the "effective distance" concept, the effects of low-permeability streambed materials and of partial penetration of the stream on drawdowns in the aquifer are compensated for by adding a fictitious increment of aquifer width between the stream and the actual aquifer.

The need to assume that the aquifer is confined above and below by impermeable beds has been overcome in developments by Hantush and Jacob (1955) and by Hantush (1960). In the earlier paper, the authors give equations that describe drawdowns in an aquifer separated from an overlying or underlying constant-head source bed by an incompressible semipermeable layer. Hantush's later paper extends this analysis to include effects of storage within the confining layer, and presents type curves showing the response of the aquifer during the early period when transient drawdown effects have not yet traversed the full thickness of the confining layer. In addition, time criteria are given to determine the period during which the type curves are applicable.

Both leaky-aquifer equations have been widely applied. The Hantush-Jacob equations are used to analyze data from aquifers semiconfined by beds that are relatively thin, permeable, and consolidated; the Hantush equation is relevant to aquifers semiconfined by thick, poorly consolidated, low permeability beds.

In tests on leaky aquifers, determination of the hydraulic properties of the semiconfining beds is often at least as important as determination of the aquifer properties. The semiconfining-bed properties can sometimes be determined from the type-curve match, but they often are better determined by analysis of drawdown in piezometers tapping the confining layer itself, using the ratio method of Neuman and Witherspoon (1972).

The above referenced leaky-aquifer equations assume that no drawdown is induced in the adjacent aquifer due to leakage into the pumped aquifer. This assumption is frequently valid if the unpumped aquifer is unconfined, but does not always hold true in multiple confined aquifer systems. Consequently, Hantush (1967) and Neuman and Witherspoon (1969) have developed equations describing drawdown distributions around a constant-discharge production well in both the pumped and unpumped aquifers. Hantush's analysis is for a system of two aquifers separated by an incompressible semiconfining layer, while Neuman and Witherspoon consider storage in the semiconfining bed and describe drawdown variations with time in that bed as well. In another development, Neuman and Witherspoon (Witherspoon and others, 1971) analyzed systems including as many as three aquifers separated by compressible semiconfining layers and also presented equations describing the time-drawdown response in the semiconfining layers. The resulting equations from all these analyses are complicated, however, and contain several parameters. Hence, in general, they are more suited for predicting aquifer-test response than for aquifer-test analysis.

Methods have also been developed by Hantush (1966a, 1966b), Hantush and Thomas (1966), and Papadopulos (1967a) to analyze data from aquifers that are areally anisotropic. These methods have not been widely applied in hydrology, because of the need for observation wells in at least three directions from the pumped well. However, unpublished analyses of some recent aquifer tests on the Floridan aquifer near Tampa, Florida, using these methods, have resulted in an excellent fit between the data and the theory, indicating that the methods are indeed useful in some situations.

Little work has been done on developing equations to handle effects of aquifer heterogeneity. However, Hantush (1962a) has developed equations to describe the effects on water levels in observation wells of pumping a well in an aquifer that thins exponentially in one direction, but is of constant thickness in the orthogonal direction, both for wells pumped at a constant rate and for flowing wells. In addition, he describes time and distance criteria for which equations assuming constant aquifer thickness can be applied. In another development, Javandel and Witherspoon (1969) have used a numerical model to compute drawdowns in piezometers tapping one of several layers of assumed different hydraulic conductivity in a layered aquifer completely penetrated by the production well. The results of their study indicate that the effects of layering on drawdown diminish with time, and that analysis of later-time drawdown data should yield the transmissivity of the full aquifer thickness.

Much recent work has been concentrated on the development of response curves for unconfined aquifers. Early important contributions on the topic were made by Boulton (1954a, 1954b). In one analysis, he assumed negligible dewatering, linear release from storage, and termination of flow lines

at the water table. In the other analysis (1954b), he investigated the effects of delayed yield from storage, expressed as an exponential function of time. Boulton's delayed-yield model has enjoyed considerable acceptance, in large part because of the applications described by Prickett (1965).

Recent work (Neuman, 1972, 1974, 1975; Streltsova, 1972; Streltsova and Rushton, 1973; Boulton and Streltsova, 1975), has centered on analyzing the aquifer as being compressible (containing internal storage), but with the flow lines terminating at the water table, as in Boulton's (1954a) analysis. These analyses result in type curves very similar to Boulton's (1954b) delayed yield curves, and have resulted in Boulton's arbitrary "delay index" being described in terms of specific yield (Sy), aquifer thickness (b), the ratio of horizontal to vertical hydraulic conductivity (Kr/Kz), and the ratio of well radius to aquifer thickness (r/b). There is considerable dispute on the exact nature of this relationship, however (Neuman, 1975; Streltsova, 1976a; Neuman, 1976; Gambolatti, 1976). On the other hand, Cooley (1972) and Cooley and Case (1973) have shown that the delay index is exactly related to the hydraulic conductivity, thickness, and specific yield of the semiconfining bed in a system in which the aquifer is overlain by a semiconfining bed containing a water table.

The recent work of Neuman, Boulton, and Streltsova supersedes earlier work by Stallman (1965) and Dagan (1967) in which flow lines were considered to end at the water table but internal storage with the aquifer was not considered. Comparison of the various response curves to test data indicate that internal aquifer storage, although quantitatively small, substantially affects the shape of the early time-drawdown data, and cannot properly be ignored.

Methods for describing drawdowns in aquifers having permeability due to fractures and to intergranular porosity have received considerable attention by the petroleum industry, but are not referenced here because another speaker is describing the state of the art in well testing in that industry. However, within the hydrologic literature, Streltsova (1976b) presents a solution for drawdowns due to pumping an aquifer exhibiting permeability due both to fracture and to intergranular porosity. Type curves developed from her paper have been used to analyze data from an aquifer test involving multiple observation wells at Reston, Virginia, by Ren Jen Sun (oral commun., 1975), and an excellent match between theory and data was obtained.

Characteristics of the Production Well

Of the assumptions regarding characteristics of the production well, that regarding its full penetration is perhaps the most significant on a practical basis. Production wells sometimes penetrate only a fraction of the aquifer thickness, and the resultant effects on drawdown in nearby piezometers can be substantial, particularly if the aquifer exhibits horizontal-vertical anisotropy. Hantush (1961a, 1961d) has presented equations to compute the effects of partial penetration in piezometers or partially penetrating observation wells, and Weeks (1964, 1969) and Mansur and Dietrich (1965) have described use of data from aquifer tests on partially penetrating wells to compute the ratio of horizontal to vertical hydraulic conductivity. Hantush has also presented equations to describe the effects of partial penetration on leaky artesian aquifers. Use of these equations to analyze aquifer-test data may not be practical, however, because of difficulty in separating the effects of radial-vertical anisotropy from those due to leakage. Neuman (1974) and Dagan (1967) have presented equations to describe effects of partial penetration on drawdowns near wells tapping unconfined aquifers, with and without internal storage in the aquifer, respectively. Neuman (1975) also describes the use of his equation to analyze aquifer-test data.

The assumption that the production well is infinitesimal in diameter is never strictly true, and, as a practical matter, storage in the well bore can cause significant effects on the early-time drawdowns in the production well, as described by Papadopulos and Cooper (1967) and in nearby observation wells, as described by Papadopulos (1967b). The equations and limiting times and distances over which they apply are not considered as often as they should be in aquifer-test design and analysis. This is true in part because the paper by Papadopulos appears in a rather obscure publication.

Analysis of the effects of head loss in the production well due to clogging of the aquifer materials adjacent to the well bore by drilling fluid, or by turbulent flow within and near the well bore has not received as wide attention in the field of hydrology as it has in petroleum engineering, in part at least because of the emphasis in hydrology on analyzing for aquifer, as opposed to well, properties. In general, well-bore effects are assumed to result from effects of turbulence, and are analyzed by step-drawdown tests. Jacob (1947) proposed that the pumped-well drawdown be expressed as a sum of two components, one linearly dependent upon discharge (the aquifer head loss) and the other upon the square of the discharge (the well head loss). Step-drawdown data may be analyzed to determine the well-loss coefficient by a simple graphical analysis using his equation.

Rorabaugh (1953) also assumed that the step-drawdown data could be separated into two components, but suggested that the well-loss portion was proportional to the discharge raised to the nth power, where n varies from 2 to 3 or more. Analysis of step-drawdown data by the Rorabaugh method requires a more complicated graphical analysis, as it is necessary to determine both the well-loss coefficient and the exponent.

Lennox (1966) presents the results of analyzing a number of step-drawdown tests by the above methods, and gives a good description of the methodology of the Rorabaugh equation.

Discharge or Drawdown Control at the Production Well

Most equations developed for aquifer-test analysis are based on the assumption that the well is pumped at some constant discharge, beginning at some initial time t=0. However, there are a number of circumstances where it is not practical to maintain pumpage at a constant rate. For example, a valve may not be available for discharge control, and the discharge of the well will decline as the water level is drawn down. Flowing wells often are not equipped with pumps, and instead are allowed to flow from the well head. The control in this case is that of constant drawdown, rather than constant discharge. Finally, particularly during test drilling, it is sometimes most practical to test the aquifer by instantaneously changing the head in the well by a constant amount, and then observing its recovery. A test run under these conditions is termed a "slug test".

Equations and methods to analyze data from tests involving variable discharge can be divided into two categories. For one approach, discharge is assumed to follow some mathematically exact variation with time. In the other approach, the discharge is assumed to vary in a sequence of discrete steps, and the effects of each step change in discharge on water levels is summed to produce a specific type curve for a given pattern of discharge variation.

Werner (1946) presents equations describing drawdowns in confined aquifers due to linearly varying discharge. Abu-Zied and Scott (1963); Abu-Zied, Scott, and Aron (1964); and Hantush (1964a, 1964b) present equations describing drawdowns in confined aquifers for exponentially decreasing pumpage rates, and Hantush (1964a, 1964b) describes the effects of hyperbolically decreasing discharge as well. In addition, Hantush presents equations for drawdown in leaky aquifers in which storage in the semiconfining bed is negligible, and in which discharge varies exponentially or hyperbolically. Lai, Karadi, and Williams (1973) present equations for drawdown in a large-diameter production well with exponentially or linearly varying discharge. Finally, Lai and Su (1974) present equations for effects of constant or exponentially varying discharge on the drawdown in a large-diameter production well that taps a leaky aquifer. In general, the various equations may be used to analyze aquifer test by preparing special type curves, as described, for example, by Hantush (1964b). However, the equations have not been widely used, possibly in part because they are complicated.

Representation of any arbitrary pumpage history as a series of finite time intervals of constant discharge has been suggested by Cooper and Jacob (1946), Stallman (1962), Aron and Scott (1965), Sternberg (1968) and Moench (1971). Of these, Stallman (1962), and Moench (1971) describe use of the full Theis or leaky aquifer equation, and the other authors suggest use of the Cooper-Jacob (Cooper and Jacob, 1946) approximation of the Theis equation to make a semilog analysis. Once again, these methods do not appear to have been widely applied, even though they would be more easily used than those based on the assumption that the discharge-time relationship follows some mathematical function.

Flowing artesian wells often are not equipped with pumps, but are opened and allowed to flow at the well head. Thus, drawdown in the production well is constant, but its discharge varies. Moreover, the use of constant-drawdown equations for prediction purposes is of interest to the construction industry, because the goal of most dewatering projects is to maintain some constant minimum drawdown, rather than to deliver water at a specified rate.

The first paper to deal with transient groundwater movement to flowing wells was by Jacob and Lohman (1952). They present a type curve to analyze the variation of discharge of a flowing well with time to determine transmissivity and the coefficient of storage. Later developments by Hantush (1964a) and Glover (1964) present type curves or tabulated functions relating the ratio of drawdown in a nearby observation well to that in the production well as a function of time and hydraulic diffusivity (transmissivity divided by the storage coefficient, or T/S). Thus, time-drawdown data for an observation well may be used to compute T/S, but not transmissivity or storage alone.

Hantush (1959b) developed equations to describe the discharge variation with time in a flowing well tapping a leaky aquifer separated from a constant-head source bed by an incompressible semiconfining bed. In addition to the infinite-aquifer equations for this situation, Hantush presents equations for the discharge variation with time of a flowing well in the center of a circular aquifer bounded either by a constant-head or by an impermeable boundary. The paper also presents drawdown equations for all three situations.

For wells not equipped with pumps, such as those installed during test-drilling operations, slug tests provide a practical tool for performing aquifer tests. In a slug test, head in the control well is instantaneously changed either upward or downward by adding a slug of water, by withdrawal of a large float or by the escape of compressed air. The recovery of head to its initial position with time is observed. The mathematical formulation governing the head recovery during a slug test on a well of infinitesimal diameter was first presented by Ferris and Knowles (1954). However, Cooper and others (1967) show that the effects of storage in the well bore generally are significant in slug tests. They present equations and type curves for analyzing slug tests when well-bore storage is significant, but inertial effects are small. Their slug-test equation, coupled with the use of an electronic pressure transducer to record rapid water-level response, has been useful to evaluate packer tests and other tests on bore holes in areas remote from pump-equipped wells.

Van der Kamp (1976) has presented an equation for analyzing slug tests on wells in which inertial effects are great enough that the response to an instantaneous head change is described by an underdamped harmonic function with time. He used the method to determine transmissivity from tests on several wells, with fair results.

ARTESIAN

Category	Nonleaky: Thiem (1906)	Theis (1935)	Jacob and Lohman (1952)	Stallman (1963)	Hantush (1964a)	Hantush (1965)	Hantush (1962b)	Streltsova (1976b)	Leaky: Hantush and Jacob (1955)	Hantush (1956)	Hantush (1960)	Multiple: Papadopulos (1966)	Hantush (1967)	Neuman and Witherspoon (1969)	Witherspoon and others (1971)
A. Type of control imposed:															
Step change Q	x	x	-	x	-	x	x	x	x	-	x	x	x	x	x
Step change s	-	-	x	-	x	-	x	-	-	x	-	x	-	-	-
Pulsed Q	-	-	-	-	-	-	-	-	-	-	-	-	-	-	-
Pulsed s	-	-	-	-	-	-	-	-	-	-	-	-	-	-	-
Variable Q	-	-	-	-	-	-	-	-	-	-	-	-	-	-	-
Variable s	-	-	-	-	-	-	-	-	-	-	-	-	-	-	-
B. Control-well Characteristics:															
Full penetration	x	x	x	x	x	x	x	x	x	x	x	x	x	x	x
Partial penetration	-	-	-	-	-	-	-	-	-	-	-	-	-	-	-
Diameter infinitesimal	x	x	x	x	x	x	x	x	x	x	x	x	x	x	x
Diameter finite	-	-	-	-	-	-	-	-	-	-	-	-	-	-	-
Seepage face	-	-	-	-	-	-	-	-	-	-	-	-	-	-	-
Well loss	-	-	-	-	-	-	-	-	-	-	-	-	-	-	-
Radial screens	-	-	-	-	-	-	-	-	-	-	-	-	-	-	-
C. Conductivity and flow conditions:															
Homogeneous, isotropic	x	x	x	x	x	x	x	-	x	x	x	x	x	x	x
Homogeneous, anisotropic	-	-	-	-	-	-	-	-	-	-	-	-	-	-	-
Heterogeneous, isotropic	-	-	-	-	-	-	-	-	-	-	-	-	-	-	-
Fracture permeability	-	-	-	-	-	-	-	x	-	-	-	-	-	-	-
Impermeable confining beds	x	x	x	x	x	x	x	-	-	-	-	x	-	-	-
Permeable confining beds (steady)	-	-	-	-	-	-	-	-	x	x	-	-	x	-	-
Permeable confining beds (nonsteady)	-	-	-	-	-	-	-	-	-	-	x	-	-	x	x
Sloping beds	-	-	-	-	-	-	x	-	-	-	-	-	-	-	-
Areally infinite	x	x	x	-	x	-	x	-	x	x	x	x	x	x	x
Areally semi-infinite	-	-	-	x	-	x	-	-	-	-	-	-	-	-	-
Areally discontinuous	-	-	-	-	-	x	-	-	-	-	-	-	-	-	-
Dewatering negligible	x	x	x	x	x	x	-	-	x	x	x	x	x	x	x
Dewatering significant[e]	-	-	-	-	-	x	x	-	-	-	-	-	-	-	-
Flow radial	x	x	x	x	x	x	-	-	x	x	x	x	-	-	-
Flow radial and vertical	-	-	-	-	-	-	x	-	-	-	-	-	x	x	x
Nonsteady flow	-	x	x	x	x	x	x	x	x	x	x	x	x	x	x
Steady flow	x	-	-	-	-	x	-	-	x	-	x	-	-	-	-
D. Storage relation:															
Linear to head	-	x	x	x	x	x	x	x	x	x	x	x	x	x	x
Head and time	-	-	-	-	-	-	-	-	-	-	-	-	-	-	-
Artesian	-	x	x	x	x	x	-	x	x	x	x	x	x	x	x
Unconfined	-	-	-	-	-	-	x	-	-	-	-	-	-	-	-
E. Emphasis on paper:															
Q versus time	-	-	x	-	-	-	x	-	-	x	-	x	-	-	-
s versus time and space	-	x	-	x	x	x	x	x	x	-	x	x	x	x	x
Analytical equation	x	x	x	x	x	x	x	x	x	x	x	x	x	x	x
Graphical type curve	-	-[1]	x[1]	x[1]	-	-	-	-	-[1]	-	-[1]	-	-	-	-
Tables, type-curve	-	-[1]	-[1]	-	x	x	-	-	x[2]	x[3]	x	-	-	-	-
Numerical or analog techniques	-	-	-	-	-	-	-	-	-	-	-	-	-	x	x
Theory development	x	x	x	-	x	x	x	x	x	x	x	x	x	x	x
Application of data	-	-	-	-	-	-	-	-	-	-	-	-	-	-	x

Category	Horizontal plane anisotropy: Hantush (1966a)	Hantush (1966b)	Hantush and Thomas (1966)	Papadopulos (1967a)	Partial penetration: Hantush (1961a)	Hantush (1961d)	Hantush (1964a)	Mansur and Dietrich (1965)	Weeks (1969)	Well Characteristics: Jacob (1947)	Rorabaugh (1953)	Lennox (1966)	Cooper and others (1965)	Bredehoeft and others (1966)	Cooper and others (1967)	Papadopulos and Cooper (1967)	Papadopulos (1967b)	van der Kamp (1976)
A. Type of control imposed:																		
Step change Q	x	x	x	x	x	x	x	x	x	x	x	x	-	-	-	x	x	x
Step change s	-	-	-	-	-	-	-	-	-	-	-	-	-	x	-	-	-	-
Pulsed Q	-	-	-	-	-	-	-	-	-	-	-	-	-	-	x	-	-	-
Pulsed s	-	-	-	-	-	-	-	-	-	-	-	-	-	-	x	-	-	-
Variable Q	-	x	-	-	-	-	-	-	-	-	-	-	-	-	-	-	-	-
Variable s	-	-	-	-	-	-	-	-	-	-	-	-	x	-	-	-	-	-
B. Control-well Characteristics:																		
Full penetration	x	x	x	x	-	-	-	-	-	x	x	x	x	x	x	x	x	x
Partial penetration	-	x	-	-	x	x	x	x	x	-	-	-	-	-	-	-	-	-
Diameter infinitesimal	x	x	x	x	x	x	x	x	x	x	x	x	-	-	-	-	-	-
Diameter finite	-	-	-	-	-	-	-	-	-	-	-	-	x	x	x	x	x	x
Seepage face	-	-	-	-	-	-	-	-	-	-	-	-	-	-	-	-	-	-
Well loss	-	-	-	-	-	-	-	-	-	x	x	x	-	-	-	-	-	-
Radial screens	-	-	-	-	-	-	-	-	-	-	-	-	-	-	-	-	-	-
C. Conductivity and flow conditions:																		
Homogeneous, isotropic	-	-	-	-	x	x	-	-	-	x	x	x	x	x	x	x	x	x
Homogeneous, anisotropic	-	-	-	-	-	-	x	x	x	-	-	-	-	-	-	-	-	-
Heterogeneous, isotropic	-	-	-	-	-	-	-	-	-	-	-	-	-	-	-	-	-	-
Fracture permeability	-	-	-	-	-	-	-	-	-	-	-	-	-	-	-	-	-	-
Impermeable confining beds	x	x	x	x	x	x	x	x	x	x	x	x	x	x	x	x	x	x
Permeable confining beds (steady)	x	x	-	-	-	-	x	-	-	-	-	-	-	-	-	-	-	-
Permeable confining beds (nonsteady)	-	-	-	-	-	-	-	-	-	-	-	-	-	-	-	-	-	-
Sloping beds	-	-	-	-	-	-	-	-	-	-	-	-	-	-	-	-	-	-
Areally infinite	x	x	x	x	x	x	x	x	x	x	x	x	x	x	x	x	x	x
Areally semi-infinite	-	-	-	-	-	-	-	-	-	-	-	-	-	-	-	-	-	-
Areally discontinuous	-	-	-	-	-	-	-	-	-	-	-	-	-	-	-	-	-	-
Dewatering negligible	x	x	x	x	x	x	x	x	x	x	x	x	x	x	x	x	x	x
Dewatering significant[e]	-	-	-	-	-	-	-	-	-	-	-	-	-	-	-	-	-	-
Flow radial	x	x	x	x	-	-	-	-	-	x	x	x	x	x	x	x	x	x
Flow radial and vertical	-	x	-	-	x	x	x	x	x	-	-	-	-	-	-	-	-	-
Nonsteady flow	x	x	x	x	x	x	x	-	x	x	x	x	x	x	x	x	x	x
Steady flow	-	-	-	-	-	-	-	x	-	-	-	-	-	-	-	-	-	-
D. Storage relation:																		
Linear to head	x	x	x	x	x	x	x	x	x	x	x	x	x	x	x	x	x	x
Head and time	-	-	-	-	-	-	-	-	-	-	-	-	-	-	-	-	-	-
Artesian	x	x	x	x	x	x	x	x	x	x	x	x	x	x	x	x	x	x
Unconfined	-	-	-	-	-	-	-	-	-	-	-	-	-	-	-	-	-	-
E. Emphasis on paper:																		
Q versus time	-	-	-	-	-	-	-	-	-	-	-	-	-	-	-	-	-	-
s versus time and space	x	x	x	x	x	x	x	x	x	x	x	x	x	x	x	x	x	x
Analytical equation	x	x	x	x	x	-	x	-	-	x	x	-	x	x	x	x	x	x
Graphical type curve	-	-	-	-	-	-	-	-	-	-	-	-	-	-	-	-	-	-
Tables, type-curve	-	-	-	-	-[4]	-	-	-	x	-	-	-	x	x	x[1]	x	x	-
Numerical or analog techniques	-	-	-	-	-	-	-	x	-	-	-	-	-	x	-	x	-	-
Theory development	x	x	x	x	x	-	x	-	-	x	x	-	x	x	x	x	x	x
Application of data	x	-	x	x	-	x	-	x	x	x	x	x	-	-	x	-	-	x

Category	Variable discharge: Werner (1946)	Stallman (1962)	Hantush (1964b)	Abu-Zied and Scott (1963)	Abu-Zied and others (1964)	Aron and Scott (1965)	Sternberg (1968)	Moench (1971)	Lai and others (1973)	Lai and Su (1974)	Miscellaneous: Hantush (1962)	Hantush and Papadopulos (1962)	Bixel and others (1963)	Moench and Prickett (1972)
A. Type of control imposed:														
Step change Q	-	-	-	-	-	-	-	-	-	x	x	x	x	x
Step change s	-	-	-	-	-	-	-	-	-	-	-	-	-	-
Pulsed Q	-	-	-	-	-	-	-	-	-	-	-	-	-	-
Pulsed s	-	-	-	-	-	-	-	-	-	-	-	-	-	-
Variable Q	x	x	x	x	x	x	x	x	x	x	-	-	-	-
Variable s	-	-	-	-	-	-	-	-	-	-	-	-	-	-
B. Control-well Characteristics:														
Full penetration	x	x	x	x	x	x	x	x	x	x	x	-	x	x
Partial penetration	-	-	-	-	-	-	-	-	-	-	-	x	-	-
Diameter infinitesimal	x	x	x	x	x	x	x	x	-	-	x	-	x	x
Diameter finite	-	-	-	-	-	-	-	-	x	x	x	-	-	-
Seepage face	-	-	-	-	-	-	-	-	-	-	-	-	-	-
Well loss	-	-	-	-	-	-	-	-	-	-	-	-	-	-
Radial screens	-	-	-	-	-	-	-	-	-	-	-	x	-	-
C. Conductivity and flow conditions:														
Homogeneous, isotropic	x	x	x	x	x	x	x	x	x	x	-	x	x	x
Homogeneous, anisotropic	-	-	-	-	-	-	-	-	-	-	-	-	-	-
Heterogeneous, isotropic	-	-	x	-	-	-	-	-	-	-	x	-	-	-
Fracture permeability	-	-	-	-	-	-	-	-	-	-	-	-	-	-
Impermeable confining beds	x	x	x	x	x	x	x	x	x	-	x	x	x	x
Permeable confining beds (steady)	-	-	x	-	-	-	-	x	-	x	-	-	-	-
Permeable confining beds (nonsteady)	-	-	-	-	-	-	-	-	-	-	-	-	-	-
Sloping beds	-	-	x	-	-	-	-	-	-	-	-	-	-	-
Areally infinite	x	x	x	x	x	x	x	x	x	x	x	x	-	x
Areally semi-infinite	-	-	-	-	-	-	-	-	-	-	-	-	-	-
Areally discontinuous	-	-	-	-	-	-	-	-	-	-	-	-	x	-
Dewatering negligible	x	x	x	x	x	x	x	x	x	x	x	x	x	x
Dewatering significant[e]	-	-	-	-	-	-	-	-	-	-	-	-	-	-
Flow radial	x	x	x	x	x	x	x	x	x	x	x	-	x	x
Flow radial and vertical	-	-	-	-	-	-	-	-	-	-	-	-	-	-
Nonsteady flow	x	x	x	x	x	x	x	x	x	x	-	x	-	x
Steady flow	-	-	-	-	-	-	-	-	-	-	-	-	-	-
D. Storage relation:														
Linear to head	x	x	x	x	x	x	x	x	x	x	x	x	x	x
Head and time	-	-	-	-	-	-	-	-	-	-	-	-	-	-
Artesian	x	x	x	x	x	x	x	x	x	x	x	x	x	x
Unconfined	-	-	-	-	-	-	-	-	-	-	-	-	-	x
E. Emphasis on paper:														
Q versus time	x	x	x	x	x	x	x	x	x	x	-	-	-	-
s versus time and space	x	x	x	x	x	x	x	x	x	x	x	x	x	x
Analytical equation	x	-	x	x	x	x	-	x	x	x	x	x	x	x
Graphical type curve	-	-	-	-	-	-	-	-	-	-	-	-	x	-
Tables, type-curve	-	-	x	x	x	-	-	-	-	-	-	-	-	x
Numerical or analog techniques	-	-	-	-	-	-	-	x	-	-	-	-	-	x
Theory development	x	x	x	x	x	x	x	x	x	x	x	x	x	x
Application of data	-	-	x	-	x	-	-	x	-	-	-	-	x	-

UNCONFINED FLOW

Category	Water table in aquifer: Boulton (1954a)	Boulton (1954b)	Boulton (1963)	Boulton (1964)	Boulton (1965)	Prickett (1965)	Stallman (1965)	Norris and Fidler (1966)	Dagan (1967)	Neuman (1972)	Streltsova (1972)	Neuman (1974)	Boulton and Streltsova (1975)	Neuman (1975)	Water table in overlying aquitard: Cooley (1972)	Cooley and Case (1973)
A. Type of control imposed:																
Step change Q	x	x	x	x	-	x	x	x	x	x	x	x	x	x	x	x
Step change s	-	-	-	-	x	-	-	-	-	-	-	-	-	-	-	-
Pulsed Q	-	-	-	-	-	-	-	-	-	-	-	-	-	-	-	-
Pulsed s	-	-	-	-	-	-	-	-	-	-	-	-	-	-	-	-
Variable Q	-	-	-	-	-	-	-	-	-	-	-	-	-	-	-	-
Variable s	-	-	-	-	-	-	-	-	-	-	-	-	-	-	-	-
B. Control-well Characteristics:																
Full penetration	x	x	x	x	x	x	-	-	-	x	x	-	x	x	x	x
Partial penetration	-	-	-	-	-	-	x	x	x	-	-	x	-	x	-	-
Diameter infinitesimal	x	x	x	x	-	x	x	x	x	x	x	x	x	x	x	x
Diameter finite	-	-	-	-	x	-	-	-	-	-	-	-	-	-	-	-
Seepage face	-	-	-	-	x	-	-	-	-	-	-	-	-	-	-	-
Well loss	-	-	-	-	-	-	-	-	-	-	-	-	-	-	-	-
Radial screens	-	-	-	-	-	-	-	-	-	-	-	-	-	-	-	-
C. Conductivity and flow conditions:																
Homogeneous, isotropic	x	x	x	x	x	x	-	-	-	x	x	-	x	-	-	-
Homogeneous, anisotropic	-	-	-	-	-	-	x	x	x	-	-	x	-	x	-	-
Heterogeneous, isotropic	-	-	-	-	-	-	-	-	-	-	-	-	-	-	x	x
Fracture permeability	-	-	-	-	-	-	-	-	-	-	-	-	-	-	-	-
Impermeable confining beds	-	-	-	-	-	-	-	-	-	-	-	-	-	-	-	-
Permeable confining beds (steady)	-	-	-	-	-	-	-	-	-	-	-	-	-	-	-	-
Permeable confining beds (nonsteady)	-	-	-	-	-	-	-	-	-	-	-	-	-	-	-	-
Sloping beds	-	-	-	-	-	-	-	-	-	-	-	-	-	-	-	-
Areally infinite	x	x	x	x	x	x	x	-	x	x	x	x	x	x	x	x
Areally semi-infinite	-	-	-	-	-	-	-	x	-	-	-	-	-	-	-	-
Areally discontinuous	-	-	-	-	-	-	-	-	-	-	-	-	-	-	-	-
Dewatering negligible	x	x	x	x	-	x	x	x	x	x	x	x	x	x	x	x
Dewatering significant[e]	-	-	-	-	x	-	-	-	-	-	-	-	-	-	-	-
Flow radial	-	x	x	x	-	x	-	-	-	-	-	-	-	-	x	x
Flow radial and vertical	x	-	-	-	x	-	x	x	x	x	x	x	x	x	-	-
Nonsteady flow	x	x	x	x	x	x	x	x	x	x	x	x	x	x	x	x
Steady flow	-	-	-	-	-	-	-	-	-	-	-	-	-	-	-	-
D. Storage relation:																
Linear to head	x	-	-	-	-	-	x	x	x	x	x	x	x	x	x	x
Head and time	-	x	x	x	-	x	-	-	-	-	-	-	-	-	-	x
Artesian	0	x	x	x	0	x	0	0	0	x	x	x	x	x	-	-
Unconfined	x	x	x	x	x	x	x	x	x	x	x	x	x	x	x	x
E. Emphasis on paper:																
Q versus time	-	-	-	-	x	-	-	-	-	-	-	-	-	-	-	-
s versus time and space	x	x	x	x	-	x	x	x	x	x	x	x	x	x	x	x
Analytical equation	x	x	x	x	x	-	-	-	x	x	x	x	x	x	x	x
Graphical type curve	x[5]	-[1]	x	-	x	x	x[1]	-	x	x	x	x	-	x	-	-
Tables, type-curve	x	-	x	x	x	-	-	-	x	x	x	x	-	x	-	-
Numerical or analog techniques	-	-	-	-	-	-	x	-	-	x	-	x	-	-	x	x
Theory development	x	x	x	x	-	-	x	-	x	x	x	x	-	-	x	x
Application of data	-	x	x	x	x	-	-	x	x	-	-	-	x	x	-	-

[e]Dupuit-Forchheimer assumptions made
[1]Lohman (1972)
[2]Hantush (1961c)
[3]Hantush (1961b)
[4]Hantush (1961e)
[5]Stallman (1962)

Table 1. Selected literature on aquifer tests showing site conditions treated and subject emphasis. (x, condition treated in this paper; 0, artesian storage release assumed to be zero.)

The various papers cited above are summarized in table 1. This table, which was adapted from Stallman (1971), categorizes the papers according to the assumptions discussed above. In addition, a category has been added on the emphasis of the paper. This category specifies whether type curves are available in the paper, specifies availability of type curves in other sources by footnotes, and mentions whether field applications are given. The table should be useful for selecting the proper response function to analyze a given aquifer test. The table also contains a few references not cited above, including those describing drawdowns in a sloping water table aquifer (Hantush, 1962b), inertial effects on water levels in observation wells (Cooper and others, 1965), seismic effects on water-level fluctuations (Bredehoeft and others, 1966), drawdowns in collector wells (Hantush and Papadopulos, 1962), and drawdowns in an aquifer undergoing conversion from artesian to water table conditions (Moench and Prickett, 1971). Three papers by Boulton (1963, 1964, 1965) are referenced including two discussing use of the delayed-yield equations (Boulton, 1954b), and one describing drawdowns in an unconfined aquifer due to production at constant drawdown. Norris and Fidler describe an application of Stallman's (1965) unconfined-aquifer test theory to analyze test data.

Despite the widespread availability of type curves for various aquifer-test situations, many others, generally involving two or more deviations from the Theis equation assumptions, remain unsolved. In these cases, as well as in some cases in which available analytical equations have not been evaluated, the hydrologist should consider use of numerical models to generate dimensionless response curves. This approach has already been applied to some extent both in hydrology and in the petroleum industry. However, such use of numerical models is presently inadequate, and needs to become part of the tool kit of many, if not all, aquifer-test analysts.

AQUIFER-TEST DESIGN

Attention to detail in the design and planning of an aquifer test is essential if the test is to be successful. This is particularly true because the response curves for different geohydrologic situations are similar in shape, and hence the shape of the observed time-drawdown curve will not by itself be diagnostic of the conditions prevailing at the well site. For example, the response curves for a well near a stream in a semi-infinite aquifer will be almost identical to those for a well tapping a leaky aquifer bounded by incompressible confining beds or to the early-time drawdown response curves for an unconfined aquifer. Alternatively, many of the response curves for a well tapping a leaky aquifer bounded by compressible beds are nearly identical to the Theis curve. Consequently, for successful aquifer-test analysis, it is absolutely essential that the set of response curves to be used for analysis of a given aquifer test be properly identified by geohydrologic site evaluation, rather than by inference from the test results themselves.

In addition to selecting the appropriate response curve for the test analysis, it is important that the observation wells be advantageously placed and that the test be run long enough that adequate time-drawdown data are obtained at all the observation wells. Pretest prediction of the response of each observation well, based on estimates of the hydraulic properties of the aquifer and semiconfining beds and on the appropriate response curve, will do much to ensure adequate design of the test. Thus, two major elements of successful aquifer-test design are site evaluation and pretest prediction.

Site Evaluation

During the site evaluation, both the physical and geohydrologic situation should be examined in detail. Such mundane items as determining the type of pump, power plant, and discharge-control equipment that are available or that can be installed on the production well, opportunity for disposal of the pumped water, accessibility for measuring discharge and water levels, rapidity of response of the observation wells, and the depths and distances of the observation wells from the production well should be determined. In addition all geologic and hydrologic data, such as drillers logs, sample logs, and geophysical logs should be collected and examined. Surface geologic features and locations of incised lakes or streams should be mapped. These data will aid in identifying the depth, thickness, and geometry of the aquifer to be tested.

During the site evaluation, estimates of all pertinent hydraulic properties of the aquifer and adjacent rocks should be made by any means feasible in order to make the pretest predictions. Estimates of transmissivity and storage coefficient should be made. Also, if leaky confining beds are suspected, leakage coefficients should be estimated. For unconfined aquifers, conductivity to vertical flow is important. In some cases, aquifer transmissivity may be estimated from the specific capacity of the well, based on equations and charts presented by Theis (1963), Brown (1963), Meyer (1963), or Hurr (1966). The effects of well loss on specific capacity is not included in these charts. However, such losses may be accounted for if step drawdown test data are available, based on equations presented by Jacob (1947) or Rorabaugh (1953). If specific capacity of the production well is not known, or if well losses are unknown and suspected to be large, transmissivity may be estimated from sample logs of wells or test holes, based on the equation:

$$T = \sum_{1}^{n} K_m b_m;$$

where n = number of layers comprising the aquifer;
K_m = estimated hydraulic conductivity of mth layer, LT^{-1};
and b_m = thickness of mth layer, L.

The hydraulic conductivity can be estimated from a table of such values versus lithology, such as that used by R. T. Hurr (Lohman, 1972, p. 53). Hurr's chart was developed for a specific aquifer (Arkansas River valley alluvium in Colorado), but similar charts might be prepared for other aquifers.

A value for the storage coefficient of an artesian aquifer may be estimated from the porosity and the barometric efficiency of the well, if known, by the equation (Jacob, 1940, p. 583):

$$S = (\gamma/E_w)nb(\frac{1}{BE})$$

where S = storage coefficient, dimensionless;
γ = specific weight of water, $MT^{-2}L^{-2}$;
E_w = bulk modulus of elasticity of water, $MT^{-2}L^{-1}$;
n = porosity, dimensionless;
b = aquifer thickness, L;
and BE = barometric efficiency, dimensionless.

Alternatively, if no data are available, S may be estimated by the rule-of-thumb equation,

$$S = 3 \times 10^{-6}b;$$

where b = aquifer thickness in meters. Note that the constant, 3×10^{-6}, has the units L^{-1}. For unconfined aquifers, specific yield may be estimated from the nature of the materials drained during the test. Rough estimates of specific yield range from 0.01 for clay to 0.1 for silt and 0.2 for sand and gravel.

The ratio of horizontal to vertical hydraulic conductivity is important in the analysis of tests using partially penetrating production wells and of tests on unconfined aquifers. This ratio is dependent upon the degree of stratification of the aquifer, and can vary from 1:1 or 2:1 to more than 100:1. Data presented by Mansur and Dietrich (1965) and by Weeks (1969) indicate that the ratio might be estimated as being about 5:1 or 10:1 in a relatively homogeneous aquifer exhibiting only slight stratification. However, in strongly stratified aquifers, the ratio would be much higher.

Two important factors in the successful design of an aquifer test are the vertical hydraulic conductivity and the specific storage of the overlying and underlying semiconfining beds. Both these factors show an extreme range. For example, a Cretaceous semiconfining clay bed in the Annapolis, Maryland, area has a vertical hydraulic conductivity of about 5 x 10^{-5}m/day (Mack, 1974), whereas several Pleistocene glacial till semiconfining beds in Ohio and Illinois have a vertical hydraulic conductivity of 0.001-0.02 m/day (Norris, 1962). The specific storage coefficient of semiconfining-bed materials also shows a wide range, depending upon the nature of the materials; their degree of consolidation and cementation; and the preconsolidation load stress, or maximum overburden load stress to which the beds have been subjected subsequent to their deposition. For example, Riley (1969) estimates the specific storage of clay beds in the valley fill deposits at a site in the San Joaquin valley to be about 1 x $10^{-5}m^{-1}$ in the range of preconsolidation load stress, as compared to a value of about 1 x $10^{-3}m^{-1}$ in the range of virgin load stress. (Virgin load stress represents stress greater than that to which the bed had previously been exposed). As another example, Wolff (1970a) found that the specific storage of an unconsolidated bed of fine sand, silt, and clay near Salisbury, Maryland, was about 3 x $10^{-5}m^{-1}$. In general, in areas for which land subsidence and semiconfining-bed compaction is not evident, an investigator might use, for his pretest design estimate, a value of 3 x $10^{-6}m^{-1}$ for the specific storage of a consolidated confining bed, and a value of 3 x $10^{-5}m^{-1}$ for an unconsolidated bed. On the other hand, if compaction has occurred, and it is anticipated that the test will be run under conditions that result in virgin load stress, the subsidence and water-level decline data themselves should be used to estimate specific storage.

The uncertainty involved in using the above examples and suggestions for estimating vertical hydraulic conductivity and specific storage of the semiconfining beds should be fully recognized. The investigator should use all available information on the geology and hydrology of the semiconfining beds to estimate their hydraulic properties.

Pretest Prediction

The site evaluation provides data on available measurement facilities and indicates the proper response equation to be used in the analysis. Success of the test can be further ensured by predicting the drawdown response of each of the observation wells before the test is performed, based on estimates of the aquifer properties made during the site evaluation. Such predictions will aid in pinpointing deficiencies in observation well locations and in determining the necessary duration of the test.

Pretest predictions are particularly important in the design of aquifer tests where leakage from or across the confining beds is anticipated. Such predictions will aid in selecting the proper set of response curves and in circumventing problems of nonuniqueness of response curve shape, as described below. If the confining layer is thin and relatively permeable and incompressible, the response curves of Hantush and Jacob (1955) will apply, whereas those of Hantush (1960) will apply if the confining layer is thick, of low permeability, and highly compressible. Quantitatively, selection of the proper set of response curves depends on one of two inequalities given by Hantush (1960, p. 3716). For example, the Hantush-Jacob (1955) response curves will apply if

$$t > \frac{5b'^2S'_s}{K'}$$

for the semiconfining layer separating the aquifer from the constant-head source bed,
where t = time since start of test, T;
b' = confining layer thickness, L;
S'_s = specific storage of the confining layer, L^{-1};
and K' = vertical hydraulic conductivity of the confining layer, LT^{-1}.

(Strictly speaking, the term $r^2S/4Tt$ in Hantush and Jacob's (1955) formulation should be replaced by the term $(r^2S/4Tt)\cdot(1+S'/3S)$ if $S' > 0.01S$, according to Hantush (1960, p. 3718),
where r = distance from observation well to production well, L;
S = storage coefficient of aquifer, dimensionless;
T = transmissivity of aquifer, L^2/T;
and S' = S'_sb', the storage coefficient of the semiconfining bed, dimensionless.)

As an example, if b' = 4 meters, K' = 0.02 m/day, and S'_s = 2.5 x 10^{-6} m, and the confining layer is overlain or underlain by a source bed, the curves of Hantush and Jacob (1955) would apply after the test had been in progress about 0.01 day, or 15 minutes. On the other hand, if K' = 5 x 10^{-4}m/day, b' = 100 m, and S'_s = 1 x $10^{-4}m^{-1}$, the Hantush (1960) response curves would apply for the first 200 days, based on Hantush's (1960, p. 3716) inequality

$$t < \frac{b'^2S'_s}{10\ K'}$$

and the Hantush and Jacob (1955) curves would not apply for 10,000 days.

Additional aquifer-test design problems arise if the response curves of Hantush (1960) apply, because the curves are nonunique for a significant range of confining bed properties. In fact, there is virtually no difference in the shape of the response curves for values of Hantush's (1960) β ranging from zero (the Theis curve) to about 0.7. The parameter

$$\beta = \frac{r}{4}\left(\frac{K'S'}{Tb'S} + \frac{K''S''}{Tb''S}\right)^{\frac{1}{2}},$$

where r = distance from production well to observation well, L;
K',K'' = vertical hydraulic conductivity of upper and lower semiconfining layers, respectively, (L/T);
S,S',S'' = storage coefficient of the aquifer and

upper and lower semiconfining beds, respectively (dimensionless);

T = transmissivity of the aquifer, L^2/T;

and

b',b'' = thickness of the upper and lower semiconfining beds, respectively (L).

If β falls within this range for a given observation well, it is not possible to determine unique values of T, S, and β using data from that well alone. On the other hand, if data for more than one observation well are available, a composite t/r^2 data plot may be prepared, and matched to the type-curve family. A unique match may then be obtained by invoking the added constraint that r values for the observation wells must fall on curves having proportional β values. For example, if data are available for wells at 100 and 200 meters from the production well, the data for the two wells must match curves having β values of the ratio 1:2. If only one observation well is available, and the pretest prediction indicates that the β value lies between zero and 0.7, consideration should be given to installing an additional observation well at some different distance to obtain separate response curves. Moreover, if knowledge of the confining bed properties is important, the investigator should consider completing a piezometer in the confining bed itself, with the plan that the data be analyzed by the ratio method of Neuman and Witherspoon (1972).

One caveat is in order on use of the Neuman-Witherspoon method. In practice, it has sometimes been found (Wolff, 1970b, for example) that piezometers completed in the semiconfining bed exhibit reverse water-level fluctuations, in that water levels in the semiconfining bed rise for some period of time after the start of pumping from the aquifer. These changes apparently are related to radial and vertical deformation of the aquifer and semiconfining beds resulting from their compressibility (Wolff, 1970b). Such phenomena were not considered in the development of the ratio method, and their effects on the accuracy of the method are not known. Additional work is needed in this area.

The nature of the problems that may be encountered in the design of a test on an aquifer bounded by compressible semiconfining beds is illustrated by actual test data in figure 1. This figure shows a match of multiple observation well data

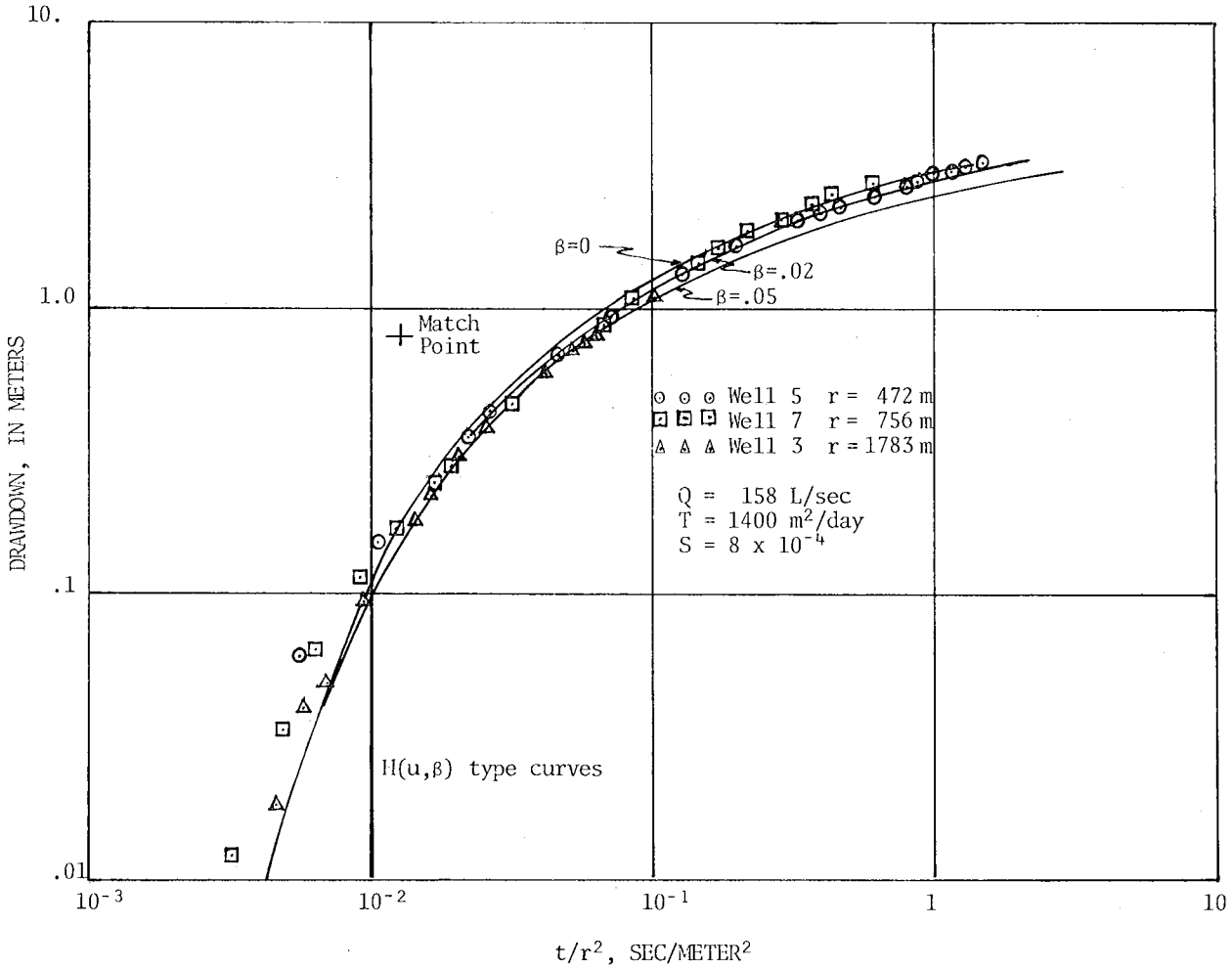

Figure 1.--Drawdown data from three observation wells for an aquifer test made near Houston, Texas matched to family of H(u,β) (Hantush, 1960) type curves.

for a well near Houston, Texas to the Hantush (1960) type curves. The test was made in an area where significant subsidence has been induced by groundwater withdrawal, and thus apparently should fit the Hantush (1960) curves. Differences in the positions of the data for well 3 from those for wells 5 and 7 are in the right direction to indicate the effects of semiconfining bed storage, but the relative positions of the data for wells 5 and 7 are not. Moreover, the data for all three wells fall so nearly on the Theis curve that the deviations could easily be caused by factors other than release from confining bed storage. Nonetheless, selection of the best-matching β curve values for wells 5 and 7, the appropriate r values for the observation wells, and an estimate of specific storage results in a hydraulic conductivity of the confining layer comparable to that used in modeling the Houston aquifer (Jorgenson, 1975). In this case, even at a distance of 1800 meters, the farthest observation well was not located far enough from the production well to produce a significant departure from the Theis curve. However, in the design of a test in a system such as this, it might not be practical to locate an observation well that does unequivocally show the effects of leakage. This is true because the well would have to be at least 4000 meters from the production well, requiring a lengthy test and increasing the hazard that the test results at the distant observation well would be masked by the effects of other production wells in the general area. Consequently, if it was important to obtain knowledge of the hydraulic properties of the semiconfining bed at this site, it would be desirable to complete a piezometer in the semiconfining layer to obtain data for application of the Neuman-Witherspoon ratio method.

The composite data-curve matching process shown in figure 1 is also important during the analysis of the test data. Such a match should always be made when data from more than one observation well are available, and single values of transmissivity, storage coefficient, and other hydraulic properties are to be determined from that match. The ability or lack thereof of the data from observation wells at different distances to fit type curves having proportional distance-based parameters, will do much to confirm or deny the validity of the selected type-curve model. Moreover, the time-drawdown plot for any given observation well is affected by many extraneous factors, such as storage and inertial effects in the observation well, deviations of natural water-level fluctuations from those predicted from the pretest trend, barometric or loading effects on the water levels, and effects of local aquifer heterogeneity. Because most type-curve families include curves exhibiting a wide range of shapes, the chance of fortuitously fitting one of them is high when data for only a single well are matched. Thus the composite data-curve matching process is useful both in confirming the validity of the selected model and in screening the data for extraneous effects.

Pretest prediction is also important in the design of tests on unconfined aquifers. Typical drawdown response to pumping such aquifers is for the water level to drop rapidly initially, to remain nearly constant for a period, and then to follow a time-drawdown response typical of a confined aquifer, particularly if the effects of dewatering on these late-time data are corrected for by use of the equation (Jacob, 1963):

$$s' = s - s^2/2b,$$

where s' = drawdown corrected for the effects of dewatering, L;
s = measured drawdown, L;
and b = saturated thickness of the aquifer at the start of the test.

However, the initial early drawdown response may occur during the first few minutes of the test, before discharge of the production well can be stabilized. Moreover, the rate of this early water-level decline may be governed by storage and inertial effects (Stallman, 1965; Bredehoeft and others, 1966) or by slow response of the observation well due to clogging of the well screen or adjacent aquifer materials in the observation well. Thus, the early-time water levels may not be representative of the actual drawdown in the aquifer itself. In the absence of reliable early-time drawdown data, it is desirable to have data extending into the time range when the response curves for a confined aquifer apply. This is true because of the lack of definition of the curve as obtained during the mid-part of the time range. Thus, it is generally desirable, even with the recent advances in unconfined aquifer test theory, to run the test long enough that the equations apply for artesian conditions.

Because of the desirability of obtaining data during tests on unconfined aquifers to match the artesian-response curves, the planned duration of such tests is important. In particular, the planned length of the test should be evaluated by use of appropriate time criteria. Boulton (1954a) gave one such time criterion:

$$t > 5bSy/K_z \quad \text{for} \quad r/b \left(\frac{K_z}{K_r}\right)^{0.5} < 0.2,$$

where t = time after which confined-aquifer equations apply, T;
b = aquifer thickness, L;
Sy = specific yield, dimensionless;
K_z = vertical hydraulic conductivity, L/T;
r = distance from observation well to production well, L;
and K_r = horizontal hydraulic conductivity, L/T.

This equation is based on the assumptions that the production well fully penetrates the aquifer, that internal storage within the body of the aquifer is negligible, and that drawdown is small compared to aquifer thickness.

Weeks (1969, p. 209-210), however, concluded that data from piezometers open near the water table match the artesian curves at $t > bSy/K_z$ for $r/b(K_z/K_r)^{1/2} < 0.4$ and $t > bSy/K_z(0.5 + 1.25\ r/b\ (K_z/K_r)^{1/2})$ for greater values of $r/b\ (K_z/K_r)^{1/2}$. (Weeks' second equation is incorrectly given in the original paper.) This conclusion was based on the comparison of field data from several tests on unconfined aquifers to the appropriate artesian

response curves. Visual examination of plots constructed from Neuman's (1975) type-curve data basically support the time-criterion equation given by Weeks for observation wells located at small radii from the production well. However, for $r/b\ (K_z/K_r)^{\frac{1}{2}} > 1.5$ or so, Neuman's data suggest that Weeks' equation substantially underpredicts the time requirement after which the artesian-response equations can be used. Hence, the equations should be used with care in evaluating the data for more distant observation wells.

As an example of unconfined aquifer-test design, assume that the site evaluation indicates that the aquifer thickness is 20 meters and that observation wells are available at 50 and 100 meters. Moreover, assume that the preliminary data indicate a transmissivity of 1000 m^2/day, a K_z of 5 m/day, and a specific yield of 0.2. Thus, $bSy/K_z = 0.8$, and $r/b\ (K_z/K_r)^{0.5}$ values for the near and far observation wells are 0.8 and 1.6, respectively. Based on Weeks' time criterion, data from the nearest well should begin to follow the artesian response curves after 1.2 days, and those from the farther well after 2 days. However, the time criterion for the second well probably underestimates the true time limit. Consequently, the test must be run at least 3 days, and preferrably 4 or 5 days, to ensure a late-data fit for both observation wells.

A third example of the utility of pretest prediction might include evaluation of a test on a large diameter well tapping an aquifer having a relatively low transmissivity. Under these conditions, Papadopulos and Cooper (1967) give a time criterion of $t > 250\ r_c^2/T$, after which drawdown in the production well follows the Theis curve,
where r_c = radius of well casing, L;
and T = transmissivity, L^2/T.

However, examination of their data indicates that the inequality may be too conservative, and might better be expressed as $t > 25\ r_c^2/T$. This time criterion represents the minimum time that a test should be run. Until the time indicated by the time criterion is exceeded, production-well drawdown is dominated by well-bore storage effects, and the aquifer properties cannot be determined. As a specific example, assume that a test is to be run on a well of 0.5 meter radius and that the aquifer has a transmissivity of 10 m^2/day. Under these conditions, the data obtained in the production well could not be used until the test had been in progress for 0.625 days, indicating that the test should be run for a minimum of at least one day.

Other examples of pretest prediction in aquifer-test design could be given, but the three described above are adequate to illustrate their desirability and utility.

SUMMARY AND CONCLUSIONS

A great many analytical equations have been derived to describe drawdown response due to pumping from aquifers under a variety of geohydrologic, well construction, and production conditions. It is important that the hydrologist be aware of the scope of available solutions in order to plan and design aquifer tests so that he is able to get full and accurate information on hydraulic properties at the test site. In addition, the hydrologist should consider the use of digital radial flow models to develop response curves for those geohydrologic conditions for which analytical equations are not available or have not been evaluated.

Careful planning and design, based on site investigation and pretest prediction, are essential in performing successful aquifer tests. The importance of identifying the geohydrologic situation during the site investigation cannot be overemphasized, because the theoretical response curves for different geohydrologic conditions tend to be similar in shape. Thus, use of the shape of the data response curve to identify the geohydrologic model applicable to the test site could be very misleading and result in erroneous conclusions. Pretest prediction, based on best estimates of the hydraulic properties of the aquifer and the adjacent confining beds, is also important for successful aquifer-test design. Such predictions can indicate the need for additional observation wells, their location, and the duration necessary for a successful test.

REFERENCES CITED

Abu-Zied, M., and Scott, V. H., 1963, Nonsteady flow for wells with decreasing discharge: Am. Soc. Civil Engrs. Proc., v. 89, no. HY3, p. 119-132.

Abu-Zied, M., Scott, V. H., and Aron, G., 1964, Modified solutions for decreasing discharge wells: Am. Soc. Civil Engrs. Proc., v. 90, no. HY6, p. 145-160.

Aron, G., and Scott, V. H., 1965, Simplified solutions for decreasing flow in wells: Am. Soc. Civil Engrs. Proc., v. 91, no. HY5, p. 1-12.

Bixel, H. C., Larkin, B. K., and Van Poollen, H. K., 1963, Effect of linear discontinuities on pressure build-up and drawdown behavior: Jour. Petro. Tech., v. 15, no. 8, p. 885-895.

Boulton, N. S., 1954a, The drawdown of the water table under non-steady conditions near a pumped well in an unconfined formation: Inst. Civil Engrs. Proc., v. 3, pt. 3, p. 564-579.

_____ 1954b, Unsteady radial flow to a pumped well allowing for delayed yield from storage: Internat. Assoc. Sci. Hydrology, Pub. 37, p. 472-477.

_____ 1963, Analysis of data from non-equilibrium pumping tests allowing for delayed yield from storage: Inst. Civil Engrs. Proc., v. 26, p. 469-482.

_____ 1964, Discussion of "Analysis of data from non-equilibrium pumping tests allowing for

delayed yield from storage," by N. S. Boulton, Inst. Civil Engrs. Proc., v. 26, 1963, p. 469-482: Inst. Civil Engrs. Proc., v. 28, p. 603-610.

_____ 1965, The discharge to a well in an extensive unconfined aquifer with constant pumping level: Jour. Hydrology, v. 3, p. 124-130.

Boulton, N. S., and Streltsova, T. D., 1975, New equations for determining the formation constants of an aquifer from pumping test data: Water Resour. Res., v. 11, no. 1, p. 148-153.

Bredehoeft, J. D., Cooper, H. H., Jr., and Papadopulos, I. S., 1966, Inertial and storage effects in well-aquifer systems--An analog investigation: Water Resour. Res., v. 2, no. 4, p. 697-707.

Brown, R. H., 1963, Estimating the transmissibility of an artesian aquifer from the specific capacity of a well, in Bentall, Ray, compiler, Methods of determining permeability, transmissibility, and drawdown: U.S. Geol. Survey Water-Supply Paper 1536-I, p. 336-338.

Cooley, R. L., 1972, Numerical simulation of flow in an aquifer overlain by a water table aquitard: Water Resour. Res., v. 8, no. 4, p. 1046-1050.

Cooley, R. L., and Case, C. M., 1973, Effect of a water table aquitard on drawdown in an underlying pumped aquifer: Water Resour. Res., v. 9, no. 2, p. 434-477.

Cooper, H. H., Jr., and Jacob, C. E., 1946, A generalized graphical method for evaluating formation constants and summarizing well-field history: Am. Geophys. Union Trans., v. 27, no. 4, p. 526-534.

Cooper, H. H., Jr., Bredehoeft, J. D., and Papadopulos, I. S., 1967, Response of a finite-diameter well to an instantaneous charge of water: Water Resour. Res., v. 3, p. 263-269.

Cooper, H. H., Jr., Bredehoeft, J. D., Papadopulos, I. S., and Bennett, R. R., 1965, The response of well-aquifer systems to seismic waves: Jour. Geophys. Res., v. 70, p. 3915-3926.

Dagan, G., 1967, A method of determining the permeability and effective porosity of unconfined anisotropic aquifers: Water Resour. Res., v. 3, p. 1059-1071.

Ferris, J. G., and Knowles, D. B., 1954, The slug test for estimating transmissibility: U.S. Geol. Survey Ground Water Note 26, 6 p.

Ferris, J. G., Knowles, D. B., Brown, R. H., and Stallman, R. W., 1962, Theory of aquifer tests: U.S. Geol. Survey Water-Supply Paper 1536-E, p. 69-174.

Gambolatti, F., 1976, Transient free surface flow to a well: An analysis of theoretical solutions: Water Resour. Res., v. 12, no. 1, p. 27-29.

Glover, R. E., 1964, Ground-water movement: U.S. Bur. Reclamation Engineering Monograph 31, p. 31-32.

Hantush, M. S., 1959a, Analysis of data from pumping wells near a river: Jour. Geophys. Res., v. 64, no. 11, p. 1921-1932.

_____ 1959b, Nonsteady flow to flowing wells in leaky aquifers: Jour. Geophys. Res., v. 64, no. 8, p. 1043-1052.

_____ 1960, Modification of the theory of leaky aquifers: Jour. Geophys. Res., v. 65, no. 11, p. 3713-3725.

_____ 1961a, Drawdowns around a partially penetrating well: Am. Soc. Civil Engrs. Proc., v. 87, no. HY4, p. 83-98.

_____ 1961b, Tables of the function H (u,β): Socorro, N. Mex., New Mexico Inst. Mining and Technology Prof. Paper 103, 13 p.

_____ 1961c, Tables of the function W (u,β): Socorro, N. Mex., New Mexico Inst. Mining and Technology Prof. Paper 104, 13 p.

_____ 1961d, Aquifer tests on partially penetrating wells: Am. Soc. Civil Engrs. Proc., v. 87, no. HY5, p. 171-195.

_____ 1961e, Tables of the function M (u,β): Socorro, N. Mex., New Mexico Inst. Mining and Technology Prof. Paper 102, 15 p.

_____ 1962a, Flow of ground water in sands of nonuniform thickness--(Part) 3, Flow to wells: Jour. Geophys. Res., v. 67, no. 4, p. 1527-1534.

_____ 1962b, Hydraulics of gravity wells in sloping sands: Am. Soc. Civil Engrs. Proc., v. 88, no. HY4, 15 p.

_____ 1964a, Hydraulics of wells, in Advances in Hydroscience, v. 1: New York, Academic Press, Inc., p. 281-442.

_____ 1964b, Drawdown around wells of variable discharge: Jour. Geophys. Res., v. 69, no. 20, p. 4221-4235.

_____ 1965, Wells near streams with semipervious beds: Jour. Geophys. Res., v. 70, no. 12, p. 2829-2838.

_____ 1966a, Analysis of data from pumping tests in anisotropic aquifers: Jour. Geophys. Res., v. 71, no. 2, p. 421-426.

_____ 1966b, Wells in homogeneous anisotropic aquifers: Water Resour. Res., v. 2, no. 2, p. 273-279.

_____ 1967, Flow to wells in aquifers separated by a semipervious layer: Jour. Geophys. Res., v. 72, no. 6, p. 1709-1720.

Hantush, M. S., and Jacob, C. E., 1955, Non-steady radial flow in an infinite leaky aquifer:

Am. Geophys. Union Trans., v. 36, no. 1, p. 95-100.

Hantush, M. S., and Papadopulos, I. S., 1962, Flow of ground water to collector wells: Am. Soc. Civil Engrs. Proc., v. 88, no. HY5, p. 221-244.

Hantush, M. S., and Thomas, R. G., 1966, A method for analyzing a drawdown test in anisotropic aquifers: Water Resour. Res., v. 2, no. 2, p. 281-285.

Hurr, R. T., 1966, A new approach for estimating transmissivity from specific capacity: Water Resour. Res., v. 2, no. 4, p. 657-664.

Jacob, C. E., 1940, On the flow of water in an elastic artesian aquifer: Am. Geophys. Union Trans., pt. 2, p. 574-586.

_____ 1947, Drawdown test to determine effective radius of artesian wells: Am. Soc. Civil Engrs. Trans., v. 112, p. 1047-1070.

Jacob, C. E., and Lohman, S. W., 1952, Nonsteady flow to a well of constant drawdown in an extensive aquifer: Am. Geophys. Union Trans., v. 33, no. 4, p. 559-569.

Javandel, I., and Witherspoon, P. A., 1969, A method of analyzing transient fluid flow in multilayered aquifers: Water Resour. Res., v. 5, no. 4, p. 856-869.

Jorgenson, D. G., 1975, Analog-model studies of ground-water hydrology in the Houston district, Texas: Texas Water-Development Board Rep. 190, 84 p.

Kazmann, R. C., 1946, Notes on determining the effective distance to a line of recharge: Am. Geophys. Union Trans., v. 27, no. 6, p. 854-859.

Lai, R. Y., Karadi, G. M., and Williams, R. A., 1973, Drawdown at time-dependent flowrate: Water Resour. Bull., v. 9, no. 5, p. 892-900.

Lai, R. Y., and Su, Choh-Wu, 1974, Nonsteady flow to a large well in a leaky aquifer: Jour. Hydrology, v. 22, p. 333-345.

Lennox, D. H., 1966, Analysis and application of step-drawdown test: Am. Soc. Civil Engrs. Proc., v. 92, no. HY6, p. 25-48.

Lohman, S. W., 1972, Ground-water hydraulics: U.S. Geol. Survey Prof. Paper 708, 70 p.

Mack, F. K., 1974, An evaluation of the Magothy aquifer in the Annapolis area, Maryland: Maryland Geol. Survey Report of Invest., no. 22, 75 p.

Mansur, C. T., and Dietrich, R. J., 1965, Pumping test to determine permeability ratio: Am. Soc. Civil Engrs. Proc., v. 91, no. SM4, p. 151-183.

Meyer, R. R., 1963, A chart relating well diameter, specific capacity, and the coefficient of transmissibility and storage, in Bentall, Ray, compiler, Methods of determining permeability, transmissibility, and drawdown: U.S. Geol. Survey Water-Supply Paper 1536-I, p. 338-340.

Moench, A. F., 1971, Ground-water fluctuations in response to arbitrary pumpage: Ground Water, v. 9, no. 2, p. 4-8.

Moench, A. F., and Prickett, T. A., 1972, Radial flow in an infinite aquifer undergoing conversion from artesian to water table conditions: Water Resour. Res., v. 8, no. 2, p. 494-499.

Neuman, S. P., 1972, Theory of flow in unconfined aquifers considering delayed response of the water table: Water Resour. Res., v. 8, no. 4, p. 1031-1045.

_____ 1974, Effect of partial penetration on flow in unconfined aquifers considering delayed gravity response: Water Resour. Res., v. 10, no. 2, p. 303-312.

_____ 1975, Analysis of pumping test data from anisotropic unconfined aquifers considering delayed gravity response: Water Resour. Res., v. 11, no. 2, p. 329-342.

_____ 1976, Reply to comments on "Analysis of pumping test data from anisotropic unconfined aquifers considering delayed gravity response" by S. P. Neuman: Water Resour. Res., v. 12, no. 1, p. 115.

Neuman, S. P., and Witherspoon, P. A., 1969, Theory of flow in a confined two aquifer system: Water Resour. Res., v. 5, no. 4, p. 803-816.

_____ 1972, Field determination of the hydraulic properties of leaky multiple aquifer systems: Water Resour. Res., v. 8, no. 5, p. 1284-1298.

Norris, S. E., 1962, Permeability of glacial till: U.S. Geol. Survey Prof. Paper 450E, p. E150-E151.

Norris, S. E., and Fidler, R. E., 1966, Use of type curves developed from electrical analog studies of unconfined flow to determine the vertical permeability of an aquifer at Piketon, Ohio: Ground Water, v. 4, no. 3, p. 43-48.

Papadopulos, I. S., 1966, Nonsteady flow to multiaquifer wells: Jour. Geophys. Res., v. 11, no. 20, p. 4791-4798.

_____ 1967a, Nonsteady flow to a well in an infinite anisotropic aquifer: Internat. Assoc. Sci. Hydrology, Pub. 73, p. 21-31.

_____ 1967b, Drawdown distribution around a large-diameter well: Proc. Nat. Symp. on Groundwater Hydrology, San Francisco, Calif., p. 157-168.

Papadopulos, I. S., and Cooper, H. H., Jr., 1967, Drawdown in a well of large diameter: Water Resour. Res., v. 3, no. 1, p. 241-244.

Prickett, T. A., 1965, Type-curve solutions to aquifer tests under water table conditions: Ground Water, v. 3, p. 5-14.

Riley, F. S., 1969, Analysis of borehole extensometer data from central California: Internat. Assoc. Sci. Hydrology, Pub. 89, v. 2, p. 423-431.

Rorabaugh, M. I., 1953, Graphical and theoretical analysis of step-drawdown test of artesian wells: Am. Soc. Civil Engrs. Trans., v. 79, Separate 362, 23 p.

_____ 1956, Ground water in northeastern Louisville, Kentucky, with reference to induced infiltration: U.S. Geol. Survey Water-Supply Paper 1360-B, p. 117-131.

Stallman, R. W., 1962, Variable discharge without vertical leakage (Continuously varying discharge), in Theory of Aquifer Tests: U.S. Geol. Survey Water-Supply Paper 1536-E, p. 118-122.

_____ 1963, Type curves for the solution of single-boundary problems, in Bentall, Ray, compiler, Short cuts and special problems in aquifer tests: U.S. Geol. Survey Water-Supply Paper 1545-C, p. 45-47.

_____ 1965, Effects of water table conditions on water level changes near pumping wells: Water Resour. Res., v. 1, no. 1, p. 295-312.

_____ 1971, Aquifer-test design, observation, and data analysis: U.S. Geol. Survey Techniques of Water-Resources Invest., Book 3, Chapter B1, 26 p.

Sternberg, Y. M., 1968, Simplified solutions for variable rate pumping test: Am. Soc. Civil Engrs. Proc., no. HY1, p. 177-180.

Streltsova, T. D., 1972, Unsteady radial flow in an unconfined aquifer: Water Resour. Res., v. 8, no. 4, p. 1059-1066.

_____ 1976a, Comments on "Analysis of pumping test data from anisotropic unconfined aquifers considering delayed gravity response" by Shlomo P. Neuman: Water Resour. Res., v. 12, no. 1, p. 113-114.

_____ 1976b, Hydrodynamics of groundwater flow in a fractured formation: Water Resour. Res., v. 12, no. 3, p. 405-414.

Streltsova, T. D., and Rushton, K. R., 1973, Water table drawdown due to a pumped well in an unconfined aquifer: Water Resour. Res., v. 9, no. 1, p. 236-242.

Theis, C. V., 1935, The relation between the lowering of the piezometric surface and the rate and duration of discharge of a well using ground-water storage: Am. Geophys. Union Trans., v. 14, pt. 2, p. 519-524.

_____ 1963, Estimating the transmissibility of a water-table aquifer from the specific capacity of a well, in Bentall, Ray, compiler, Methods of determining permeability, transmissibility, and drawdown: U.S. Geol. Survey Water-Supply Paper 1536-I, p. 332-336.

Thiem, Gunther, 1906, Hydrologische Methoden (Hydrologic methods): Leipzig, J. M. Gebhardt, 56 p.

van der Kamp, Garth, 1976, Determining aquifer transmissivity by means of well response tests: the underdamped case: Water Resour. Res., v. 12, no. 1, p. 71-77.

Weeks, E. P., 1964, Field methods for determining vertical permeability and aquifer anisotropy: U.S. Geol. Survey Prof. Paper 501-D, p. D193-D198.

_____ 1969, Determining the ratio of horizontal to vertical permeability by aquifer-test analysis: Water Resour. Res., v. 5, no. 1, p. 196-214.

Werner, P. A., 1946, Notes on flow-time effects in the great artesian aquifers of the earth: Am. Geophys. Union Trans., v. 27, no. 5, p. 687-708.

Witherspoon, P. A., and others, 1971, Sea water intrusion: Aquitards in the coastal ground water basin of Oxnard Plain, Ventura County: Calif. Dept. of Water Resour. Bull. 63-4, 569 p.

Wolff, R. G., 1970a, Field and laboratory determination of the hydraulic diffusivity of a confining bed: Water Resour. Res., v. 6, no. 1, p. 194-203.

_____ 1970b, Relationship between horizontal strain near a well and reverse water level fluctuation: Water Resour. Res., v. 6, no. 6, p. 1721-1728.

TECHNOLOGY AND NEEDS FOR DRILLING AND WELL TESTING INSTRUMENTATION

WILLIAM J. McDONALD
MAURER ENGINEERING INC.
HOUSTON, TEXAS

SUMMARY

Detailed information on the physical properties of geothermal reservoirs is required for effective and economic development and operation of these energy resources. Since drilling and reservoir development accounts for approximately half of geothermal energy development costs, it is important that this information be available as quickly and as accurately as possible. While many methods are available to obtain needed information, two of the most important are measurements-while-drilling and well testing. These are complementary in time and in information provided.

Methods of well testing include pressure build-up, draw-down, flow, injection, interference, pulse, and drill-stem tests. All require sensitive, accurate, and reliable measurement of pressure and temperature. Recent developments promise improved data acquisition by surface automation and computer processing, while reducing instrumentation costs by improved pressure sensors. Temperature limitations remain a problem and are one of the great needs in geothermal applications.

Measurements-while-drilling systems are of great interest because they offer an opportunity to obtain data from the reservoir as it is penetrated by the bit and drill in relatively undamaged condition. Also MWD systems offer improved safety while reducing drilling costs. Four telemetry methods for MWD are under development: mud pulses, hard-wire, acoustic and electromagnetic systems. Over forty-five companies are involved in this work with at least fifteen hardware systems under development. Commercial systems should become available within the next one to two years. These instruments must be simple, reliable, and economical. They must offer a broad range of capability from directional measurements to formation and formation fluid properties. With these capabilities, costs for geothermal development can be reduced while increasing the effectiveness of geothermal energy recovery.

INTRODUCTION

Development of a geothermal resource requires detailed information about the reservoir so that reliable analyses may be made on how to drill, develop, produce and operate that reservoir. As illustrated in Figure 1, information on the reservoir may be obtained in several ways, two of which (Production or Well Testing and Measurements-While-Drilling) are addressed here.

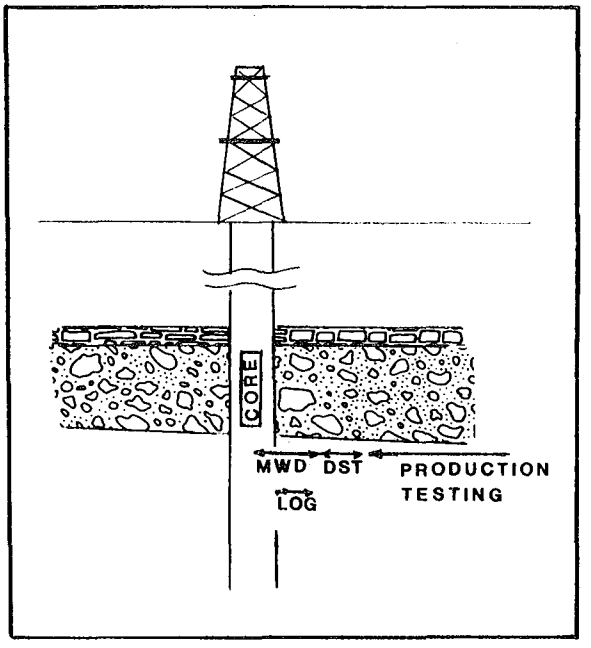

Figure 1. Relative Depth of Investigation for Measurements of Reservoir Properties

Well Testing provides a deep investigation method of determining properties such as reservoir extent, boundaries and faults, permeability and well damage. Measurements-While-Drilling (MWD) investigate only the wellbore and near wellbore reservoir but are important because they are the "first look" at the reservoir. Substantial downhole and surface hardware can be required for carrying out the needed measurements, particularly for well testing. It is the purpose here, however, to concentrate on the present technology and needs for instrumentation for Well Testing and MWD data gathering systems.

WELL TESTING

Well testing originated in the 1920s with application of downhole pressure measuring equipment. Experience soon showed that the measurements of shut-in pressures were highly time dependent. One of the milestone papers in petroleum engineering is the 1937 publication of Muskat[1] setting forth a method for interpreting reservoir pressure data. Many hundreds of papers on well testing and well test analysis have been added to the literature since that time. Reference to many good ones are found in Matthews & Russell[2] and Earlougher.[3]

Production well testing requires extensive equipment. In general, the surface equipment needs (listed in Table 1) are much greater than the subsurface equipment (Table 2).

Table 1

SURFACE WELL TESTING EQUIPMENT

Safety Equipment
- Safety Valve
- Sand Detector

Pressure Measuring
- Dead Weight Gauges
- Barometer

Flow Equipment
- Chokes and Choke Manifolds
- Flow Meters

Treating and Separating Equipment
- Heaters
- Separators
- Traps

Disposal Equipment
- Surge Tanks and Pumps
- Flares and Tanks

Table 2

SUBSURFACE EQUIPMENT

- Lubricator
- Sub-surface Test Tree
- Hydraulic Packers
- Borrom Hole Pressure Bomb

With the exception of high temperature packers, the hardware needed for geothermal well testing is usually available and generally reliable. That is not always true for the most important tool used in well testing, the downhole pressure and temperature equipment.

The most recent developments in well test instrumentation are in the area of more sensitive, more reliable pressure gauges and the addition of automatic data acquisition equipment.

Table 3 from SPE Monograph 5 by Earlougher[3] summarizes available pressure measuring equipment. The Amerada gauges (RPG3 and RPG4) are probably the most common subsurface recording gauges. They have a stated accuracy of 0.2% of full-scale with higher precision if carefully calibrated. The Kuster gauges have a similar accuracy. Leutert and Sperry Sun gauges have an order of magnitude better accuracy (.025 and .05% accuracy respectively) but lack temperature capability, being rated at about 150°C compared with 340°C for the Amerada gauges.

Surface recording gauges are more expensive and require a conductor cable. The Hewlett Packard with .025% accuracy and extreme sensitivity is the most accurate. This is a fairly expensive device and often requires careful scheduling if multiple tests or interference tests are to be run. A fairly new surface recording gauge on the market is the Amerada EPG-512 shown in Figure 2.

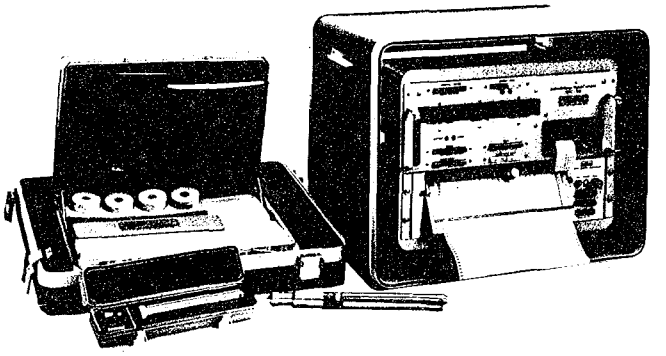

Figure 2. Amerada EPG-512 Pressure/Temperature Gauge and Recorder (Ref. 4)

Accuracy of the EPG-512 is stated at .04%. Major limitations include the present 10,000 psi, 150°C stated specifications. Work is being done to expand these operating ranges.

Temperature probe capabilities have not presented problems in sensitivity or range for most applications. At geothermal temperatures, expectations for performance of this equipment is great and improvements in performance at high temperatures might be necessary.

One important point of test design is to try to make flow measurements near the point of pressure and temperature measurement. Fluid gradients, flowing temperatures, friction loss and phase changes significantly impact data correction and interpretation.

Data Aquisition and Display

In most cases well test data are acquired and posted manually. This leads to delays between readings and possible errors. Recent advancements in well test instrumentation include development of integrated systems to poll, post, display and process the test data.

Table 3

PRESSURE GAUGES FOR WELL TESTING

DOWN-HOLE PRESSURE GAUGES.*

SECTION 1: SELF-CONTAINED WIRELINE GAUGES

Gauge	Maximum Pressure[1] (psi)	Sensitivity, Percent of Full Scale	Accuracy, Percent of Full Scale	OD (in.)	Approximate Length[2] (in.)	Maximum Service Temperature[3] (°F)	Type Pressure Element[4]	Maximum Time Down Hole[5] (hours)	Approximate Chart Size, $p \times t$ (in.)
Amerada RPG-3	25,000	0.05	0.2	1.25	77	650	B	360	2x5
Amerada RPG-4	25,000	0.056	0.2	1	76	650	B	144	1.8x5
Amerada RPG-5	20,000	0.05	0.25	1.5	20	450	B	120	2x5
Kuster KPG	25,000	0.05	0.2	1.25	66	700	B	360	2x5
Kuster K-2	20,000	0.05	0.25	1	41	500	B	120	2x3
Kuster K-3	20,000	0.042	0.25	1.25	43	500	B	120	2.4x4
Kuster K-4	12,000	0.067	0.25	0.75	42	450	B	72	1.5x2.5
Leutert Precision Subsurface Pressure Recorder	6,400	0.005	0.025	1.25	139	300	P	360	9.8x3.1
Leutert Precision Subsurface Pressure Recorder	10,000	0.005	0.025	1.42	139	300	P	360	9.8x3.1
Sperry-Sun Precision Subsurface Gauge	16,000	0.005	0.05	1.5	108	300	B	672[6]	2.3x7.1

SECTION 2: PERMANENTLY INSTALLED, SURFACE-RECORDING GAUGES

Gauge	Maximum Pressure[1] (psi)	Sensitivity, Percent of Full Scale	Accuracy, Percent of Full Scale	OD (in.)	Approximate Length[2] (in.)	Maximum Service Temperature[3] (°F)	Type Pressure Element[4]	Type Signal[7]	Type Conductor[8]
Amerada EPG-512[9]	10,000	0.002	0.02	1.25	13	300	D	F	S
Amerada SPG-3	25,000	0.04	0.2	1.25	49	350	B	R	S
Flopetrol	10,000	0.001	0.06	1.42	29	257	S	F	S
Lynes Pressure Sentry MK-9PES	10,000	0.2	0.2	1.5	33	300	B	B	S
Maihak SG-2	5,700	0.1	1.0	3.54	11.54	176	D	F	S
Maihak SG-5	5,700	0.1	1.0	1.65	8.43	176	D	F	S
Sperry-Sun Permagauge	10,000	0.005	0.05	1.66	120 or 240	no max.	G	G	T
BJ Centrilift-PHD System[10]	3,500		3[11]	N/A[12]	N/A[12]		B	C	P

SECTION 3: RETRIEVABLE SURFACE-RECORDING GAUGES

Gauge	Maximum Pressure[1] (psi)	Sensitivity, Percent of Full Scale	Accuracy, Percent of Full Scale	OD (in.)	Approximate Length[2] (in.)	Maximum Service Temperature[3] (°F)	Type Pressure Element[4]	Type Signal[7]	Type Conductor[8]
Amerada EPG-512[9]	10,000	0.002	0.02	1.25	13	300	D	F	S
Amerada SPG-3	25,000	0.04	0.2	1.25	49	350	B	R	S
Flopetrol[13]	10,000	0.001	0.06	1.42	29	257	S	F	S
Hewlett Packard HP-2811B	12,000	0.00009[14]	0.025[15]	1.44	39	302	Q	F	S
Kuster PSR	5,000	0.04	0.02	1.38	36	212	Q	F	S
Lynes Sentry MK-9PES	10,000	0.2	0.2	1.5	33	300	B	B	S
Maihak SG-3	5,700	0.1	1.0			176	D	F	S
Sperry-Sun Surface Recording	15,000	0.006	0.05	1.5	72	300	B	D	S

*Other gauges are available — no endorsement is implied by inclusion in this table. Data are from information supplied by the manufacturer and other sources believed to be reliable. Although we have been careful in assembling this table, neither the author nor SPE-AIME can guarantee accuracy of the data supplied. The reader should contact the manufacturer for specifics. Blank values could not be obtained by the author.

1. Normally, elements are available in several ranges, with the lowest being about 0 to 500 or 0 to 1,000 psi.
2. Length may vary depending on tool configuration; value is approximate normal length without weight sections.
3. Normally, temperature above which gauge cannot be used, not maximum temperature for normal calibration.
4. B — Bourdon tube.
   D — Diaphragm.
   G — Gas chamber with transducer at surface.
   P — Rotating piston.
   Q — Oscillating quartz crystal.
   S — Strain gauge.
5. Time depends on clock chosen. Clocks normally come in several ranges, starting as low as about 3 hours.
6. Clock is electronic without mechanical linkage to recorder.
7. B — Binary signal.
   C — Current.
   D — Digital.
   F — Frequency.
   G — Gas column to surface.
   R — Resistance.
8. P — Normal power cable for pump, no special conductor.
   S — Single-conductor armored cable, ground return.
   T — 3/22-in.-OD steel tubing.
9. Also measures temperature to an accuracy of 0.1 °F and a sensitivity of 0.01 °F.
10. Part of the BJ Centrilift submersible pump. Gauge is an integral part of the motor assembly.
11. Approximately 3 percent of reading.
12. Imbedded in pump motor assembly.
13. Flopetrol has under development a slick-line retrievable surface-recording gauge. The gauge is set in a side pocket mandrel; a conductor cable goes from the mandrel to the surface on the outside of the tubing.
14. Sensitivity is constant across the entire pressure range: 0.01 psi with nominal 1-second count time, 0.001 psi with nominal 10-second count time.
15. Accuracy, if temperature is known with 1° C: ±0.5 psi to 2,000 psi; ±0.025 percent of *reading* above 2,000 psi.

Companies such as Otis,[5] Gearhart-Owen[6] and Johnston[7] are developing systems. The Gearhart-Owen system, shown schematically in Figure 3 produces printed and strip chart output. The Otis system presently being field tested has an option for magnetic tape output. One advantage to tape output is the capability of direct input to sophisticated software packages that are becoming available for interpretation of well test data.

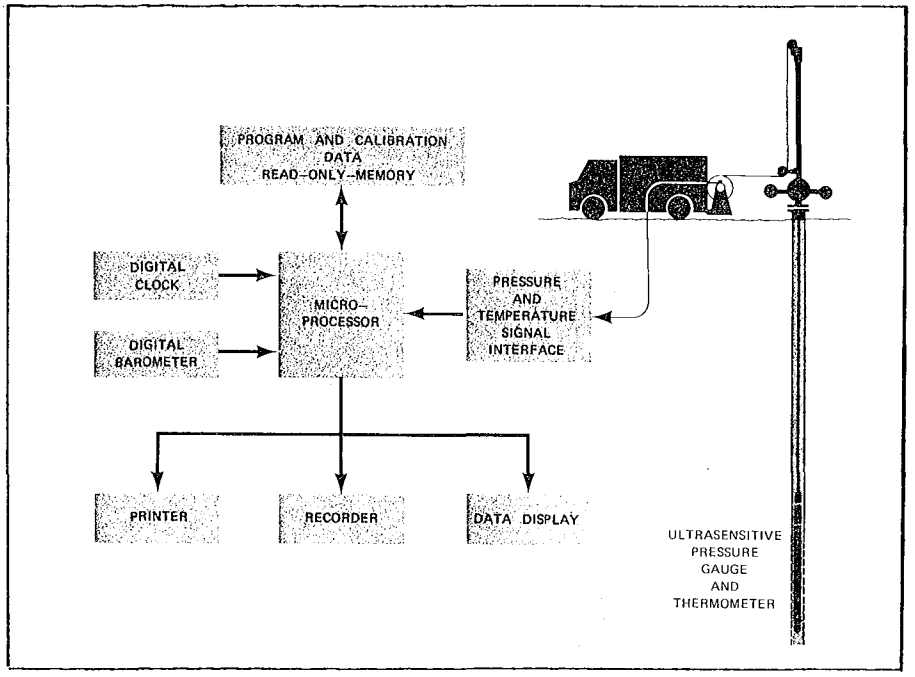

Figure 3. GO Ultrasensitive Pressure Gauge System

MEASUREMENTS-WHILE-DRILLING

Measurements during drilling can help improve well testing interpretation by examining near wellbore properties before damage occurs. This simplifies the early time interpretation and provides a basis for assessing damage and stimulation. MWD provides a source of information for wells which may be lost or not completed, thus expanding the geothermal reservoir data base since a significant portion of wells drilled are not producers.

In addition to formation evaluation, real time drilling measurements significantly impact drilling safety and efficiency.[8] The types of borehole measurements are summarized in Table 4.

Table 4

BOREHOLE MEASUREMENTS

Formation Evaluation
- Porosity
- Permeability
- Fluids

Drilling Safety and Efficiency
- Well Control
- Directional Information
- Drilling Efficiency

Table 5 lists potential formation evaluation measurements and priorities for measurement capability. Due to the detail and complexity of

Table 5

FORMATION EVALUATION MEASUREMENTS

TYPE	PRIORITY
Lithology	
Porosity	H
Permeability	H
Rock Density	M
Mineral Component	M
Natural Radioactivity	H
Bedding Plane Strike & Dip	M
Formation Depth & Thickness	H
Correlation	H
Mechanical Properties	M
Magnetic Properties	M
State of Stress	M
Pore Fluid Properties	
Type	H
Saturation	H
Salinity	H
Density	M
Depth of Invasion	H
Pore Pressure	M
Fluid Flow	M
Dissolved Minerals	L
Well Geometry	
Gauge (Size & Shape)	H
Fractures	
Location	H
Dip	M
Strike	M

H - High
M - Moderate
L - Low

information needs, it is not expected that MWD will replace conventional logging and well testing. Rather, better coring, logging and well testing programs can be planned and executed.

A borehole telemetry, or MWD, system must accomplish two basic functions while drilling: 1) needed data must be acquired at the bottom of the hole and 2) data must be transmitted to the surface. Downhole recording systems such as those developed by Exxon and Texaco in the early 1960s demonstrated that sensors do not present insurmountable problems. Therefore, emphasis has been placed on development of the communication or telemetry system.

BASIC SYSTEMS

Four basic types of systems are being developed as transmission methods. These are: mud pressure pulses, electromagnetic methods, insulated conductor or hardwire systems, and acoustic methods. Each of these types of systems is under investigation by more than one company, illustrating that there is no consensus as to which method offers greatest promise overall. In fact, it is quite possible that a successful system may result from a combination of methods. The potential and limitations of these four methods are outlined in Table 6.

Based on research and development experience to date, and applying subjective judgments as to required data rate, system cost, field acceptability and other factors, the four systems would be ranked in the order in which they are presented in Table 6. It should be noted, however, that this is a new technology and continued evolution of systems is anticipated for many years to improve on cost, reliability, data rate and overall system performance.

The four basic systems are discussed below.

Mud Pressure Pulses

In the mud pressure pulse system, the resistance to the flow of mud through the drill string is modulated or pulsed by means of a valve and control mechanism mounted in a special drill collar sub near the bit. The pressure pulse travels up the mud column at near the velocity of sound in the mud, about 4,000 to 5,000 ft/sec [9]. This system is illustrated in Figure 4. The rate of transmission of measurements is relatively slow due to pulse spreading, modulation rate limitations and other limitations characteristic of mud systems.

Table 6

BASIC MEASUREMENTS-WHILE-DRILLING SYSTEMS

System	Depth Capability	Transmission Time (One Word)	Requires Downhole Power Supply	Two-Way System Possible	Reliability	Development Cost	Estimated Capital Cost/Unit ($1,000)	Evaluation	Comments
Mud Pressure Pulses	>20,000 ft; reduced data rate at deeper depths & higher mud weight & viscosity	6-60 sec.	Yes	?	Good	Moderate	100-300	Excellent	Presently most advanced in development. No problems foreseen in handling majority of applications.
Electro-magnetic Methods	2,000-20,000 ft; is highly system dependent	.1 sec or greater	Yes	Yes	Good	High	100-300	Excellent-Good	Wide variety of systems proposed and being studied. Inherent capabilities and limitations not well defined. Has good potential for combination with hard wire system.
Hard-Wire System	>20,000 ft.	Very High	No	Yes	Fair	High	300-500	Fair	Major breakthroughs will be required to overcome objectionable interference with standard rotary drilling practices.
Acoustic Methods	∿3,000 ft; greater depth capability for production applications	.1 sec. or greater	Yes	Yes	Good	Low	25-150	Fair	Extensive work to date has not overcome signal to noise limitations in the drilling environment.

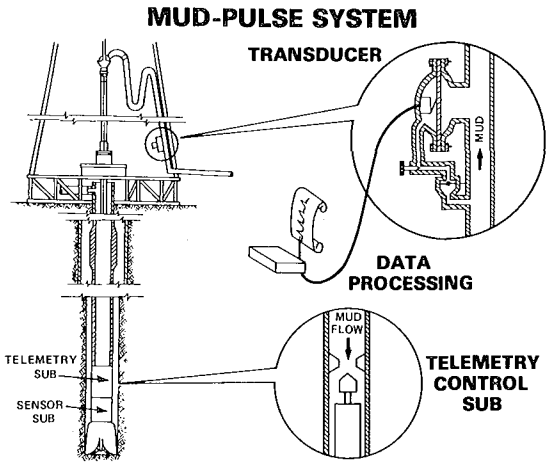

Figure 4. Mud Pressure Pulse System (Ref. 8)

In the mud pulse system, the power source for telemetering data is the pressure field developed by the mud pumps on the surface. Modulation of the mud pressure is accomplished downhole and power for modulation of the mud pressure must be available downhole. While mud pressure can be used to cock springs or cams as in the 'Teledrift' system, most advanced systems use either batteries or a mud turbine generator. The mud pressure pulse system should not be confused with acoustic systems which do not depend on having the pumps running to transmit the signal.

Basic mud pressure pulse systems are under development by Teleco and Gearhart-Owen. The Teleco system, shown schematically in Figure 5, requires a downhole power generator and needs approximately one minute to transmit each measurement. The Gearhart-Owen system is simpler mechanically and uses batteries for downhole power. Both of these systems are being field

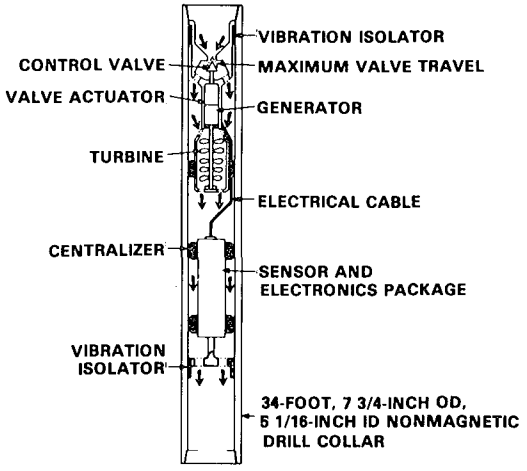

Figure 5. Teleco System (Ref. 10)

proven and commercial availability is expected soon. The cost will be on the order of $1,000 - $2,000 per day.

Schlumberger is actively working on an alternative mud-pressure pulse concept developed by Mobil.[11] A rotary valve is used to generate a continuous sonic pressure wave signal in the range of 10-300 Hz in the mud inside the drill string. Data are transmitted digitally in 10 bit words, plus a parity check, thus allowing 0.1% accuracy. Transmission can be at 3, 1.5 or 0.75 bits/second. Schlumberger is actively field testing the system and is expected to market it soon.

The inherent advantages of the mud-pressure pulse concept are that neither insulated cables nor special drill pipe are required. Power for the system is derived from the mud stream. The mud pulse systems are basically mechanical and should be reliable. The primary disadvantages are that the system has a relatively slow data rate and the signal must be extracted from a fairly noisy environment. The Schlumberger system has a higher data rate, but is mechanically more complicated thus incurring problems in cost and reliability relative to some simpler forms of mud pulsing systems. Sensor systems presently in use require cessation of drilling during acquisition of directional data.

Electromagnetic Methods

Transmission of electronmagnetic (EM) signals both through the earth and over drillpipe has been studied as a telemetry method for downhole measurements while drilling. Numerous companies have worked on EM systems. Many of these investigations were on government contract relating to coal mine safety or relating to military applications. Develco developed an EM system under an AEC contract for data transmission for underground nuclear testing. ENSCO has worked on torroidal coupling of EM signals on drill pipe. Westinghouse and Telcom worked on several systems under government contract including work for the USBM on the "mine rescue" project.[12]

With the EM method, a relatively high data rate may be possible, and there is no need for special drill pipe. There are several possible disadvantages. Only very low frequency EM signals have low enough attenuation for deep transmission through the earth to be feasible. Unfortunately these frequencies are near telluric frequencies. Thus background noise makes detection and information recovery with the EM signals very difficult. Attenuation of the EM signals on drill pipe also limits application of this approach. Repeaters add cost and reliability problems. An EM system would probably require a downhole power generator.

Insulated Conductor Systems

Wireline systems are presently used for logging and other borehole operations. The adaptation of the electrical conductor or hard-wire system to a continuous drilling operation would solve the borehole telemetry problem.

However, problems associated with connecting and maintaining such an electrical line under rotary drilling conditions have not met requirements for an easy to use, economical and reliable system.

Hardwire systems are currently being developed by two major oil companies, Shell and Exxon. In the Shell system the electrical conduit and cable is a part of the drill pipe.[13] Special connectors manufactured into the tool joints are used to provide a rapid and easy means of making electrical connections. Figure 6 is a schematic of the Shell system. A disadvantage of this system is that it requires a special string of expensive pipe, estimated to be three times the cost of ordinary drill pipe; also, it requires high reliability of many electrical connectors.

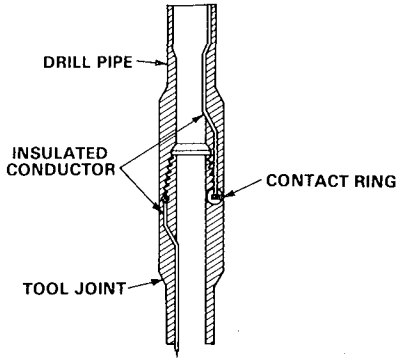

Figure 6. Shell Hardwire System (Ref. 13)

A concept under development by Exxon Production Research Company uses a continuous electrical cable lowered inside the drill string (Figure 7).[14] The excess cable is pulled out as additional joints of drill pipe are added. All of the cable is removed before tripping out of the hole. This system eliminates the need for an electrical connector for each length of drill pipe. However, problems associated with storing the cable in the drill pipe have not yet been overcome.

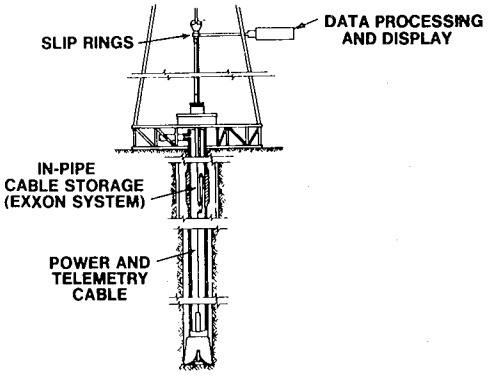

Figure 7. Exxon Cable System

Two special applications of cable systems are the French Petroleum Institute "Flexidrill" (Figure 8)[15] and the GE/Cullen Electrodrill.[16] In the "Flexidrill" system, conductors built into the flexible drilling hose allow monitoring downhole motor performance and other downhole parameters.

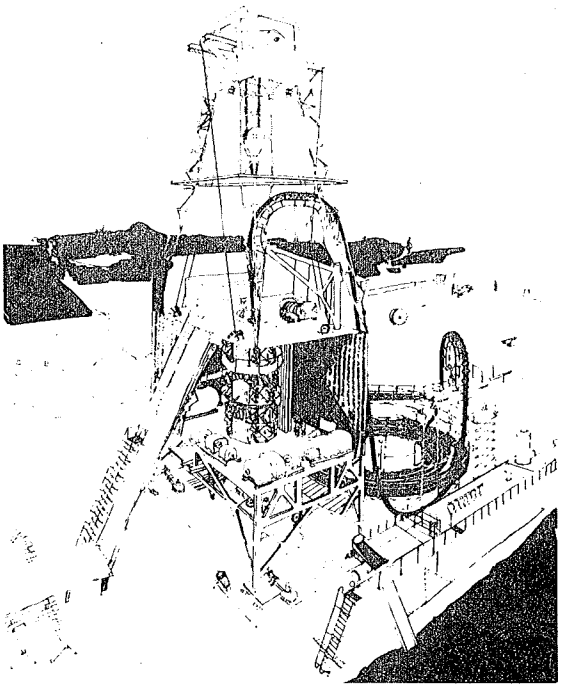

Figure 8. IFP Flexidrill Rig

In the GE system, the cable transmitting electric power to the downhole motor contains one conductor for data transmission. Since a conductor to the surface exists, there is no practical limit on the data link.

Special purpose hardwire systems such as the "EYE" marketed by Scientific Drilling Controls[17] are available. These systems require a continuous single conductor wireline inside the drill string during the drilling operation.

Major advantages to a hardwire system are that data rate can be extremely high, two-way communications are simple and electrical power can be supplied over the conductor system. Disadvantages include costs, reliability (especially of connectors), wear and failure of cable due to mud abrasion and pipe rotation, potential interference with fishing operations, and requirements for special equipment and supplies such as cable handling reels and non-conductive and non-conductive doping compounds.

Acoustic Methods

Another potential method for borehole telemetry is by transmission of acoustic or seismic signals through the drill pipe or the earth. As discussed earlier, the acoustic system should not be confused with mud pressure pulse systems. Acoustic systems do not depend on having the mud pumps running for signal transmission. The very low intensity of the signal which can be generated downhole, along with the acoustic noise generated by the drilling system, makes signal detection difficult. Reflective and refractive

interference resulting from changing diameters and thread make-up at the tool joints compounds the signal attenuation problem.

Acoustic systems have been worked on by Sperry Sun, Sperry Research, Motorola, Del Norte Technology and others. The primary advantages to acoustic systems are simplicity and cost. A disadvantage is that high signal attenuation and acoustic noise generated in drilling limit range. Repeaters incur reliability and cost problems. Downhole power consumption could be a problem.

Other Methods

Other methods and special applications which have been studied include tracers (radioactive and chemical), and drill pipe vibration and torque. While these measurements can be useful, attempts to use these and other surface indications of drilling performance to infer formation pore pressure, bit tooth and bearing condition, etc., have not met with broad acceptance.

CONCLUSIONS

Pressure sensors with excellent accuracy and improved reliability at lower cost have recently become available for well testing. Temperature remains a major limitation to the high sensitivity gauges (both self contained and surface readout). Surface automation promises greater ease accuracy and speed of well testing. Such systems could be directly coupled to home office facilities for processing and interpretation.

Measurements-While-Drilling will have significant impact in reducing drilling and reservoir development costs. Commercial systems are expected to be available soon at an estimated cost of $1,000 - $2,000 per day. Continued improvement to reduce cost, improve reliability and broaden the scope of available sensors is expected.

ACKNOWLEDGEMENT

The support of the Division of Geothermal Energy of US-ERDA in this work is gratefully acknowledged. Special appreciation is expressed to Clifton Carwile of ERDA and M. M. Newsom of Sandia Laboratories for their assistance, and to innumerable friends in industry for their contributions of material and information for this technology review.

REFERENCES

1. Muskat, M., "Use of Data on the Buildup of Bottom Hole Pressures," Trans., AIME (1937) 123, p. 44.

2. Matthews, C. S. and Russell, D. G., "Pressure Buildup and Flow Tests in Wells," SPE Monograph No. 5, Society of Petroleum Engineers of AIME, Dallas (1967).

3. Earlougher, R. C., Jr., "Advances in Well Test Testing," SPE Monograph No. 5, Society of Petroleum Engineers of AIME, Dallas (1977).

4. _____, Amerada EPG-512 and GSC-501 Surface Recording Pressure/Temperature System, Geophysical Research Corporation, Tulsa (1977).

5. Ochler, Carl, "Well Testing Data Gathering and Display System," Otis Engineering Company, Dallas (1967).

6. _____, "Ultrasensitive Pressure Gauge System," Gearhart-Owen Industries, Ft. Worth (1977).

7. Erdle, J. C., et al, "Early Fluid Entry Determination; Key to Safe, Optimum Drill Stem Testing," SPE Preprint 6884, presented at the 52nd Annual SPE Meeting, Denver, Col., October 9-12, 1977.

8. McDonald, W. J., "Borehole Measurements While Drilling - Systems and Activities," ERDA - Division of GEothermal Energy Report IDO/0091-1, June, 1977.

9. Arps, J. J., "Continuous Logging While Drilling: A Practical Reality," Society of Petroleum Engineers, Preprint No. SPE 710, September, 1963.

10. Anon., "New Tool Accelerates Directional Surveying," World Oil, Vol. 181, No. 5, October, 1975, pp. 91-95.

11. Patton, B. J., et al, "Development and Successful Testing of a Continuous Wave Logging-While-Drilling Telemetry System," paper SPE 6157, presented at the Annual SPE Meeting, New Orleans, October 3-6, 1976.

12. Anon., "Trapped Miner Location and Communication System Development Program," prepared for Bureau of Mines, PB-235 605, May, 1973.

13. Dennison, E. B., "Making Downhole Measurements Through Modified Drill Pipe," World Oil, Vol. 183, No. 5, October 1975, pp. 86ff.

14. Heilhecker, Joe K., "Method For Mounting An Electrical Conductor in a Drill String," USP 3,825,079.

15. Thiery, J., "Report on the Flexorig 3000-1 Drilling Operation in Leemens From October 1974 Till May 1975," Floraflex Technical Report No. 33-R, June 1975, pp. 3 and 12.

16. Cullen, Roy H., et al, "Methods And Apparatus For Mounting Electrical Cable in Flexible Drilling Hose," USP 3,285,629.

17. Russell, M. K., "The Design and Development of a Surface Reading Orienting and Survey Instrument," API Production Division, Pacific Coast District Meeting, Paper No. 801-46R, Los Angeles, California, May 12-14, 1970.

Session Introduction

Instrumentation

G. B. Miller
Occidental Research Corporation
La Verne, California

Technological advances in downhole instrumentation have been phenomenal in the past ten years. It is interesting to note, however, that the advances are not couched primarily in techniques to evaluate new or previously unmeasured parameters but, rather, in dramatic refinement of evaluation of the common ones such as pressure, temperature, flow, porosity, permeability, and so on.

Much progress has been made in the resolution, accuracy and, most importantly, long-term reliability of such instrumentation. For example, downhole fluid pressure can be measured with resolution as great as a part per million at 20,000 psi. It seems that in the near future, instrumentation will be capable of operating reliably in thermal environments as high as $300^{o}C$.

The theory of fluid flow in porous media is well developed. Although advanced instrumentation will contribute to the refinement of theory, its principal value lies in the permission of long awaited application of theory to solve real world problems. It turns out, in general, that the dynamic phenomena of real interest in underground fluid reservoirs are manifest in only small, slow perturbations of their intensive properties. Therefore, the advent of highly stable and resolute instrumentation is surely to be welcomed in our fields of endeavor.

OIL AND GAS INSTRUMENTATION

W. E. Kenyon
Schlumberger-Doll Research Center
Ridgefield, Connecticut

Summary

"Well testing" is usually considered to mean the flow testing of a well to determine its producibility. This paper reviews some wireline measurements which are applied in the somewhat larger context of predicting and managing the performance of oil and gas reservoirs: nuclear spectroscopy, electromagnetic propagation, production logging, and the wireline formation tester. The emphasis is on underlying principles.

Nuclear Spectroscopy

Neutrons in traversing a formation interact with the nuclei in the formation. These interactions can be detected and related directly to certain properties of the formation which are of interest to the oil industry. For example, the spatial distribution of slowed-down neutrons is used to determine porosity in standard neutron porosity logging[1]. The penetrating power of neutrons is such that they can be used to measure formation properties behind casing as well as in open hole.

The gamma rays which are emitted as a result of neutron-nucleus interactions have energies which are characteristic of the particular nuclear species involved. An analysis of the energy spectrum of these gamma rays should therefore permit a quantitative determination of the elements present in a formation. The possibility of doing this in the borehole has been under investigation for more than 20 years.

There are several types of nuclear reactions which are useful; all use similar instrumentation to detect and analyze the gamma-ray spectrum. The components of this instrumentation are illustrated in Figure 1.

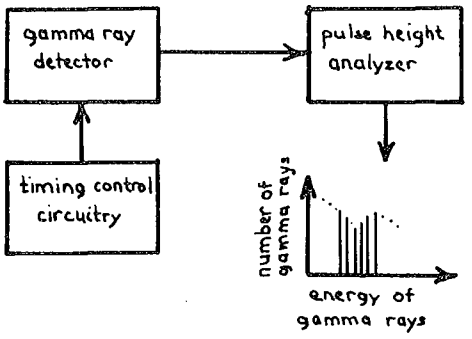

Figure 1. Elements of a Spectrometer

The detector, when struck by a gamma-ray resulting from a neutron-nucleus interaction in the formation, produces an electrical impulse whose amplitude is related to the energy of the gamma-ray. A pulse-height analyzer counts the number of pulses which occur in each of a number of amplitude ranges. In the case where the neutron source is pulsed, timing control circuitry gates the detector on and off at appropriate times.

To simplify the discussion of the different types of nuclear interactions, consider what happens when a short burst of neutrons is emitted by a downhole source. Such sources, using tubes operating at high voltages to produce microsecond-range bursts of neutrons, have existed for about 20 years.[2] The neutrons emitted have an energy of 14 meV.

Inelastic Spectroscopy (Carbon/Oxygen)

The 14 meV neutrons have collisions both inelastic and elastic with the nuclei in the formation, losing energy and slowing down. In the case of an inelastic collision, the target nucleus is raised to an excited state; that is, its internal energy is increased. De-excitation occurs by the emission of characteristic gamma rays.

The inelastic reactions of most interest for logging purposes are with carbon and oxygen. The excited carbon nucleus emits a 4.43 meV gamma ray, and the oxygen nucleus one at 6.1 meV. These reactions are likely to occur only when the energy of the incident neutron is above 7-8 meV. Ideally, the neutron pulse should only last a few microseconds to avoid generating interfering gamma rays from reactions which occur when the neutrons have reached lower energies. Correspondingly, the detector is gated "on" for only a short period.

The significance of measuring carbon and oxygen is that it offers a means for determining oil/water saturations behind casing. Furthermore, this determination is independent of chlorine content of the water, an advantage over some other types of measurements. Inelastic spectroscopy is therefore of great interest to monitor reservoir production. Unfortunately, there are a number of technical difficulties. The main one is that the measured carbon/oxygen ratio is strongly influenced by lithology changes (e.g., from sandstone to limestone) and by the liquid in the borehole. Some users have gone to the trouble of choosing drill and casing sizes especially to minimize the borehole effect. Despite the difficulties, interest in inelastic spectroscopy is strong, and there are some experimental tools in the field.[3-7]

Capture-Gamma-Ray Spectroscopy:

When the energy of the neutron has dropped below about 1 meV, inelastic collisions no longer occur. The neutron continues to slow down due to elastic collisions, in which hydrogen nuclei play the dominant role. Once the neutrons have been slowed to thermal energy (i.e. in equilibrium with their surroundings) they will diffuse until they are finally captured by the nuclei in the formations.

The decay of the thermal neutron population proceeds exponentially, at a rate determined by the propensity ("cross section") of the formation nuclei to capture them. Of the common formation elements, the chlorine nucleus has by far the largest capture cross section. Thus, the decay rate of the thermal neutron population is essentially a measure of the chlorine content of the formation. This is Thermal Decay Time logging.[1] It has been used widely and successfully for some years to determine water saturation behind casing.

As a thermal neutron is captured, it excites the capturing nucleus, which releases the excess energy by emitting gamma rays. These are referred to as "thermal capture" gamma rays. Elements most easily detected by capture spectroscopy are those which have large capture cross sections, and which subsequently emit gamma rays of fairly high energy. Elements with these properties which are of interest in the oil/gas world are chlorine, calcium, silicon, hydrogen, oxygen and iron. A capture spectroscopy tool thus offers the possibility of determining chlorine content, porosity, and lithology behind casing, by properly combining the measured proportions of these elements.

Both capture spectroscopy and decay-time logging have the property that borehole effects can be reduced by careful design. Capture spectroscopy, however, is not as seriously disturbed by the presence of strong absorbers other than chlorine (for example, boron, which sometimes occurs in formation waters), which can seriously affect decay-time logs in lower salinity ranges. But, the chlorine content of the water must be known or inferred in order to determine water saturations by either method.

Over the last 15 years, several capture spectroscopy tools have been built.[8, 9]

Activation Spectroscopy:

As a result of interactions, some of the nuclei will become radioactive; that is, some of the reactions will produce unstable isotopes, which subsequently decay with a characteristic half-life, by emitting both gamma rays and other products. We speak of these nuclei as having been "activated". An element may then be identified by either the characteristic energy of the gamma rays emitted, or by the time required for the activated nuclei to decay. The gamma rays can be detected by a logging tool if the half-life is short enough but not too short: seconds or minutes for continuous logging, longer for stationary measurements. Among the elements which can be detected by this technique are oxygen and silicon. Oxygen is of particular interest because it is much more abundant in water than in oil. Some experimental activation tools have been built.[10-13]

Applications:

One of the main applications of the types of spectroscopy discussed above is in monitoring fluid types behind casing as a reservoir is produced.

Different techniques will be applicable under different conditions. Natural gamma-ray spectroscopy and thermal decay-time logging can distinguish between water and oil only when there is a significant contrast in chlorine content. Inelastic spectroscopy also distinguishes between oil and water, but does not depend on chlorine content. However, in its present form, it is more sensitive to hole and lithology effects. For distinguishing between gas and liquid, a standard neutron-porosity tool is best.

Reservoir monitoring is mainly concerned with the movement of an interface between two phases in the reservoir, say oil and water. If "before" and "after" measurements are available, then the logs can be interpreted successfully without knowing some of the parameters which are otherwise required; for example, shaliness effects.

One simple use of this technique is to update estimates of the hydrocarbons in the reservoir according to the change in interface level since last logging and the amount of hydrocarbons produced in the same period.

In a water-drive reservoir, coning (see Figure 2) is a potentially serious problem which can be detected by these logging techniques.

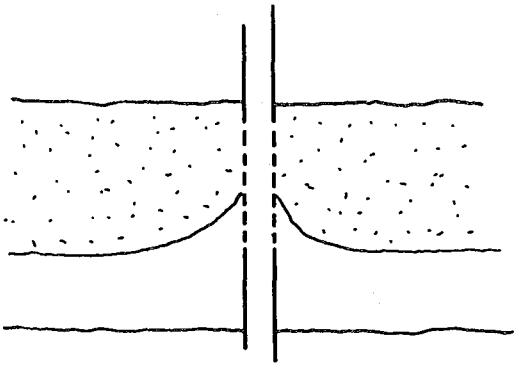

Figure 2. Coning at an Oil-Water Interface

If the water produced due to coning is expensive or difficult to dispose of, remedial action may be required.

The possibility of breakthrough (Figure 3) is an important concern, particularly in water-flooded reservoirs since it may result in the bypassing of oil.

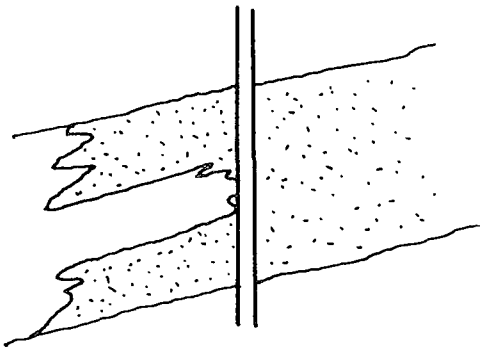

Figure 3. Breakthrough

It may be even more important in tertiary recovery, where the injected fluids are often quite expensive.

High-resolution Spectroscopy:

In most existing spectroscopy logging tools, the detector uses a sodium-iodide scintillation crystal. In contrast, solid-state detectors such as high-purity germanium produce a dramatically cleaner spectrum, as illustrated in Figure 4.

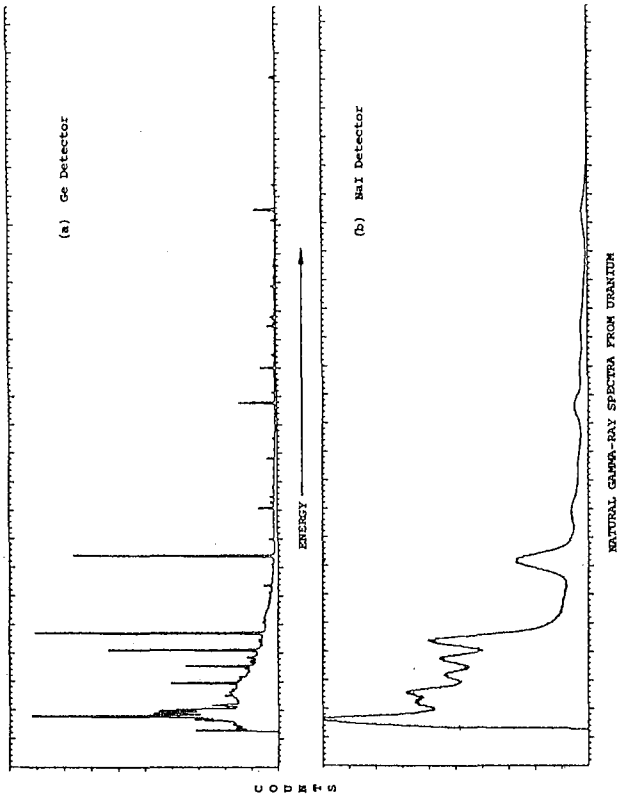

Figure 4.
Sodium Iodide and Solid State Detector Spectra

With a high-resolution detector such as this, many more elements can be clearly distinguished than is possible with a sodium iodide detector.

The high-resolution solid-state detector has drawbacks. It must be operated at temperatures below about minus one hundred degrees Celsius. This is difficult to achieve in a tool which needs to operate in ambient temperatures of at least 175° C. Furthermore, its detection efficiency at reasonably high energies (e.g. 1.5 meV) is much less than that of sodium iodide, thus lowering count rates. Moreover, it is very expensive. There are, however, some high-resolution tools in the field; for example, the United States Geological Survey has one.[14]

High-resolution spectroscopy is of particular interest for detecting tracers, for example for flood-front profiling in secondary or tertiary recovery. In these cases, logging for chlorine or carbon/oxygen may not distinguish the flood fluid from the fluid existing before flooding. Tracers can then be added to the injected fluid, chosen so that they can be easily detected at the producing wells. The ability of the high-resolution spectrometer to see small concentrations of elements should permit economical use of tracers even in large projects.

Electromagnetic Propagation (Dielectric) Logging[15]

Electrical resistivity measurements are the classical way of determining water saturation in open hole; Archie's equation (1) gives*

$$S_w = \sqrt{\frac{a \cdot R_w}{\phi^m R_t}}$$

But, this requires a knowledge of water resistivity, which varies over several orders of magnitude depending on its salinity. In cases where salinity is unknown or variable, this causes a corresponding uncertainty in the inferred water saturation. An additional uncertainty may exist when water resistivity is very high and other conduction mechanisms become comparatively important.

Consider now the relative dielectric constant (ε) of water. It contrasts strongly with that of oil or rocks, but varies by less than a factor of two with varying salinity (Table 1).

*Symbols are defined at the end of the paper.

Material	Relative Dielectric Permittivity (ε)	Loss-Free Propagation Time (t_{po}) nanoseconds/meter
Gas or air	1.0	3.3
Oil	2.2	4.9
Water	56-80	25-30
Quartz	4.7	7.2
Limestone	7.5	9.1
Dolomite	6.9	8.7
Anhydrite	6.5	8.4

Table I. Relative Dielectric Constants and Propagation Times of Some Representative Materials

Thus, measurements of the relative dielectric constant of formations should permit determinations of water saturation which are much less sensitive to variations in salinity.

It turns out that a convenient way to determine dielectric constants in a borehole is to measure the velocity of propagation of electromagnetic waves through the formations. For simplicity, consider a plane electromagnetic wave. Its velocity is $1/\sqrt{\varepsilon\mu}$. Since μ is almost constant for most sedimentary rocks, propagation over a fixed distance is proportional to $\sqrt{\varepsilon}$. Table I gives propagation times for representative materials.

Such a tool has been built and is being used successfully in the field. (See Figure 5) It works in the following way. An upper transmitter T_1 radiates an electromagnetic wave which propagates in the formation. The phase difference and amplitude ratio of the wave are measured at the two receivers R_1 and R_2. These measurements are combined in a borehole-compensating mode with those from the lower transmitter T_2 to provide a correction for tool tilt or washouts. Variables recorded are the propagation time $t_{p\ell}$, in nanoseconds per meter, and attenuation A_ℓ in decibels per meter. Receiver spacing is 4 cm., producing excellent vertical resolution.

Where conductivities are high, the wave is attenuated strongly as it propagates and cannot be consistently detected at the receivers. However, the tool operates successfully at conductivities up to about 1 S/m.

The tool operates at a frequency of 1.1 giga-Hertz. At this frequency, the main contributions to the dielectric constant are electronic and dipolar polarization; more complicated effects such as interfacial polarization (seen at lower frequencies) are not present. At this frequency, depth of investigation is very small.

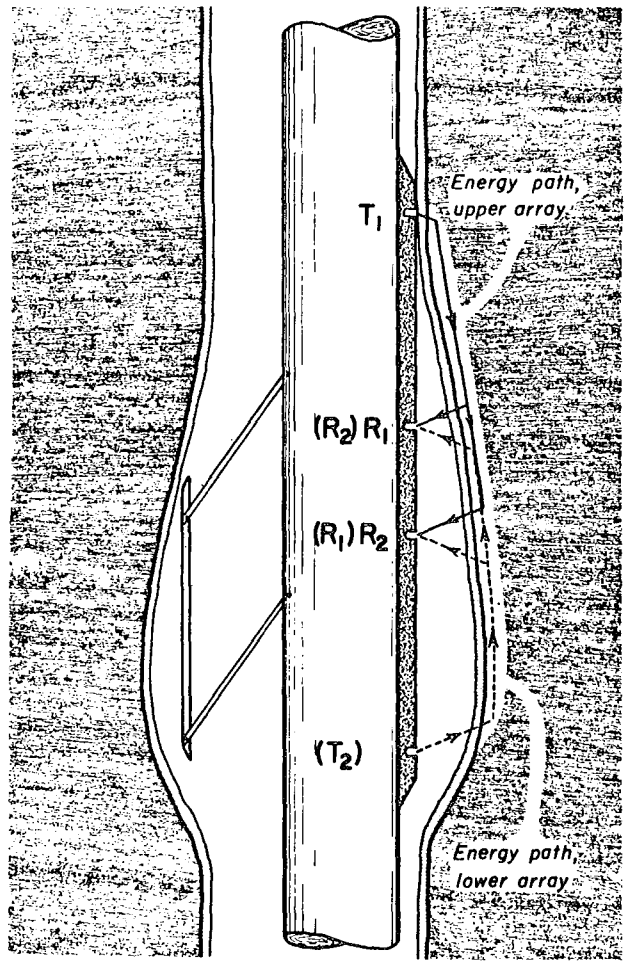

Figure 5. Schematic of Operation of Electromagnetic Propagation Tool

For interpretation, it has been determined that an analog to the Wyllie time-average formula for sonic logging applies:

$$t_{p\ell} = \phi_w t_{pw} + (1 - \phi_w) t_{pma}$$

The electromagnetic propagation tool has been used quite successfully in areas where water salinity is low or unknown. It has been particularly successful in detecting heavy (high viscosity) hydrocarbons in the presence of fresh water.

A special area of application for this tool is in the evaluation of established reservoirs as candidates for tertiary-recovery projects. In this case, the objective is to determine the residual oil content of the reservoir after waterflooding is completed. Newly drilled evaluation wells permit the use of open-hole tools, but frequently the water salinity is unknown, because the flood-water salinity was unknown or varied during the secondary recovery phase. In

this case, the electromagnetic propagation tool can be used to determine water saturation without knowledge of the water salinity. Because the reservoir is already close to residual oil saturation, not much additional flushing occurs during drilling, so the tool measures close to the true formation saturation.

Production Logging

Production logging has been defined as the measurement of "how much of what flows where". Another definition is the measurement versus depth of what is inside the casing-- for example, its movement, temperature, density, etc. Table 2 lists some of the measurements that are made in production logging.

Sensor	Range	Accuracy	Resolution
Fullbore Flowmeter	50 B/D min	±2%	0.5 rps
Continuous Flowmeter	400 B/D min	±2%	0.5 rps
Gradiomanometer	0 to 1.6 gm/cc	zero shift = .03 gm/cc sens. shift = 3%	0.005 gm/cc
High Resolution Thermometer	0 to 350°F	±3%	0.04°F
Manometer	0 to 5,000 psi 0 to 10,000 psi 0 to 15,000 psi	±2% of full scale	0.3% of full scale
Caliper	2" to 18"	±.2"	0.1"

Table 2. Some Production Logging Measurements

Production logging has demonstrated its ability to give very valuable information. For example, the cost of diagnosing and plugging a water-productive interval which has killed a gas well may be returned in a few days of production. But, in fact, production logging is, so far, a very small market compared to formation-evaluation logging. It therefore has not received the same degree of attention to the development of measuring devices and interpretation.

Production logging has a variety of uses, but one which should be emphasized here is the determination of type and amount of fluid produced versus depth. One of the greatest obstacles to such determination is the complex nature of multiphase flow. Combined fluids may flow in a variety of configurations: bubble, plug, froth slug, mist.

A recent development by Schlumberger is aimed at determining the flow rates of individual phases in multiphase flow. The mass flow rate of each phase is [16]

$$Q_i = y_i v_i A$$

The holdup (y_i) can usually be determined fairly well from gradiomanometer or other measurements. However, the individual phase velocities are very difficult to measure. Now in use is a dual tracer ejector, which will allow selective ejection of either of two different radioactive tracer fluids. The two tracers are chosen so that each is miscible with only one of the phases present in the casing; for example, an oil-miscible and a water-miscible fluid are often paired. The tool has three gamma-ray detectors, two above and one below the ejectors, which are used to determine the speed with which the ejected tracer shot moves. Ideally, this should permit measurements of the velocity of each of the two phases. In practice, it can measure the velocity of the continuous phase quite successfully using the corresponding tracer; the gradiometer reading can be used to infer which is the continuous phase of ejection level so that the correct tracer is chosen. Velocity of the other phase can then be determined by mass balance, using the spinner velocity.

Another recent improvement is a tool which permits the simultaneous measurement of all of the variables listed in Table 2 (the dual-tracer ejector is also included in this tool). Previously, these measurements could only be made sequentially. The major impact of simultaneous measurements should lie in the elimination of confusion caused by changes in flow characteristics between runs.

Repeat Formation Tester

The Repeat Formation Tester[17, 18] is a wireline device which can measure formation pressures, make small-volume drawdown tests, and recover formation fluid samples. A schematic drawing of the tool is shown in Figure 6. This tool is intended for use in uncased boreholes.

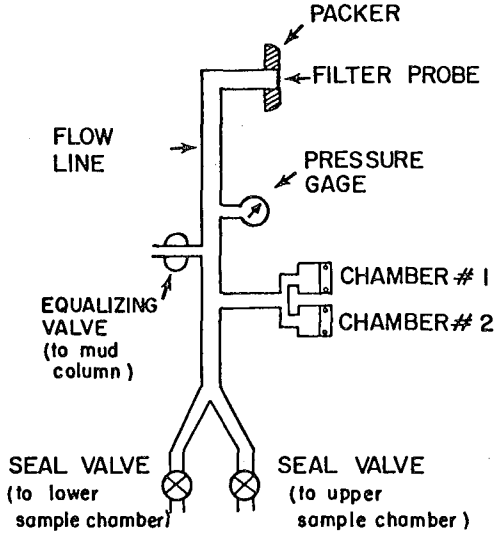

Figure 6. Schematic of Repeat Formation Tool (First published in Paper SPE 6822. Used by permission of SPE of AIME)

In operation, the tool is positioned opposite the formation of interest. A hydraulic system deploys a back-up shoe and forces a small probe into the borehole wall. An automatic test sequence then proceeds; the equalizing valve closes; the piston within the probe is withdrawn, admitting formation fluid; a piston allows the flow of 10cc of fluid into Chamber #1; this is followed immediately by the withdrawal of another 10cc at a higher flow rate into Chamber #2. Total time to fill the two chambers is about 20 seconds. Ratio of the two flowrates is about 2.5:1. During the test sequence, pressure measured by the gauge is recorded at the surface. A sketch of the pressure waveforms is shown in Figure 7, and a summary of tool specifications is given in Table 3.

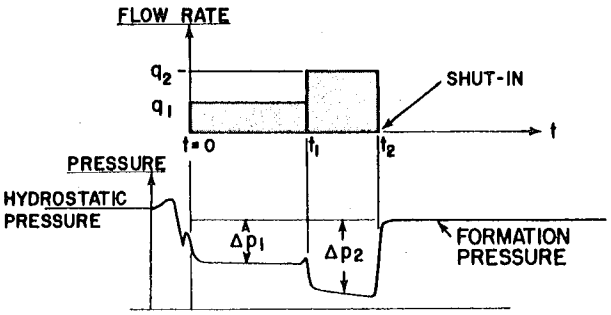

Figure 7. Sketch of Pressure Waveforms (First published in Paper SPE 6822. Used by permission of SPE of AIME)

Repeat Formation Tester Specifications.

Pressure Rating	20,000 psi
Temperature Rating	350° F
Minimum Hole Size	6 inches
Maximum Hole Size	14 3/4 in.
Basic Make-up Length (excluding options)	33 feet
Formation-Pressure Readings per Trip in Hole	Any Number
Sample Chamber Sizes	1, 2 3/4, 6 & 12 gal.

Pressure Measurement Specifications:

	Accuracy*	Resolution	Repeatability*
No Temperature Correction	.98%	1.0 psi	.05 %
With Temperature Correction	.29%	1.0 psi	.05 %
Special "At Temperature" Calibration	.18%	1.0 psi	.05 %

*Based on % Full-scale, 10,000 psi Gage

Table 3. Repeat Formation Tester Specifications

After the test sequence, at the operator's choice, one or both of the sample chambers may be filled, or the tool may be disengaged and set at another depth. When the tool is disengaged, the pistons and valve reset to their original position. This empties the test chamber and closes the probe opening, at the same time cleaning the probe of any plugging material. Thus, an unlimited number of intervals can be pressure tested on one trip in the well. This constitutes a major advantage over previous wireline formation testers.

The tool has a number of applications. Smolen and Litsey[18] describe an application in which 643 pressure measurements were made in 25 infill wells in a waterflooded reservoir. Pressure profiles plotted from the measurements defined portions of the reservoir which communicated poorly with the rest of the reservoir and needed additional water flooding.

Another important application is in determining permeabilities by analysis of the drawdown curves. Although all three portions of the flow test can be analyzed, we mention here only the simple relationship.[18]

$$k = \frac{CFq\mu}{\Delta p}$$

Here, F is a shape factor which ranges between ½ for spherical flow, and 1 for hemispherical flow, corresponding to very small and very large boreholes respectively. Numerical calculations have established a value of 0.75 for 8-inch borehole ("quasi-spherical" flow).

Summary

This paper has surveyed four categories of wireline measurements which have shown themselves useful in predicting and managing the production of oil and gas wells.

Nuclear spectroscopy is not yet an established logging technique. It is potentially useful for monitoring fluid types behind casing. The development of high-resolution spectroscopy tools may permit improved tracer techniques particularly in flood-front profiling.

Electromagnetic propagation logging is an open-hole logging technique that is useful where water salinities are unknown, variable, and/or very low. One of its potential applications is in the evaluation of oil fields for tertiary recovery. Introduced recently, it appears very promising.

Production logging is the measurement of "what flows where" in the casing. Although a long-established technique, it is not as widely used as formation evaluation logging. Current developments are aimed at measuring phase velocities and at making all important measurements simultaneously.

The Repeat Formation Tester is an improved fluid and pressure-sampling tool introduced a few years ago. It represents a significant advance over previous wireline formation testers, and is becoming widely used. Its applications include not only the self-evident determinations

of formation pressures and fluid types, but also the evaluation of reservoir permeability by analysis of pressure buildup data.

Acknowledgements

The author is grateful for help received from a number of people, among whom are H. Sherman, A. Becker, R. Hertzog, G. S. Huchital, J. F. Perry, E. E. Finklea and D. H. Rust.

Symbols Used

a	empirical constant in formation-factor porosity relationship: $F = a/\phi^m$
A	area of pipe
C	constant in permeability equation
F	shape factor in permeability equation; formation factor: $F = R_w/R_o$
k	permeability
m	see a
Δp	pressure drop
q_i	mass flow rate of phase i
R_o	resistivity of formation saturated with water of resistivity R_w
R_t	formation resistivity
R_w	resistivity of water
$t_{p\ell}$	electromagnetic propagation time measured by tool
t_{pma}	electromagnetic propagation time in matrix
t_{pw}	electromagnetic propagation time in water
v_i	velocity of phase i
y_i	holdup of phase i; i.e., the fractional area occupied by phase i within the pipe
ϵ	relative permeability or dielectric constant
μ	magnetic susceptibility; fluid viscosity
ϕ	porosity
ϕ_w	water-filled porosity

References

(1) Schlumberger Log Interpretation. Volume I - Principles. Schlumberger Limited, New York, 1972.

(2) Frentrop, A. H. and Sherman, H.: "Schlumberger Tube: For Oil-Well Logging", Nucleonics, No. 18, 1960, pp. 72-74.

(3) Schultz, W. E. and Smith, H. D.: "Field Experience in Determining Oil Saturation From Continuous C/O and Ca/Si Logs Independent of Salinity and Shaliness", Trans. SPWLA 15th Annual Logging Symposium, June 2-5, 1974. Paper K.

(4) Lawson, B. L. and Cook, G. F.: "A Theoretical and Laboratory Evaluation of Carbon Logging: Part II - Theoretical Evaluation of Oxygen Interference", Trans. SPWLA 11th Annual Logging Symposium, May 3-6, 1970, Paper B.

(5) Lock, G. A. and Hoyer, W. A.: "Carbon Oxygen (C/O) Log: Use and Interpretation", J. Pet. Tech., 1974, p. 1044.

(6) Schultz, W. E. and Smith, H. D.: "Laboratory Evaluation of a Carbon-Oxygen (C/O) Well Logging System", J. Pet. Tech., 1974, pp. 1103-1110.

(7) Culver, R. B., Hopkinson, E. C. and Youmans, A. H.: "Carbon-Oxygen (C/O) Logging Instrumentation", Soc. Pet. Eng. J. No. 14, Oct. 1974, pp. 463-470.

(8) Dewan, J. T., Stone, O. L. and Morris, R. L.: "Chlorine Logging in Cased Holes", J. Pet. Tech. No. 13, June 1961, pp. 531-537.

(9) Peatross, R. F.: "A New Lithology Compensated Capture Gamma-Ray System", Trans. SPWLA 17th Annual Logging Symposium, June 9-12, 1976. Paper M.

(10) Keys, W. S. and Boulogne, A. R.: "Well Logging with Cf-252", Trans. SPWLA 10th Annual Logging Symposium, May 25-28, 1969. Paper P.

(11) Scott, H. D. and Smith, M. P.: "The Aluminum Activation Log", Trans. SPWLA 14th Annual Logging Symposium, May 6-9, 1973. Paper F.

(12) Hoyer, W. A.: "Induced Nuclear Reaction Logging", J. Pet. Tech. No. 13, Aug. 1961, pp. 797-802.

(13) Caldwell, R. L. and Mills, W. R. Jr.: "Activation Analysis in Petroleum Exploration Research", Nucl. Inst. Meth. No. 5, Nov. 1959, pp. 312-322.

(14) Senftle, F. E., Moxham, R. M., Tanner, A. B., Boynton, G. R., Philbin, P. W. and Baicker, J. A.: "Intrinsic Germanium Detector Used in Borehole Sonde for Uranium Exploration", Nucl. Inst. Meth. No. 138, 1976, pp. 371-380.

(15) Calvert, T. J., Rau, R. N. and Wells, L. E.: "Electromagnetic Propagation. . . A New Dimension in Logging", 47th SPE-AIME Regional Meeting, Bakersfield, Calif., April 13-15, 1977.

(16) Schlumberger Production Log Interpretation. Schlumberger Limited. New York, 1973.

(17) Schultz, A. L., Bell, W. T., and Urbanosky, H. J.: "Advances in Uncased-Hole Wireline-Formation-Tester Techniques", 49th Annual SPE-AIME Meeting, Oct. 6-9, 1974. Paper SPE 5035.

(18) Smolen, J. J. and Litsey, L. R.: Formation Evaluation Using Wireline Formation Tester Pressure Data", 52nd Annual SPE-AIME Meeting, Oct. 9-12, 1977. Paper SPE 6822.

CONTINUOUS BOTTOM-HOLE PRESSURES ARE MEASURED BY NON-ELECTRIC SYSTEM

T. J. Ashby
Sperry-Sun
Denver, Colorado

The Sperry-Sun Pressure Transmission System (P.T.S.) continuously monitors bottom-hole pressure from any surface control point. The reliable and rugged down-hole package uses no electronics or moving parts; therefore, the possibility of having problems with the down-hole package is very remote. The bottom-hole pressure are transmitted to the surface unit through a small stainless steel capillary tube that is .094" O.D. and .054" or .026" I.D., that is charged from the surface with an inert gas (Nitrogen or Helium) to establish a single phase gas system.

The down-hole system utilitzes two (2) types of chambers -- suspension and concentric chambers. The suspension chamber is 1.66" O.D. X 10 feet long, although other sizes can be made for special applications. The suspension chamber can be run in wells through a stuffing box and lubricator in the same manner as conventional gauges are run. There are depth limitations when running the suspension chamber due to the strength and long continuous lengths of the capillary tube. Generally, when using the .094" or .026" I.D., #1 temper, fully annealed tubing, the depth is limited to approximately 3000 feet; the .094" O.D. X .054" I.D. tubing limited to approximately 7000 feet. This tubing is a #3 temper, cold drawn, with a tensile strength of 145,000 to 165,000 P.S.I. Additionally, the size of tubing to be used will depend on the pressure range to be measured.

The reason for the two (2) different I.D.'s of tubing is that in some instances, with large B.H.P. changes, the .026" I.D. tube has to be used in order that a standard chamber can be used. For example, the small I.D. tubing (.026-inch) has a volume of 6.37 cubic inches per 1000 feet. The large I.D. tubing (.054-inch) has a volume of 27.48 cubic inches per 1000 feet or 4.3 times more. The larger I.D. tube will require that the down-hole chamber be 4.3 times larger than one used with the small I.D. tubing. At low pressures, say 10 to 510 psi which is a 500 psi change, a 10-foot concentric chamber will work with the small I.D. tubing 1000 feet deep, but a 43-foot concentric chamber would be required using the larger I.D. tube. The same 500 psi change between 2000 and 2500 psi would require only a 1-foot concentric chamber for either size tube.

The concentric chambers are made from a full joint of production tubing with an outer jacket welded to the joint of tubing. The jacket length is normally 25 feet long on a 30 foot joint of tubing. These chambers are made from J-55 and N-80 EUE 8rd. tubing and are available in most sizes of standard production tubing.

The .094" capillary tube is banded to the outside of the production tubing in the annulus. To date, the deepest installation made has been approximately 11,300 feet. The highest angle hole ran to date is 58° angle, 6000 feet deep, utilizing a new type collar tubing protector developed by Sperry-Sun.

There is no apparent depth or temperature limitations of the down-hole package. Installations have been made in geothermal wells up to 625° F., utilizing both types of down-hole chambers. Either down-hole package can be permanently installed for measuring B.H.P. in Rod Pump wells, gas storage wells, oil and gas wells, etc., where build-up and draw-down pressures, as well as long term dynamic pressure test at high temperatures are required.

The major problem area of using the Pressure Transmission System in geothermal wells the type material used in the capillary tube to withstand the high temperatures and hostile environments for prolonged periods of time. To date, we have used 304, 304L, 316, 316L, 321, and E-Brite 26-1 to make the capillary tube. The 300 Series metals lasted from as short as four (4) hours (304 and 321) to as long as one (1) year with the 304L, 316 and 316L. The E-Brite 26-1 material looked extremely good in the initial test of this metal, tubing was made with a .032" I.D. in a #2 temper. Failure of this tubing downhole occurred as short as 30 days after installation to as long as six (6) months from the twelve installation that were made. This tubing also failed from severe pit corrosion and chloride stress corrosion cracking. Additional problems were enountered in welding the strip material as the weld would start cracking as the tubing was pulled to the small .094" size.

At this time, we are evaluating several other materials to make tubing with, with primary emphasis on resistance to chloride stress corrosion cracking and pit corrosion, that has good welding characteristics and can be pulled in long lengths. Some of these materials are Carpenter 20, Monel 400, Inconel 625, and Incoloy alloy 825. A short length of tubing made from the Incoloy 825 is presently being tested in a laboratory now and will soon be installed in a geothermal well for evaluation.

The accuracy of the Pressure Transmission System has been proven in oil and gas wells and geothermal wells. However, when this system is to be installed in these high temperature wells, where there will be flowing and shut-in test, the use of Helium is recommended as the transmission media, as it is more stable than Nitrogen to the large average temperature changes that will occur.

The Pressure Transmission Surface Recorder is a precise measuring instrument which continuously displays psi gauge pressure in digital form and provides a paper tape print-out of pressure

and delta time, at time print modes from 18 seconds to 30 minutes. A built-in battery pack is available so that no information will be lost in the event of an AC power failure. The standard pressure ranges are 0 - 1,000 PSI, 0 - 5,000 PSI, and 0 - 10,000 PSI. Other ranges are available special order. The accuracy is .05%± of the full scale range of the sensing element. Sensitivity is .005% of the full scale range of the sensing element. Response time is 15 seconds for full scale transition, depending on the pressure range. The pressure sensing element utilized a Bourbon tube and a force-balance servo system in which the pressure system is combined with an electro-mechanical feedback system. The force developed by the Bourdon tube in response to an input pressure is matched by an equal force developed by a temperature-stable linear feedback spring which returns the system to a null (balanced) position. This eliminates losses in sensitivity and accuracy, commonly associated with conventional mechanical linkages, and limited sensing element-tip travel minimizes temperature and hysteresis effects.

A Digital Pressure Monitor that only displays pressure in digital form is also available.

These units may also be used in place of dead weight testers, as they are more accurate, faster, and easier to read.

Additionally, these units may be used for calibrating pressure instruments in the laboratory or in the field, Process Control Instrumentation and Production Line Instrumentation.

Within the past two (2) years, another service has been developed and field proven. When the .054" I.D. tubing is used in the Pressure Transmission System to measure bottom-hole pressures, a chemical can be injected down the capillary tube to treat the wellbore fluids, near the perforations, as it rises in the production tubing. Less chemicals can be injected at the correct rate on a continued basis at the desired depth downhole for maximum efficiency of the well. When pressure data is again desired, the capillary tube is purged of the chemical by injecting a solvent to remove the chemical film on the inside of the tube and then injecting an inert gas (Nitrogen or Helium), to obtain the single phase gas system required. One thing to check is the temperature flash point of the chemical to be injected, as some chemicals have a low flash point and will tend to plug the tubing. When bottom-hole pressure is not desired, a chemical injection sub has been installed in the production string for continuous injection of chemicals. Field tests to date havebeen as deep as 10,400 feet. Injection rates using methanol of up to 50 gallons per day have been obtained in gas wells to keep the well from freezing up and shut-in, which has resulted in substantial increased production. Approximately 25 to 30 such systems have been installed to date.

Sperry-Sun has another precision subsurface pressure gauge. This gauge is widely used in the oil and gas industry. With an accuracy of .05%± and sensitivity of .055% of the full-scale range of the sensing element, and at near calibration temperature, this gauge is ideally suited for draw-down test, build-up test, interferance test, static test, gradient test, variable flow rate test, and drill stem test, to provide necessary information for a thorough analysis of any type reservoir.

This gauge has eight pressure sample rates, ranging from 15 seconds to 32 minutes, with a maximum sample time of twenty-eight (28) days, depending on temperature. This is a self-contained gauge and is a solid state electronic instrument that uses a Bourdon tube as the primary sensing device, but does not have a physical connection between the Bourdon tube and the recording section. The gauge is powered by batteries and has a temperature limitation based on the electronics and batteries available to the industry.

Sperry-Sun also provides gyroscopic single shot and multishot instruments for surveying cased holes in the oil and gas industry. Additional magnetic single shot and multishot instruments are available for surveying of uncased or open holes. When the magnetic instruments are run inside a thermal shield, records can be obtained in holes up to 600° F. for a shot duration of time, normally, 6 to 8 hours.

Sperry-Sun recently made a major break through in the design of a gyroscopic directional instrument, utilizing a thermal shield, that is capable of surveying wells with temperatures up to 600° F. This instrument has been run in geothermal wells as deep as 10,000 feet successfully, surveying the cased and open holes.

In the oil and gas industry, a survey steering tool is available to monitor down-hole conditions when drilling with a mud motor in directional controlled holes. This tool is run on a conductor wireline and provides a continuous reading on the surface of toolface, (high side and magnetic) drift, directional bearing, and mud temperature above the mud motor.

HIGH TEMPERATURE INSTRUMENTATION

Anthony F. Veneruso
Sandia Laboratories - Division 5736
Albuquerque, New Mexico 87115

Abstract

Methods for obtaining geothermal borehole measurements and making appropriate interpretations are limited at present by technical deficiencies in that logging tools developed for the oil and gas industry rarely encounter temperatures above 150°C. Also, most of the available logging tools, cables and seals are rated to only 180°C whereas in geothermal wells temperatures frequently range up to 350°C. This paper reviews the Geothermal Logging Development Program being conducted by Sandia Laboratories for DOE's Division of Geothermal Energy. This program is an industry-based effort to develop and apply the high temperature instrumentation which is needed by the wireline logging industry to serve a rapidly expanding geothermal market. In order to satisfy critical existing needs, the near-term goal is to develop instrumentation for use at or above 275°C in pressures up to 48.3 MPa (7,000 psi) by the end of FY80. The long-term goal is for operation up to 350°C and 138 MPa (20,000 psi) by the end of FY82. To meet these goals, existing hardware will be upgraded and new components will be developed and evaluated in critically needed prototype tools such as the temperature, flow rate and high resolution downhole pressure sondes. Most of the development and service activities will be contracted to industry with work by Sandia and other DOE laboratories as necessary to expedite the industry effort.

Introduction

Methods for obtaining borehole measurements and making the appropriate interpretations are limited at present by technical deficiencies in that logging tools developed for the oil and gas industry rarely encounter temperatures above 150°C.[1] In geothermal wells, temperatures frequently range up to 350°C, but most of the logging tools, cables and seals, are rated to only 180°C. Above their temperature rating in the often corrosive "hostile" environment of a geothermal well, logging tools and cables have have significantly reduced reliability and life expectancy. These deficiencies as well as the less than satisfactory results obtained through the use of existing "hostile" environment logging tools in geothermal wells were confirmed by the 1975 Geothermal Workshop hosted by Sandia Laboratories.[2]

Industries that are expected to make major financial investments in geothermal power plants, space heating or process heating are not inclined to risk large sums on construction without confidence that geothermal resources exist with temperatures, flow rates and production longevity sufficient for long-term commercial operation. It is the purpose of the Geothermal Logging Development Program to provide the means to establish that confidence with information from new high temperature instrumentation which will operate in hot, corrosive geothermal wells. This program is being conducted by Sandia Laboratories for the Department of Energy's (DOE) Division of Geothermal Energy (DGE) and is a portion of DGE's Long Range Geothermal Well Technology Program.

The existing, highly developed hydrocarbon and mineral logging services and their interpretation procedures form the basis for the technical developments in this program. Research in geothermal reservoir engineering and log interpretation is being pursued by the evolving geothermal production industry. In addition, the logging service companies are conducting in-house R & D to correct technical deficiencies so they may adequately serve the geothermal market. The basic impediments they face involve special technologies which are not normally required in their trade and for which there are insufficient incentives for them to develop. These technologies are precisely those which are being pursued by this program.

In order to satisfy critical existing needs, the near-term goal is for operation at 275°C and 48.3 MPa (7,000 psi) by the end of 1980. The long-term goal is for operation up to 350°C and 138 MPa (20,000 psi) by the end of 1982. To meet these goals, existing hardware is being upgraded and new components are under development. Prototypes of critically needed tools for temperature, flow rate and high resolution, downhole pressure will be constructed with the components and their performance

evaluated under laboratory and field conditions. Our strategy involves direct cooperation with industry where most of the development and service activities are contracted. Work is done by Sandia and other DOE laboratories whenever it is necessary to significantly expedite the industry effort with supporting research, development, and testing. Operationally, this program combines the advanced, high temperature materials and components capabilities of Sandia Laboratories with the know-how of the logging service industry to develop appropriate technology which will fulfill the logging needs of the rapidly expanding geothermal market.[3]

In establishing its design goals and overall direction, the Geothermal Logging Development Program will address the needs of geothermal reservoir engineering through formal participation in the Reservoir Engineering Management Program which is being conducted by the Lawrence Berkeley Laboratory (LBL). Also, the borehole measurements obtained in this program's geothermal well field tests will serve as a data base for the Geothermal Log Interpretation Program underway at the Los Alamos Scientific Laboratory (LASL).

Geothermal Borehole Measurements

Making measurements in geothermal wells with high temperature instruments is only one step in a process that begins with needs of reservoir engineering. Figure 1 is a schematic of this process. A list of the parameters desired for open borehole exploration and reservoir assessment is given in Table 1. The repertoire of tools, their development priority and performance requirements are described in Table 2. This information was compiled by the 1975 Geothermal Workshop and updated by the Geothermal Logging Steering Committee at their June 28, 1977 meeting.

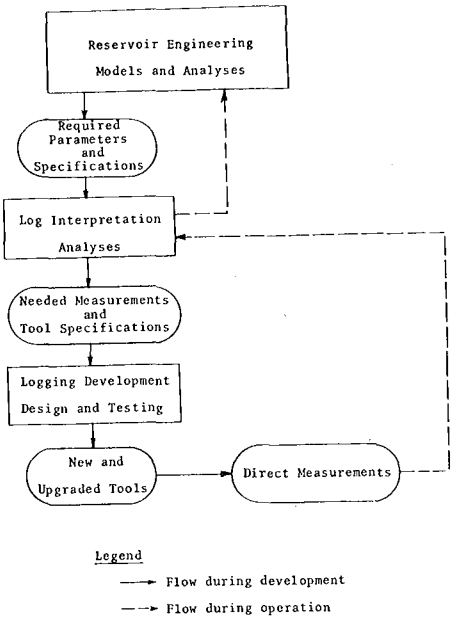

Figure 1-1. Schematic of Geothermal Logging Activities

Table 1. Borehole Parameter Priorities

Priorities of parameters may vary among resource types. However, certain parameters are essential for evaluation of most geothermal resources in the near-term. These are arranged to indicate ranking and importance.

1. Temperature
2. Formation Pressure
3. Flow Rate
4. Hole Geometry (may be critical in log interpretation)
5. Fracture System (location, orientation, permeability, etc.)
6. Fluid Compositions (pH, dissolved solids and gases)
7. Permeability
8. Porosity (interconnected and isolated)
9. Formation Depth and Thickness

Other parameters which are important but which may not need to be measured in every well or which may be reliably predicted or calculated from other physical parameters include:

1. Thermal Conductivity
2. Electrical Conductivity or Resistivity
3. Heat Capacity
4. Lithology and Mineralogy
5. Acoustic Wave Velocity

Table 2

PROTOTYPE GEOTHERMAL LOGGING TOOLS
(up to 275°C operation)

Tool	Performance Goal
Temperature	1.0°C accuracy, 0.5°C resolution
Pressure	0-7000 psi, 0.1 psi accuracy, 0.01 psi resolution
Flow	0-2000 gpm in diphasic flow
Caliper	6 arm borehole geometry, 0.1 in. accuracy with fracture indication
Casing Collar Locator	Detect standard collars
Formation Resistivity	To be determined
Fracture Mapping	To be determined
Casing and Cementing Inspection	To be determined
Directional Survey	To be determined
Sonde Refrigerator	50 watts cooling to 125°C for at least 100 hours

Geothermal Logging Development

The technical development of geothermal borehole instrumentation is divided into three tasks: 1) severe environment components development, 2) prototype system development, and 3) borehole test and evaluation. Efforts in components development are directed toward alleviating existing technical deficiencies by identifying, testing and evaluating devices, materials, and components suitable for use in geothermal logging systems. Specific developments are underway in 275°C electronics, high temperature-high resolution pressure transducers, acoustic transducers, and high temperature corrosion resistant elastomers, ceramics and metals. Results in this area will have immediate impact on improving near-term industry capabilities for geothermal logging. Special efforts are therefore being made to rapidly transfer these technological developments to the logging industry to stimulate their own inventions and contributions to geothermal logging.

To evaluate these components in complete systems, a few experimental prototype borehole instruments will be built and tested in both the laboratory as well as in actual geothermal boreholes.

Severe Environment Components Development

High Temperature Electronics - The thrust of the efforts for near-term 275°C electronics is directed toward thick film hybrid microcircuits technology. This technology is widely used commercially for small quantity production of special electronics albeit for applications up to 125°C. However, this technology can be adapted for use in the required higher temperature range, has the required ruggedness and gives the desired level of miniaturization. The hybrid thick film process is analogous to a silk screen process in which special inks are squeezed through a mask and then baked at 900-1000°C onto a ceramic substrate. Different patterns of different inks yield the desired conductors, resistors and capacitors. After the thick film portion of the circuit is made, discrete semiconductor devices and multi-layered capacitors, too large to print in thick film, are mounted onto the substrate and electrically bonded to the circuit. Adaption of this process for high temperature operation requires selection of resistor inks specially formulated for low values of thermal coefficient of resistivity as shown in Fig. 2. Similarly, dielectric inks, for fabricating capacitors, are formulated to maintain stable low loss properties over a wide temperature range. These inks are now commercially available and can be processed on standard equipment. Hundreds of hybrid thick film resistor and capacitor devices have been laboratory tested for thousands of hours at 300°C. Efforts are continuing to further develop thin film dielectrics, together with the necessary bonding and circuit interconnection techniques.

Figure 2

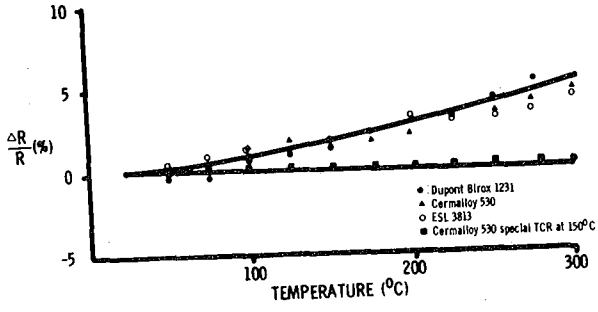

THICK FILM RESISTANCE CHANGE AS A FUNCTION OF TEMPERATURE. THE THREE INK SAMPLES THAT WERE EXTENSIVELY TESTED PERFORMED ROUGHLY THE SAME. IT IS IMPORTANT TO STATE THAT ALL INK MANUFACTURERS CAN MIX SPECIAL INKS SO THAT THE TOTAL CHANGE ΔR/R IS 1-2% OVER THIS TEMPERATURE RANGE.

In the 275-300°C temperature range, the popular bipolar silicon transistors are intrinsically limited. However, a few commercially available silicon semiconductors have been found to operate satisfactorily at these high temperatures. These devices are the so-called field effect transistors (FETs). FETs operate by means of electrostatic control of majority carrier current flow whereas the more common bipolar transistors operate by means of a small injected control current modulating a more temperature sensitive minority carrier current. Figure 3 displays temperature performance curves for a commercially available FET specially selected for its high temperature qualified construction. Several have been qualified for 275°C operation through active circuit tests for 1000 hours at 300°C.

Figure 3

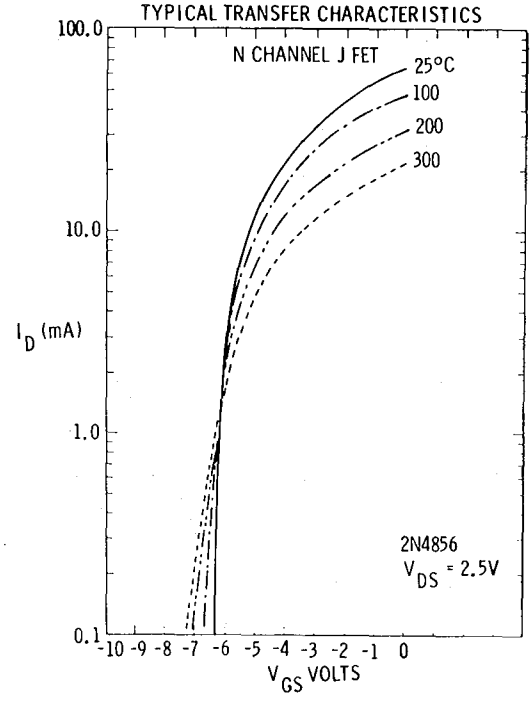

Through the above laboratory testing of active and passive electronic devices, a sufficient, though somewhat limited, line of commercial components and fabrication techniques is now available for 275°C operation to fulfill basic circuit needs for amplification, switching and filtering. Development work is continuing toward expanding the repertoire of available devices suitable for 275°C operation. For higher temperatures, such as 300-325°C, alloy semi-conductors such as gallium arsenide FETs are being explored because they continue to exhibit semiconductor properties at temperatures where silicon crystal devices cease to function and become intrinsic conductors. Above 325°C suitable semiconductors are presently not acceptable. Therefore, special vacuum tube-based circuits called Integrated Thermionic Circuits (ITCs) are under development by LASL.[4] These ITCs are planar vacuum tube structures which are

metal vapor deposited onto miniature sapphire substrates and packaged in a special glass ceramic container. LASL has operated ITCs in temperatures up to 900°C. Although they are not now commercially available, they will be further developed because they offer a relatively high assurance of performing satisfactorily at extremely high temperatures.

High Temperature Mechanical Components - Elastomers and seals capable of withstanding temperatures of at least 275°C and 7,000 psi in the presence of geothermal brine for up to 100 hours are required for geothermal well logging applications in seals, gaskets, connectors, cable sheathing and wire insulation. An important aspect of these applications is the protection of sensitive electronic components from the corrosive fluids in a geothermal reservoir. Elastomers are also needed in borehole packers for geothermal well testing and completion. Unfortunately quantitative performance data on commercially available materials and components are lacking for these applications. Therefore the approach taken to fulfill these deficiencies includes the following: 1) Coordination of material needs and developments with DGE's Geochemical Engineering Program, 2) test and evaluation of available high temperature, steam resistant elastomers and metals as moisture barrier seals, and 3) investigation of special coatings to enhance the chemical and steam resistance of elastomers made from available polymers.

As shown in Tables 3 and 4, test and evaluation of available materials has identified several promising candidates for use in specific components such as seals and wire insulation. Other materials, along with specific prototype designs of cables, cableheads and tool seals will be tested in the coming months.

TABLE 3

HIGH TEMPERATURE ELASTOMERS

TRADE NAME	TYPE	DECOMPOSITION TEMPERATURE °C	COST $/LB	COMMENTS
BUNA N	NITRILE	150	6	GOOD OIL RESISTANCE POOR RESISTANCE TO H_2S AND STEAM
VITON E- -C	FLUORO ELASTOMER	290	35	FAIR RESISTANCE TO STEAM POOR FOR H_2S
VITON G (Peroxide Cure)	FLUORO ELASTOMER	290	40	IMPROVED STEAM RESISTANCE POOR FOR H_2S
KALREZ	FLUORO ELASTOMER (Fully Fluorinated)	400	2000	BEST FOR H_2S FAIR FOR STEAM
EPR	POLYOLEFIN	250	8	EXCELLENT STEAM RESISTANCE H_2S UNKNOWN
SILOXANE	SILICONE	300	17	POOR STEAM AND POOR H_2S RESISTANCE

TABLE 4

HIGH TEMPERATURE SEALS

TYPE	TEMPERATURE LIMITATION		COMMENTS
ELASTOMERIC O-RINGS	POLYMER DECOMPOSITION	300 C	REUSE PERMITTED LEAST DIRT SENSITIVE
METAL O-RINGS	METAL SOFTENING	500 C	REUSE NOT RECOMMENDED SOFT PLATING RECOMMENDED NICK AND SCRATCH SENSITIVE
CONO-SEALS	METAL SOFTENING	500 C	REUSE NOT RECOMMENDED NICK AND SCRATCH SENSITIVE MINOR JOINT MOTION TOLERATED
WAVE RINGS	METAL SOFTENING	500 C	REUSE NOT RECOMMENDED SOFT PLATING RECOMMENDED NICK AND SCRATCH SENSITIVE

Prototype System Development - To satisfy critical existing needs of geothermal reservoir engineering, prototypes of the most critically needed tools are being developed for geothermal applications. Table 2 is a list of these tools in the order of their priority. The temperature, pressure, flow and caliper tools have the highest priority and are therefore being addressed first.

Temperature - Both printed circuit board and hybrid microcircuits for a 275°C temperature tool have been completed and are presently being assembled with the tools housing and interconnections.

The printed circuit is quicker and easier to fabricate and modify than the hybrid circuit; however at high temperatures the hybrid is more rugged and reliable. The design is based on a platinum resistance transducer with active downhole electronics: a voltage-to-frequency converter, voltage regulator and a line drive. The tool is compatible with both multi- and monoconductor cables. To date, a printed circuit board version of the temperature tool has successfully completed 62 consecutive hours of laboratory testing at 275°C. Test results indicated a drift error of less than 0.28°C. Also each of the four major subassemblies of the more rugged and reliable hybrid circuit version has been successfully tested for at least 25 hours at 275°C. Efforts are now underway to test the complete hybrid circuit temperature tool.

Pressure - This development is directed toward a high resolution quartz crystal based pressure sensor which strives for 0.01 psi resolution in temperatures up to 275°C. Currently available, high resolution pressure gauges utilize quartz crystals but these gauges are temperature limited because of limitations in the crystal geometry employed, in the bonding of the crystals to the substrate and in the limited temperature range of the associated electronics. The approach taken for the high temperature design begins with a new quartz crystal configuration that is specifically designed to operate optimally at 275°C rather than over a wide range of temperatures. The crystal is small enough to fit inside a miniature oven which precisely maintains the quartz crystal at the optimum temperature. Deficiencies in the associated electronics are corrected by utilizing the repertoire of high temperature hybrid thick film circuit components already developed.

Flow - A high temperature impeller type flux gate transducer signal feedthrough mechanism has been constructed. The associated hybrid electronics for 275°C operation are presently under development.

Caliper - A caliper tool is a necessary adjunct to the impeller type flow tool in order to compute flow rate. The caliper is also necessary to identify open borehole geometry and thereby establish a basis for log interpretation and well completion strategy. In addition, a caliper is also useful in gross fracture mapping where the fractures are at least 0.1 inches wide. Development efforts are directed at correcting major deficiencies in existing caliper's susceptibility to the corrosive, high temperature geothermal environment.

Other Prototypes - Complementing the above prototype borehole instruments effort is the development of a sonde refrigerator. Available thermal protection devices such as eutectic heat sink equipped dewar flasks are presently the industries' staple in packaging and protecting state-of-the-art electronics for logging geothermal wells. However, the best available dewars are limited to no more than 12 hours of operation in boreholes up to 275°C. A reliable instrumentation refrigerator, capable of operating for 100 hours or more, will enable operation of existing downhole electronic packages and thereby open up the geothermal logging market to conventional logging services. This approach is technically challenging and outside the normal endeavors of the logging industry. Due to the high potential payoffs, this sonde refrigerator is currently being contracted to industry with appropriate technical support from Sandia. Table 5 lists the industry contracts presently underway for geothermal logging development.

Table 5
Industry Contracts in Geothermal Logging Development

Company	Area of Work	Contact
Gearhart Owen Ind. Ft. Worth, TX.	Prototype Tool Fabrication	Jack Burgen (817) 921-3761
Geoscience Ltd. Solans Beach, CA.	Heat Flux, Thermal Conductivity Probe	Heintz Poppendiek (714) 755-9396
IRT Corp. San Diego, CA.	Neutron Formation Temp. Tool	Don Steinman (714) 565-7171
Los Alamos Scientific Laboratory Los Alamos, NM	Integrated Thermionic Circuits	Steve Deppe (505) 667-5974
Measurement Analysis Corp. Palos Verdes Estates, CA.	Instrumentation Systems Contracts Monitoring	Mike Lamers (213) 378-8868
Southwest Research Institute San Antonio, TX	Optical Logging Methods	Bob Swanson (703) 684-5111
Spectra Systems Springfield, VA.	Chemical Well Temp. Measuring	Joe Gaven (703) 321-9240
System Development Corp. Santa Monica, CA.	Sonde Refrigerator Ceramic Tube Amplifier	Ron Kelly (213) 829-7575
Systems, Science & Software La Jolla, CA.	Passive Sonde for T, P, ΔP	Don Grine (714) 453-0060
University of Arizona Tucson, AZ.	Passive Electronic Components Autoclave Testing	Doug Hamilton Archie Deutschman (602) 793-2651
Westinghouse Pittsburg, PA.	Improved Acoustic Tools	Jim Wonn (412) 256-3635

Borehole Test and Evaluation - The above experimental prototypes will be tested in geothermal boreholes using a special trailer mounted skid unit, a 50 foot mast truck and auxiliary support equipment such as pressure controls and line lubricators. The skid unit is equipped with 16,000 ft. of seven conductor and 15,000 ft. of monoconductor high temperature cables. The unit also has generators and on-broad instrumentation to support long term experimental tests of prototype borehole instruments.

After successful completion of initial tests and evaluation of the above hardware, a limited number of prototype sondes, cable heads and supporting electronics will be supplied to other DGE experimental facilities at other labs and geothermal sites to both expedite sonde evaluation and to provide additional support for their respective borehole measurement needs. For example, reservoir engineers at LBL and log interpreters at LASL are working with geothermal wells from which they need accurate, reliable, high temperature downhole information. The hardware under development by this program will attempt to fulfill these needs on an interim basis while stimulating industries' involvement. Both logging service companies and geothermal producers are involved in this endeavor because ultimately they must supply and utilize the logging sevices needed to support the expanding geothermal industry.

REFERENCES

1. Martin, C. A. and Rust, D. H., Hostile Environment Logging, The Log Analyst, Vol. 12, No. 2, 1976.

2. Baker, L. E., Baker, R. P., and Hughen, R. L., Report of the Geophysical Measurements in Geothermal Wells Workshop, Sandia Laboratories Report, SAND75-0608, December 1975.

3. Palmer, D. W. and Krauss, G. L., 275°C Microcircuits, Resistors, Capacitors, Conductors, Substrates, and Bonding, Sandia Laboratories Report, SAND76-0611, December 1976.

4. McCormick, J. B., Depp, S. W., Hamilton, D. J., and Kerwin, W. T., A New Electronic Gain Device for High Temperature Applications, LASL Report, LA6339 MS, July 1976.

Session Introduction

Field Applications

R. Ershaghi
University of Southern California

Theoretical developments in the area of well testing have been rather extensive in recent years. Unfortunately, published reports describing extensive field applications have been limited in number.

Technical sessions on field applications of well-testing methods are always refreshing and draw a great deal of attention, and this meeting was no exception. The four papers selected for this session presented some aspects of tool and/or interpretation problems associated with field data. Bill Miller from Shell Oil Company gave the first talk on the concept of total formation evaluation using coupling of a non-linear least-square-fit computer program to a general purpose reservoir simulator. A paper by Jerry Pickens from the University of Waterloo discussed problems associated with sampling devices used in tracer studies for modeling of shallow waste-burial operations. Well-testing problems in geothermal reservoirs was the subject of the next two papers. T. N. Narasimhan from Lawrence Berkeley Laboratory presented a talk on the nature of collected data, methods for preprocessing of raw data to eliminate extraneous noises, and the need for improved methods to interpret the data. Similar discussions for geopressured reservoirs were given by Myron Dorfman from the University of Texas at Austin.

The active participation of the audience in the question and answer period following each paper was a clear indication of the great interest generated by the speakers and the topics.

ABSTRACT

WELL TESTING ANALYSIS:

A GUIDE TO PRACTICAL OIL AND GAS FIELD DECISIONS

William C. Miller
Shell Oil

Examples from oil and gas field evaluation, development, well stimulation, and supplemental recovery projects emphasize the wide scope of questions which can be effectively answered with comprehensive interpretation of both routine and specially designed well tests. In our experience, far too often the complex nature of the reservoir properties and processes demand more powerful analysis methods than those provided by the literature. But flexible couplings of a non-linear least-squares-fit computer program to a general purpose reservoir simulator is extending our interpretation of such engineering problems.

From the examples presented, it is obvious that such "automated" history matching of well-test response (multi-fluid production, observation well pressures, post-fracturing performance) should not be regarded at all as an "automatic" procedure. The engineer's ingenuity and experience are much more critical factors than the mathematical elegance of the computation scheme. Furthermore, despite the prevalent concern voiced about the possible non-uniqueness of the prototype which is deduced by such a well-test analysis procedure, from a decision-making standpoint, without such a method, complete inability to explain the observed performance of an expensive field test occurs all too frequently and is a much more serious obstacle.

FIELD STUDIES OF DISPERSION IN A SHALLOW SANDY AQUIFER

J.F. Pickens, J.A. Cherry, R.W. Gillham
Department of Earth Sciences
University of Waterloo
WATERLOO, Ontario, Canada. N2L 3G1

W.F. Merritt
Atomic Energy of Canada Limited
Chalk River Nuclear Laboratories
CHALK RIVER, Ontario, Canada. KOJ 1JO

Summary

Field studies of dispersion in granular aquifers can be conducted by means of tracer experiments using radioactive or non-radioactive solutes. Studies of the concentration distributions at sites at which contaminant enclaves already exist can also yield information on the dispersive properties of the geologic materials. This study reports on a single-well injection-withdrawal and a two-well recirculating withdrawal-injection tracer test that have been conducted in a shallow sandy aquifer at a waste management area of the Chalk River Nuclear Laboratories of the Atomic Energy of Canada Limited. A detailed three-dimensional monitoring network was used to monitor the tracer movement within the aquifer. Evaluation of the test results have demonstrated the effect of sampling from wells slotted over the entire aquifer versus point samples from an individual layer within the aquifer.

Introduction

As a solute is transported in a groundwater flow system it gradually spreads, occupying an increasing portion of the flow domain beyond the region that it would be expected to occupy according to fluid convection alone. This spreading phenomenon, called hydrodynamic dispersion, includes mechanical dispersion which is advection dependent and molecular diffusion which is concentration dependent. In aquifers, mechanical dispersion is normally the dominant of these two processes. The property of theporous medium that is a measure of its capability to cause mechanical dispersion is known as dispersivity. Dispersivity is considered to have two components, one in the direction of groundwater flow called longitudinal dispersivity and one normal to the direction of groundwater flow called transverse dispersivity. In laboratory experiments the value of the longitudinal dispersivity is generally found[1] to be larger than the transverse dispersivity by a factor of 10 to 20. From laboratory column experiments using relatively homogeneous granular porous media, published values of dispersivity[2,3] determined from breakthrough curves are usually of the order of 10^{-2} to 1 cm. In contrast, dispersivity values for granular deposits obtained by calibration of digital models to large-scale field contamination zones[4,5,6,7] or from the modelling of field dispersivity test results[7,8] are usually in the range of 10 to 10^2 m, which is 3 to 6 orders of magnitude larger than typical laboratory values. If dispersivity at the field scale is as large as is suggested by this model calibration approach it can be expected that contaminants transported in active groundwater flow systems will undergo strong dilution and spreading as a result of dispersion. Narasimhan *et al.*[9] concluded on the basis of simulation studies of well sampling effects that large dispersivity values computed from concentration data obtained in the usual manner of well sampling may not be representative of the true dispersivity of the geologic materials. Childs *et al.*[10] and Palmquist and Sendlein[11] have observed in detailed field studies in sand and gravel deposits that contaminants tend to follow the most permeable beds, which because of complexity in distribution, can cause a lensing or fingering of contaminant zones rather than strong spreading due to intergranular dispersion. These field studies [10,11] indicate, that indeed, there may be little spreading found when detailed three-dimensional monitoring of the contamination plumes is performed.

Fig. 1 illustrates three mechanisms that result in hydrodynamic dispersion. The patterned regions in this figure represent the individual grains. The first two mechanisms (a) and (b) are caused by fluid advection. The first mechanism (a) is the spreading or mixing caused by the groundwater velocity variation across a pore channel. This results in solutes being transported at different rates within an individual pore. The second mechanism (b) is the spreading caused by the pore-to-pore velocity variations. On a larger scale, spreading may also be caused by variations in velocity between micro or macro stratigraphic units. The third mechanism (c) is the spreading as a result of molecular diffusion. An important effect of heterogeneities relates to the problem of sampling.

This study deals with the investigations of the process of dispersion in field tracer tests. The field studies consist of a two-well recirculating withdrawal-injection tracer test and a single-well injection-withdrawal tracer test. These two types of tests are well documented in the contaminant transport literature. The unique aspect of our version of these tests is that we used a detailed three-dimensional monitoring network. As a

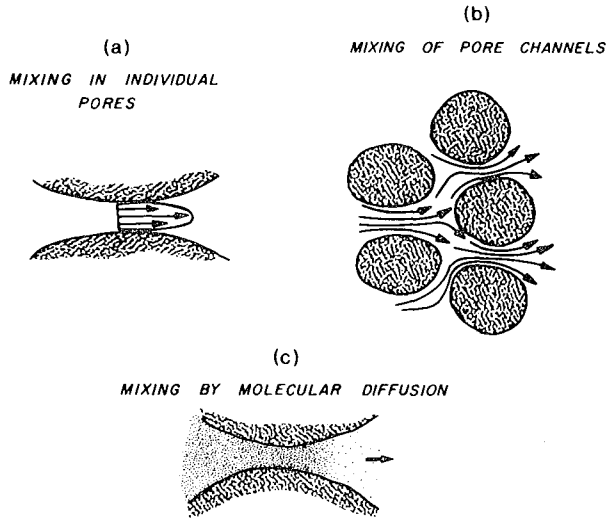

Fig. 1. Mechanisms of hydrodynamic dispersion

result, we were able to examine the dispersion process at different sampling scales including scales considerably smaller than have been used previously in field dispersion studies reported in the literature. An evaluation of the mixing caused by the groundwater sampling method has been done. The objective of this and other studies in progress is to examine the effect of the scale of measurement on the measured dispersivity values in heterogeneous hydrogeologic environments. The tests were conducted in a sandy aquifer at one of the radioactive waste management areas of the Chalk River Nuclear Laboratories of the Atomic Energy of Canada Limited, Chalk River, Ontario, Canada. The general hydrogeology of the basin in which the tests were conducted is given by Cherry *et al.*[12].

Scale of Sampling

Soil or groundwater sampling generally implies an averaging of the conditions existing at that point or region. Fig. 2a which was originally introduced into the groundwater literature by Hubbert[13] illustrates scales that can be defined with reference to a porous medium. This diagram is a hypothetical plot of the porosity as it might be measured on samples of increasing volume V_1, V_2, V_3... at a point within the porous medium. Sampling at a scale which is small with respect to the size of a pore or a grain is called the microscopic scale. The volume V_3 represents what is normally referred to as the representative elementary volume (Bear[14]) and is the lower limit of the macroscopic scale. Where the scale of analysis involves volumes, such as V_7 or greater, that may encompass several stratigraphic units or several heterogeneities this scale can be referred to as megascopic. A similar scaling system, as shown in Fig. 2b, can also be visualized for sampling of groundwater for tracer or contaminant concentrations. A schematic representation to further illustrate scales of sampling is shown in Fig. 3. In this study we attempt to show the effect on measured dispersivity of going from a measurement

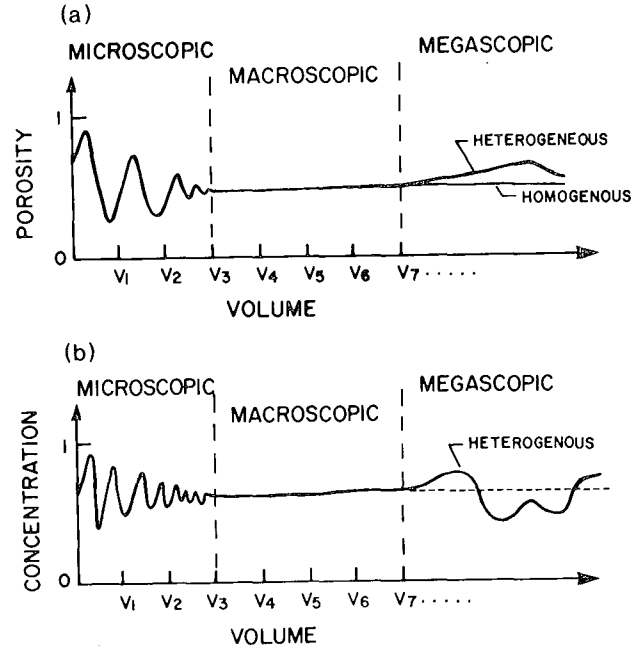

Fig. 2(a). Scales of measurement of porosity within a porous medium
(b). Scales of groundwater sampling within a porous medium

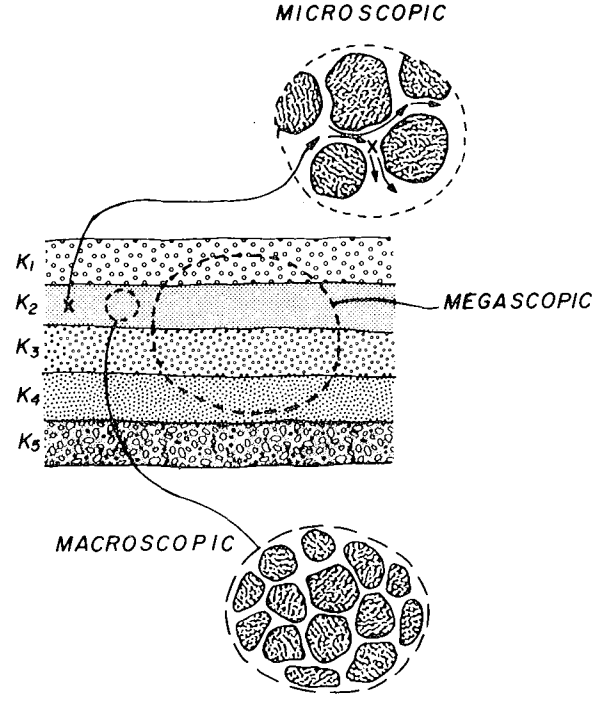

Fig. 3. Schematic representation of scales within a layered porous medium

scale which we believe to be approaching the macroscopic scale, to a larger, megascopic scale.

Field Experiments

Geology

The geology of the basin in which the study site is located is shown in Fig. 4. The field investigations were conducted in the middle sand unit referred to as the middle aquifer. This aquifer is indicated by the arrow on the cross-section (Fig. 4). The aquifer sand, which is approximately 8.5 m thick, was deposited in a deltaic environment that existed during a period of glacial melting during Pleistocene or early Holocene time. The sand is fine- to medium-grained and well sorted. At outcrops elsewhere in the vicinity of the basin, sands of this type have minor laminations and small-scale cross bedding. Some core samples from within the aquifers at the study site exhibit laminations. The middle aquifer is confined below by a silty clay bed that is about 1 m in thickness and above by a much thinner zone of bedded silt and clay. The results of various types of hydraulic conductivity tests conducted in the aquifer are described by Pickens *et al.*[15] and Woldetensae[16].

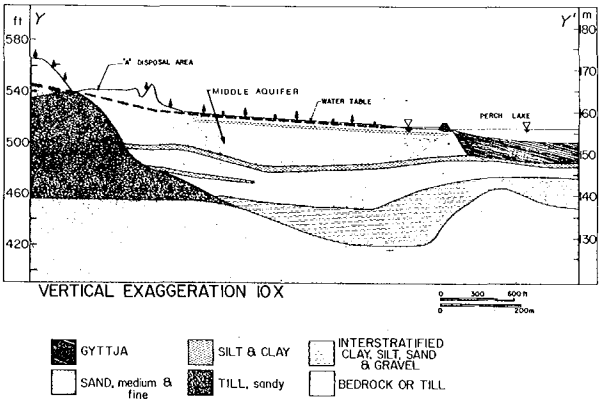

Fig. 4. Geologic cross-section through the study area

Instrumentation

The field site has 32 piezometers, 2 wells and 13 multi-level samplers. The layout of the instrumentation for the field tests is shown in Fig. 5.

The piezometers were used for monitoring of the piezometric heads in the aquifers during the tracer tests. They were installed through a steel casing that was driven by the combined effect of mechanical vibration and jetting. After installation of the piezometer pipe to the desired depth, the casing was removed by jacks. Since the sands of these deposits caved immediately upon removal of the casing, it was not necessary to grout the hole above the piezometer tip. The piezometers were constructed of 3.4 cm diameter PVC pipe. The intake portion at the bottom of the piezometer is

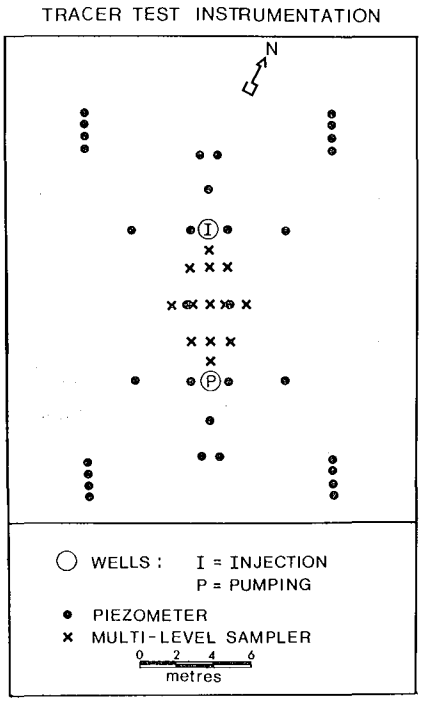

Fig. 5. Instrumentation at field site

about 50 cm in length and was constructed by slotting with saw cuts and wrapping with fibreglass cloth tape to prevent fine-grained material from entering. This type of piezometer is inexpensive and provides reliable data in cohesionless granular deposits. The piezometers were installed to various depths in order to monitor the hydraulic head in the different stratigraphic units.

The wells which were used in the tracer tests were constructed of PVC pipe with ABS plastic-wrapped screens having slot openings of about 0.1 mm. They were screened from 3 m to 10 m below ground surface which is approximately the extent of the middle sand aquifer. The wells were installed through a steel casing driven by a cable-tool drilling rig. The borehole was grouted as the casing was removed in the upper 2.5 m to prevent hydraulic connection of the upper and middle sand aquifers.

The network of multi-level samplers permitted the three-dimensional monitoring of the concentration of the tracer in the aquifer during the tracer tests. The 13 samplers contained a total of 160 sampling points. A schematic diagram, showing a field installation of the sampler and a cross-section of an individual sampling point on the sampler, is shown in Fig. 6. Each sampler consists of a PVC pipe with a number of sampling points positioned at predetermined levels along its length. The sampler is inexpensive and it can be easily constructed in the field. Samples were collected by connecting the polypropylene tubing which extends to above ground surface to a vacuum flask and applying suction. The samplers were installed by the washboring method as described for the piezometer installations.

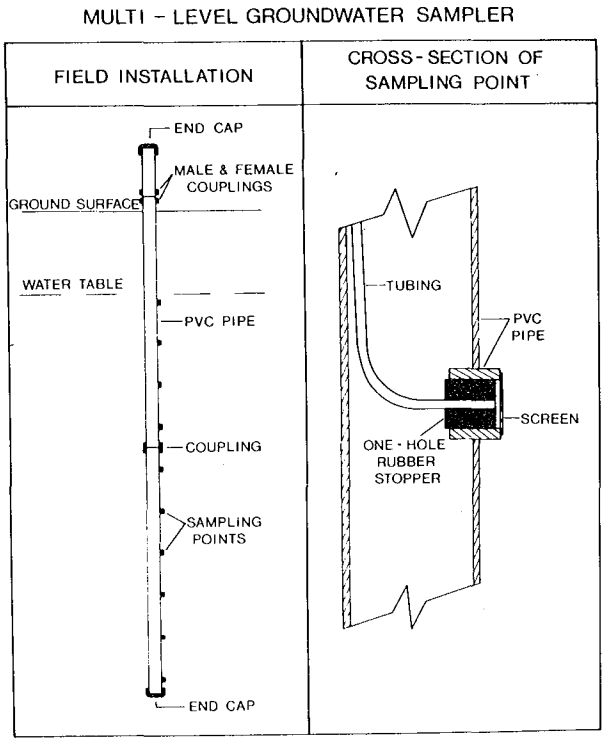

Fig. 6. Schematic diagram of the multi-level sampling device for monitoring tracer movement

Point Dilution Tests

The physical processes that cause transport of contaminants or tracers in groundwater flow systems are advection and dispersion. The parameters that are required to quantify these processes are groundwater velocity and dispersivity. One method that allows a direct estimation of groundwater velocity is a down-hole tracer test known as the point dilution or borehole dilution technique.

A comprehensive review of the uses and limitations of the borehole dilution technique for groundwater velocity measurements has been given by Halevy *et al.*[17]. Essentially, the technique consists of labelling the water in a section of the well screen with a tracer and observing the rate of dilution. The rate of dilution in the well screen is related to the velocity of the groundwater. Details of the analysis procedure are presented by Halevy *et al.*[17] and Merritt[18].

The apparatus used in this study was designed to fit inside a 10 cm plastic well screen. It uses inflatable packers to isolate a section 41 cm in length in the well. An oscillator pump, sealed in a waterproof case, is positioned just above the top packer and is used to keep the dilution volume between the packers well mixed. The effect of vertical currents is minimized by using a pressure equalizing tube across the packers. Rhodamine WT was used as the tracer. Water from the dilution volume between the packers was recirculated to above ground surface and passed through a fluorometer to record changes in the tracer concentration.

The velocity distribution under natural gradients was determined throughout the depth of the aquifer at one of the wells using point dilution tests. The results are shown in Fig. 7; the solid bars indicate the packed-off interval in the well for each test. The results show that significant velocity variations may exist within an aquifer which appears to be homogeneous and that these variations can occur over relatively short depth intervals. The technique allowed for detailed velocity profiling; however, we have no assurance that the distance between packers (41 cm) in the apparatus is approaching the macroscopic measurement scale. A smaller measurement interval would likely show even greater velocity variations.

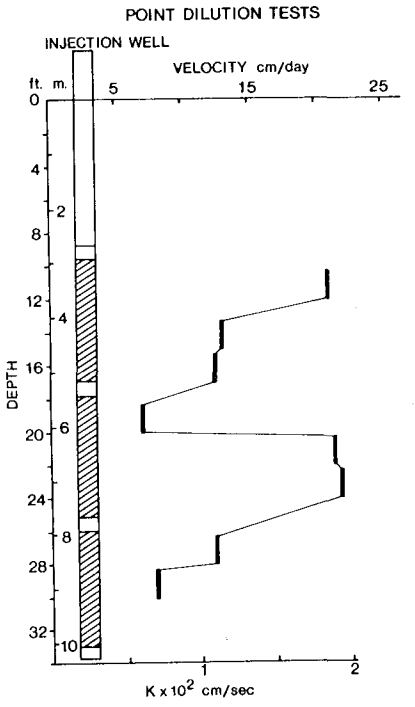

Fig. 7. Groundwater velocity distribution in the aquifer determined from point dilution tests.

Two-Well Recirculating Withdrawal-Injection Tracer Test

A two-well withdrawal-injection tracer test was conducted using the instrumentation shown in Fig. 5. Water was withdrawn from one well and recharged in the other well at a rate of 27 L/min. In order to establish a steady-state flow field the withdrawal and injection system was in operation for several days prior to introducing the tracer. The piezometer network was monitored daily to determine the hydraulic head distribution during the test. Approximately 100 mCi (3.7 GBq) of the tracer, ^{51}Cr-EDTA having a half-life of 27.8 days, were added to the injection water at a continuous rate over a period of 3.2 days. The input concentration at the injection well was maintained at about 57 cpm/mL. Recirculation of tracer in the pumping water occurred after about three days. The tracer test was continued for 15 days with

monitoring of the ^{51}Cr-EDTA concentration in the injection well, withdrawal well and multi-level samplers. All sample activities were corrected for radioactive decay to the time at which the tracer test was started.

The relative velocity distribution throughout the depth of the aquifer was determined by analyzing the concentration profiles from the five multi-level samplers located directly between the two wells. The results (Fig. 8) show reasonable agreement with the results obtained using the point dilution technique (Fig. 7). This provides further evidence of the potential of the point dilution technique in identifying zones of high transport rate in a groundwater flow system.

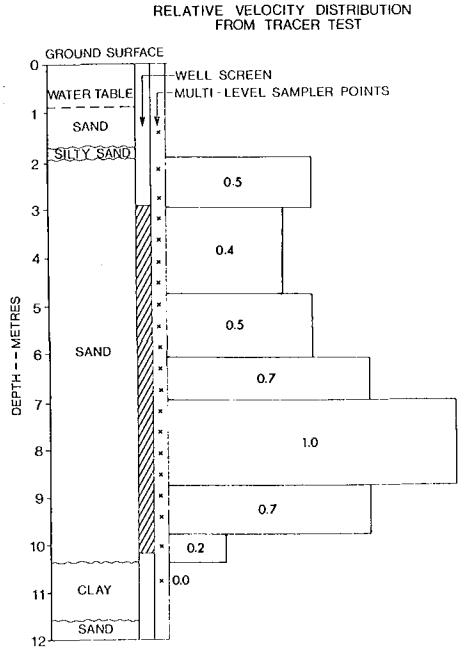

Fig. 8. Relative velocity distribution in the aquifer determined from monitoring tracer movement

A field dispersivity value was obtained from the results of the two-well withdrawal-injection tracer test using the method described by Grove and Beetem[19]. In this method the flow field induced by the withdrawal and injection wells is divided into a series of crescentic flow tubes that approximate columns of known length from the injection to the withdrawal well along which the tracer is assumed to pass. The breakthrough curve concentrations, generated using an analytical solution for the advective-dispersive transport of the tracer with an assumed value of dispersivity, from each arc or flow column are summed to produce a composite breakthrough curve at the withdrawal well for the entire flow field. Various values for dispersivity are used as input in the computer model until the calculated composite breakthrough curve closely matches the experimental one measured in the field. Tracer material passing through the withdrawal well and continuously returned to the injection well is accounted for in the calculation procedure. The computer program is listed in the report by Grove[20]. The following conditions necessary for application of the Grove model have been met in this experiment: the aquifer is horizontal and confined; a constant withdrawal-injection rate was used; the natural areal groundwater velocity is low; and the tracer was added continuously for a set time period. Results from the network of multi-level point samplers showed that the tracer movement was uniform at any particular depth and hence that the aquifer was areally homogeneous. The concentration profiles for the multi-level samplers between the two wells indicate that even though the aquifer appears on the basis of visual inspection of core samples to be vertically homogeneous, the tracer did not travel evenly throughout the vertical thickness of the aquifer. It is well known that satisfying the assumption of aquifer homogeneity is impossible in any natural geologic environment. The data from this test enabled the effect of minor stratigraphic heterogeneities to be evaluated in terms of their influence on the dispersivity determinations. The initial breakthrough of the ^{51}Cr-EDTA in the withdrawal well occurred about three days after the start of introduction of the tracer. The peak concentration was reached at about seven days. The results of the two-well model analysis are given in Fig. 9. This compares the ^{51}Cr-EDTA breakthrough curve obtained by measuring samples from the withdrawal well (shown as dots) to the breakthrough curve generated by the computer model (shown as the solid line) using a dispersivity of 50 cm. This dispersivity produced the breakthrough curve that most closely matched the field data.

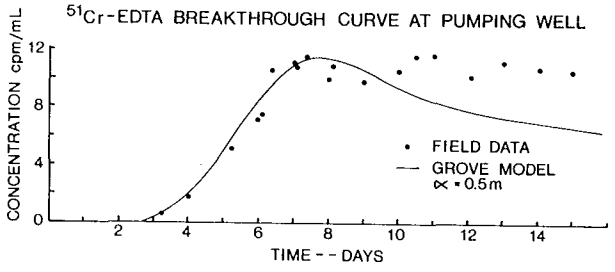

Fig. 9. Breakthrough curve at withdrawal well for two-well tracer test

A computer model based on the finite element method was used to simulate in a horizontal plane the movement of the tracer in the two-well tracer test. The model used is a modified version of that described by Pickens and Lennox[21] for computer simulation of solute transport in cross-section, through a steady-state saturated groundwater flow system. In this analysis, a horizontal slice at any specified depth in the aquifer was assumed to be homogeneous and isotropic. The finite element model solved for the hydraulic head distribution, groundwater velocities and transient concentration distribution. The calculated hydraulic head distribution was consistent with the measured values from the piezometer network. The concentration data from the network of multi-level samplers

indicated that the tracer movement was essentially horizontal at all levels in the aquifer. For simulation of the movement of the ^{51}Cr-EDTA, a horizontal slice at depth 8.1 m was chosen. This slice is representative of the zone of most rapid tracer movement. Fig. 10 shows the concentration profiles directly between the two wells at this depth. A longitudinal dispersivity of 10 cm in the finite element model gave the best fit to the field data. This is one-fifth of the value of dispersivity obtained using the two-well Grove model.

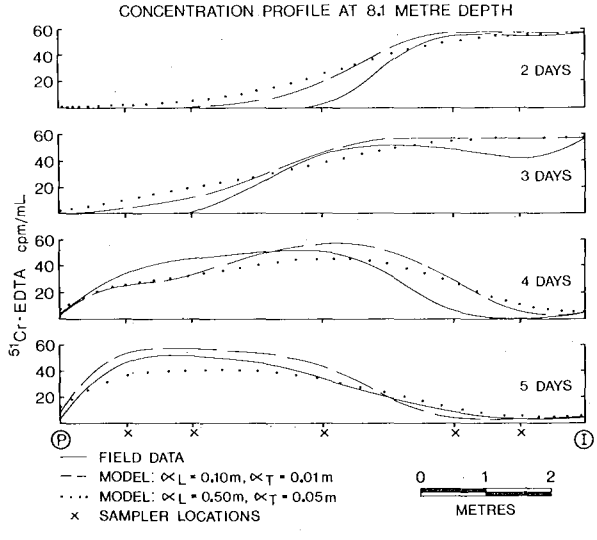

Fig. 10. Concentration profiles between wells at 8.1 m depth for two-well tracer test

Single-Well Injection-Withdrawal Tracer Test

A single-well injection-withdrawal tracer test was conducted using the instrumentation shown in Fig. 5. The well denoted "P" was not used and only the multi-level samplers located directly between the two wells were monitored. Water was recharged to the well denoted "I" at a rate of 54 L/min until steady-state flow conditions were attained. The piezometer network was monitored to establish the hydraulic head distribution during the test. Approximately 50 mCi (1.8 GBq) of the tracer, ^{131}I having a half-life of 8.07 days, were added to the injection water for a period of 30 hours. The input concentration was maintained at about 225 cpm/mL. At the end of 30 hours of injection of tracer, water was withdrawn from the well at a rate of 54 L/min for three days. The concentration of ^{131}I was monitored in samples taken from the well during injection and withdrawal, and from the multi-level samplers. All samples were corrected for radioactive decay to the time at which the tracer test was started.

A field dispersivity value was obtained from the results of the single-well tracer test using the method described by Mercado[22]. The relation between relative concentration of tracer in the pumped water during the withdrawal phase and the ratio of the pumped volume to the recharged volume yields a value of dispersivity in the direction of flow. The dispersion in radial flow (during the recharge and discharge phases) is assumed to be the same as for a longitudinal flow case. The radial flow field is assumed to be in steady-state during injection and withdrawal. The breakthrough curve determined from water samples during pumping is shown in Fig. 11. The sample concentrations are given by the solid dots and the average input concentration during injection is shown as a dashed line. The ratio of pumped to recharged volumes is equal to unity at time 30 hours. Analysis of this breakthrough curve from sampling the well (equivalent to full aquifer depth) yielded a dispersivity of 3.4 cm.

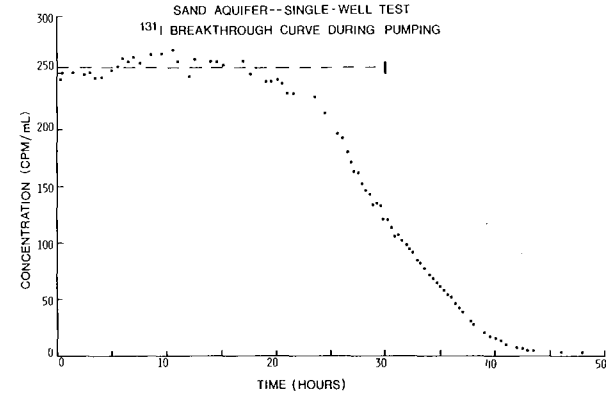

Fig. 11. Breakthrough curve during withdrawal for single-well tracer test

Breakthrough curves during the injection phase obtained from water samples from sampling points at the 8.1 m depth at distances of 1, 2 and 4 m from the injection well were analyzed using an analytical solution by Hoopes and Harleman[23]. Various values of dispersivity were used as input to the analytical solution until the computed breakthrough curve approximated the field values obtained. The field results and the analytical solution results for dispersivities of 3.4 and 10 cm are shown in Fig. 12. These dispersivity values produced breakthrough curves which are reasonably close to the field measured concentrations.

Discussion of Results

The value of dispersivity of 50 cm obtained by analysis of the breakthrough curve for the withdrawal well in the two-well tracer test is much larger than the value of 10 cm obtained from analyzing tracer movement in an individual layer. Based upon the measured velocity profile in the aquifer, we believe the large dispersivity value to represent the effect of mixing in the well of water of differing tracer concentrations from the various levels within the aquifer. This method of sampling and analysis could be considered to be at the megascopic scale whereas sampling from an individual layer within the aquifer using the multi-level point samplers is approaching the macroscopic scale. The dispersivity results for this two-well test are shown in Table I which also lists for comparison other values reported in the literature.

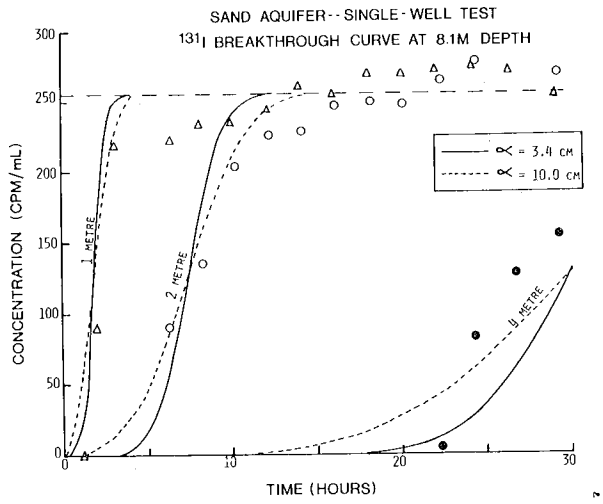

Fig. 12. Concentration breakthrough curves at 8.1 m depth for single-well tracer test

In the single-well tracer test, the value of dispersivity of 3.4 cm obtained by analysis of the breakthrough curve produced during pumping is similar to the value obtained by analysis of the concentration variations in the point samplers located in the high transport layer. Analysis of tracer movement in this layer yielded a value of about 3.4 to 10 cm. Although the water samples from pumping the well represent water contributed from the full depth of the aquifer, the effect of stratification within the aquifer was much less pronounced than for the two-well tracer test. Also

	BETWEEN WELLS, m	SCREEN LENGTH, m	DISPERSIVITY, m: FULL AQUIFER	DISPERSIVITY, m: PLANE OF HIGH VELOCITY
ROBSON	6	27	15	—
WILSON	79	4	15	—
THIS STUDY	8	8	0.5	0.1

Table I. Values of dispersivity of granular materials for two-well tracer tests

the zone of influence for the single-well test is much less (mean radius of 3 m) than that for the two-well test. The above reasons may account for the observation that the full-aquifer dispersivity obtained from the single-well test is approximately the same as for the high velocity layer within the aquifer. The dispersivity results for the single-well test are shown in Table II. For comparison this table lists other values from single-well tests reported in the literature. A comparison of the single-well and two-well test results (Tables I and II) for situations where dispersivity values were computed from concentration data obtained from full-aquifer withdrawal wells indicates that the single-well dispersivities are much lower than the two-well dispersivities. The two-well dispersivity value obtained in our study using the plane-of-highest-velocity analysis however, yielded a value which is only slightly larger than the single-well test value and which is within the range of single-well values reported by other investigators.

	SCREEN LENGTH, m	DISPERSIVITY, m: FULL AQUIFER	DISPERSIVITY, m: PLANE OF HIGH VELOCITY
MERCADO	33	0.09-0.15	—
PERCIOUS	15	0.08-0.25	—
THIS STUDY	8	0.034	0.034-0.10

Table II. Values of dispersivity of granular materials for single-well tracer tests

Conclusions

The following conclusions have been developed from analysis of the field investigations:

(1) The point dilution technique is an efficient and reliable method for identifying high transport zones within aquifers.

(2) The detailed field tracer experiments indicate that the multi-level point sampling device used in this investigation is an efficient and relatively inexpensive means of monitoring the migration of tracers or contaminants in shallow cohesionless geologic materials.

(3) In the single-well test, the value of dispersivity obtained for the full aquifer depth was 3.4 cm. This is approximately the same as that obtained (3.4 to 10 cm) for an individual layer and is only slightly smaller than the value (10 cm) obtained from the individual layer analysis for the two-well test. A much higher value (50 cm) was obtained from the analysis of the breakthrough curve at the withdrawal well in the two-well test. Based on the results of our test, it is apparent that dispersivity values obtained from two-well tests are greatly influenced by the type and distribution of sampling devices used to obtain the concentration data for analysis. Our studies suggest that in two-well tests the large dispersivity values obtained from analysis of the breakthrough curve at the withdrawal well are mainly a result of mixing that occurs in the well bore of water from different levels in the aquifer.

Acknowledgements

The authors appreciate the assistance of G.E. Grisak, K.J. Inch, R.E. Jackson, B.A. Risto, E.A. Sudicky and H. Vandor in various aspects of the field experiments and their analysis. Financial support for this research has been provided through the Atomic Energy of Canada Limited, Environment Canada and National Research Council of Canada Grant No. A8184.

References

1. Shamir, U.Y. and D.R.F. Harleman, "Numerical solutions for dispersion in porous mediums", Water Resour. Res. 3(2), 557-581, 1967.

2. Bear, J., "Some experiments in dispersion", J. Geophys. Res. 66(8), 2455-2467, 1961.

3. Lai, S-H. and J.J. Jurinak, "Numerical approximation of cation exchange in miscible displacement through soil columns", Soil Sci. Soc. Amer. Proc. 35, 894-899, 1976.

4. Konikow, L.F., "Modeling solute transport in groundwater", Environmental Sensing and Assessment (Proc. Int. Conf., Las Vegas, Nevada, U.S.A. 1975), Institute for Electrical and Electronics Engineers Inc., U.S.A. Article 20-3, 6 p., 1976.

5. Konikow, L.F. and J.D. Bredehoeft, "Modeling flow and chemical quality changes in an irrigated stream-aquifer system", Water Resour. Res. 10(3), 546-562, 1974.

6. Pinder, G.F., "A Galerkin-finite element simulation of groundwater contamination on Long Island, New York", Water Resour. Res. 10(3), 546-562, 1973.

7. Robson, S.G., "Feasibility of water-quality modeling illustrated by application at Barstow, California", Water Resourc. Invest. Rep. 46073, U.S. Geol. Survey, Menlo Park, Calif., 66 p., 1974.

8. Wilson, L.G., "Investigations on the subsurface disposal of waste effluents at inland sites". U.S. Dept. Interior, Research and Development Progress Report No. 650, 106 p., 1971.

9. Narasimhan, T.N., J.A. Cherry, D.L. Bingham and P.A. Witherspoon, "Interpretation of water quality data from observations wells in stratified aquifers", Abstract in Transactions American Geophysical Union 57(12), 912, 1976.

10. Childs, K.E., S.B. Upchurch and B. Ellis, "Sampling of variable waste-migration patterns in groundwater", Ground Water 12(6), 369-377, 1974.

11. Palmquist, R. and L.V.A. Sendlein, "The configuration of contamination enclaves from refuse disposal sites on floodplains", Ground Water 13(2), 167-181, 1975.

12. Cherry, J.A., R.E. Jackson, D.C. McNaughton, J.F. Pickens and H. Woldetensae, "Physical hydrogeology of the lower Perch Lake basin". In: Hydrological Studies on a Small Basin on the Canadian Shield, Ed. by P.J. Barry, Atomic Energy of Canada, Chalk River Nuclear Laboratories, AECL-5041, Vol. 2, p. 625-680, 1975.

13. Hubbert, M.K., "The theory of groundwater motion", J. Geol. 48(8), 785-944, 1940.

14. Bear, J., "Dynamics of fluids in porous media", American Elsevier Publ. Co. Inc., 764 p., 1972.

15. Pickens, J.F., W.F. Merritt and J.A. Cherry. "Field determination of the physical contaminant transport parameters in a sandy aquifer". In: Proc. IAEA Advisory Group Meeting on The Use of Nuclear Techniques in Water Pollution Studies, Cracow, Poland, 6-9 December 1976. In press.

16. Woldetensae, H., "Comparative hydraulic conductivity studies in the lower Perch Lake basin". M.Sc. Thesis, University of Waterloo, Waterloo, Ontario, Canada, 228 p.

17. Halevy, E., H. Moser, O. Zellhofer and A. Zuber, "Borehole dilution techniques: A critical review". In: Isotopes in Hydrology (Proc. Int. Symp. Vienna 1966), IAEA, Vienna, 531-564, 1967.

18. Merritt, W.F., "Groundwater conductivity measurements by point dilution". In: Hydrological Studies on a Small Basin on the Canadian Shield, Ed. by P.J. Barry, Atomic Energy of Canada Limited, Chalk River Nuclear Laboratories, AECL-5041, Vol. 2, p. 615-624, 1975.

19. Grove, D.B. and W.A. Beetem, "Porosity and dispersion constant calculations for a fractured carbonate aquifer using the two-well tracer method", Water Resour. Res. 7(1), 128-134, 1971.

20. Grove, D.B., "U.S. Geological Survey tracer study, Amargosa Desert, Nye County, Nevada, Part II: An analysis of the flow field of a discharging-recharging pair of wells". U.S. Geol. Survey Report USGS-474-99, 56 p., 1971.

21. Pickens, J.F. and W.C. Lennox, "Numerical simulation of waste movement in steady groundwater flow systems", Water Resour. Res. 12(2), 171-180, 1976.

22. Mercado, A., "Recharge and mixing tests at Yavne 20 well field", Underground Water Storage Study Technical Report No. 12, TAHAL-Water Planning for Israel Ltd., Tel Aviv, P.N. 611, 62 p., 1966.

23. Hoopes, J.A. and D.R.F. Harleman, "Dispersion in radial flow from a recharge well". J. Geophys. Res. 72(14), 3595-3607.

24. Percious, D.J., "Aquifer dispersivity by recharge-discharge of a fluorescent dye tracer through a single well". M.Sc. Thesis, University of Arizona, Tuscon, Arizona, 80 p., 1969.

Application of Well Testing to Liquid Dominated Geothermal Systems

T. N. Narasimhan

Lawrence Berkeley Laboratory
University of California
Berkeley, California 94720

Introduction

Since September 1975 the Lawrence Berkeley Laboratory has been engaged in well-testing of liquid dominated geothermal reservoirs in the Raft River Valley of Idaho and at East Mesa in southern California (Witherspoon, et al., 1976; Narasimhan and Witherspoon, 1977; Narasimhan, et al., 1977). These tests have established that well-testing, based on the techniques developed in the fields of petroleum engineering and hydrogeology, is invaluable in estimating the in situ parameters and in deciphering the geometry of geothermal reservoirs. However, due to high temperatures of geothermal fluids (generally in excess of 300°F) and due to the highly corrosive nature of geothermal brines, the instruments needed to make various measurements in a geothermal well must be capable of performing over prolonged periods of time in highly hostile environments. Moreover, the spacing of wells in geothermal reservoirs may often be of the order of a few to several thousand feet. As a result, highly sensitive pressure measuring devices are needed if interference effects on these wells are to be observed and interpreted.

During the course of the well-testing experiments at Raft River and at East Mesa, different types of instruments were used and considerable experience was gained in regard to their operational utility. In addition, the data forthcoming from these tests had special features which had to be given due consideration before attempting interpretation. The purpose of this paper is first to summarize the knowledge gained during the aforesaid tests in regard to: a) instrumentation and data collection, b) the quality and nature of the data forthcoming, c) control of test conditions, and d) interpretation. Based on this, some of the problems that currently exist in regard to testing liquid-dominated geothermal reservoirs are identified and suggestions are made on the directions in which further research might be directed.

Before proceeding further, it is in order to provide some background information on the geothermal reservoirs at Raft River and at East Mesa.

The Raft River Valley geothermal field (Witherspoon, et al., 1976; Narasimhan and Witherspoon, 1977) is located in southeastern Idaho. The geothermal resource here occurs in sedimentary and volcanic rocks of tertiary age overlying a pre-Cambrian quartz-monzonite. The resource, at a temperature of about 295°F, is tapped by means of three wells, reaching down to a maximum of 6,000 feet.

The East Mesa geothermal anomaly in southern California is currently being explored by the U.S. Bureau of Reclamation and by two private companies, Republic Geothermal Company to the north and Magma Power Company to the south. Currently there are fourteen geothermal wells in this area (five owned by the U.S. Bureau of Reclamation; six by Republic Geothermal Company; and three by Magma Power Company). In general, the wells range in depth from 5,000 to 8,000 feet and derive fluids from tertiary sediments. The temperature of the resource ranges from 300 to 400 °F (?).

Since both the Raft River and the East Mesa sites are of exploratory nature and since very little data was available on the in situ reservoir characteristics of the reservoirs, the well tests were designed with the aim of estimating overall reservoir parameters and to decipher reservoir geometry. The tests conducted included productivity index tests as well as interference tests. These tests ranged in duration from a few days to several weeks.

Instrumentation and Data Collection

The primary data to be collected during geothermal well tests include mass flow rates, pressure and temperature. In addition to the instruments required to measure these quantities, appropriate equipment are also needed to automatically record them to facilitate data storage and retrieval. Finally, the use of a variety of sophisticated instruments in the field requires that skilled technical help be available to operate and maintain the equipment.

Since the reservoirs tested were liquid dominated, there was no flashing of the fluids within the reservoir. However, there may or may not be flashing within the well-bore. In order to measure flows, therefore, it is convenient to pass the output from the well into a steam separator, pass the separated steam and water through different orifice plates and measure flow rates, using the appropriate equations connecting orifice configurations, pressure drop and mass flow rates. If there is no flashing in the well-bore, the output from the well could be directly passed through an orifice plate to measure the liquid mass flow rate. In this case it may be necessary to provide sufficient back pressure so that there is no flashing at or in the vicinity of the orifice plate. A less accurate, and sometimes acceptable, method of measuring liquid flowrates is to use a weir box.

One problem that may often arise in using orifice plates is that of scaling. Even though the East Mesa geothermal brine is relatively low in dissolved solids (less than 30,000 ppm, TDS), it was found that significant scale deposition occurred downstream of the orifice which affected the accuracy of flow calculations. To avoid this an extra by-pass line was provided to enable cleaning or replacement of orifice plates without shutting in the well.

In the tests conducted so far, the principal aim was to decipher the reservoir characteristics by assuming the reservoir to be isothermal and directly applying the well-testing methods of petroleum engineering and hydrogeology. As a result, the measurement of temperatures has not been critical. The temperature data collected during the tests (mostly at the well-head and the spearator and occasionally downhole) were for the purpose of either calculating steam quality or for the purpose of applying temperature corrections to the pressure data.

By far the most critical data from the point of view of well testing relate to pressure transients. In general it is preferable to be able to measure these data in the well-bore, opposite the reservoir. Although this is not always possible in geothermal wells, under certain conditions, measurement of well-head pressures can yield the same pressure differential data that can be monitored downhole. During the tests at Raft River and East Mesa, three different kinds of pressure measuring instruments were used. These were:

a. An ultra sensitive downhole pressure gauge employing a piezo-electric quartz crystal, manufactured by Hewlett-Packard Company,

b. An ultra sensitive well-head pressure gauge employing a piezo-electric quartz crystal, manufactured by Paroscientific Company, and

c. A downhole pressure gauge employing a gas column, manufactured by Sperry-Sun Company.

The Hewlett-Packard downhole pressure gauge is designed to provide pressure measurements accurate to 0.01 psi up to a maximum of 10,000 psi and to withstand up to 300 °F for prolonged periods of time. The downhole instrument communicates with a surface based computer and recording device through a conductor cable. The frequency response of the crystal caused by pressure changes is converted automatically to pressure data which is displayed continuously and printed out at desired time intervals. Since quartz possesses pyro-electric properties in addition to piezo-electricity, a temperature correction is essential before frequency response can be converted to pressure. For this purpose, the pressure tool is connected in tandem with a temperature tool which facilitates in situ temperature measurements. The HP gauge was successfully used for periods of up to several days at temperature of 295 °F at Raft River in Idaho. However, at East Mesa it operated for about 40 hours at a temperature of 318 °F before breaking down due to electronics failure.

It is well known that in interpreting well test data one is interested in pressure differentials rather than absolute pressures. Because of this, it is sometime possible to get around the difficulty of measuring downhole pressures in geothermal wells and obtain the required data from well-head measurements. Thus, in shut-in artesian wells (i.e., wells with positive well-head pressures) the downhole pressure changes at the sandface are transmitted instantaneously to the well-head. Both at Raft River and at East Mesa, all the geothermal wells have positive well head pressure ranging from 60 to 150 psi shut-in. Therefore, it is possible to use the Paroscientific well head pressure gauge on these wells. Like the H.P. gauge, the Paroscientific instrument also takes advantage of the piezo-electric properties of quartz and measures the frequency response of the crystal to fluid pressure changes. This instrument too provides accuracy of 0.01 psi up to 900 psi and yields automatic printouts at desired intervals in addition to providing continuous visual display of pressures.

In Figure 1 a comparison is shown of the downhole data collected with the H.P. gauge and the well-head data collected with the Paroscientific gauge. These data were collected from the same well, with the HP gauge set at approximately 1,000 feet below ground level. As can be seen from the Figure, both instruments agree very well in regard to the observed changes in pressure. The only point that may be added here is that, during this test, the Paroscientific instrument had a column of air acting as a buffer between the geothermal fluid and the quartz crystal. This air column expanded and contracted in response to diurnal variations in temperature, causing slight distortions in the pressure profile. This problem was eliminated in subsequent tests by replacing the air column with silicone oil. Incidentally, the conspicuous fluctuations seen in Figure 1 show the influence of earth tides on reservoir pressures.

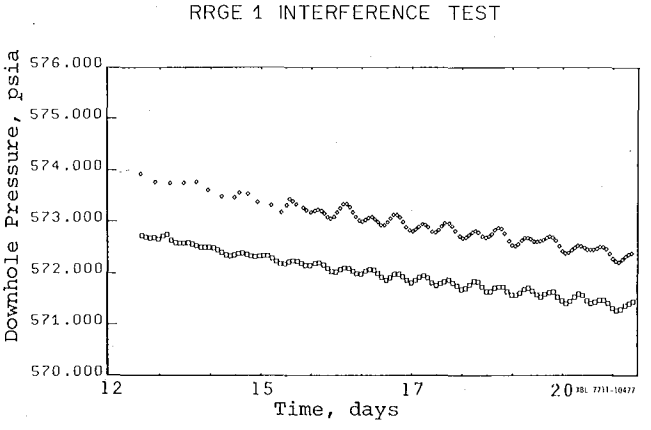

Figure 1. Example of data collected downhole with the Hewlett Packard gauge (◇) and at the well-head with Paroscientific gauge (□). Well RRGE 1, Raft River Valley, Idaho.

One of the great advantages of the automatic recording devices is that they enable the collection of very early time drawdown or build up data which are invaluable in the interpretation of such features as fractures, well-bore damage and skin effects. In Figure 2 is shown the buildup data from Well RRGE 2 in Idaho. In this test, data printout was obtained at one-second intervals and about 50 data points were available within the first minute of buildup.

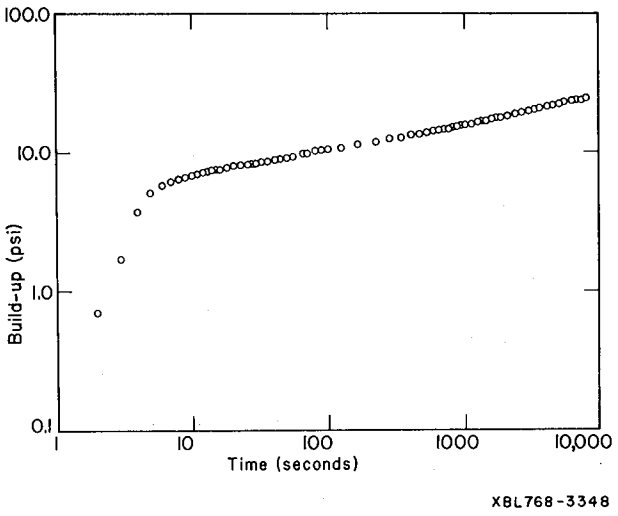

Figure 2. Short-term production test on RRGE 2, Raft River Valley, Idaho: Log-log plot of pressure buildup.

A problem that is frequently encountered in the use of the downhole pressure gauge is that of data noise. Such noise is generally random and may have magnitudes of one psi or more. Figure 3 shows a segment of the noisy data collected from Well 6-1 at East Mesa during early 1976.

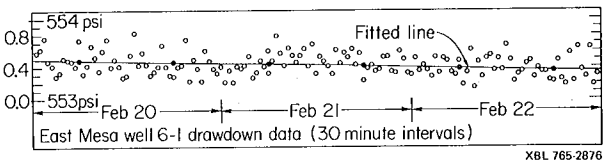

Figure 3. Drawdown data from observation well 6-1 at East Mesa. Data recorded by a downhole pressure (H.P.) gauge at approximately 1500 feet below ground level.

The cause of this noise, which may be electronic or electrical is being investigated.

The Sperry-Sun downhole pressure gauge measures downhole pressures by using a small diameter (≈0.05" I.D.) tube filled with Helium or Nitrogen to transmit pressures readings from downhole to the surface. In addition to providing visual readout, this instrument set up can also provide automatic printout at desired intervals. At East Mesa, this instrument was used to measure pressures in the range of 2,000 to 2,500 psi, at which pressures the accuracy is probably about 0.1 psi. An advantage with this set up is that it is not constrained by any temperature limitations. The experience gained at East Mesa with this instrument indicates that care might have to be exercised in choosing a proper inner diameter size for the gas filled tube. In Figure 4 a segment of pressure data is presented collected from a depth of 5000 feet using a tubing with an inner diameter of .026 inches and using nitrogen gas. The downhole temperature at the depth is known to be about ≈360°F while the shut-in well-head temperature at the time of installing the instrument was atmospheric. Shortly after installation, production was commenced at a rate of 60 gpm.

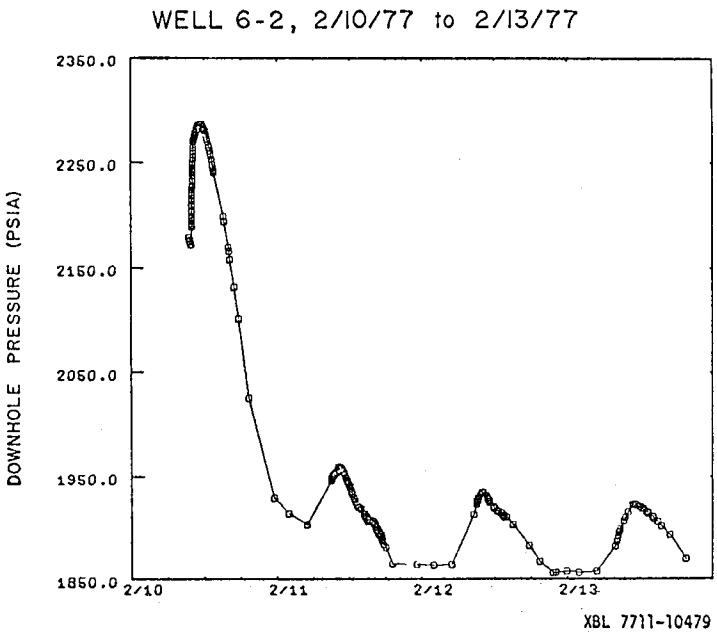

Figure 4. Downhole pressures measured with Sperry-Sun gauge using a .026 inch I.D. tube.

As seen from Figure 4, the downhole pressures significantly increased (≈125 psi) for the first 90 minutes after commencement of production, before starting to decline. During this period the well-head temperatures rose to ≈320 °F. This anomalous increase in pressure is attributable to the gradual heating of the tube as the geothermal changes from the static temperature profile to the flowing temperature profile. A serious consequence of this temperature perturbation of pressure is that it is extremely difficult to define a proper value for initial reservoir pressure with reference to which drawdowns are to be evaluated.

Also during this test, approximately 1000 feet of the excess tubing length remained on the spool at the surface and could only be crudely insulated. The gas in this part of the tubing was subject to the diurnal variations in temperatures causing the three peaks (once daily between 2/11 and 2/13/77).

In a subsequent test, a larger diameter tubing (.054 inches I.D.) was used and the results obtained using nitrogen gas are shown in Figure 5. As can be seen from this Figure, the initial perturbation to pressures soon after the start of production has been short-lived and small and there are no perceptible diurnal effects.

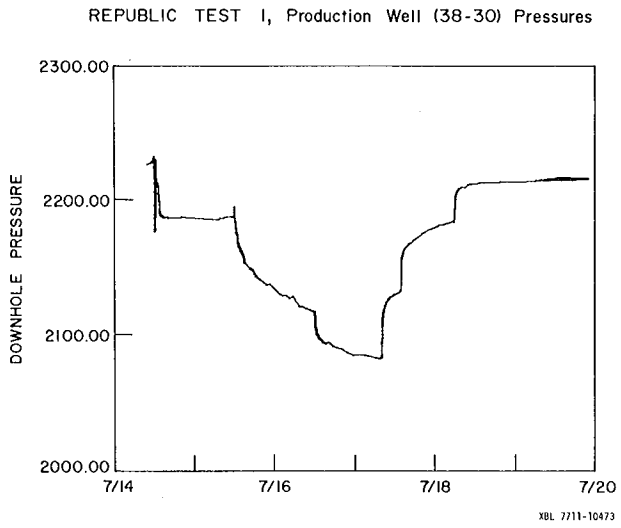

Figure 5. Downhole pressures measured with a Sperry-Sun gauge using a .054 inch I.D. tube.

It is also pertinent to point out here that a suitable correction for the weight of nitrogen has to be applied to the pressure readings if it is desired to obtain absolute bottom hole pressures. Such correction depend on both the temperature profile in the well and the length of tubing in the well.

The susceptibility of the transmission tubing to the corrosive effects of geothermal brines can sometimes cause serious problems in using the Sperry-Sun system over prolonged periods of time. Since the geothermal fluids at Raft River and at East Mesa are relatively low in dissolved solids, the problem of corrosion was of no concern. However, it is reported that at Niland near Salton Sea, where the geothermal fluids are highly corrosive, it is diffiuclt to keep the tubing functional for more than a few days at a time. The only possible method of avoiding this problem, it appears, is to look for more corrosion resistant tubing materials.

The tests so far conducted have clearly established that meaningful testing of geothermal reservoirs may often involve simultaneous data gathering from several wells over a period of several weeks. In order that subtle variations in pressure changes, which may yield important information on the reservoir, are not missed, it is advisible to monitor pressures continuously at intervals of ten to fifteen minutes throughout the test. This, leads to the accumulation of a volume of data too difficult to be gathered manually. To overcome this problem, it is essential to have an automated, a centralized data gathering system where all data from different instruments is gathered and recorded. At present, the LBL field unit has a central recording van to which all the well-head or downhole instruments communicate by telephone wires. A data logger which is currently being designed at LBL, will enable the automatic recording of the data on to multi-channel magnetic tapes, which will greatly help minimize data handling efforts in the future.

The use of sophisticated measurement devices as well as sophisticated centralized recording instruments in the field renders it imperative to have a well trained crew of technical persons capable of assembling and maintaining the required instruments. In addition to the availability of experienced electrical and mechanical engineers to design and fabricate various peripheral equipment, the LBL well-testing effort is aided by the round-the-clock availability of a crew of highly skilled electrical and mechanical technicians.

Quality and Nature of Data

The availability of highly accurate measuring devices as well as automatic recording equipment at very frequent intervals has tremendously enhanced the breadth of information that can now be elicited from the well tests. The extensive pressure transient data collected at Raft River and East Mesa has indicated that fluid pressures in these liquid dominated geothermal systems respond to seismic events. The presence of earth tide and siesmic effects in pressure transient data lead to two practical consequences in relation to well-testing. First, it is necessary to filter out these extraneous noises and isolate the pressure transient trends caused exclusively by well tesiing. Such filtering could be either carried out by careful eye judegement or be achieved through regression analyses, fast Fourier transform and and other such techniques. Secondly, the magnitude of the fluid pressure response in a well and its relation to the carefully measured or computed earth-tides may provide valuable clues about the elastic properties or permeability of the reservoir. Or again, the response of some wells in a well field to some microseisms but not others may help infer the presence of faults or other boundaries in the reservoir.

In Figure 6 is presented a segment of data collected from an observation well, 16-29, at East Mesa (owned by Republic Geothermal Company). This well is located about 4,200 feet from Well 38-30 (Figure 14), which commenced production at 1200 hours on July 14, and was shut in at 0600 hours on 18, 1977. The marked drop in the pressure seen in Figure 6 subsequent to July 16 denotes the response of Well 16-29 to the production from 38-30. The periodic fluctuation of pressures having two maxima and two minima everyday denote earth tide effects. In this particular well the amplitude of tidal variation ranges from 0.2 to 0.4 psi.

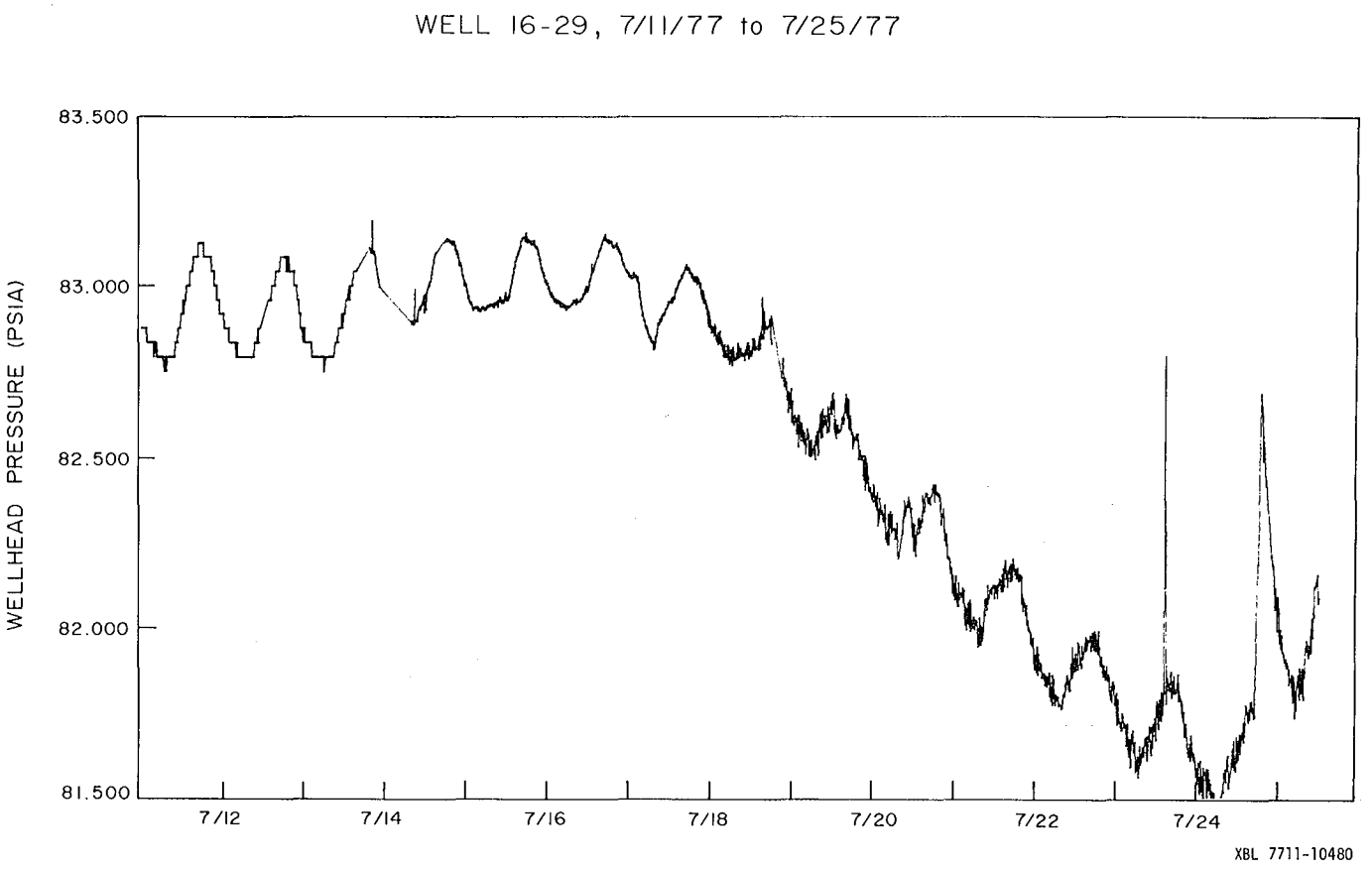

Figure 6. Well-head pressures from Well 16-29 owned by Republic Geothermal Company at East Mesa.

In Figure 7 is shown the pressure data collected from the Bureau of Reclamation's Wells 6-1 and 8-1 at East Mesa. Note in this figure that, despite the general noise in the data, two prominent peaks could be seen in Well 8-1 occurring approximately at 0340 hours and at 0410 hours on Feb. 13, 1976. Examination of microseismic records collected within the well field show that during the same period, there was considerable microseismic activity within the area. It is also interesting to note that Well 6-1 does not show any anomalous increase in fluid pressure during the same time, suggesting that perhaps there may be certain energy absorbing discontinuities in the vicinity of Wells 6-1 and 8-1.

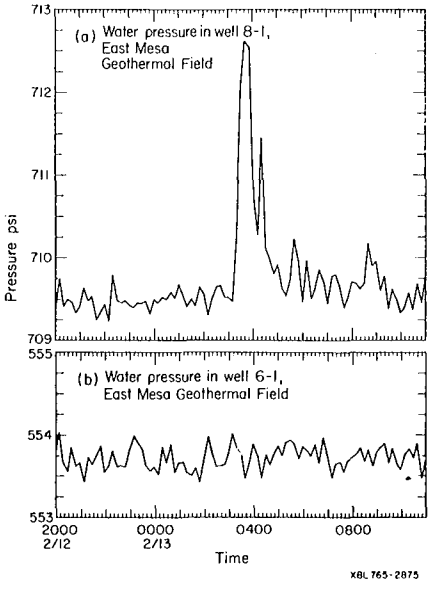

Figure 7. Pressure transient data from wells: A. 8-1 and B. 6-1 at East Mesa showing response of fluid pressures to microseisms.

In addition to the diurnal trends in earth-tide effects, the data may also show low frequency fluctuations with periodicity of one week or more. Figure 8 is a plot of well-head pressures measured on Well 31-1 (owned by the U.S. Bureau of Reclamation) at East Mesa for a period of over two months. During this period, Wells 6-2 and 6-1, (also owned by the same agency) located approximately a mile and a half away, were producing continuously with a combined discharge of about 100 gpm. A careful scrutiny of this Figure will show that in addition to showing diurnal earth-tide effects, there exist low frequency fluctuations with periodicity of ranging from one to two weeks. Also, despite the presence of these extraneous influences one could still decipher an overall decline in fluid pressures amounting to approximately 0.15 psi over the two-month period, caused by the production at Wells 6-2 and 6-1.

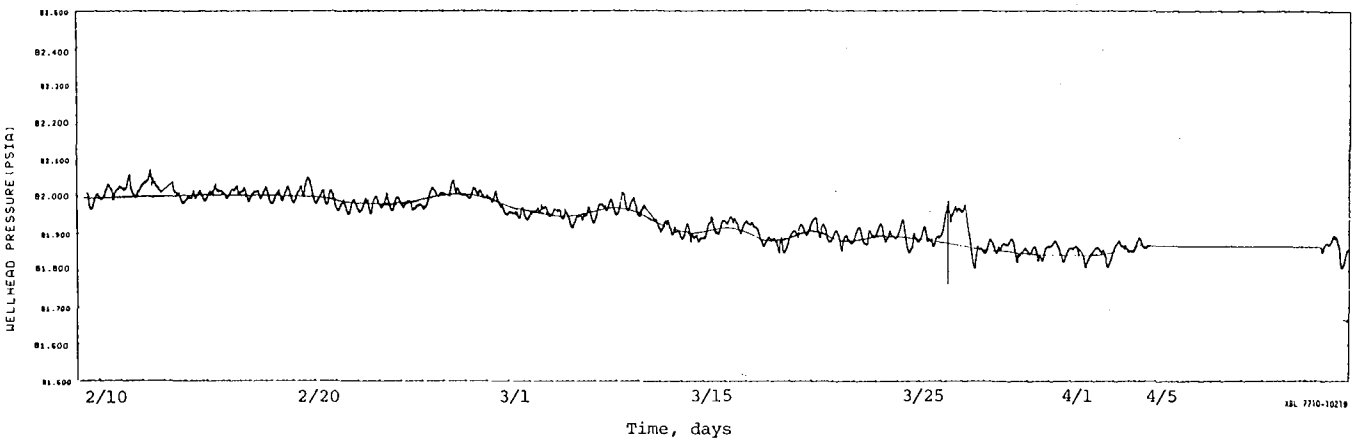

Figure 8. Well-head pressures from well 31-1 owned by the U.S. Bureau of Reclamation at East Mesa.

Control of Test Conditions

As in the case of any scientific experiment, the design and controlled execution of a well test are of utmost importance. The design of a well test depends on the goals to be achieved. In the Raft River and the East Mesa examples the tests were designed to obtain information principally on reservoir characteristics and geometry in order to assess resource size and recoverability. Once a well test is designed, the test conditions must be controlled as much as possible to fit the design conditions. Nevertheless, there are several factors which render the control of geothermal well test conditions difficult. For example, the magnitude of discharge may be restricted because disposal of the fluids into holding ponds or through injection wells may be necessary. Or it may so happen that other activities such as heat exchanger experiments and corrosion or scaling studies may be in progress, making specific demands on the control of flow rates. Or, again, it may be necessary to produce the well for short periods of time before the actual test in order to stimulate the well or to test out equipment. Some of these activities are unavoidable and will have to be given due consideration in developing appropriate techniques of interpretation. Yet another difficulty that may frequently crop up is the uncontrolled production or injection of fluids into nearby wells. The problems arising out of these uncontrolled activities are of two kinds. These are: a) variable flow rates and ambiguities in defining the starting time and b) ambiguities in defining the static or initial reservoir pressure.

Most analytical solutions developed in hydrogeology and petroleum literature pertain to the case of constant flow rates. These solutions are of very little use when flow rates become arbitrarily variable due to unavoidable reasons. However, a recently developed computer-assisted mathematical technique (Tsang, et al., 1977) enables interpretation of data from arbitrarily variable discharge tests in the presence of boundaries, well-bore storage and skin effects. In order that this method is efficiently employed, it is imperative that a very careful record is kept of all the productions and shut-in activities that have to be performed before and during the tests.

The ambiguities in defining a proper static reservoir pressure may often greatly minimize the utility of the data that is gathered at great expense and effort. This may particularly be a problem in outlying observation wells in which the pressure response may be measurable but not strong. It is therefore essential to monitor background pressures at least several days prior to a test and also avoid any unscheduled production or injection activities in wells located close to an observation well. As an example, Figure 9 shows the pressure transient data from Well 44-7 at East Mesa, owned by Magma Power Company. This observation well is located about 5,000 ft from Well 6-2 which started production on February 10, 1977 at approximately 60 gpm and continued to flow for several weeks. A shallow well, 46-7, proposed to be used as an injection well, was drilled in late January, about 2,000 feet from 44-7 and some unscheduled injection and production activities were carried out on this well between February 8 and February 20, 1977, as indicated in the diagram. Note from Figure 9 that just prior to and immediately following the start of the interference test on February 10, the mean pressure in 44-7 has been gradually increasing from 92.63 psi to 92.8 psi. Is this increase caused by the shallow zone injection prior to February 10? If so, what is the static reservoir pressure? It is difficult to provide clear answers to these questions and the result is a significant ambiguity in estimating pressure drawdown.

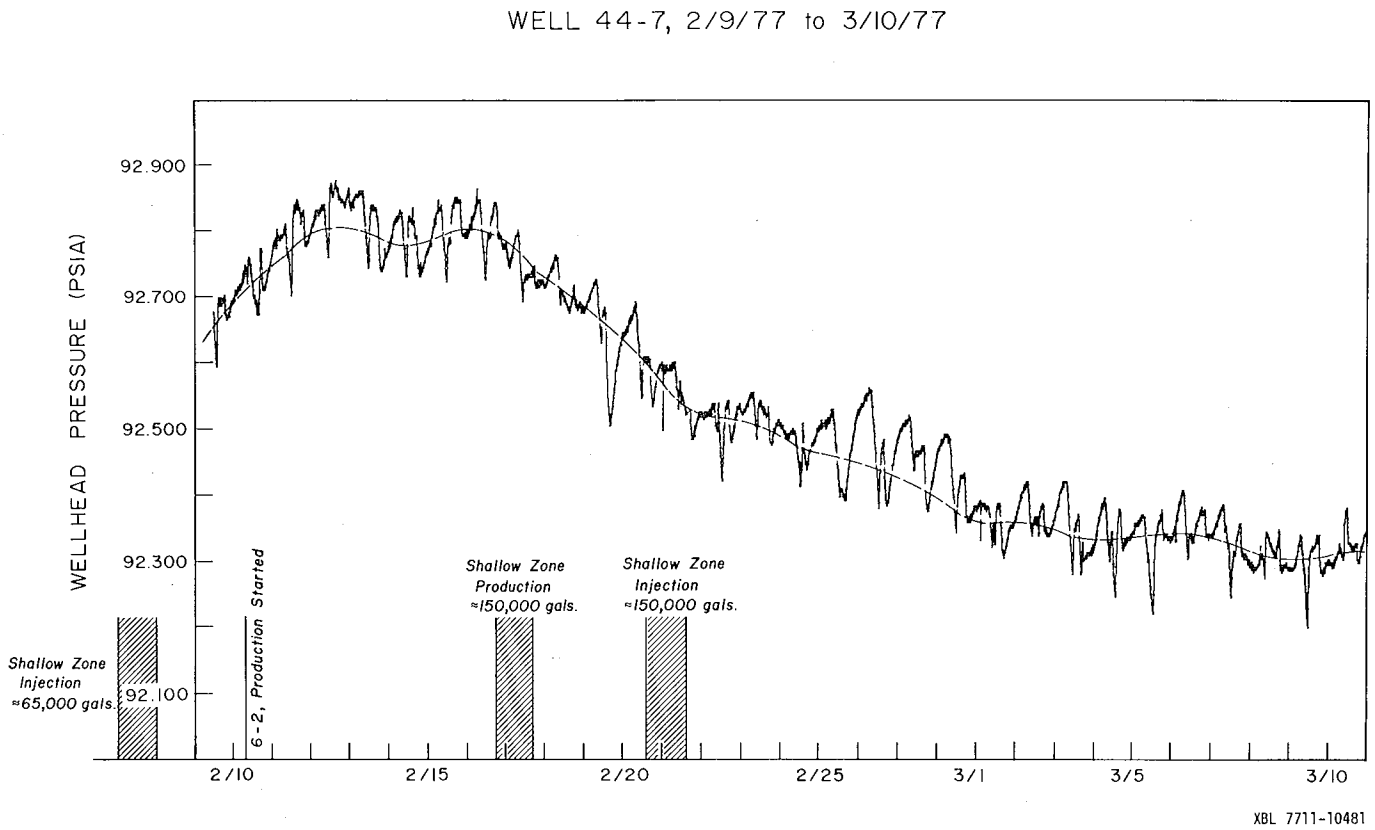

Figure 9. Well-head pressures transient data from well 44-7 at East Mesa owned by Magma Power Company, showing possible perturbations due to shallow zone activities.

Interpretation

Once a test is carried out under favorable conditions, the pressure data are preprocessed to filter out extraneous noises and a good record of the flow history is available, it is relatively a straight forward matter to interpret the data for reservoir characteristics and geometry. As an illustration, let us consider the tentative interpretation of the interference data collected from a recent well test conducted in the well field owned by Republic Geothermal Company at East Mesa.

The test itself was a multipurpose, productivity-index cum interference test. The producing well was Well 38-30 which produced at a variable rate shown in Figure 10. Although the main test started at t = 4,000 minutes, the two isolated productions at 0 and 1,200 minutes had to be carried out to check-out equipment and thus were unavoidable. During this test pressures were measured in 38-30 with a Sperry-Sun device, while well-head pressures were measured in the observation Wells 16-29, 56-30 and 31-1 using Paroscientific gauges. For purposes of this illustration, let us consider the interference data from 56-30, shown in Figure 11. As seen from this Figure, the static reservoir pressure is approximately 97 psi

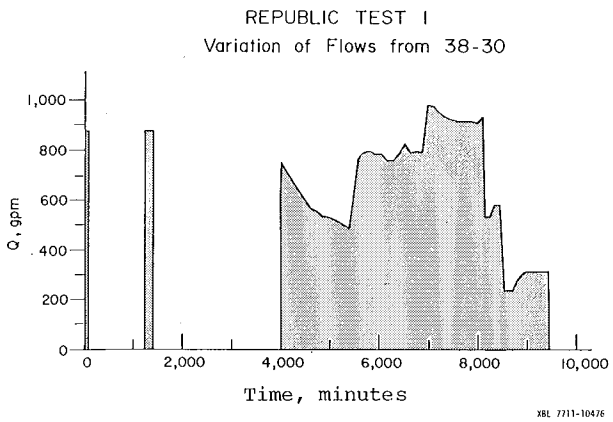

Figure 10. Republic Test 1. Flow history from well 38-30.

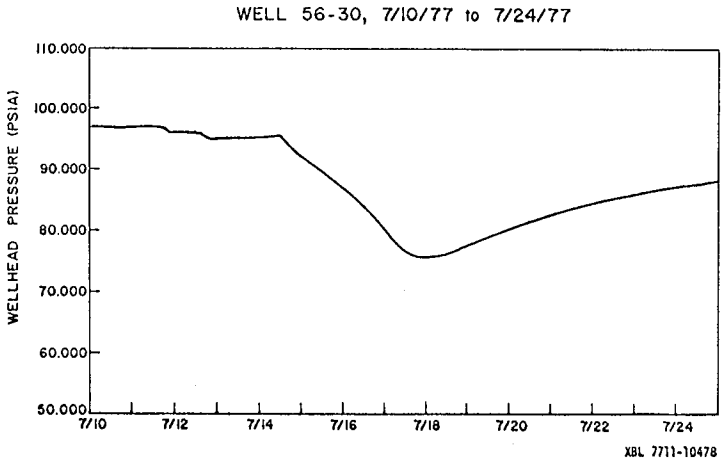

Figure 11. Republic Test 1. Pressure transient data from well 56-30.

and the two small step-like pressure drops seen on July 11 and July 12, 1977 correspond to the two isolated productions in Figure 10. Although the main test did not commence until about 1000 hours on July 14, the inital time t_o in this case was assumed to be 1,700 hours on July 11, 1977.

The data shown in Figures 10 and 11 were interpreted using the computer program COMPFIT developed by Tsang, et al., (1977). Two cases were considered in the interpretation. In the first, Figure 12, the reservoir assumed to be horizontally infinite and the data was interpreted for the two parameters, kH and ϕCH. This yielded kH = 15,200 md-feet and $\phi CH = 4.6 \times 10^{-4}$ feet/psi, with a χ^2 value of 1.664. In the second case, the data

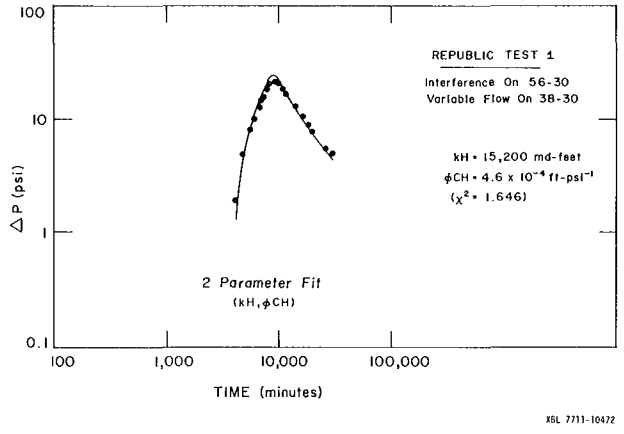

Figure 12. Republic Test 1. Analysis of data from well 56-30 for two parameters, kH and ϕCH.

was interpreted for three parameters, kH, ϕCH, and the radius to an image well equilvalent to a linear barrier boundary. This interpretation is shown in Figure 13. This interpretation yielded

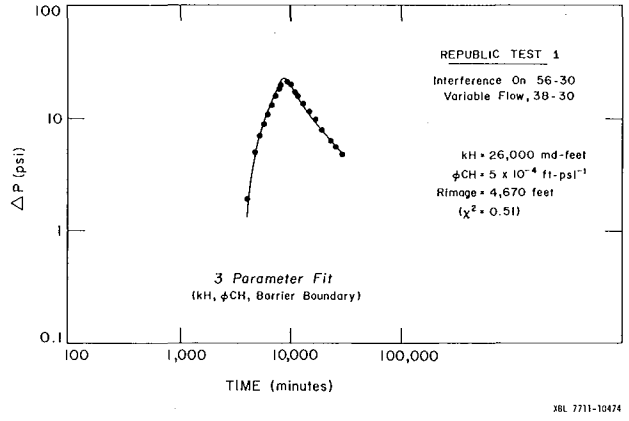

Figure 13. Republic Test 1. Analysis of data from well 56-30 for three parameters, kH, ϕCH, and radius to an image well equivalent to a linear, barrier boundary.

an estimate of kH = 26,000 md-feet, $\phi CH = 5 \times 10^{-4}$ feet/psi and R_{image} 4,670 feet with $\chi^2 = 0.51$. Noting that χ^2 yields a relative estimate on the goodness of fit, the three parameter model is better than the two parameter one. A similar interpretation of the data collected from 31-1 indicated a R_{image} of about 2,800 feet from the image well, while observations made on Well 16-30 (Figure 14) during a subsequent test indicated that this well did not respond to production in Well

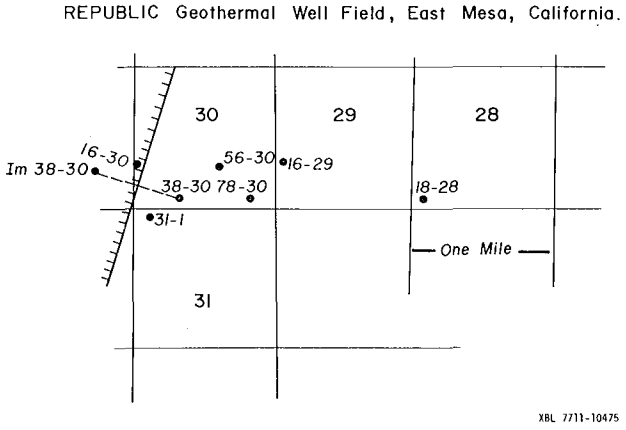

Figure 14. Republic Test 1. Location of wells and disposition of barrier boundary tentatively inferred from well tests.

38-30. Using these three pieces of information, a barrier boundary, trending approximatley NNE can be inferred to exist as shown in Figure 14.

It is interesting to mention here an earlier interference test was conducted between Wells 31-1 and 38-30 in February 1976 during which Well 31-1 was flowed at a near constant rate of 130 gpm. In addition to suggesting a kH of 29,500 md-feet and ϕCH of 2.13×10^{-3} feet/psi, this test also suggested the possible presence of a barrier boundary located between 1,100 and 2,400 feet from 38-30, depending on orientation. However, since measurements were made on only one observation well (38-30) during this test, it was not possible to uniquely located the barrier boundary. As seen in Figure 14, the boundary is about 1,600 feet from 38-30. It is evident that both the tests agree reasonably with reference to reservoir characteristics as well as the presence of the barrier boundary.

Problems and Suggestions

From the experiences presented in the foregoing pages it is clear that a strong theoretical foundation is currently available for designing and execution of well tests on liquid dominated geothermal reservoirs and for interpreting the ensuing results. However, several practical problems do exist in implementing the tests. A few of these problems are summarized below.

There is an immediate need for reliable downhole instrumentation for measuring pressures, temperature and flows. These instruments, in addition to being amenable to automated data recording, must be capable of functioning at elevated temperatures for prolonged periods of time. In addition, there is currently extreme difficulty

in keeping downhole instruments operational for more than a few days when the brine is corrosive. This is another area of instrumentation that needs immediate attention.

In controlling test conditions, the determination of initial reservoir pressure, especially in outlying observation wells, is of considerable interest. This problem could be minimized by proper scheduling of well test activities and the recognition of the importance of background data by the principals involved in well testing.

From the point of view of interpretation, perhaps the most important feature to be noted is the need to eliminate extraneous noise, especially when the interference signal is weak. This is an area in which the ideas and practices of information theory and data analysis must have many valuable applications.

Looking into the future, there are certain other aspects of well testing which have not been covered so far but need to be looked into carefully in order to advance the science of well testing.

The aspect that sets geothermal systems conspicuously apart from hydrogeological and petroleum systems is that in a geothermal system it is not the fluid itself we aim to use as a resource, but the energy transported by the fluid. Yet, the phrase well-testing as it is now applied to geothermal systems totally ignores the role of energy or energy related parameters. In fact, it would appear from our present knowledge that very little theoretical work has been done to identify the most important concepts, models and parameters relevant to the evaluation of energy related parameters of geothermal reservoirs through well tests. Moreover, the exploitation of a geothermal reservoir is very much dependent on the geochemistry of the fluids. Here again, very little has been done to relate the variation of the chemical quality of the fluids during the test to reservoir characteristics. The idea of incorporating measurement of energy related parameters as well as the geochemistry of the fluids into the field of well-testing has arrived. A great deal of benefit is foreseeable if research is actively directed in these two areas.

Acknowledgements

The experiences and ideas contained in the previous pages have been accumulated by many who actively participated in the well-testing activities of the Lawrence Berkeley Laboratory. These include: P. A. Witherspoon, Ron Schroeder, Colin Goranson, D. G. McEdwards and C. F. Tsang, all of whom have been involved with design, planning, and execution of the tests and interpretation of data; Gene Binnall and Carlos Riveros, who have helped design and fabricate specialized electronic equipment; Milt Moebus, Ray Solbau, Don Lippert and Bob Davis, all of whom have assured the operation and maintenance of field equipment; and Sally Benson and Jeannie Mullaney who have been responsible for the processing, storage and retrieval of field data. Exchange of ideas and discussion with all the above is gratefully acknowledged.

Nan Parsons helped with drafting of the figures and editing of the manuscript.

This work was supported by the U.S. Department of Energy.

References

Narasimhan, T.N. and P. A. Witherspoon, "Reservoir Evaluation Tests on RRGE 1 and RRGE 2, Raft River Geothermal Project, Idaho," report LBL-5958, Lawrence Berkeley Laboratory, University of California, Berkeley, 1977.

Narasimhan, T. N., D. G. McEdwards and P. A. Witherspoon, "Results of Reservoir Evaluation Tests, 1976, East Mesa Geothermal Field, California," report LBL-6369, Lawrence Berkeley Laboratory, University of California, Berkeley, 1977.

Tsang, C. F., D. G. McEdwards, T.N. Narasimhan and P. A. Witherspoon, "Variable Flow Well Test Analysis by a Computer Assisted Matching Procedure," SPE paper No. 6547 Society of Petroleum Engineers AIME Annual California Regional Meeting, Bakersfield, California, April 1977.

Witherspoon, P. A., T. N. Narasimhan and D. G. McEdwards, "Results of Interference Tests from Two Geothermal Reservoirs, paper No. SPE 6052, Society of Petroleum Engineers, AIME Fall Annual Meeting, New Orleans, October 1976; also to appear in Journal of Petroleum Technology.

TESTING AND SAMPLING PROCEDURES FOR A GEOPRESSURED WELL

M. H. Dorfman and W. E. Boyd
The University of Texas at Austin

Summary

Test wells to tap and sample geothermal-geopressured formations at 15,000-20,000 feet in the Gulf Coast area can be drilled routinely utilizing available equipment and methods. Electrical logs, surveys and fluid samplers can be used to obtain accurate and reliable information as to depths, temperatures, pressures, and fluid content of the geopressured formations before the well is completed. But it will be necessary to set casing and flow the well, at least temporarily, to secure fluid production volume and pressure data to evaluate the producibility of the geopressured resource. Electric logging and wireline survey methods are fully developed techniques for measuring the parameters needed to assess a geopressured zone before setting casing. Formation subsidence, though it may be slow to develop, can be measured using radioactivity tracer surveys.

Introduction

Geological assessment studies indicate that commercially attractive geothermal-geopressured resources exist in several "Fairways" in Texas and Louisiana at depths of 12,000 to 20,000 feet near the coast of the Gulf of Mexico. Brines in porous formations at these depths have pressures ranging from 9,000 psi to more than 15,000 psi and temperatures from 250°F to over 350°F. Wells to tap these resources can be drilled routinely using existing technology. Electrical well logs and surveys taken in those wells will produce reasonably accurate and reliable information of temperatures, pressures, and porosity to estimate the worth of the geopressured resource, but data regarding dissolved solids and gas in the water must be obtained from fluid samples taken out of a well. Producibility of the resource will be an open question. Relative porosity and permeability indices can be estimated from electric logs, but actual reservoir testing is necessary to learn the producing rates that can be maintained and the volumes of gas and fluid that can be obtained.

Seismic survey methods can be used to outline the depths and area where geopressures (abnormal formation pressures) will be found, but it is necessary to drill a hole to determine the actual depth where high formation pressures will be encountered and whether porous and permeable rocks are present. Seismic surveys can profile the shape and size of an underground structure and delineate the major faults that may be present.

Prior to drilling the well electric logs and other data from nearby wells, plus regional geological studies, can give considerable insight on the pressures and temperatures that will be found in a well at a specific location. But a drilled hole and/or cased well is needed for complete factual data on the porosity and permeability of the reservoir rocks, their mechanical strengths, and the producing capacity of the well. An accurate estimate of free methane and other hydrocarbons can be obtained from electric logs but gases in solution must perforce be measured from water samples taken under bottomhole conditions of temperature and pressure. Dissolved solids in the geopressured brines will have a large bearing on the mechanical handling of the geopressured fluids on the surface. Equivalent salinity of the water in the geopressured zones can be determined from resistivity measurements of the underground waters using electric log data. But the kind and amount of dissolved solids in the geopressured fluids will have to be measured by analysis of samples taken under bottomhole conditions. Producibility of underground waters from porous and permeable rocks can be accurately measured only by actual production tests.

Testing and sampling of geopressured formations can be best obtained from a hole drilled and completed specifically for a geothermal test. This will insure that the casing and tubing sizes are large enough for the flow volumes needed to exploit the resource and that the requisite testing-sampling devices can be run through the well bore. A well drilled for oil or gas production but converted to a geothermal test hole will enable considerable information to be obtained from logs and fluid samples, but flowing rates may be limited by the size of the tubing or casing. Minimum information concerning geothermal purposes can be obtained from a hole being drilled for oil or gas. It will have all the limitations of the second case and would not likely be available for geothermal testing after the well was completed. Although considerable information can be obtained from all three types prior to their completion, actual fluid production test must be conducted to measure the quality and quantity of heated water, thermal output and geohydraulic power under dynamic conditions, and the quantity of methane that can be obtained on a continuing basis. Short-term production tests may give an indication of fluid pressure and volume relationship, but flowing tests of a year or more will be needed to accurately predict long-term reservoir performance.

Static testing procedures will include techniques and surveys needed to drill into the geopressured zone with safety and to penetrate the sand intervals so that the hole can be logged, cased, and completed as a producing well. This will involve the application of known drilling technology to overbalance formation pressure, thus to avoid well kicks, and to minimize the hazard of lost circulation. Either situation can lead to a blowout, lost hole, and added well expense. Drilling parameters will be monitored by experienced mud loggers on a 24-hour basis to insure safe operations. Conventional cores will be taken to measure formation porosity, permeability, and mechanical properties by laboratory analysis. After the hole is drilled to final depth, a complete "suite" of electric logs will be made to determine lithology, porosity, and other characteristics of the exposed formations. Surveys will be made to measure the angle and direction of formation dip, to plot the course of the hole and its bottomhole location. Temperature and pressure tests can be made and fluid samples obtained from the porous intervals. Casing will then be set and cemented in the well; subsequently tests utilizing wireline equipment will be made to assess the quality of the cement bond between the pipe and wall of the hole. The casing can then be perforated at the porous zones and produced for dynamic flow tests.

Dynamic testing procedures will involve flowing each productive interval to obtain fluid samples under bottomhole and surface conditions, to determine the maximum rate of flow with negligible sand production, as well as temperatures and pressures. It may be necessary to open several of the zones for commingled production to obtain the desired rate of flow, temperature and pressure. If sand movement appears to be a problem, it may be necessary to set a screen liner and gravel pack the perforated interval.

Testing and Sampling Techniques

A well drilled specifically for geopressured-geothermal tests will be arranged to provide reliable and accurate information for the overall assessment and evaluation of the geopressured resource. Standard methods will insure reliable tests and safe operations for personnel, the well, and environment. Within the past five years, ultra-deep drilling technology has resulted in the drilling and completion of wells to depths of 25,000 feet in areas of abnormally high pressures. Bottomhole pressures exceeding 13,000 psi and temperatures more than 300°F in geopressured formations can be reached at nominal depths of 15,000 feet, depending on the geographic location of the well. Casing and tubing sizes, weights, and grades of steel, to satisfactorily handle the required pressures and fluid volumes with safety and reliability are available. The wells can be drilled routinely using the drilling rigs, methods and procedures normally employed for 20,000-foot wells in the oil business.

Testing and sampling methods for a geopressured well are the same as those employed for a deep oil or gas well. Electrical surveying devices lowered into the well on multi-conductor wirelines can be used to define the kind of rocks, contained fluids, temperatures, pressures, and physical characteristics. Resistivity, sonic and radioactivity logs make it possible to estimate porosity, density, and the apparent permeability of the reservoir rocks, though actual fluid production tests are needed to determine well performance. Actual cores are needed to precisely evaluate porosity and permeability of a reservoir rock. Cores will be needed to predict actual mechanical strength of the rocks penetrated, but electric log data can be used to estimate their apparent mechanical strengths. Prior to setting casing through geopressured strata exposed in a borehole, wireline instruments can be employed to measure the fluid pressures in the permeable formations and to secure samples of the contained fluids. Cored samples from the sidewall of the well can be taken by wireline methods; sidewall samples may be used for laboratory analysis to confirm lithology, porosity and original fluid content of the geopressured formations. After casing is set in a well, acoustic surveys can be used to determine the quality of cement and the bond between the pipe and wall of the hole. Directional survey data, obtained by wireline methods, can be employed to plot the course of the borehole from the surface location and thus to map the bottomhole position of the well. Shaped-charge explosives (jets) will be used to perforate the casing to permit formation fluids to enter the well bore; the perforations will be made at the most porous zones of the reservoir face in the hole, using radioactivity surveys for depth control. Radioactive markers (bullets) will be shot into the well bore at certain levels to be used as references for subsidence observations as the well is produced. Other wireline surveys will be run periodically to observe bottomhole temperature, pressure, to secure fluid samples, and for fluid flow data to evaluate reservoir performance.

Table I lists the parameters measured or derived for geothermal-geopressured tests and sampling procedures, the instruments or techniques employed, and the quality of the information obtained.

Drilling Safeguards

More than 400 wells are being drilled annually for oil or gas to 15,000 feet or greater depth in the United States. About fifty of these reach 20,000 feet or more. Some 6,000 deep wells have been drilled in the U.S. during the past twenty years. Approximately 4,000 were located in the Gulf Coast area of Texas and Louisiana. Drilling machinery, tools and equipment for deep wells have been very much improved during this time and are considered quite satisfactory for the mechanical loads, pressures, and temperatures that will be encountered in 20,000-foot geopressured wells.

Tubular products, i.e., casing and tubing, in the sizes, weights, and grades of steel needed for 20,000-foot wells are readily available — though delivery time for some sizes and grades may be quite lengthy. Related wellhead equipment, including 10,000 psi working pressure valves and fittings, are available.

Materials are in good supply for the 17-18 ppg (pound per gallon) muds often required to contain the very high pressures found in geopressured formations. Mud expense is considerable for the specially treated, high density fluids needed; cost of mud materials for a 15,000-foot well may be $200,000 (1976) or more. Blowout preventer equipment suitable for 5,000-psi working pressure will be installed for protection against the high formation pressures that may be encountered while drilling. The production string of casing that will be set to complete the well will be fitted with 10,000-psi working pressure equipment because of the possibility of high pressure gas at the wellhead. With a given bottomhole formation pressure of, say 12,000 psi , shut-in pressure may be only 5,000 psi with a column of salt water extending to the surface, but with gas in the well could be about 10,000 psi.

Casing and blowout preventers are very important safeguards against "Kicks" and "Blowouts". Casing must be set and cemented to such depths as to provide a solid, pressure-tight, foundation for the wellhead and blowout preventers in case a high-pressured formation is drilled into. Although the drilling fluid normally provides sufficient hydrostatic head to overbalance and contain the formation pressure, high pressure blowout preventers, wellhead and casing are needed to provide a safeguard in case excessive formation pressure is encountered. Blowout preventers, in such case, will make the difference between a kick, which is formation fluid or gas that is circulated out of the well under controlled conditions, or a blowout, which is an uncontrolled flow of fluid or gas from a well. In the latter case, flow to the surface becomes uncontrollable and the hazard of an explosion and fire is created.

The "art" of prediction and detection of geopressured formations is a fairly exact procedure today. Many of the parameters that indicate the proximity of high pressure can be measured within the time needed to circulate from the bottom of the well to the surface, about two hours on a deep hole. Table II lists the techniques available to predict and detect geopressured formations. Continuous plots of mud temperature, fluid weight, cuttings density, and normalized drilling rates make it possible to anticipate dangerous high pressures by departures from straightline trends. Electric logs, from which formation conductivity, resistivity and shale density can be obtained, will give after-the-fact evidence that geopressured formations have been penetrated.

Table I

INSTRUMENTS OR TECHNIQUES USED TO DERIVE INFORMATION ON GEOPRESSURED FORMATIONS

Parameters Measured or Derived		Instrument or Technique	Quality of Information
1. Lithology		Electric Logs	Good
		Mud Logging	Good
		Cuttings Analysis	Fair
		Drilling Rate of Penetration	Fair
		Sidewall Samples	Good
		Conventional Cores	Good
2. Formation Porosity		Resistivity Logs	Good
		Sonic Logs	Good
		Density and Pulsed Neutron Logs	Good
		Sidewall Samples	Poor
		Conventional Cores	Good
3. Formation Permeability		Electric Logs	Porosity Only
		Computer Proc. Logs	Indices-Fair
		Sidewall Samples	Poor
		Conventional Cores	Good
	(1)	RFT	Fair
	(2)	DST	Good
4. Fluid Identification		Mud Logging	Fair
		Resistivity Logs	Good
		Density and Pulsed Neutron Logs	Good
	(1)	RFT - Fluid Sample	Poor-Good
	(2)	DST - Fluid Sample	Good
	(3)	Fluid Sampler	Good
5. Geopressured Strata		Drilling Rate of Penetration	Fair
		Mud Logging	Fair
		Shale Density	Fair
	(4)	Electric Logs	Good
	(4)	Sonic Log	Good
	(4)	Density Log	Fair
6. Fluid Pressure		Drilling Rate of Penetration	Poor
		Electric Logs	Fair
	(1)	RFT - Pressure	Good
	(2)	DST - Pressure	Good
	(3)	Bottomhole Pressure Gauges	
		Amerada**	Good
		Hewlett Packard**	Good
		Sperry Sun	Good
7. Formation Temperature		Temperature Electric Log	Good
	(3)	Bourdon-Tube Temperature Gauge	Good
	(3)	Electrical Remote Temperature Gauge	Good
	(3)	Maximum Reading Thermometer	Good
8. Formation Mechanical Strength		Electric Logs)	
		Sonic Log)	
		Density Log) Mech. Prop. Log	Poor
		Nuclear Log)	
		Conventional Cores	Good
9. Formation Subsidence	(3)	Radioactivity Tracer Surveys	Poor
	(3)	Strain Gauges	Fair
10. Sand Movement	(3)	Sonic Detector	?

(1) Schlumberger Repeat Formation Tester
(2) Drill Stem Test
(3) After the well is completed
(4) After the Fact of Drilling
** Limited to 12,000 psig

Detection of Abnormal Pressure

The scientific principles involved in the process of shale compaction and geopressured sands are fairly well defined. We can predict the pressures to be found in abnormally pressured shales and to some extent predict their occurrence with a fair degree of accuracy, using shale-density and electric-log information from nearby wells. High formation pressures can be detected by —

- Drilling rate;
- Sloughing shale;
- Shale density;
- Gas-cut mud;
- Chloride increase in the mud;
- Mud-temperature increase; and
- Electric-log data.

Table II

PRESSURE DETECTION TECHNIQUES

Source of Data	Parameters	Time of Recording
Seismic Methods	Formation Velocity	Prior to spudding the well
Drilling Parameters	Drilling rate "d" - Exponent Drilling Rate Equations Drill Stem Torque Drill Stem Drag Drilling Porosity Log	While drilling
Drilling Mud	"Kicks" Gas content Flow line mud weight Flow line temperature Chlorides in the mud Drill pipe pressure Pit level, volume Flow rate Hole fill up	While drilling Delayed by the time required for mud return.
Shale Cuttings	Shape and size Bulk density Shale factor Electrical resistivity Volume	While drilling Delayed by the time required for sample return.
Well Logging	Electrical surveys Resistivity Conductivity Shale formation factor Salinity variations Interval transit time Bulk density Hydrogen index Thermal neutron capture cross section	After hole is drilled.
Direct Pressure Measuring Devices	Pressure bombs Drill stem test Wire line formation test	When well is tested or completed.

Other methods more or less direct but generally not as accurate as those indicated above include:

(1) Borehole fluid kicks while drilling caused by formation pressures in excess of hydrostatic mud pressures. Such kicks establish minimum formation pressures.

(2) Surface tubing pressure measurements. The hydrostatic pressure of the fluid in the column must be added to the surface measurements to get the formation pressures.

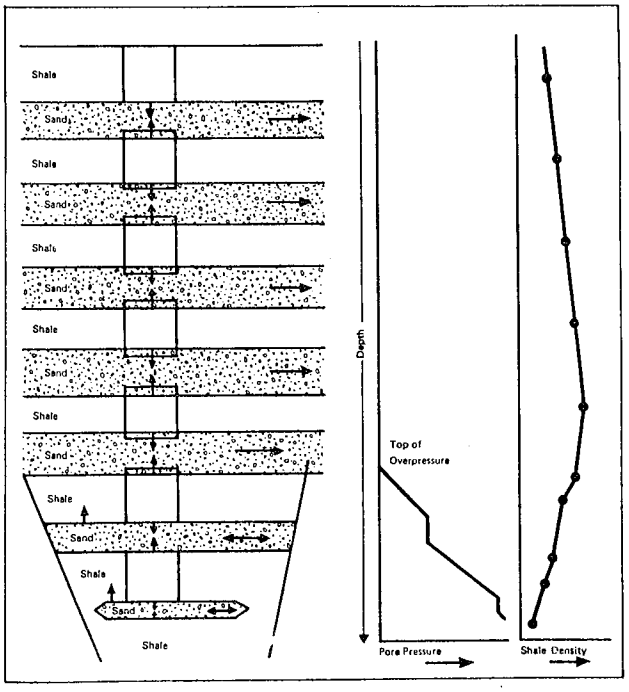

Figure 1. Effect of Shale Compaction on Shale Pore Pressure and Density

Drilling rate is a direct means of detecting shale or sand formations containing high pressures. It should be remembered that the rate of penetration is affected by changes in the kind of rocks, bottomhole cleaning by the circulating fluid, bit weight, rotary speed, fluid properties of the mud, and by the type of bit and its condition.

Sloughing shale is usually the result of formation pressure in excess of hydrostatic pressure, particularly in the softer shales of coastal areas of the United States.

Shale density normally increases with depth because the unit weight of shale is greater when water is squeezed out due to compaction. Figure 1 shows the normal trend of shale density; when density decreases below the normal-trend line, increased formation pore pressures may be expected. Actual use of this means of detecting formation-pressure increase is difficult because of problems in selecting representative particles of shale and in making precise measurement of density.

Gas-cut mud has always been considered a warning of high formation pressure, but its appearance is not always a serious problem. Gas may enter the mud as a result of the following —

1. gas in shale, the so-called high pressure/low volume shows that are frequently associated with thick shale sections;
2. gas from drilled gas-bearing sands may cause temporary changes in the gas concentration in the mud.

Chloride increase in the mud is not as easily recognized as changes in gas content. Regular checks should be made of the chloride content of the mud going into and circulated out of the hole. A comparison of the trend levels may confirm that formation fluid is entering the mud due to increasing pore pressure.

Mud temperature increase may or may not be an aid in detecting an increase in pore pressure. Flow-line temperatures, if correctly plotted against depth, can be used to predict the presence of abnormal formation pressure, as shown in Figure 2.

Electric Log Indications of Geopressures

An induction electric log (I-ES) will indicate the top of a geopressured shale by increased conductivities and lowered resistivities, as clearly indicated on the log illustrated in Figure 3. Conductivity, the irregular curve on the right, increased from approximately 1,000 millimhos/m that had been registered from 12,900 to 13,500 feet to about 3,000 millimhos at 13,700 feet. Note that casing was set in this well just below the top of the geopressured shale. In the same intervals

resistivity decreased from about 2.0 ohm-meters to less than 0.5. This is evidence that there is more porosity in the geopressured shales, therefore more water, than would be expected for the depth. Conductivity and resistivity measurements are affected by formation water salinity, temperature, and instrument calibration problems.

Shale conductivity, resistivity, density and acoustic travel time are some of the characteristics measured by electric logs that will confirm that geopressures have been penetrated. Normal compaction of shale with depth as the weight of the overburden increases will result in decreased porosity. For this reason, resistivity should normally increase with depth, sonic travel time should decrease, and shale density should decrease. If deviation from these trends are observed, abnormal pressure (geopressure) will be present.

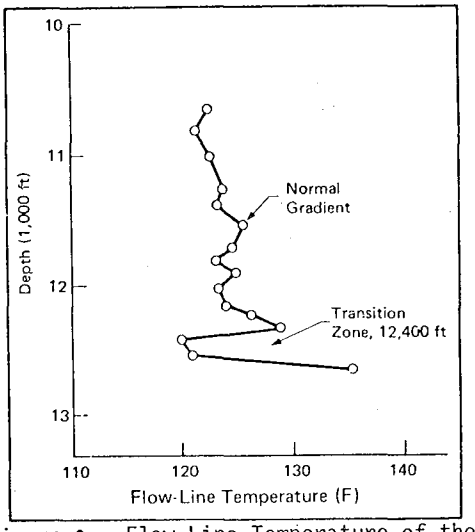

Figure 2 Flow-Line Temperature of the Mud Can Be Used to Detect Geopressured Formations.

Problem Areas of Test Data

Although electric logging procedures leave little to be desired in the classification of the formations and the lithological sequence there are many problems when correlating the formations from well to well in the Gulf Coast area, particularly in geopressured shales and sands. This is due to the manner in which these strata were deposited, the amount of compaction that has taken place in geological time, the large number of faults, and the near impossible task of correlating shale formations. Micropaleontology studies, whereby certain micro-fossils were identified in rocks of specific age, have been used with rather indifferent success to correlate shale formations thus to predict geopressured sands. Mud logging techniques, in which gas and cuttings in the mud returns are measured and logged versus well depth, have

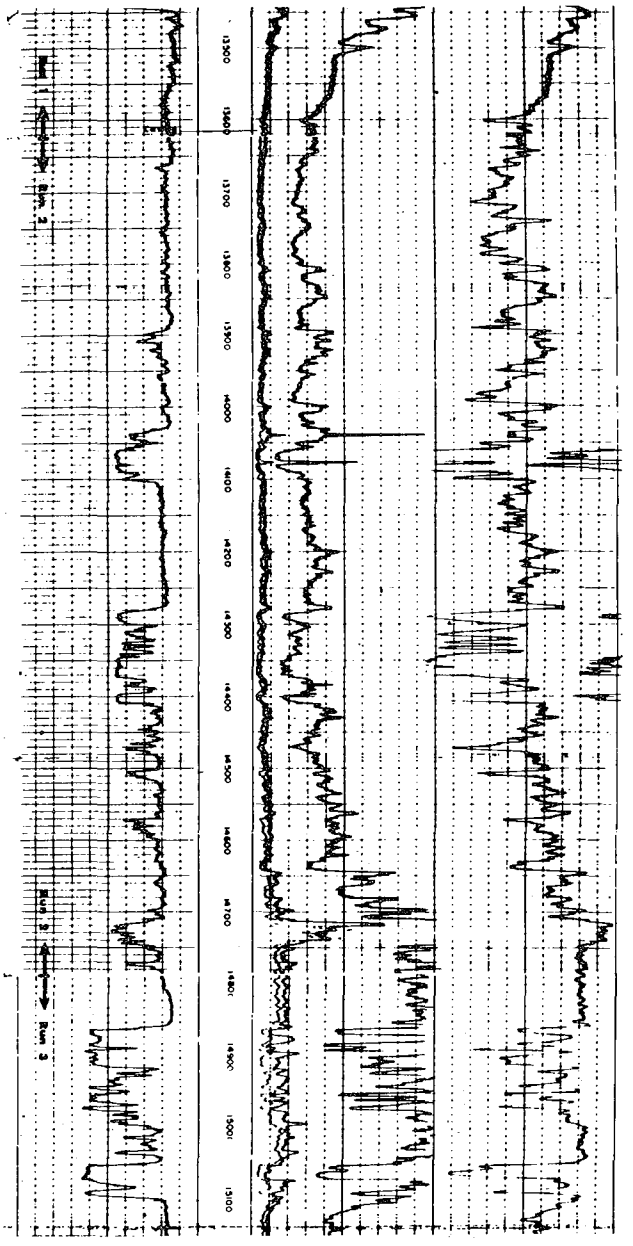

Figure 3 Induction-Electric Survey (I-ES) of a Geopressured Well

proven to be fairly reliable, particularly to identify shale and sand strata and the kind of fluids in the pore space. Shale density plots have been found to be good indicators of geopressured rocks, but problems arise (1) to properly identify new cuttings from bottom, (2) properly clean, and (3) shale density determinations. Geopressured shales are more porous, thereby less dense, than the trend of shale densities plotted against depths. A drilling-rate log may give valid indication that an over-pressured sand or shale has been entered, but but the affects of hydrostatic pressure versus formation pressure, rotary speed, drilling weight and

bit size must be considered. These can be normalized, thus plots of drilling rate versus well depth can be used to indicate that a geopressured formation has been encountered. Sidewall samples, will give good indications of lithology. The manner in which these samples are obtained disturbs the matrix of the core, thus porosity and permeability measurements are of little value. Conventional cores, properly packaged and analyzed, will enable true porosity and permeability values to be obtained. Bulk compressibility and shear moduli can be measured from core samples loaded in a testing machine.

Electric resistivity logs are valid indicators of average resistivity values for sands and shales, but it is necessary to obtain these readings far enough from the borehole to be true formation fluid, rather than mud filtrate, in the pore space of the rocks. Induction logs will measure true resistivity because the radius of investigation is some distance from the well. Other focused logs will obtain true formation resistivity at the bottomhole temperature involved. Resistivity values can be converted to apparent porosity and apparent salinity of the formation fluid in clean water sands. Sonic and density logs will indicate total porosity, which can be converted to apparent porosity when the type of fluid in the pore space is known. Conventional cores can be measured precisely for porosity and permeability.

Formation permeability cannot be measured directly by electric log methods, though permeability can be inferred from the displacement of formation fluid by mud filtrate invasion. Porosity measurements will permit some estimate of permeability because permeable rocks must have porosity. Where porosity is known, the so-called Archie equation, and similar expressions, can be used to calculate the Formation Factor "F" which can be used for saturation determinations. Computer processed logs, when provided with sufficient log data, can calculate permeability indices by taking all log information into account. Conventional cores will permit good assessment of permeability by means of laboratory analytical methods. The Schlumberger RFT formation tester can be reset until intervals of good permeability are located in a porous zone; the tendency of this tool to stick may limit its usefulness for geopressured sands. A full-scale test of permeability can be made by a drill stem test, though the need to make the DST through perforations in casing for geopressured formations may effect the result.

Formation fluid identification can be made by resistivity and other electric logs using quantitative interpretation methods. Formation fluid resistivity values, corrected for bottomhole temperature, can be directly related to apparent salinity on the basis of an equivalent sodium chloride solution, but other minerals cannot be identified. Drill stem test fluid samples, particularly after a lengthy flow test, will be quite valid as to pressure, temperature, dissolved gas and chemical composition. The sample chambers for these devices can be removed for transport to a laboratory for analysis. Several sampler devices that can be run on a wireline are available; these are equivalent to open-end tubes which can be closed by timer, mechanical, or electrical means. These tools can obtain a fluid sample under bottomhole conditions of temperature and pressure, but the sample will cool as it is pulled to the surface and its pressure will be lowered. This will mean precipitation of dissolved gas and silica, etc., unless the samples are quickly diluted when taken from the well.

Geopressured formations have been the bane of rotary drillers for a long time; disasterous and expensive blowouts have taken place when such formations were encountered unexpectedly. Casing strong enough to contain the geopressure must be set before the formation is penetrated and the hole filled with drilling fluid of appropriate density to hold back the geopressured fluids. Drilling parameters such as rate of penetration, shows of gas, oil or saltwater in the mud returns, shale cuttings density, and other indicators are fairly obvious signs that a geopressured formation has been encountered. Gathering this information depends to a great extent on the competence and alertness of the observers. Well kicks, which are incipient blowouts caused when hydrostatic pressure is lower than formation pressure, are usually slow to develop and sometimes are most unobtrusive when they begin.

Formation pressure determinations can be made using electric log data, by drilling rate, and by direct measuring devices such as the Schlumberger RFT tool, drill stem test equipment, or downhole pressure gauges. Electric log data does not permit measurement of formation pressure, but instead a family of curves can be drawn relating depth to resistivity and conductivity values to geostatic pressure gradients in a given area. These curves can be used as an overlay on plots of well depth versus resistivity or conductivity trends; when the values fall between formation pressure gradients, formation pressure at specific well depth can be estimated. Drilling rate of penetration will permit only a poor assessment of formation pressure. Differential between hydrostatic and formation pressures is an important factor affecting drill bit performance; at high differential the bit will drill slower than at low differential, other factors being constant. When negative differential exists, i.e., formation pressure greater than hydrostatic, the bit will make hole with little applied mechanical or hydraulic effort. But a blowout will be underway if the formation is porous and the negative pressure differential is appreciable. The Schlumberger RFT tool will produce valid readings of formation pressure; these values can be monitored on the surface, thus waiting time can be regulated to obtain stabilized pressure readings. Drill stem test equipment includes pressure gauges that are run to or near the depth of the producing formation. Static or dynamic pressure readings

will thus be about the same as formation pressure when the well is shut in or flowing. DST pressures are recorded on 24-72 hour clock-driven charts, thus the record would be limited to 1-3 days time. Several types of bottomhole pressure gauges, which are run on wirelines, are available; these are run to the depth desired and pressures recorded on clock-driven charts. Hewlett-Packard makes a quartz crystal bottomhole pressure gauge that is run on an electric cable, thus readings are obtained and recorded on the surface. Sperry-Sun has a remote reading bottomhole gauge which utilizes a downhole chamber connected to a surface monitor by a small diameter tube filled with nitrogen gas. Tube temperature affect must be taken into account.

Formation temperatures can be recorded by electrical logging means, by a mechanical bourdon tube temperature gauge, or by maximum reading mercury thermometers. Electrical-conductor remote reading gauges utilizing downhole temperature sensors are also available.

Formation mechanical strength estimates utilizing electric log data to infer the intrinsic strength from the values of the shear modulus and bulk compressibility are probably of little value. There is some evidence that there is a correlation between intrinsic strength and the dynamic elastic constants, as determined from sonic-velocity and density measurements. Sonic log values may not be correct because the tool is not close enough to the wall of the hole, thus mud will interfere with the acoustic readings obtained. Actual compressibility tests on cored samples will give valid information of rock strength.

Formation subsidence measurements can be taken from radioactive markers placed at carefully measured increments of depth in a well specifically for geothermal testing. These markers can be surveyed at various time intervals and the apparent compaction and/or subsidence measured by comparison with the original depths and measurements between the markers.

Sand movement from the productive zone into the well may be a problem. Sand particles in the water flowing into the well may abrade and wear the mechanical equipment to such an extent that the well cannot be produced; alternatively sand entry into the well bore can plug the casing or tubing thus to shut off fluid flow. Production of minor quantities of solid material is sometimes difficult to measure.

Bibliography

Abnormal Subsurface Pressure — A Study Group Report Houston, Texas: Houston Geological Society, 92 pp., 1971.

Boatman, W.A., Jr. Measuring and Using Shale Density to Aid in Drilling Wells in High Pressure Areas. Jour. Petrol. Tech., V. 19: 1423-29, 1967.

Boyd, W.E. (editor), Blowout Prevention — 2nd Edition. Petroleum Extension Service; The University at Austin; Austin, Texas: 73 pp., 1976.

Eaton, B.A. Fracture Gradient Prediction and its Application in Oil Field Operations. Jour. Petrol. Tech., V. 21: 1353-1360, 1964.

Fertl, Walter H. Abnormal Formation Pressures. Elsevier Scientific Pub. Co.: 382 pp., 1976.

Gill, J.A. Applied Drilling Technology, an Engineered Packaged for Pressure Detection and Control. Drilling Contractor: 128-140, 1968.

Goins, W. C., Jr. Blowout Prevention. Houston, Texas: Gulf Pub. Co.: 260, 1968.

Hottman, C.E. and Johnson, R.K. Estimation of Formation Pressure from Log Derived Shale Properties. Jour. Petrol. Tech., V. 17: 717-723, 1965.

Jorden, J.R. and Shirley, O.J. Applications of Drilling Performance Data to Overpressure Detection. Jour. Petrol. Tech., v. 18: 1387-1394, 1966.

Lewis, C.R. and Rose, S.C. A Theory Relating High Temperatures and High Pressures. Jour. Petrol. Techn., v. 22: 11-16, 1970.

Schlumberger Ltd. Publications. Log Interpretation, Volume I - Prinicples: 1972; Log Interpretation, Volume II - Application: 1974; Cased Hole Applications: 1975; Open Hole Repeat Formation Tester: 1974.

Sonic Sand Detector. In-House Report. Dallas, Texas: Mobil Research and Dev. Corp.: 23 pp., 1974.

Tixier, M.P., Loveless, G.W., Anderson, R.A. Estimation of Formation Strength from the Mechanical Properties Log. Soc. Petrol. Eng. AIME Paper No. 4532: 14 pp., 1973.

Wallace, W.E. Abnormal Subsurface Pressures Measured From Conductivity or Resistivity Logs. 6th Prof. Well Log Analysis Symp.: Dallas, Texas, 1965.

Session Introduction

Analysis and Interpretation

H. K. van Poollen
H. K. van Poollen and Associates, Inc.
Littleton, Colorado

Well testing is an art and science of long standing. The first application was applied to water wells. In later years we saw its application to the petroleum industries. There, separate developments took place in the oil and gas industries. Hence, one observed different approaches in the latter two. Today most scientists recognize the similarity between water-well testing, gas-well testing and oil-well testing. Yet in more recent years, we recognize that the principles of well testing apply equally for geothermal wells.

In well testing, one produces a well or injects into it and observes the pressure changes in the well or neighboring wells. The latter application is frequently called interference testing and finds major application in the water industry.

Analysis techniques may be categorized as follows:

- Simple use of graph paper. Here one evalutes straight-line relationships when pressure and/or rate functions are plotted versus time functions. Cartesian, semi-logarithmic and log-log paper are favorites. By the use of these techniques one calculates reservoir pressure, transmissibility, and wellbore effects. Sometimes it is possible to determine geometry and distances to barriers or other discontinuities.

- Type curves. For various boundary conditions and flow geometry, typical log-log plots are prepared beforehand with dimensionless pressure rate functions on one axis and dimensionless time functions on the other axis. Next, similar real pressure rate functions and real time functions are plotted on the same scale paper. By overlaying the two curves, one may match the curves in at least certain portions. Again, one may (under the right circumstances) learn the before-mentioned reservoir parameters. This technique has long since been used in ground-water applications. These techniques work best if observation wells render data. With all data being obtained at a single well, uniqueness is basically nonexistent. However, there they still render general results about flow regimes and geometry.

- Computer matching. In this technique one uses numerical grid-type models and assigns reservoir properties to each. By comparing observed field data and modifying the reservoir parameters, eventually a match is obtained. This technique is limited to complicated problems of geometry such as multi-layered reservoirs. Cost, both in time and money, is a major detriment of this method.

GENERAL REMARKS

Although complicated mathematical solutions can be derived for varying rates and pressures, a word of caution is justified. When rates and pressures vary greatly, field measurement becomes difficult. Hence, interpretation becomes nearly meaningless.

A good test procedure is to evaluate data as they become available. The first method of plotting data on various kinds of graph paper is the simplest and recommended.

Probably the most important word of advice is to keep all tests as simple as possible.

ABSTRACT

ANALYSIS AND INTERPRETATION OF OIL, GAS, AND GEOTHERMAL WELL TESTS

William E. Brigham
Stanford University

The purpose for any well test is to determine quantitative information about the reservoir which the well (or wells) penetrates and quantitative information about the condition of the well. These data, in turn, can be used to answer a variety of important questions--What will be the long term producing rate versus time? What are the total reserves? Should we attempt to stimulate the well? How has the reservoir pressure changed?--and a host of others. At the heart of these analyses is the fact that the pressure changes linearly with the logarithmic of time; and the quantitative answers are extracted from the slope and intercept of such a graph.

Unfortunately, we find in practice that it is often difficult to identify the correct semi-log slope. At early times the condition of the well causes distortion of the pressure-time curve. Such things as the wellbore volume or the presence of fractures at the well will often cause such distortions. At later times the reservoir geometry will similarly affect the semi-log slope; nearby faults, abrupt changes in the reservoir flow properties, or multiple zones are examples.

Since 1970 there has been a virtual explosion of information on ways to handle these early and late time problems. Many of them have now been solved analytically. Further, through the use of log-log type curve matching one can often diagnose the well behavior and be certain that the correct slope has been found and the analysis of the data is correct.

Most of these techniques were developed for oil and gas flow, but in recent years they have been applied to geothermal systems--both hot water and steam--with considerable success.

In interference testing the properties between wells are analyzed by determining the pressure-time behavior of a shut-in well when the production rate is changed in an offset well. Historically, this has been used successfully in both the oil and gas industry and in hydrology through use of log-log type curves and the classic line source solution. This technique has also been used successfully in geothermal systems.

Recently, well test problems have been attacked that appear unique to geothermal systems. A number of new solutions have been generated that embody differing reservoir geometries and have been found to match field data. Other problems need to be addressed quantitatively; for example, the problem of water boiling near a producing well. In addition, reliable measuring equipment needs to be developed which can stand the high temperatures and salinity seen in geothermal systems. Since well testing has been found to be useful in geothermal systems, there is considerable incentive to expand its use to the fullest extent possible. For this reason, I am confident that many new and useful solutions to well testing problems will become available in the near future.

INTERPRETATION OF TRACER TESTS BY MEANS OF TYPE CURVES
APPLICATION TO UNIFORM AND RADIAL FLOW

J. P. SAUTY

BUREAU DE RECHERCHES GEOLOGIQUES ET MINIERES

(Service Géologique National - French Geological Survey)

ABSTRACT

It is shown that in uniform or radial flow it is possible to characterize the response to continuous injection or instantaneous pulse by a set of type curves in dimensionless coordinates depending only on one parameter similar to a Péclet number. These curves allow a simple and efficient eye identification of dispersion parameters - dispersivity and kinematical (or effective) porosity - by graphical matching.

Application to field experiments shows that:

- in practice, tracer tests in uniform flow should be avoided in absence of precise knowledge of the effective direction of flow;
- on the contrary, pulse injection into satellite piezometers of a central pumping well yields a good and economical method when the flow is effectively radial.

ACKNOWLEDGEMENTS

The method and its application have been developed in Sauty (1977). The data used have been measured in the field by BRGM* and CEA**, and initially published in Gaillard, Guizerix, Margat, Molinari and Peaudecerf (1976) and Gaillard (1976) for uniform flow, in Rousselot (1977) for experiments in radial flow. Methods of interpretation and applications have been partially published in recent papers, Sauty (1977), Gaillards, Rousselot and Sauty (1976), and Molinari and Peandecest (1977). An advanced paper[10] containing the main theoretical developments and results of Sauty (1977) is under preparation for submittance to Water Resources Research.

INTRODUCTION

Aquifers contain large amounts of water of a quality generally superior to that of surface water. It is naturally protected from surface pollution by confining layers or a non-saturated zone of variable thickness and by filtrating properties of soils. But increasing sources of contamination (factory disposal, nitrates, pesticides, nuclear waste disposal) are such that groundwater is not safe any more.

It is important to be able to evaluate the transfer of contaminants with the movement of water in order to predict the evolution of concentrations in vulnerable spots, and eventually examine by mathematical simulation the efficiency of protection devices.

Today there exist quite a number of numerical codes theoretically able to simulate mass transfer, but the program user generally misses knowledge of the physical parameters necessary to feed correct data for an accurate modeling of the considered aquifer: it is necessary to develop simple, unexpensive and easy to interpret field experiments to get this data in situ.

---

* Bureau de Recherches Géologiques et Minières

** Commissariat à l'Energie Atomique - Centre d'Etudes Nucléaires de Grenoble

PHYSICS OF MASS TRANSFER

Transfer of pollutants is governed by the following factors (ref. 1 and 2):

(i) convection: transfer by water particles in their average displacement at a macroscopic scale;

(ii) hydrodynamic (or kinematic) dispersion, resulting from travel time differences between water particles inside the pores mainly due to streamlines tortuosity;

(iii) molecular diffusion due to thermal agitation of fluid molecules;

(iv) adsorption - desorption by the solid phase and eventually exchanges with immobile water;

(v) chemical and organic reactions.

The equation of mass transfer is (ref. 1):

$$\underbrace{\frac{\partial C}{\partial t}}_{\text{concentration variation}} = \frac{\partial}{\partial x_i}\underbrace{\left(\underbrace{D_{ij}\frac{C}{\partial x_j}}_{\text{kinematic dispersion}} - \underbrace{Cu_i}_{\text{convection}}\right)}_{\text{-}} + \underbrace{D_m \frac{\partial^2 C}{\partial x_i^2}}_{\text{molecular diffusion}} - \underbrace{R}_{\text{various reactions}}$$

with
- $C(x_i,t)$: concentration
- x_i, i=1,3 : cartesian coordinates
- t : time
- u_i, i=1,3 : effective pore velocity
- D_{ij} : dispersion tensor
- D_m : molecular diffusion
- R : fixation or destruction by various chemical or organic reaction

considering that:

$\vec{u} = \frac{\vec{V}}{\omega}$ is related to DARCY velocity (which results from permeability and head gradient) by ω, kinematical porosity

and:

$$D_{ij} = R^T \begin{vmatrix} \alpha_L & 0 & 0 \\ 0 & \alpha_T & 0 \\ 0 & 0 & \alpha_T \end{vmatrix} \cdot |\vec{U}| \cdot R$$

with α_L and α_T longitudinal and transversal dispersivities and R rotation matrix between reference coordinates and local velocity coordinates.

Usual modeling of aquifer pollutions only deal with phenomena (i) to (iii). The last two are more difficult to handle, and the numerical values of reaction parameters (which very strongly depend on chemical and physical properties of solutes and rocks) are very difficult to determine.

However, their consequences contribute to safety : concentration peaks are lowered and delayed.

TRACER TESTS

The first objective is to evaluate in situ values of α_L, α_T and ω. This can be performed by means of tracer tests : a substance, the concentration of which can be easily measured, is injected through a well into the flowing groundwater. After a certain displacement, water is sampled and analysed for concentrations. If the tracer is little subject to reactions (chemical or others) its transfer fits with the hydrodispersive model (perfect tracer), and the restitution curve yields dispersivities and porosity which are intrinsic parameters of the aquifer ready to be used for predictions of hydrodispersive mass transfer in different flow conditions.

Two main flow patterns are usual for this kind of experiment : uniform flow (constant velocity vector) or radial flow in the horizontal plane (condition satisfied in the vicinity of a well subject to injection, withdrawal or both successively).

In each of these flows (Fig. 1 to 3), for matters of interpretation simplicity, the tracer injection is generally chosen as close as possible to either instantaneous injection (i.e. DIRAC pulse) or continuous injection (with a constant mass rate of tracer). The interpretation of more complicated injection conditions requires convolutions and specific type curves.

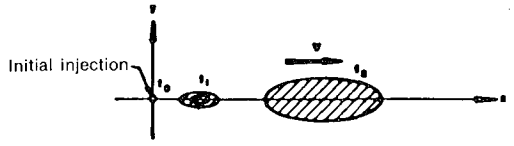

Fig. 1. Bidimensional flow, migration of the tracing spot after a brief injection.

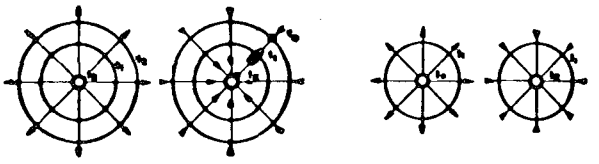

Fig. 2.

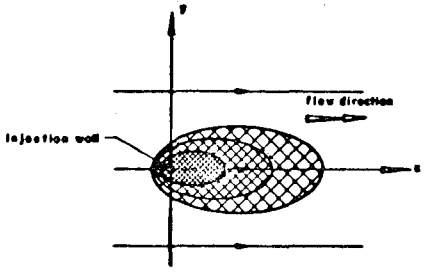

Fig. 3.

TYPE CURVES

For each combination of flow pattern and injection process, a set of universal type curves has been established which only depends on one dimensionless parameter similar to a PECLET number (Ref. 9). As an example, two of these type curves are given below for instantaneous injections in uniform flow (Fig. 4) and radial converging flow (Fig. 5).

DIRAC PULSE IN UNIFORM FLOW

In the case of instantaneous injection in 2D uniform flow (Fig. 2), with transversal dispersion, the equation of concentration variations versus time at any point (x,y) of the aquifer is well known (Ref. 1) :

$$C(x,y,t) = \frac{m}{4\pi\omega u\sqrt{\alpha_L \alpha_T}} \cdot \frac{1}{t} \cdot \exp - \left(\frac{(x-ut)^2}{4\alpha_L ut} + \frac{y^2}{4\alpha_T ut} \right)$$

A judicious choice of dimensionless variables (subscript R stands for reduced variable) :

$$t'_R = ut/\alpha_L$$
$$C_R = C/C_{max}$$
$$x_R = x/\alpha_L$$
$$y_R = y/\sqrt{\alpha_L \alpha_T}$$
$$a = \sqrt{x_R^2 + y_R^2} = \sqrt{\frac{x^2}{\alpha_L^2} + \frac{y^2}{\alpha_L \alpha_T}}$$

leads to a simplified expression for the tracer restitution curve in sampling well :

$$C_R(t'_R) = k \cdot t'^{-1}_R \cdot \exp \left(- \frac{a^2 + t'^2_R}{4t'_R} \right)$$

where k is a function of a, independent of t'_R.

This equation allows to establish a universal set of type curves depending on the only parameter a (Fig. 4a and 4b). "a" is the dimensionless distance between injection well and sampling well ($a = \sqrt{x_R^2 + y_R^2}$). It has the dimension of a Péclet number : on the x axis, $a = x/\alpha_L = ux/D_L$.

It is a mixed Péclet number (taking into account both longitudinal and transversal disperivities), characterizing simultaneously aquifer (α_L and α_T) and flow plus experimental device (x and y are distances between wells in a system of coordinates related to flow direction).

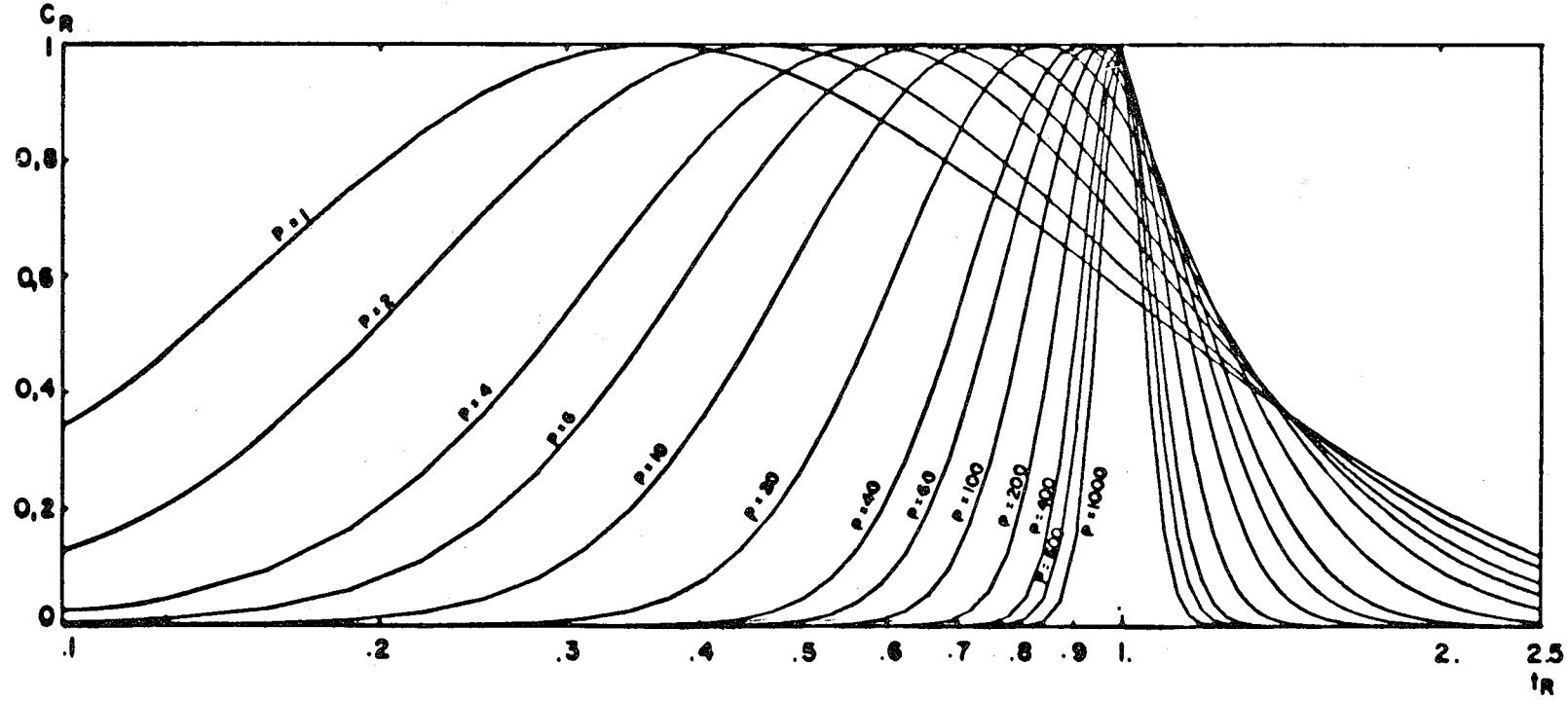

Fig. 4. Schematic for an instantaneous injection in a convergent flow.

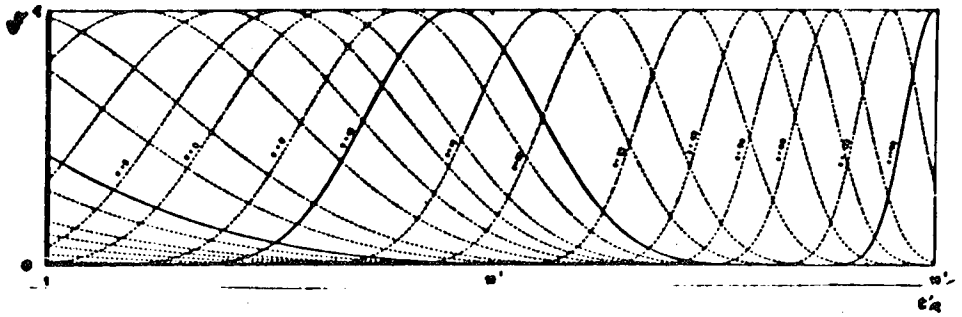

Fig. 4a. DIRAC pulse in 2D uniform flow - Reduced concentrations function of reduced time for different mixed Peclet number a. Semi-logarithmic coordinates.

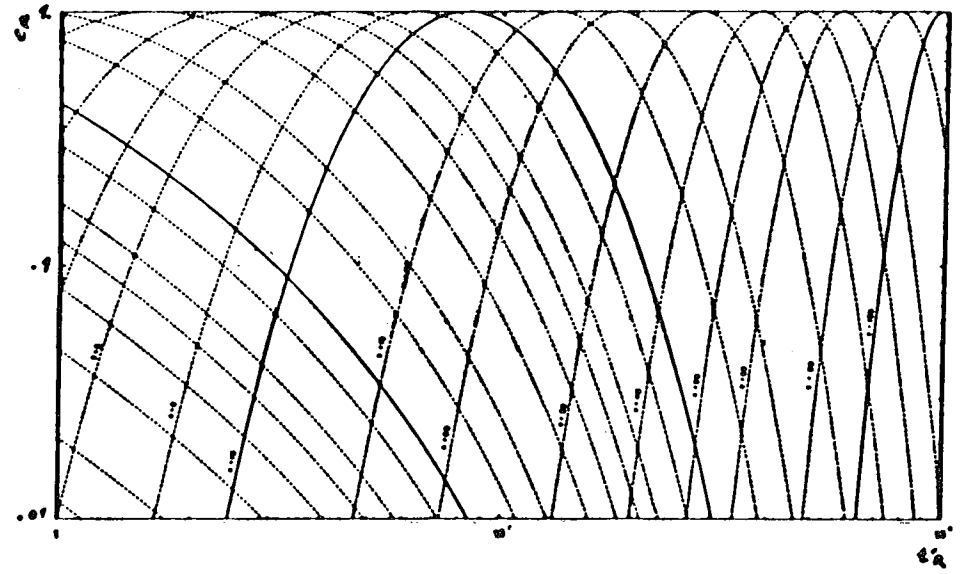

Fig. 4b. DIRAC pulse in 2D uniform flow - Reduced concentrations function of reduced time for different mixed Peclet numbers a. Bi-logarithmic coordinates.

The peak concentration (maximum value) can be expressed as follows :

$$C_{max} = \frac{m/\omega}{4\pi\alpha_L\sqrt{\alpha_L\alpha_T}} \cdot \frac{1}{x_R\, t_{Rmax}} \cdot \exp - \left[\frac{x_R}{4} \cdot \frac{(1-t_{Rmax})^2}{t_{Rmax}} + \frac{y_R^2}{4x_R\, t_{Rmax}} \right]$$

with

$$t_{R_{max}} = \sqrt{1 + \left(\frac{2}{x_R}\right)^2 + \left(\frac{y_R}{x_R}\right)^2} - \frac{2}{x_R}$$

The relative peak values have been plotted in function of dimensionless coordinates : x_R, y_R (Fig. 5).

For a longitudinal Péclet number (x/α_L) of 20 and in the hypothesis that $\alpha_L/\alpha_T = 10$, an angular error θ = Arctg y/x of 10° on the flow direction divides peak value by 5, while an error of 20° divides it by 500.

DIRAC PULSE IN RADIAL CONVERGING FLOW

In the case of instantaneous injection in a satellite piezometer of a pumping central well (second case of Fig. 3), as far as we know, no exact analytical solution has been derived. A numerical integration is then necessary. A method, free of the effect of numerical dispersion (classical error due to discretisation of convection term), has been developed (Ref. 8).

The choice of dimensionless variables :

$t_R = \frac{Q}{\pi h\omega} \frac{t}{R^2}$ with Q : flow rate
h : aquifer thickness
ω : kinematical porosity
t : time
R : distance between lateral piezometer and central well axis

$r_R = \frac{r}{\alpha}$ (for r = R, r_R = P, Péclet number associated to the aquifer with its experimental device)

$c_R = C/C_{max}$

allows to represent restitution curves $C_R(t_R)$ depending on the sole Péclet number. The resulting set of type curves is given by Figure 6.

INTERPRETATION OF DISPERSION PARAMETERS WITH TYPE CURVES

Using these type curves plotted in semi-log or log-log coordinates, dispersion parameters can readily be identified from experimental results of a tracer test by mere graphical matching.

On semi-log paper (Fig. 4a - logarithmic time scale), observed concentrations are normalized by peak value ($C_R = C/C_{max}$) and plotted versus real time on a transparent paper. This experimental graph is slided along time axis, until it matches with one of the theoretical curves (Fig. 7).

Curve shape yields Péclet number hence dispersivity α; correspondence between experimental time scale and dimensionless time gives the effective pore velocity u hence kinematical porosity ω.

Log-log graphs (Fig. 4b) are to be used when information lacks in the vicinity of peak value : real concentrations are plotted (without normalization). The experimental graph is slided both along time axis and in the direction of C axis, thus determining peak value.

This procedure is very similar to those used for well tests interpretation by THEIS (or other) curves. Log-log method is more general, but does not provide as good a precision as semi-log. Cartesian coordinates yield the best precision, but their use is rather cumbersome (Ref. 8).

APPLICATION TO IN SITU TRACER TESTS

This method has been applied to numerous field tracer experiments (Ref. 5, 8 and 9) performed by DIRAC pulse in either uniform flow or radial converging flow, with various tracer, sites and wells distances.

These various tests lead to common conclusions:

- Tests performed on small distances (order of 1 meter) show strong evidence of heterogeneities even in an apparently homogeneous aquifer.

- Often, tracer experiments performed with mean distances (order of 10 meters) in aquifers geologically known as homogeneous can only be interpreted satisfactorily by a two layers effect, showing evidence of privileged paths.

- In the same aquifer, but at higher distances (examples have been obtained for 30 meters, in other cases for more than 100 meters), the experimental points fit exactly with a theoretical curve for a monolayer aquifer. Coupled experiments performed in uniform flow, with three wells B, C and D in line with the groundwater velocity, lead to restitution curves characteristic of a two layered aquifer when performed between B and C (13 m) or C and D (13 m); while results of a test between B and D (26 m) is typical of an homogeneous (monolayer) aquifer.

- At first, dispersivity increases with distance, until a certain length is reached above which dispersivity seems to stablize; generally, at this distance, the fit with a monolayer type curve is obtained. It is known as scale of heterogeneity : at a smaller scale, consequences of local non homogeneities are equivalent to that of a multilayer aquifer, while at a larger scale, transverse dispersivity gets the opportunity of homogeneising their effects, macroscopically leading to an equivalent homogeneous aquifer. In the same order of ideas, parameters are homogeneous in an REV of aquifer (Representative Elementary Volume according to J. BEAR, Ref. 1) in spite of the presence of strong heterogeneities at the scale of pores.

- Tracer tests performed in natural flow have an important drawback : flow direction is not known with precision; at a dimensionless distance (Péclet number), between 10 and 20, an angular error of 10° to 20°, which is very probable, considerably lowers the response amplitude (Fig. 5). In many cases, the concentrations do not reach sensibility threshold, or at least are of the order of magnitude of analyses imprecisions.

  It is then necessary to drill several sampling wells on a line perpendicular to flow direction or on a circle centered on injecting well, in order to get sampling as close as possible to flow axis (Ref. 2).

- With tracer tests in radial converging flow, it is possible to take advantage of existing wells often equipped with satellite piezometer(s) (primarily used in order to get storage coefficient), and a pump. Expenses are then reduced to tracer injection, regulation of flow rate and automatic sampling device, analyses and interpretation.

- This last type of test does not yield transverse dispersivities : for that purpose it would be preferable to operate with uniform flow and a set of sampling wells (Ref. 9). However, field experiments performed in different sites and velocities indicate dispersivity anisotropy ratios (α_L/α_T) always of the order of 20. If more experiments still show the same ratio, the measure of longitudinal dispersivity α_L will clearly be sufficient.

REFERENCES

1. BEAR, J., Dynamics of fluids in porous media, *New York, American Elsevier,* 1972.

2. FRIED, J.J. and M.A. COMBARNOUS, Dispersion in porous media, In: *Advances in hydroscience, New York, London, Academic Press,* Vol. 7, p. 169-282, 1971.

3. GAILLARD, B., J. GUIZERIX, J. MARGAT, J. MOLINARI AND P. PEAUDECERF, Etude methodologique des caracteristiques de transfert des substances chimiques dans les nappes - 5ème rapport - Synthèse de la recherche, *Paris, Centre national de la recherche scientifique, Action thématique programmée Hydrogéologie,* 1976.

4. GAILLARD, B., Méthode de traceurs pour la determination des paramètres de transfert de subtances en solution dans l'eau des aquifères, *Grenoble, these, Universite,* 1976.

5. GAILLARD, B., D. ROUSSELOT AND J.P. SAUTY, Applications d'une méthode économique de determination sur le terrain des paramètres de dispersion, *Hydrodynamic diffusion and dispersion in porous media, Symposium A.I.R.H., Pavie,* 1977.

6. MOLINARI, J. and P. PEAUDECERF, Essais conjoints en laboratoire et sur le terrain en vue d'une approche simplifiée de la prevision des propagations de substances miscibles dans le aquifères réels, *Hydrodynamic diffusion and dispersion in porous media, Symposium A.I.R.H., Pavie,* 1977.

7. ROUSSELOT, D., Etude hydrogéologique de la zone de Blyes-Saint-Vulbas (01) France, *BRGM, rapport inédit 77 SGN 157 JAL,* 1977.

8. SAUTY, J.P., Identification of hydrodispersive mass transfer parameters in aquifers by interpretation of tracer experiments in radial converging and diverging flow, (In French), *Journal of Hydrology* (submitted: March 1977, accepted: 1977).

9. SAUTY, J.P., Contribution a l'identification des paramètres de dispersion dans les aquifères par l'interprétation des expériences de tracage, *Thèse: doct.-ing. Grenoble,* 1977.

10. SAUTY, J.P., Hydrodispersive transfer in aquifers. Identification of dispersion parameters. Paper in preparation for submission to *Water Resources Research.*

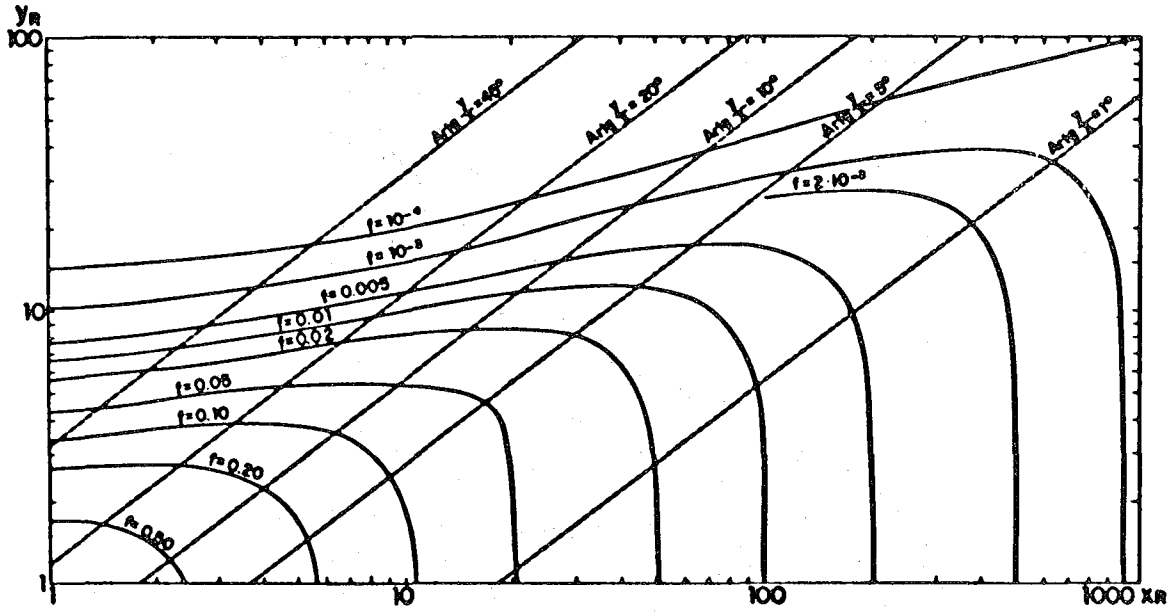

Fig. 5. Instantaneous injection in a bidimensional and uniform flow. Amplitude relative to the top of the restitution curve relative to Xr and Yr mapped by logarithmic coordinates.

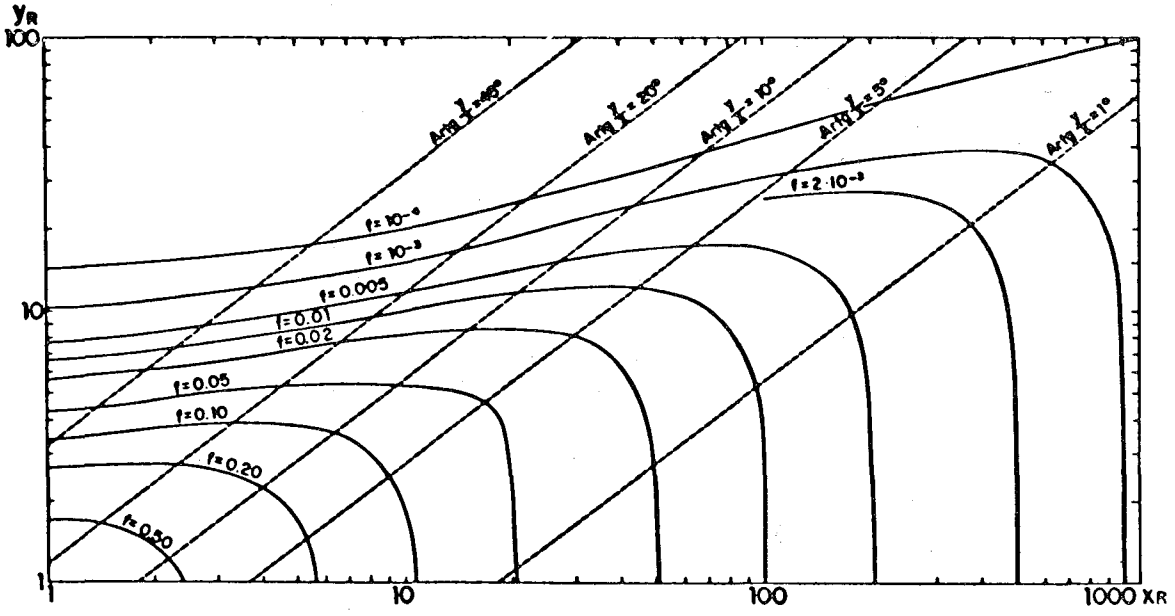

Fig. 6. DIRAC pulse in uniform flow. Relative peak values in function of dimensionless coordinates.

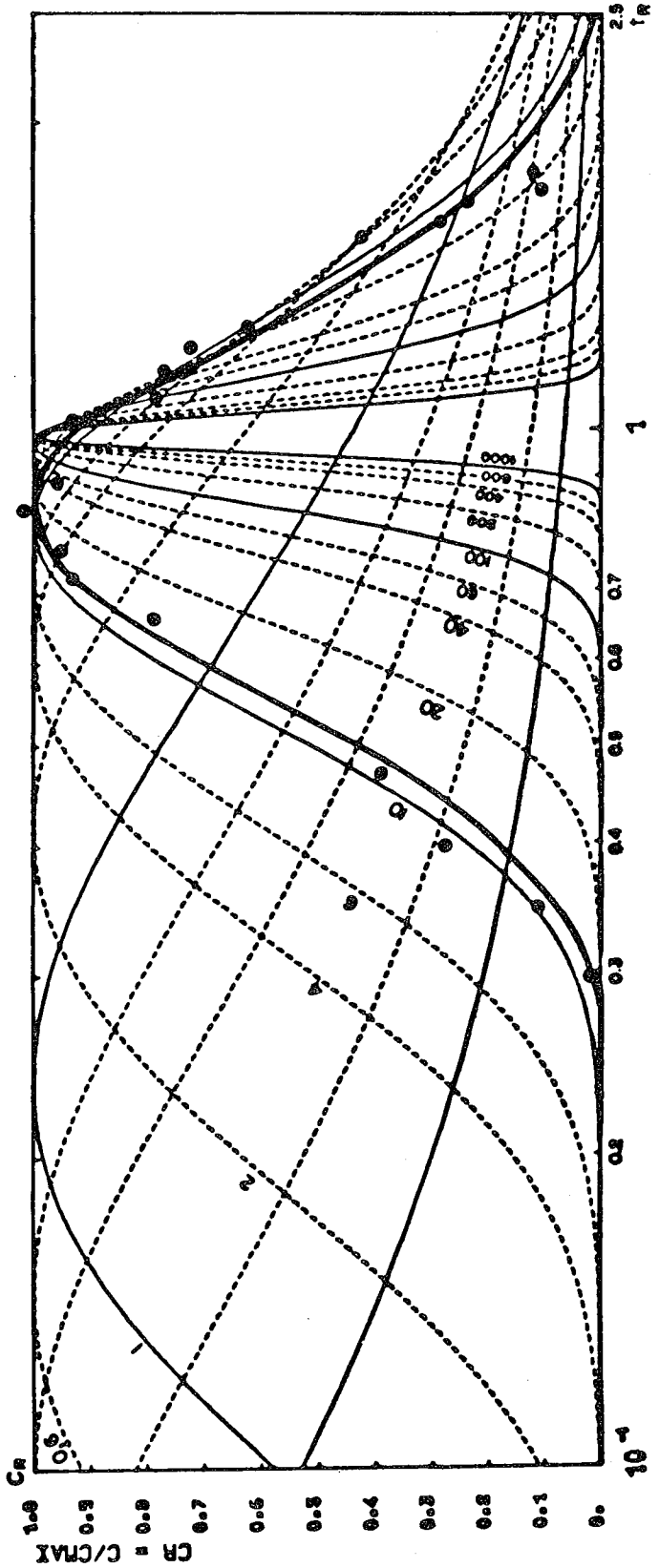

Fig. 7. Example of dispersion parameters identification from in situ tracer tests.

ABSTRACT

ROLE OF PARAMETER IDENTIFICATIONS IN THE DESIGN AND ANALYSIS OF PUMPING TESTS

Shlomo P. Neuman
University of Arizona, Tucson

The results of conventional pumping tests are usually interpreted on the basis of analytical solutions in which the aquifer (or reservoir) is assumed to be homogeneous and possesses an idealized geometry. Such tests rely further on the introduction into the system of a single control signal (e.g., a constant or piece-wise constant rate of pumping) at a single well location. In practice, aquifers tend to be inhomogeneous and have a complex geometry. The need to maintain a prescribed rate of pumping in only one well, while shutting down neighboring wells to prevent interference with the test, is often costly and at times impractical. Moreover, the parameters determined for such tests tend to have only a local significance.

It is suggested that numerical modeling coupled with parameter identification techniques should make it possible to design large scale tests in which several wells pump simultaneously at variable rates. Such tests will cause minimum interference with normal field operations and will yield more reliable parameter estimates than those obtained by conventional methods. A blue print for the design of such tests is presented in this paper.

Variable Rate Multiple Well Testing Analysis

D. G. McEdwards and C. F. Tsang

Lawrence Berkeley Laboratory
University of California
Berkeley, California 94720

Introduction

The graphical type-curve matching technique of analyzing well test data is widely known in the fields of petroleum engineering and hydrology. A recent treatment given by Earlougher[1] demonstrates its utility as an analytical tool. As useful as it is, however, the technique may in some cases be inappropriate. All type curve solutions model the behavior of one producing well whose flow rate follows a functional form; a type curve solution therefore, is not available for well test data that reflect the effects of two or more producing wells each of which may have a unique (arbitrary) flow rate history. To permit convenient analysis of well test data obtained under conditions that do not meet the assumptions of a type curve solution, a computer-based least-squares fitting technique similar in principle to the graphical curve matching technique has been developed.

The analysis technique presented herein accounts for the effects of two or more flowing wells, unique flow rate histories, the presence of a linear boundary (leaky or barrier), well bore storage, and skin effect. Two parameters, the mobility-thickness product, kh/μ, and the porosity-compressibility-thickness product, ϕch, are usually sought. Additionally, for production or interference tests involving one or more producing wells, the image well distance, r_i, is found if a boundary is felt.

For a one-well production test, values of kh/μ and skin are determined using known values of C, the well bore storage coefficient, and ϕchr_w^2, the porosity-compressibility-thickness-radius squared product. When production data reflect the effects of a second producing well, independent estimates of kh/μ, ϕchr^2, and skin are made using a known (input) value of the well bore storage coefficient.

The computational basis of the method is a least-squares minimization routine[2], developed at Lawrence Berkeley Laboratory, that adjusts the values of the fitting parameters X_i, i = 1 to NPAR, such that the sum of the squares of the differences between the log of the calculated drawdown and the log of the observed drawdown is a minimum. The parameters associated with a minimum are directly related to either reservoir or well bore properties.

Written mathematically, we minimize

$$\chi^2 = \sum_{j=1}^{IDATA} \left[\ell n \Delta P^j(X_i) - \ell n \Delta P_o^j(X_i) \right]^2 \qquad (1)$$

with respect to X_i, i=1 to NPAR, where IDATA is the number of observed drawdowns (data points). As (*1*) indicates both calculated and observed pressure changes may, in principle, be functions of certain fitting parameters X_i.

The paper comprises five main sections: I, an analytical development section which presents the ways in which variable flow rates, boundaries, well bore storage, skin effect, and two or more producing wells are treated; II, a section describing the operation of the minimization procedure; III, a section concerning validation of the method in light of known solutions; IV, a section containing examples of the method applied to field data; and V, a section discussing the proper use of the least-squares well test analysis program.

I. Analytical Development

A. *Variable Flow Rate*

The pressure change around a line source of instantaneous strength q^* is given by[3].

$$\Delta P(r,t) = \frac{q^*}{4\pi\eta t} e^{-r^2/4\eta t} \qquad (2)$$

where $\eta = \frac{k}{\mu\phi c}$, is the hydraulic diffusivity.

With q as the amount of fluid released instantaneously per unit length of line source, we may write

$$q = q^*\phi c \; ; \quad \text{or} \quad q^* = \frac{q}{\phi c} \; . \qquad (3)$$

Further, with h as the length of the line source (thickness of the aquifer with a fully penetrating well) Q, the total amount of fluid released instantaneously by the line source is

$$Q = qh = q^*\phi ch \; ; \quad \text{or} \quad q^* = \frac{Q}{\phi ch} \; . \qquad (4)$$

Substituting (*4*) into (*2*) we obtain the pressure change at any time and radius caused by the instantaneous release of a volume of fluid Q from the line source:

$$\Delta P(r,t) = \frac{Q\mu}{4\pi kht} e^{-r^2/4\eta t} \; . \qquad (5)$$

We may think of a time varying flow rate as a time sequence of instantaneous Q's, whose magnitudes correspond in time to the flow rate value. With $Q_n(\tau)$ representing the flow rate from τ_n to τ_{n+1}, we integrate the instantaneous response (*5*) in time to get

$$\Delta P_n(r,t) = \frac{\mu}{4\pi kh} \int_{\tau_n}^{\tau_{n+1}} \frac{Q_n(\tau)}{t-\tau} e^{-r^2/4\eta(t-\tau)} d\tau \qquad (6)$$

which is the pressure response due to a line source active from τ_n to τ_{n+1} with a flow rate $Q_n(\tau)$. With $Q_n(\tau) = Q$, a constant, and letting $\tau_n = 0$, and $\tau_{n+1} = t$, (6) becomes

$$\Delta P(r,t) = \frac{Q\mu}{4\pi kh}\int_o^t \frac{e^{-r^2/4\eta(t-\tau)}}{t-\tau}\,d\tau$$

$$= \frac{Q\mu}{4\pi kh}\int_{r^2/4\eta t}^{\infty}\frac{e^{-u}}{u}\,du \qquad (7)$$

$$= \frac{Q\mu}{4\pi kh}\left[-Ei\left(\frac{-r^2}{4\eta t}\right)\right] = \frac{Q\mu}{4\pi kh}\,W(U)$$

$$= \frac{Q\mu}{2\pi kh}\,P_D(t_D)$$

where $-Ei\left(\frac{-r^2}{4\eta t}\right)$, the exponential integral, is known to hydrologists as the well function $W(U)$ (where $U = \frac{r^2}{4\eta t}$) and by petroleum engineers as twice the dimensionless pressure, $2P_D(t_D)$ (where $t_D = \frac{\eta t}{r^2} = \frac{1}{4U}$).

To handle variable flow rate $Q(t)$, we assume that any production rate history can be adequately represented by a series of sequential straight line segments, each of different length and inclination. We prescribe $Q(t)$ to vary linearly within the interval τ_n to τ_{n+1} as,

$$Q_n(\tau) = A_n + B_n(\tau-\tau_n) \qquad (8)$$

With these definitions (of two fitting parameters)

$$X1 = \frac{\mu}{4\pi kh} \quad \text{and} \quad X2 = \frac{r^2}{4\eta},$$

and in light of (8), (6) becomes

$$\Delta P_n(r,t) = X1\int_{\tau_n}^{\tau_{n+1}}\left[A_n + B_n(\tau-\tau_n)\right]\frac{e^{-X2/(t-\tau)}}{t-\tau}\,d\tau \qquad (9)$$

Summing (9) for N time intervals we obtain

$$\Delta P(r,t) = \sum_{n=1}^{N}\Delta P_n(r,t) \qquad (10)$$

Where $\Delta P(r,t)$ is now the pressure response due to N linearly-varying production rate segments.

To obtain $\Delta P(r,t)$ we require a convenient computational form of (9). We may write (9) differently as

$$\Delta P_n(r,t) = X1\int_{\tau_n}^{t}\left[A_n + B_n(\tau-\tau_n)\right]\frac{e^{-X2/(t-\tau)}}{t-\tau}\,d\tau$$

$$-X1\int_{\tau_{n+1}}^{t}\left[A_n + B_n(\tau-\tau_n)\right]\frac{e^{-X2/(t-\tau)}}{t-\tau}\,d\tau \qquad (11)$$

Because the two integrals in (11) are identical except for the lower limit of integration, it is necessary to operate on the first integral only, and then by exact analogy, extend all analytical results to the second integral to arrive at a convenient form of (9).

Making use of the relations

$$\int_{\tau_n}^{t} e^{-X2/(t-\tau)}\,d\tau = X2\int_{U_n}^{\infty}\frac{e^{-u}}{u^2}\,dU \qquad (12)$$

and

$$\frac{e^{-u}}{u^2}\,dU = \frac{e^{-u}}{u} - \int\frac{e^{-u}}{u}\,dU \text{ , we obtain} \qquad (13)$$

$$\Delta P_n(r,t) = X1\Big\{\left[A_n + B_n(t-\tau_n + X2)\right]\left[W(U_n) - W(U_{n+1})\right] + B_n\left[(t-\tau_n)\,e^{-U_n} - (t-\tau_{n+1})\,e^{-U_{n+1}}\right]\Big\} \qquad (14)$$

which is convenient computational form of (9) that we may use in (10). Note that (14) reduces to (7) when $\tau_n = 0$, $\tau_{n+1} = t$, $B_n = 0$, and $A_n = Q$, a constant.

It may be of interest to write the solution corresponding to a line source whose flow rate starts at zero and increases linearly. For this case $\tau_n = 0$, $\tau_{n+1} = t$, $A_n = 0$, $B_n = B$, a constant:

$$\Delta P(r,t) = \frac{\mu Bt}{4\pi kh}\left[U\cdot W(U) + W(U) + e^{-U}\right] . \qquad (15)$$

In dimensionless form, in the hydrologists' notation, we may define

$$W_1(U) = \frac{4\pi kh\Delta P}{\mu Bt} = U\cdot W(U) + W(U) + e^{-U} \qquad (16)$$

and in petroleum engineers' notation, we may define

$$Pd_1 = \frac{2\pi kh\Delta P}{\mu Bt} = \frac{P_D(t_D)}{4t_D} + P_D(t_D) + \frac{e^{-1/4t_D}}{2} \qquad (17)$$

Equations (15) through (17) are presented for the sake of completeness and in the belief that they are not widely known in literature.

In summary, variable flow rates are accounted for by use of equations (14) and (10):

$$\Delta P(r,t) = X1\sum_{n=1}^{N}\Big[\left[A_n + B_n(t-\tau_n + X2)\right]\left[W(U_n) - W(U_{n+1})\right] + B_n\left[(t-\tau_n)\,e^{-U_n} - (t-\tau_{n+1})\,e^{-U_{n+1}}\right]\Big] \qquad (18)$$

B. Boundaries

The influence of a linear boundary is seen by the inclusion of another parameter X3;

$$X3 = \frac{r_i^2}{4\eta} \qquad (19)$$

where r_i is the distance of an image well from the observation well. The component of pressure change due to an image well, or its equivalent linear boundary, is gotten from (18) with X3 in place of X2, thus the total drawdown is

$$\Delta P(r,t) = \sum_{n=1}^{N}\Delta P_n(r,t) \pm \Delta P_n(r_i,t) \qquad (20)$$

where the positive sign indicates a barrier boundary and the negative sign indicates a leaky boundary.

C. *Well Bore Storage*

For production tests, the well bore storage[4] effect is handled relatively easily. We replace $Q_n(\tau)$ by the sandface flow rate $Q_{SF,n}(\tau)$, which is of the same form as $Q_n(\tau)$:

$$Q_{SF,n}(\tau) = A_{SF,n} + B_{SF,n}(\tau-\tau_n)$$

$$\text{where,} \quad A_{SF,n} = A_n - C \left.\frac{\partial \Delta P_w}{\partial \tau}\right|_{\tau=\tau_n} \qquad (21)$$

$$\text{and } B_{SF,n} = B_n - \frac{C}{(\tau_{n+1}-\tau_n)} \left[\left.\frac{\partial \Delta P_w}{\partial \tau}\right|_{\tau=\tau_{n+1}} - \left.\frac{\partial \Delta P_w}{\partial \tau}\right|_{\tau=\tau_n} \right]$$

In (*21*), C, the well bore storage coefficient is equal to $V_w/h\gamma\ell$ if the well has a free liquid level, or equal to $V_w C\ell$ if the well is completely filled with fluid, and is in principle a known value. In determining sandface rates, (*21*) shows that it is necessary to known the time rate of change of the drawdown in the well bore at the times of the A_n specifications. The sandface flow rate derivation given above assumes that a sufficiently small time interval, $\tau_{n+1}-\tau_n$, is taken such that the sandface rate variation can be taken as linear with time within the time interval.

D. *Skin Effect*

A steady state skin effect[5] is included in a production test analysis by noting that

$$\Delta P(r_w,t) = \Delta P(r,t) + X1 \cdot 2S \cdot Q_{SF}(t) \qquad (22)$$

in which $\Delta P(r,t)$ on the right side denotes the pressure change on the formation side of the well bore. In the least-squares program, the product $X1 \cdot 2S$ is treated as another parameter, X4, and (*22*) becomes

$$\Delta P(r_w,t) = \Delta P(r,t) + X4 \cdot Q_{SF}(t) \qquad (23)$$

E. *Many Production Wells*

A straight forward modification of (*1*) is necessary to analyze data influenced by two or more production wells. Each production well will cause a pressure change according to its production rate variation and its distance from the point of observation. The pressure change is calculated using equation (*18*). The total pressure change caused by NW production wells is obtained by summing the contributions of each well:

$$\Delta P(r,t) = \sum_{k=1}^{NW} \Delta P_k(r_k,t) \qquad (24)$$

where $\Delta P_k(r_k,t)$ is calculated from (*18*) with the values of A_n, B_n, and X2 taking on values that correspond to the k'th well's production rate and its distance r_k, from the point of observation. To accomodate various radii r_k (whose values are known), in the X2 term, it is necessary to redefine X2. Recalling that previously $X2 = \frac{r^2}{4\eta}$ in the case of one producing well, we let $X2 = \frac{1}{4\eta}$ in the case of two or more producing wells and calculate $\Delta P_k(r_k,t)$ from (*18*) using $X2 \cdot r_k^2$ in place of the former X2. With these changes, equation (*1*) written to reflect the influence of two or more production wells, is

$$\chi^2 = \sum_{j=1}^{IDATA} \left[\ell n \sum_{k=1}^{NW} \Delta P_k^j \,(Xi) - \ell n \Delta P_o^j \,(Xi) \right]^2 \qquad (25)$$

To include the effect of boundaries in the case of two or more production wells, we must add another parameter for each production well that we include in the analysis. These additional parameters correpond to the locations of each production well's image well. For example, the drawdown component of the kth production well in the presence of a linear boundary is

$$\Delta P_k = \Delta P_k(r_k,t) \pm \Delta P_k(r_{ik},t) \qquad (26)$$

where $\Delta P_k(r_{ik},t)$ is calculated form (*18*) using a redefined value of X2, as before. Because r_{ik} is unknown we simply let the product $X2 \cdot r_{ik}^2$ be X(k), an additional fitting parameter.

II. The Procedure of Curve Matching

The minimization procedure used in the least-square program is very similar to graphical curve matching. The program in essence computes an analytically predicted pressure response record that corresponds with the given production wells' flow rates, distances to the point of observation, and particular set of reservoir (fitting) parameters. A measure of how well the predicted values match the observed values are given by the χ^2 statistic, Equation (1). Many response records are calculated and their χ^2 values are compared in a computer search for the smallest χ^2 value. The response record with the smallest χ^2 value is taken to be the best fit and the corresponding set of fitting parameters are taken to represent the reservoir or well bore properties. Starting with the set of initial guess values, proceeding from one response record to another, the fitting parameters are simultaneously changed in directions corresponding to a decreasing value of χ^2. This requires knowing the gradient of χ^2 with respect to each fitting parameter. Knowing the gradient $\partial\chi^2/\partial X_i$, a numerical extrapolation scheme is used in calculate new trial values of X_i that correspond to the X_i values changing in the direction of decreasing gradient. As each gradient may be functionally dependent on all the fitting parameters, the calculation of new trial values of X_i requires matrix multiplication and inversion operations. The search for a lower χ^2 value is terminated when one or more of several criteria (regarding the absolute value, or the successive change in the value, of either the gradients of χ^2 or χ^2) are met.

A modified version of a computer program called LSQVMT[2], a non-linear least-squares procedure, is used to form χ^2. The minimization procedure incorporated in LSQVMT is based on a iterative gradient method that used a variable metric (computer routine VARMIT[6]). The program LSQVMT can handle up to 40 fitting parameters. Both LSQVMT and VARMIT are available as library routines at the computer center of the Lawrence Berkeley Laboratory.

III. Validation

The validity of the variable flow rate equations derived earlier has been shown by four examples given in a previous work[7]. We present one of these examples, a well test involving well bore storage and a constant surface rate as indicative of the program's ability to handle variable production rate accurately. A second example, a interference test involving three production wells, each of different rate and starting time, is given to show the ability of the program to handle more than one production well. Examples involving skin effect and boundaries are given in the field applications section.

Table 1. Data Used in Verification Examples.

Production Well with Well Bore Storage		3 Staggered Production Wells, Different Q's & r's	
kH = 484,000 md-ft. ϕcH = 2.128 ft/psi. Q = 100 gpm r = 1 ft. C = 1000 gal/psi.		kH = 30,000 md-ft. ϕcH = 1.0×10^{-3} Q, gpm (Figure 3) r, ft. (Figure 3)	
Time Minutes	ΔP psi	Time Weeks	ΔP psi
1	9.9717×10^{-4}	.2	1.96
2	1.9934×10^{-3}	.5	5.99
5	4.9773×10^{-3}	1.0	10.28
10	9.9382×10^{-3}	2.0	15.16
20	1.9821×10^{-2}	3.5	19.35
50	4.9206×10^{-2}	5.0	32.72
100	9.7432×10^{-2}	7.0	48.60
200	1.9146×10^{-1}	9.0	58.45
500	4.5722×10^{-1}	11.0	73.22
1,000	8.5575×10^{-1}	15.0	109.73
2,000	1.5337	20.0	132.67
5,000	2.8668		
10,000	4.0120		
20,000	4.9150		
50,000	5.6617		
100,000	6.0823		
200,000	6.4615		
500,000	6.9382		
1,000,000	7.2919		

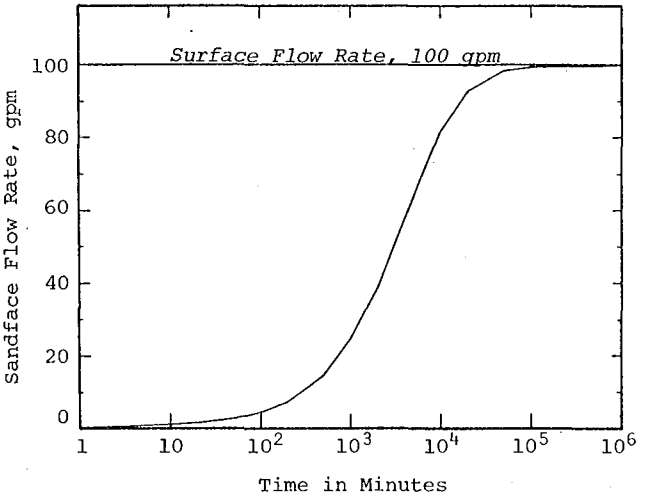

Figure 1. Sandface Flow Rate as a Function of Time.

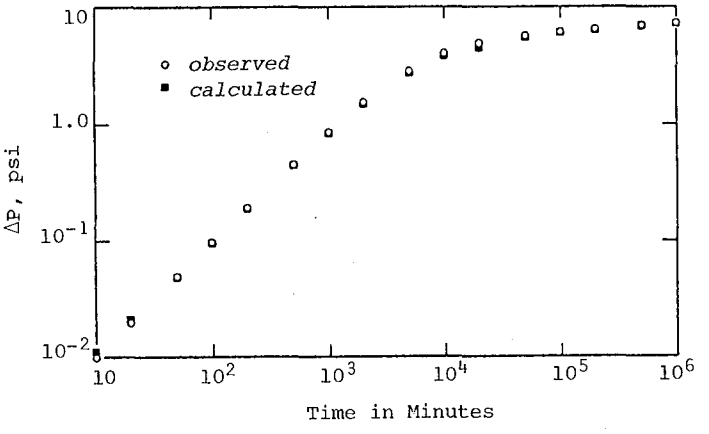

Figure 2. Computer Assisted Match of Predicted and Theoretical Drawdowns.

A. *Constant Flow with Well Bore Storage*

This verification problem relates to a well with significant well bore storage but no skin (s=0). The dependence of P_D on t_D for such a system has been provided by Wattenbarger and Ramey[8]. The hypothetical reservoir considered has kh = 484,300 md-feet and ϕch = 2.128 feet/psi and is pierced by a well with a well bore capacity C = 1000 gal/psi. The well produces at a constant surface rate of 100 gpm. The drawdown history of the aforesaid well as computed using Wattenbarger and Ramey $P_D(t_D)$ values is shown tabulated in Table 1.

The time dependent variation of the sandface flow rate $Q_{SF,n}$, as determined using *(21)* is presented in Figure 1. The analysis performed (Figure 2) yield kh = 485,000 md-feet and ϕch = 2.299 feet/psi.

B. *Three Staggered Production Wells of Different Rates and Distances*

Interference test data expected for one observation well located some distance from three producing wells is given in Table 1. The assumed reservoir properties are kh = 30,000 md-feet and ϕch = 1.0×10^{-3} feet/psi. A plot of the observation well's pressure change and the distances and rates of each production well are shown in Figure 3. Using perturbed values (±5%) of the values in Table 1, an analysis was run whose results are shown in Figure 4. Agreement is quite good as seen by the returned values of kh = 30,300 md-feet and ϕch = $.987 \times 10^{-3}$ feet/psi.

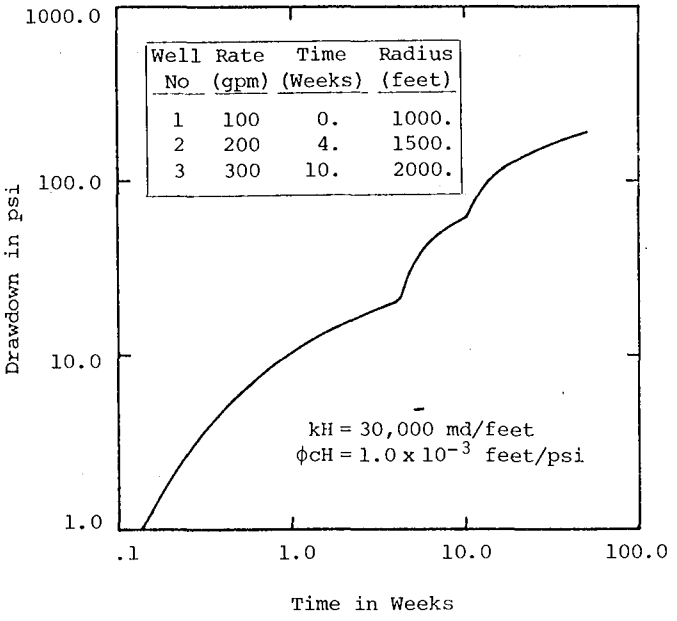

Figure 3. Three Staggered Production Wells.

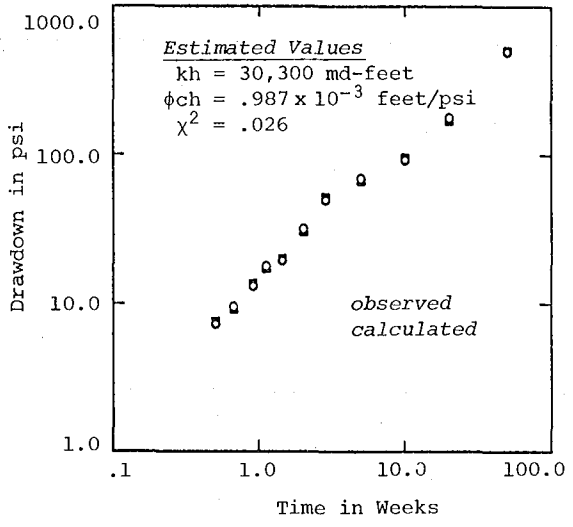

Figure 4. 3 Staggered Production Wells.

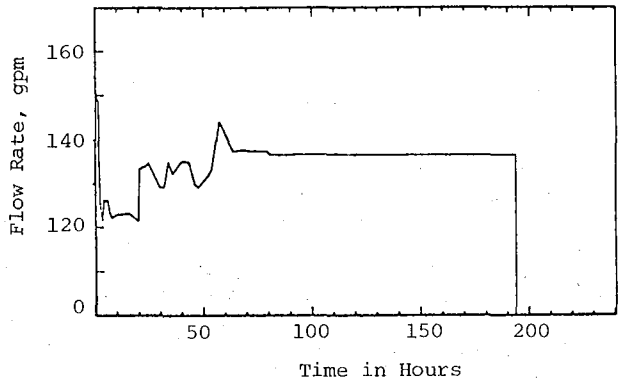

Figure 5. Production Test on Well RRGE 3, Raft River Valley; Flow Rate as a Function of Time.

IV. Field Applications

We have applied this method of analysis to well tests conducted in two geothermal reservoirs, one at Raft River Valley, Idaho and the other at East Mesa in the Imperial Valley of southern California[9]. As several of these field examples have been published[7], we present two representative analyses:

1. A production test on Well RRGE 3 in Raft River Valley, Idaho, and
2. An interference test involving Wells 31-1 and 38-30 at East Mesa in California.

Skin effect is treated in the first analysis and the detection of a barrier boundary is demonstrated in the second analysis.

A. *Production Test on Well RRGE 3, Raft River, Valley, Idaho*

During this test the well was flowed for 193.5 hours. Due to practical difficulties the flow rate could not be regulated properly during the first 20 hours of the test. The observed variable flow rate history is presented in Figure 5.

In addition to the variable flow rate, the interpretation of the drawdown data collected during the test is complicated by the fact that Well RRGE 3 is a whipstock well, with three differently inclined legs, with bottoms ending at different elevations over a radius of roughly 400 feet. Furthermore, drilling operations indicated that each leg produced different quantities of water, suggesting that the formations pierced by each leg had different local permeability characteristics. The data interpretation which follows is therefore only a tentative interpretation as far as the actual reservoir characterization is concerned.

Using the computer program, the data are analyzed both with and without storage, C, and skin effect, s. For each case, data collected during the first 18 hours of production history as well as the full range of data of 0 to 328 hours (Figure 5) are analyzed. Note that the latter calculation includes both the production (193 hours) and build-up (135 hours) data in the same analysis, pointing our a further advantage of the present technique. The results of these analyses are summed up in Table II. For each of the analyses shown in the Table, several runs were made using different initial guesses with both positive and negative values for the skin, s. In all cases the same results were obtained (within 1% of each other), thus indicating the strength of the fit.

The well bore storage coefficient, C, as discussed earlier, is a known quantity. However, in this case where we have a whipstock well with three differently inclined legs, the estimation of C is rather uncertain. Hence we analyze the data with values of C equal to 0, 5, 10, 13, and 20 gallons/psi. It turns out much to our surprise that the fit and the optimal values of parameters depend very little on the value of C chosen. When the

Table II. Variable Discharge Interpretations. Well RRGE 3, Raft River Valley, Idaho.

Assumed Parameters	Data Period	Input C gal/psi	kh (md-feet)	ϕchr_w^2 ft^3/psi	s
Without Well Bore Storage and Skin Effect	0 - 18 hours	-	11,900	1.31	-
	0 - 328 hours	-	6,400	0.86	-
With Well Bore Storage and Skin Effect	0 - 18 hours	5	7,400	27.2	0.7
		10	7,600	28.1	0.7
	0 - 328 hours	5	7,000	0.01	-2.7
		10	7,000	0.01	-2.4

sandface flow-rate is calculated by equation *(21)* it is found that it differs from the surface flow-rate only for a very short time (<30 minutes) after each change in the flow-rate.

Now compare the results for the short-term analysis of 0-18 hours data with and without well bore storage and skin effect, Figures 6 and 7. This is the region where the flow-rate is markedly varying. The Figures show a much better fit when well bore storage and skin are taken into account. A good fit and similar parameters are also obtained when we set C = 0. Hence this shows that in our case the effect of skin is very significant. Though the value obtained for the skin factor, s = 0.7 is quite small, its inclusion in the time dependent term $Xl \cdot 2s \cdot Q_{SF}(t)$ of equation *(22)* is what is needed to yield a good fit.

There is also an improvement in the fit of the long range data, 0-328 hours, when well bore storage and skin are taken into account. In Figure 8 we show the results when well bore storage, C = 10 gallon/psi, and the skin effect are included. In this analysis, the kh value obtained is very similar to that obtained in short term data. However, skin factor, s, turns out to be negative s = -2.4, and the ϕchr_w^2 value is also different from the short term result. By making several runs with the same data, these values are found to be independent of different sets of initial guesses. A possible explanation of these results follows (we are aware that alternative interpretations may exist). The well RRGE 3 has three different inclined legs with bottoms ending over a radius of roughly 400 feet. At early times the water is released from storage from the region with the 400 feet radius, with the three legs *competing* for water between themselves. This may be represented by a single well of a large effective r_w (hence large ϕchr_w^2 value) and a positive skin factor. On the other hand, at large times, the water is being drawn from regions away from the legs, r > 400 feet. The system may then be represented by a single well with a smaller effective r_w (hence smaller ϕcHr_w^2 value) and a negative skin factor, implying that the effect of the three legs can be treated as equivalent to that of a highly conductive fracture.

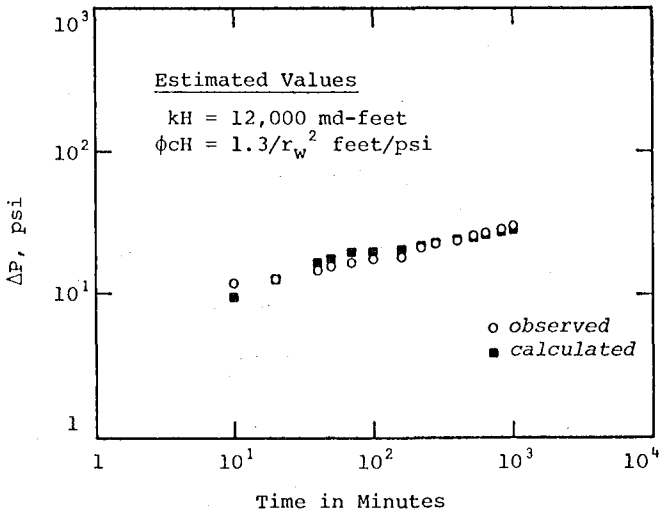

Figure 6. Production Test on Well RRGE 3, Raft River, Idaho; Computer Assisted Match of Calculated and Observed Drawdowns During the First 20 Hours of Production. C = 0; s = 0.

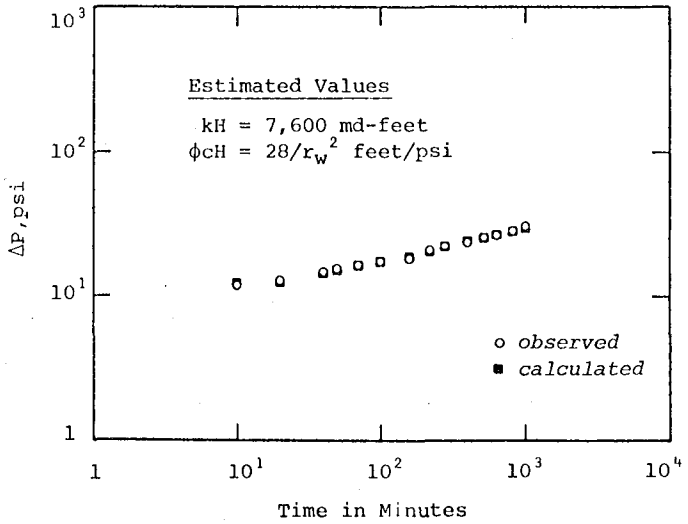

Figure 7. Production Test on Well RRGE 3, Raft River Valley, Idaho; Well Bore Storage and Skin Effect. C = 10; s = 0.7.

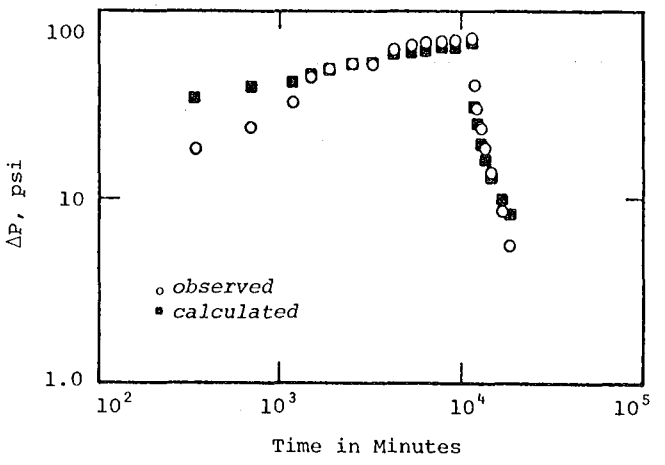

Figure 8. Production Test on Well RRGE 3, Raft River Valley, Idaho; Computer Assisted Match of Calculated and Observed Drawdowns; 0 → 328 Hours. C = 10 gal/psi; s = -2.4.

B. *Interference Test between Wells 31-1 and 38-30, East Mesa, California*

During this test, Well 31-1 was produced at a flow rate of about 130 gpm for about 237 hours and pressure drawdowns were observed in Well 38-30 about 1250 feet away. In this case the observed data was matched against calculated data generated with three parameters, X1, X2, X3, the last one being included to take into account boundary effects. The computer aided fit, Figure 9, indicates kh = 36,800 md-feet, $\phi ch = 2.1 \times 10^{-3}$ feet/psi and the possible presence of a barrier boundary which is effectively equivalent to an image well at a distance of r_i = 3000 feet from the observation well. The observed data, when analyzed by the graphical curve-matching technique, indicated kh = 29,500 md-feet, $\phi ch = 2.1 \times 10^{-3}$ feet/psi and r_i = 3000 feet.

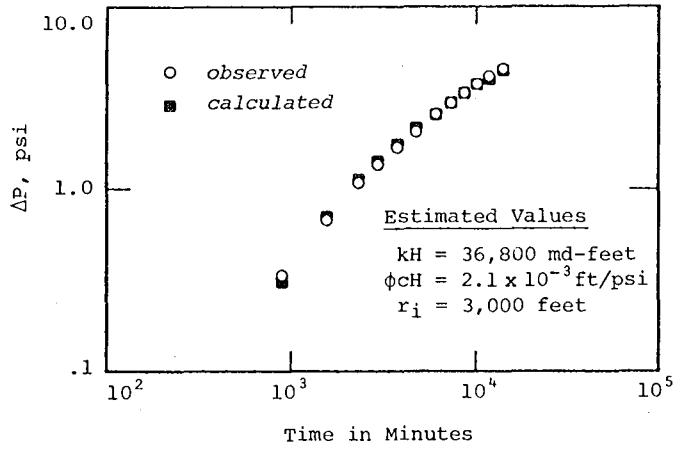

Figure 9. Interference Tests Between Wells 31-1 and 38-30, East Mesa, California; Computer Assisted Match of Calculated and Observed Drawdowns.

V. Proper Use of the Least-Squares Program

The use of the fitting program for well test analysis is not a completely automatic process. Engineering judgement must be used to gauge the reasonableness of any result. In many cases, because of the quality of the data, there may exist several χ^2 minimum candidates, each corresponding to a particular set of optimal parameters. This being the case, the particular minimum and associated parameters returned by the program are dependent on the values of the initial guesses given for the parameters, i.e., in χ^2 country, which minimum you encounter first will depend on where you begin looking. This situation normally presents no difficulty however, as the correctness of a minimum is readily seen in an on-line log-log plot of observed vs. predicted drawdowns and in the values of the parameters returned. For correct order-of-magnitude initial guesses, using reasonably good data, the proper minimum is usually achieved. The final selection of fitted parameter values should be based on a comparison of several computer runs each of which considers different effects (with skin, without skin, etc.) and each of which are judged to have returned proper minimum χ^2 values. The final set of reservoir parameter values should be then taken from the computer run having the smallest χ^2 value.

To date we recognize two well test situations for which a reliable set of reservoir values is impossible to obtain by the least-squares method. These are: 1) a single production well with a nominal well bore radius whose observed in-well pressure changes are to be analyzed for kh, ϕch, and skin; and 2) an interference test with one production well for which the observation well data are to be analyzed for kh, ϕch, and r_i, the distance to a *leaky* boundary. The root cause of difficulty in both cases is that two of the three parameters interact in such a way as to permit nearly identical χ^2 minimum values to be returned for differently-valued parameter pairs. This does not mean, however, that it is not possible to analyze for skin or for a leaky boundary. We anticipate these analyses may be performed with no difficulty provided that the observed data reflect the effects of more than one production well, and that the analysis properly accounts for all production wells' effect. It is well to note here that the field application of the program was successful for the RRGE 3 well test because of the well's unique three-leg character (large effective radius).

VI. Future Work

We are currently extending this method of analysis to handle variable flow from a vertical fracture intersecting the well bore, and to account for nonstatic background pressure. The analysis of many production wells in the presence of a linear boundary has not been implemented as yet, but this presents no difficulty as it merely requires slight modification of the existing program structure. We also hope to extend the method to simultaneously analyze data from two or more observation wells in the presence of two or more production wells.

Conclusions

We have demonstrated the feasibility of conveniently analyzing complicated well test situations by use of the digital computer. Much greater flexibility of well test design can now be accomodated and well test data previously through to be of little value may in some cases be utilized, Furthermore, the availability of portable, telephone coupled computer terminals makes such a computer assisted method practical in on-site field applications.

Acknowledgements

We thank the Earth Sciences Division of LBL for supporting and encouraging our research effort, both in the form of the Well Testing Symposium and in the financial aspect.

Nomenclature

A_n -Coefficient used in defining variable flow rate, L^3/T.
B_n -Coefficient used in defining variable flow rate, L^3/T^2.
c -Total compressibility, LT^2/M.
$c\ell$ -Compressibility of liquid, LT^2/M.
C -Well bore storage coefficient, L^4T^2/M.
h -Thickness of reservoir, L.
k -Absolute permeability of reservoir, L^2.
P -Pressure, M/LT^2.
P_D -Dimensionless pressure.
ΔP -Total pressure drawdown at distance r and time t, M/LT^2.
ΔP_n -Pressure drawdown due to flow during the time interval $\tau_{n+1}-\tau_n$, M/LT^2.
ΔP_o -Pressure drawdown observed during test, M/LT^2.
ΔP_w -Pressure drawdown at the well bore, M/LT^2.
q -Quantity of fluid instantaneously released per unit length of line source, L^3.
q* -Strength of line source, ML/T^2.
Q -Flow rate from line source, L^3/T.
Q_n -Flow rate during the interval, $\tau_{n+1}-\tau_n$, L^3/T.
$Q_{SF,n}$ -Sandface flow rate during the interval $\tau_{n+1}-\tau_n$, L^3/T.
r -Distance to point of observation, L.
r_i -Distance to image well from point of observation, L.
r_w -Well radius, L.
s -Steady state skin coefficient.
t -Time, T.
U -Dimensionless variable, $X2/(t-\tau)$.
U_n -$X2/(t-\tau_n)$.
V_w -Volume of well, L^3.
X1 -$\mu/4\pi kh$, M/L^4T.
X2 -$\phi\mu cr^2/4k$, T; or $\phi\mu c/k$, T/L^2.
X3 -$\sigma\mu cr_i^2/4k$, T.
X4 -2sX1, M/L^2T.
η -Diffusivity, L^2/T.
$\gamma\ell$ -Specific weight of liquid, M/L^2T^2.
μ -Dynamic viscosity, M/LT.
τ_n, τ_{n+1} -End points of nth time segment, T.
ϕ -Porosity.
χ^2 -Sum of the squares of deviations used in least square fit.

References

1. Earlougher, Robert C., Jr., Advances in Well Test Analysis, Monograph Series, Society of Petroleum Engineers of AIME, Dallas (1977), 5.

2. Beals, E.,LSQMVT, A Computer Program for Non-Linear Least Squares Procedure, No. E2 BYK-LSQVMT Computer Center Library, Lawrence Berkeley Laboratory, Berkeley, California, 1966.

3. Carslaw, H.S., and Jaeger, J.C., Conduction of Heat in Solids, 2nd Edition, Oxford at Claredon Press, 258 and 261, 1959.

4. vanEverdingen, A.F., and Hurst, W., *The Application of the Laplace Transformation to Flow Problems*, Transactions, AIME, 196, pages 305-324 (1949); Agarval, R.G., Al-Hussaniny, R., and Ramey, H.J., *An Investigation of Well Bore Storage and Skin Effect in Unsteady Liquid Flow: I-Analytical Treatment*, Society of Petroleum Engineers Journal, pages 279-290, 1970.

5. vanEverdingen, A.F., *The Skin Effect and Its Influence on the Productive Capacity of a Well*, Transactions, AIME 198, pages 171-176, 1953. Hurst, W., *Establishment of the Skin Effect and Its Impediment to Fluid-Flow in a Well Bore*, Society of Petroleum Engineers, 25, B-6, 1953.

6. Beals, E., VARMIT, A Computer Program for Non-Linear Least Squares Procedure, No. E2 BYK-LSQVMT, Computer Center Library, Lawrence Berkeley Laboratory, University of California, Berkeley, California, 1966.

7. Tsang, C.F., McEdwards, D.G., Narasimhan, T.N., and Witherspoon, P.A., *Variable Flow Well Test Analysis by a Computer Assisted Matching Procedure*, Paper No. SPE-6547, 47th Annual California Regional Meeting of SPE of AIME, Bakersfield, California, April 13-15, 1977.

8. Wattenbarger, R.A. and Ramey, H.J., Jr., *An Investigation of Well Bore Storage and Skin Effect in Unsteady Liquid Flow: II-Finite Difference Treatment*, Society of Petroleum Engineers Journal, pages 291-297, 1970.

9. Witherspoon, P.A., Narasimhan, T.N., and McEdwards, D.G., *Results of Interference Tests from Two Geothermal Reservoirs*, Paper No. 6052, 51st Annual Fall Meeting of SPE of AIME, New Orleans, Louisiana, October 3-6, 1976.

Session Introduction

Special Problems

J. H. Howard
Earth Sciences Division
Lawrence Berkeley Laboratory

INTRODUCTION

This writing discusses six comments I want to make which pertain either to the session for which I was chairman or to the subject of well testing in general.

The comments are on:

- The justification for well testing
- The geological reasonableness of the conclusions of any analysis done of well-test data
- The non-unique but limited number of reasonable solutions for the analysis of well-test data
- Progress on new analyses for boundary value problems of interest to analysts of well-test data
- Development of instruments of use in acquiring well-test data
- The conceptualization of "rules" for describing mass, energy, and reactants transport in essentially non-porous, fractured media

The following paragraphs elaborate on these comments.

JUSTIFICATION OF WELL TESTING

There was little indication at the well testing symposium that anyone was especially concerned with the question of whether or not a well should be tested. The responsibility of a well tester should, however, include determination of answers to questions as: "Why should this well be tested?"; "What chance have I of obtaining data that will influence future decisions regarding exploitation of the resource of interest?"; "What risks do I run as I undertake to obtain data from a given well?"

In some instances (e.g., within a geopressured section of hole), there may be substantial risk in losing the hole because of running the test. In some instances (e.g., a southeast Asia offshore rig) the cost of time during testing may be impressively high. In some instances (e.g., an in-filling well in a reservoir having good subsurface control) practically no useful additional value may be obtained from well testing. Value of information, risk, and costs need be compared.

GEOLOGICAL REASONABLENESS OF SOLUTION

Regardless of the elegance of a mathematical analysis of well-test data, or its internal consistency, the physical reasonableness of the conclusion toward which the analyst is led should be considered. It is not reasonable, for instance, for one to conclude that a 20 meter interval produces, as indicated by test data, from a 17 meter horizontal fracture. Geologic constraints on the solution must be considered and alternative solutions sought if the conclusion is geologically unreasonable.

NON-UNIQUE BUT LIMITED NUMBER OF SOLUTIONS

It appears that in view of the scatter of data and in view of the variety of boundary and internal conditions that can lead to almost the same pressure-time signature that well test analysts should pay more attention to the different situations that could explain their data. As in geology, there is need for multiple working hypotheses. Distinction and selection among possible choices can be made based perhaps on independently acquired geologic data or on additional testing under somewhat different circumstances.

There also appears to be a need for the cataloging of situations which lead to similar pressure-time behavior so that analysts can know quickly what alternatives can yield almost the same result. How many variations on fracture width, height, length, and numbers can produce the same "answer"? Can any highly permeable, porous formation produce the same pressure-time data as a fracture-dominated reservoir?

NEW ANALYSES OF BOUNDARY VALUE PROBLEMS

The talent available for mathematical analyses of new boundary value problems and/or available for computer-assisted solutions was very impressive. One gets the impression that almost no solution is intractable. As suggested in the previous paragraph, the problem in well-test analysis may soon become one of fully appreciating all the solutions that can yield a similar result--and then selecting among them.

DEVELOPMENT OF INSTRUMENTS

The development of new instruments for collection of data by well-test analysts has, as many at the symposium noted, been most impressive. Probably new extensions to well-testing capability could be realized if one assumed the availability in the future of high sensitivity temperature recording downhole operation and of improved flow meters. I suggest that the atmosphere for instrument development is such that new analysis might be directed at problems for which data are not now available.

"RULES" FOR MASS ENERGY AND REACTANTS TRANSPORT IN ESSENTIALLY NON-POROUS FRACTURED MEDIA

The conceptualization of flow in fractured media leaves me uneasy, although I am unable to argue on an entirely rational basis for my uneasiness. Based on geologic observations I suggest, however, that much more needs to be done on analyzing pressure-time behavior of a media in which flow occurs from a network of fractures connected in dendritic form with each branch having its own flow characteristic. What branch throttles the system? How many reasonable dendritic patterns are there? (The analysis of river flow during cloud bursts may offer a useful insight to this problem.) I also suggest that experiments be conducted to verify the reliability of darcy flow in very small aperture fractures (micron range) when three phases are present (steam, water, rock; air, water, rock). I would like to see evidence supporting choice of a mass transport--pressure gradient function in very low permeability fractured rocks. I am not aware that such confirmation exists.

TRANSIENT FLOW IN TIGHT FRACTURES

J. S. Y. Wang, T. N. Narasimhan, C. F. Tsang, P. A. Witherspoon

Lawrence Berkeley Laboratory
University of California
Berkeley, California 94720

ABSTRACT

Methods are developed to analyze packer-test data from a well intersected by one or more tight fractures. In a geological formation such as granite in which fractures are the main conduits of water, the permeability of fractures to the movement of water is an important consideration in deciding the suitability of a site for radioactive waste storage. In a packer test, a pressure pulse is applied to water sealed between two packers and the pressure decay in the wellbore is monitored. When the well intersects fractures, the pressure decline is due to the flow into the fractures. In this study, the diffusivity equation governing the transient flow in the fracture is solved and the boundary conditions at the wellbore-fracture interface are discussed. Analytic and numerical solutions are given for geometrical arrangements of single infinite fractures, single finite fractures, multiple identical fractures, two fractures in series, and two fractures in parallel. "Short-time" pressure decay tests can be effectively used to estimate the fracture aperture. Further information about the continuity and connectivity of the fracture system requires "long-time" tests.

I. INTRODUCTION

Spent fuel of a nuclear reactor or waste created by fuel reprocessing contains fission products and long-lived transuranic elements. These wastes must be isolated until the radioactive isotopes have decayed to insignificant levels. We are investigating whether long-term isolation of high level radioactive wastes can be achieved by storage in a deep continental geologic formation. The hydrogeologic condition of the formations is one of the most important considerations. If radionuclides move from the storage site to the earth's surface, it will be mainly through groundwater transport.

Groundwater flow in most hard rock formations is primarily through fractures. A crystalline rock such as granite has very low intrinsic permeability, less than one microdarcy[1]. Even for a tight fracture with an aperture of the order of one micron, existing possibly at depths of one to two kilometers, the permeability of the fracture is a million times larger than that of granite. Thus, water intrusion and leakage at a waste storage site will be mainly through fractures. To estimate the rate of possible spread of the waste, it is important to have reliable measurements of the aperture size and the connectivity of the underground fracture network.

A test hole several inches in diameter provides direct access to study the formation during site exploration. The challenge of using well-testing methods for in-situ study of the fracture system is similar to the challenge faced by a reservoir engineer trying to make reliable estimations of the reservoir properties from the data at wells penetrating a permeable formation. There is, however, a difference in the test conditions. Most well testing to study reservoirs monitors the effects of given flow rates from the wellbore. The transient pressure behavior is recorded during, or immediately after, the injection or withdrawal of massive quantities of fluid or gas from the well. Maintaining a flow is not usually a problem when the well penetrates an aquifer, or a petroleum or geothermal reservoir containing large amounts of easily-removable liquid or gas. HOwever, when the well is located in an almost impermeable rock formation, the flow rate from or to the formation at the wellbore will be very low and difficult to measure. Therefore, to study tight fractures in deep crystalline rock masses, it is desirable to test the well without maintaining a flow.

Pulse packer testing:

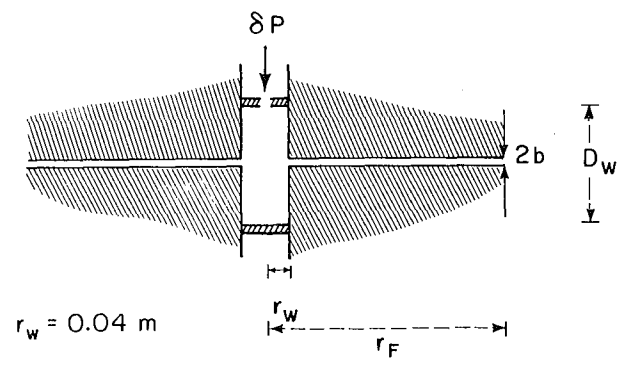

Figure 1. Schematics of a wellbore intersecting a fracture.

In a pulse-packer test (Figure 1), a section of the well is sealed between two impermeable packers. In a fully-saturated zone underground, the wellbore space between the packers is filled with water at ambient pressure. At some initial time, t = 0, an

additional pressure increase is applied by a slight squeeze of the sealed water. If the wellbore between the packers intersects fractures, the pressure will decrease toward the ambient pressure as water flows from the bore into the fractures. Since water is viscous, the smaller the fracture aperture, the larger the resistance to flow or the slower the pressure decline. By measuring pressure change as a function of time the fracture properties can be analyzed. Early in the test the pressure change depends mainly on the near-wellbore fracture resistance. By analyzing this "short-time" data, fracture aperture can be estimated. Later, the fracture geometry will affect pressure change. Thus the "long-time" data contains further information about the continuity and connectivity of the fracture system.

The driving mechanism for the wellbore water flowing into the fractures is the compressibility of the water. Since there is no production or injection to induce pressure change in the pulse-packer test, the pressure decline is solely due to this compressibility-wellbore storage effect. In the conventional reservoir study, wellbore storage effect[2-4] is regarded as a distortion which masks the early-time line-source response of the data. Log-log plots are used to diagnose the well behavior and to identify the start of the semi-log straight line from which the reservoir properties are then deduced. For a producing reservoir well, penetrating a permeable sandy formation, the effective wellbore volume is usually an unknown parameter due to wellbore damage. The early-time data cannot effectively be used to deduce both the wellbore condition and reservoir properties. On the other hand, for a well located in a hard rock formation the wellbore space between the packers will have a regular shape, and the volume between the packers can be easily measured. With the knowledge of the wellbore volume, early-time data may be used with more confidence to estimate the formation properties such as fracture aperture.

In the present study, changes of pressure as a function of time are calculated. The geometrical dimensions of the wellbore shown in Figure 1 are used when the results are expressed in real time. A wellbore of these dimensions is useful to study fractures with apertures in the micron range. Scaling to different dimensions will be discussed. The calculated pressure decay at the wellbore is shown in Figure 2 for intersecting fractures of 1μm and 10μm apertures. The results show that when the fracture aperture changes by one order of magnitude, the decay time changes by almost three orders of magnitude. This dependence, together with the governing equations and boundary conditions of the transient flow from the wellbore to the fractures are discussed in Section II. Dimensionless quantities useful for scaling are described. The derivation of the analytic expressions of the pressure changes are given in the appendix. In Section III, the curves of infinite and finite fractures with no flow or constant-pressure fracture-boundary conditions are given. Based on early-time behavior, a simple relationship between the aperture and the observed time of a given pressure drop is derived. The effect of multiple identical fractures intersecting the wellbore and the effect of the orientation of the fractures are discussed with simple scaling arguments. To study the effect of fracture connectivity, the pressure change of a finite fracture in series or parallel to an infinite fracture are calculated. Finally, the pressure changes in the fracture away from the wellbore are discussed. The assumptions and results of this study are summarized in the last section. Definitions of symbols are defined in the section on nomenclature.

II. GOVERNING EQUATIONS

The fundamental equation of transient water motion is the mass conservation equations:

$$-\int_A \rho \vec{u} \cdot \vec{n}\, dA = \frac{D}{Dt}\int_V \rho dV. \qquad (1)$$

The change of water mass within a volume is determined by the flow across the surface. For the case of a single tight fracture intersecting the wellbore, the mass conservation equation for the wellbore volume is simply

$$-\rho_w u_w(t) L_{wF} \cdot (2b) = V_w \frac{d\rho_w}{dt} \qquad (2)$$

(the density is approximated as uniform throughout the wellbore). This assumes that rock material is impermeable and that the water leaving the wellbore flows into the fracture only. $u_w(t)$ is the flow velocity at the wellbore-fracture intersection. The wellbore-fracture contact length, L_{wF}, is equal to the circumference $2\pi r_w$ for a single fracture intersecting the well normally (Figure 1). L_{wF} times the aperture, 2b, is the wellbore-fracture contact area. The volume V_w is $\pi r_w^2 D_w$ for an ideal wellbore between the packers. The notations, L_{wF} and V_w, are retained for general cases.

From the definition of the compressibility, β, the density change can be expressed as the pressure change:

$$\frac{d\rho_w}{dt} = \frac{d\rho_w}{dp_w}\frac{dp_w}{dt} = \beta\rho_w \frac{dP_w}{dt} \qquad (3)$$

$$\left(\beta \equiv \frac{1}{\rho}\frac{d\rho}{dP}\right).$$

From equations (2) and (3), the flow velocity

$$u_w(t) = -\frac{V_w}{L_{wF} \cdot (2b)}\beta\frac{dP_w}{dt} = -\frac{r_w}{\alpha}\frac{dP_w}{dt}, \qquad (4)$$

where the dimensionless parameter, α, is introduced:

$$\alpha \equiv \frac{r_w L_{wF} \cdot (2b)}{V_w} \qquad \left(= \frac{2(2b)}{D_w}\right). \qquad (5)$$

α is proportional to the ratio of the well-bore fracture contact area to the wellbore volume. It represents the leaking capacity of the wellbore water. For the simple geometry of Figure 1, α is simply twice the geometric ratio of the aperture, 2b, to the packer separation, D_w (the parenthetic

statement in equation (5)). Typically for D_w in meters and 2b in the micron range, α is a small parameter.

For low fluid velocities (laminar flow) or fluids with high viscosities, the flow velocity averaged over the aperture between two smooth-walled plates is:

$$\vec{u} = -\frac{k}{\mu}\vec{\nabla}P \tag{6}$$

with

$$k = \frac{(2b)^2}{12}. \tag{7}$$

Equation (6) is analogous to Darcy's law. This dependence of the permeability, k, on the aperture (parallel plate model of fracture) has been shown to be a good approximation for fracture flow in small[6] and large[7,8] rock samples.

The governing equation for the transient flow in the fracture is the diffusivity equation for $P(\vec{r}, t)$. When expressed in radial coordinates it is

$$\frac{\partial^2 P}{\partial r} + \frac{1}{r}\frac{\partial P}{\partial r} = \frac{1}{\kappa}\frac{\partial P}{\partial t} \tag{8}$$

with

$$\kappa = \frac{k}{\beta\mu} \tag{9}$$

By expressing r in terms of dimensionless radius $r_D = r/r_w$, equation (8) can be rewritten as

$$\frac{\partial^2 P}{\partial r_D^2} + \frac{1}{r_D}\frac{\partial P}{\partial r_D} = \frac{\partial P}{\partial t_D} \tag{10}$$

with t_D the familiar dimensionless time of the diffusivity equation [9]

$$t_D = \frac{\kappa}{r_w^2}t \qquad \left(= \frac{(2b)^2}{12 r_w^2 \beta\mu}t\right), \tag{11}$$

t_D is proportional to $(2b)^2$.

The boundary condition at the wellbore radius, $r = r_w$, is the continuity of flow velocities

$$u\Big|_{r=r_w} = u_w.$$

With equations (4) and (6),

$$-\frac{k}{\mu}\frac{\partial P}{\partial r}\Big|_{r=r_w} = -\frac{r_w}{\alpha}\beta\frac{dP_w}{dt} \tag{12}$$

or equivalently, with $P(r_w, t) = P_w(t)$,

$$\alpha\kappa\frac{\partial P}{\partial r} = r_w\frac{\partial P}{\partial t} \qquad \text{at } r = r_w. \tag{13}$$

In terms of r_D, equation (13) becomes

$$\frac{\partial P}{\partial r_D} = \frac{\partial P}{\partial t_{DF}} \qquad \text{at } r_D = 1 \tag{14}$$

with

$$t_{DF} = \alpha t_D = \frac{\alpha\kappa}{r_w^2}t \qquad \left(= \frac{L_{WF}(2b)^3}{12 r_w V_w \beta\mu}t\right) \tag{15}$$

This dimensionless time is proportional to $(2b)^3$ instead of $(2b)^2$. As noted in Figure 2, the pressure decay times are almost scaled as $(2b)^{-3}$. Thus for this boundary condition, dimensionless time t_{DF} is more appropriate for scaling than the differential equation dimensionless time t_D. The boundary condition at the wellbore-fracture interface dominates the transient pressure change at the wellbore.

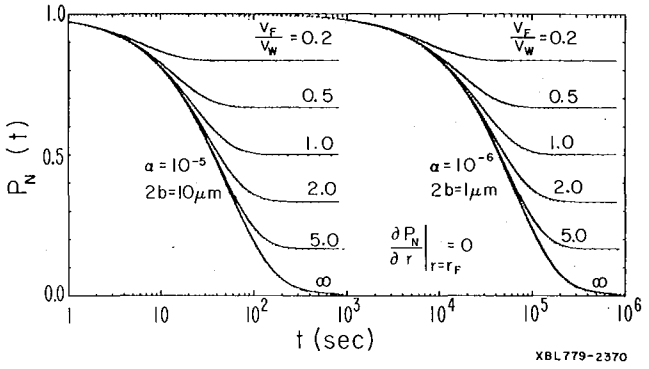

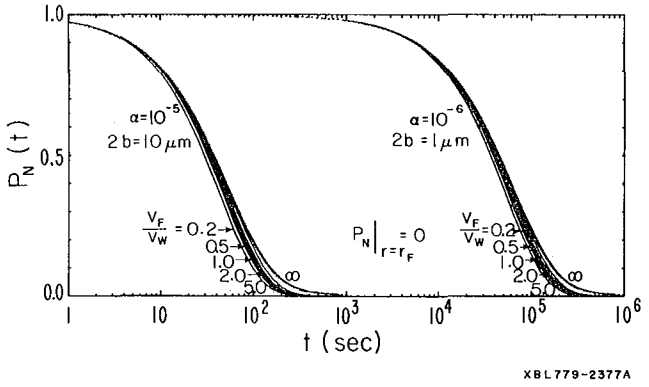

Figure 2(a), (b). Normalized pressure decay at a wellbore intersected by a single fracture of aperture 2b and fracture-wellbore volume ratio V_F/V_w. The fracture boundaries at radius r_F are either closed (zero pressure gradient in (a)) or open (zero pressure in (b)). α is the dimensionless leaking capacity. Solid lines = analytic solutions. Dots = numerical results.

It is interesting to compare this zero-flow-rate, closed, transient boundary condition with the more-familiar conditions of an open-flowing well. The obvious difference is that equations (12) and (14) have no source or sink term of a given flow rate. By identifying α with the inverse of the dimensionless wellbore storage constant $\bar{C}$ ($\alpha = 1/\bar{C}$ and $t_{DF} = t_D/\bar{C}$), equation (13) or (14) is the analog of wellbore storage without skin effect boundary condition of a flowing well (see equation (6) of reference 4). For a flowing well, the wellbore storage effect dominates the transient behavior at early times. If one replots the type curves of short-time

solutions with wellbore storage (Figure 2 of reference 4) in terms of $t_{DF} = t_D/\bar{C}$ instead of t_D, it is obvious that the type curves for different $\bar{C}$ will fall on top of each other. Thus t_{DF} is more interesting for scaling the early-time behavior. For the packer well transient problem, wellbore storage is the only driving mechanism. Thus scaling with t_{DF} is applicable over the whole time range.

In addition to the difference in regard to the presence or absence of source terms in the two problems, the initial conditions are also different. For an open well, both the wellbore pressure and the formation pressure are assumed equal to some initial pressure at $t = 0$ in deriving solutions. For the packer well, the wellbore pressure is different from the fracture pressure at $t = 0$. When a slight squeeze (pressure pulse) is applied to the sealed water in the wellbore with almost impermeable walls, the pressure build-up in the wellbore is very fast because of the small compressibility of the water. Due to the resistance to flow in the fracture, the pressure at the fracture is still at the ambient pressure at $t = 0$. By setting the ambient pressure as zero pressure, the initial condition is

$$P(r, 0) = \begin{cases} \delta P & \text{for } r = r_w \\ 0 & \text{for } r > r_w \end{cases} \qquad (16)$$

δP is the applied pressure pulse. Since the differential equation and the boundary conditions are linear in P, it is convenient to define the normalized pressure [9]

$$P_N(r, t) = \frac{P(r, t)}{\delta P} = \frac{P(r, t)}{P(r_w, 0)}. \qquad (17)$$

For a given r, the argument r in P is usually dropped and the symbol $P_N(t)$ is used, as in the figures.

III. RESULTS

Transient pressure changes are calculated for several geometrical arrangements of single and multiple fractures intersecting the wellbore. Analytic and numerical methods are used to solve the diffusivity equation. The numerical code is the "TRUST" program developed at Lawrence Berkeley Laboratory[10]. The analytic method using the Laplace transformation procedure[2,9] is given in detail in the appendix. Results are discussed in this section.

A. Single fracture

The simplest case is a single fracture sheet which extends to infinite and is intersected by the wellbore perpendicularly. The pressure at $r = r_w$ (see appendix) is

$$P(t) = \frac{4\alpha P(0)}{\pi^2} \int_0^\infty \exp\left(-\frac{\kappa t u^2}{r_w^2}\right) \frac{du}{u\Delta(u)} \qquad (18)$$

with

$$\Delta(u) = [uJ_0(u) - \alpha J_1(u)]^2 + [uY_0(u) - \alpha Y_1(u)]^2.$$

This expression has been derived and calculated in the analogous heat conduction problem[9] and in the analysis of the slug test[11,12]. The solutions of the diffusivity equation with infinite flow region are typically in the form of an integral from 0 to ∞.

For the case of a finite fracture closed at radius r_F, no flow passes through the external fracture boundary. The pressure transient is in the form of an infinity series (see appendix, equations (A20) and (A25))

$$P(t) = P(0)\frac{V_w}{V_w + V_F} + P(0) \sum_{n=1}^{\infty} (Res)_n \exp(-\kappa\beta_n^2 t) \qquad (19)$$

The leading term is a manifestation of the volume effect. The initial pressure build-up P(0) within the wellbore volume V_w is distributed evenly over the sum of V_w and the fracture volume V_F as $t \to \infty$.

If the external boundary of the finite fracture is maintained at the ambient pressure, the pressure function is also a series but without the volume term (see appendix, equations (A27), (A28)).

$$P(t) = P(0) \sum_{m=1}^{\infty} (Res)_m \exp(-\kappa\beta_m^2 t). \qquad (20)$$

The pressure declines at the wellbore for infinite and finite fractures with 10μm and 1μm apertures are plotted in Figure 2. The solid lines are solutions calculated with equations (18)-(20). The dots are numerical solutions using the program TRUST[10]. The finite fractures with no-flow boundaries decay more slowly than the infinite fracture. The finite-volume effect at long-time is evident. For the finite fractures with constant pressure boundary the declines are slightly faster than the infinite fractures. For a 10μm fracture, the pressure changes occur within several minutes. For a 1μm fracture, it takes almost an hour before an appreciable pressure change is noted and several days to complete the pressure decline. By monitoring the pressure change, the fracture aperture can be sensitively estimated. The finite fracture boundary effect has no influence on the early pressures and all curves of a given aperture tend to coincide.

To explore the early-time behavior and the scaling of different apertures, log-log type curves of the pressure drop $1-P_N(t)$ versus the dimensionless time t_{DF} are plotted in Figure 3 for the 10μm and 1μm fracture. Over the range of t_{DF} plotted, the two sets of curves are very similar. If the set of 10μm curves is shifted slightly to the right, it will almost coincide with the 1μm curves. The slight shift indicates that $P_N(t)$ depends not only on t_{DF} but also weakly depends on the parameter α over this range of t_{DF} values. This is more evident in the type curves on Figure 4 with α ranging from 10^{-3} to 10^{-8}. The slopes for different α at early-time are slightly different. By plotting measured pressure drop versus real time on a log-log paper with the same log-cycle, and shifting the data with axes remaining parallel to Figure 4 to fit the type curves, α and $\alpha\kappa$ (from t_{DF}) can be deduced separately from the best fit.

To estimate the aperture directly from the pressure-drop time, one may use the approximate scaling with t_{DF}, the insensitivity of early-time

data to the fracture boundary condition, and the model relation $k = (2b)^2/12$. For different aperture, the time required for the pressure decline to a given value differs. In Figure 5, the aperture is plotted against the time required for the pressure to reach 0.95, 0.90, or 0.85 of the initial value. For lower P_N, the effect of finite fracture boundary leads to larger uncertainty in the required time. The set of curves for the infinite fracture can be fitted (with least square equal to 0.002 for α ranging from 10^{-3} to 10^{-8}) to straight lines of the form

$$\log[2b(\mu m)] = -0.32 \log [t(sec)] + C \qquad (21)$$

with $C = 1.09$, 1.20, 1.27 for $P_N = 0.95$, 0.9, 0.85, respectively. For wellbore dimensions other than those of Figure 1, or for fluids with different viscosities and compressibilities, equation (21) can be generalized with the substitution

$$C \rightarrow C + 0.32\left(2 \log \frac{r_w(m)}{0.04} + \log \frac{(\beta\mu)(sec)}{4.177 \times 10^{-13}}\right) + \frac{1}{3} \log \frac{D_w(m)}{2} \qquad (22)$$

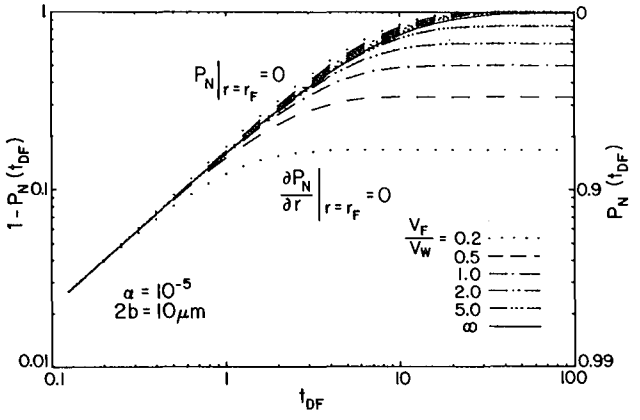

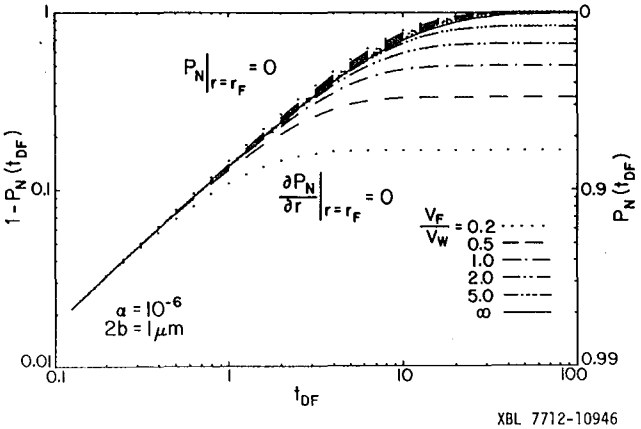

Figure 3(a), (b). Type curves of wellbore pressure changes due to 10μm (a) and 1μm (b) fractures. The pressure change at small dimensionless time t_{DF} is insensitive to the different fracture volumes and fracture boundary conditions.

Equations (21) and (22) can be used for a quick estimation of the apertures, 2b, before fitting the data with type curves of Figure 4.

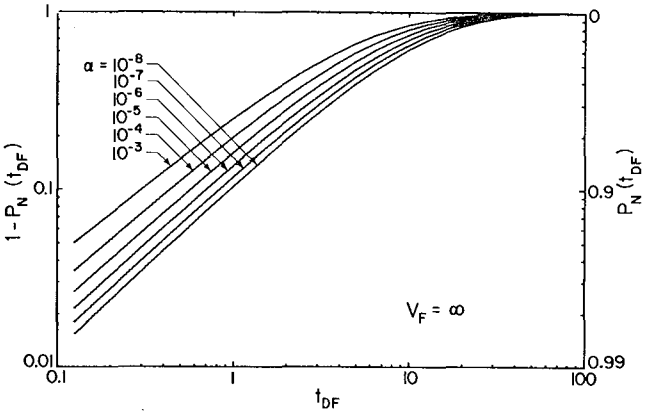

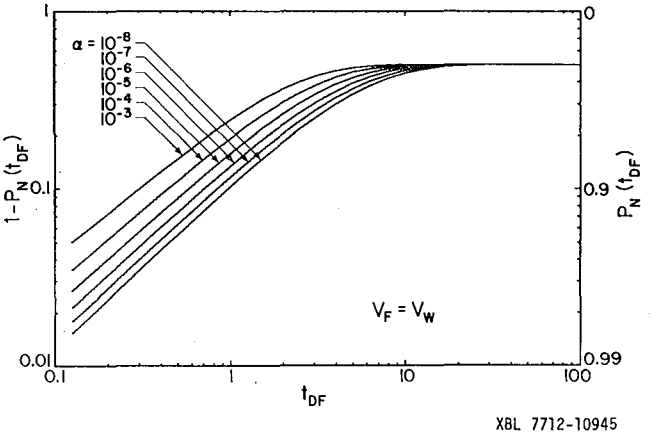

Figure 4(a), (b). Type curves of wellbore pressure change. The slopes of the straight line portion at small dimensionless time t_{DF} is weakly dependent on the dimensionless leaking capacity α and is insensitive to the fracture volume (infinite in (a) and finite in (b)).

In addition to the semi-log plot ($P_N(t)$ - log t of Figure 2) and the log-log plot ($\log[1-P_N(t)]$ - log t of Figure 3), another informative plot of $\log([P_N(t) - P_N(\infty)]/[1 - P_N(\infty)])$ is shown in Figure 6. $P_N(\infty)$ is the volume effect term of equation (19) for the no-flow finite fracture and is zero for other cases. This type of plotting may be useful for laboratory study with knowledge of the fracture volume and boundaries or for diagnosis of long-time field data when the finite volume effect with non-zero $P_N(\infty)$ is evident. The approximate straight lines of Figure 6 reflect the exponential decay nature associated with diffusive flow. For small fractures one exponential term of the series solution (equation (19)) is sufficient to describe the pressure decline. The dominant exponential is the term with the smallest $\kappa\beta_n^2$. As the fracture volume increases, more exponential terms contribute

to the series. With infinite fracture volume the solution is then in the form of an integral instead of a series.

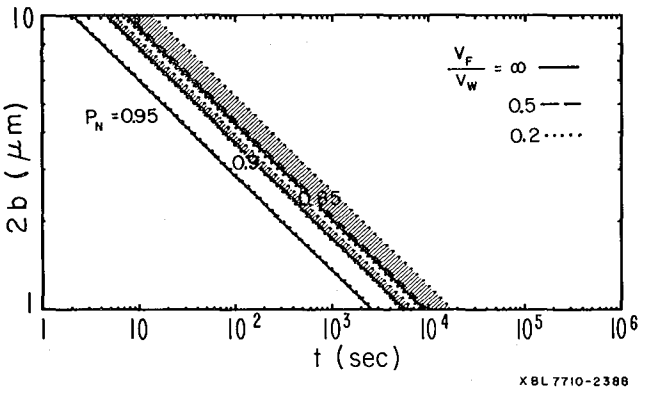

Figure 5. The relation of the aperture 2b and the time required for the pressure to decay to a given fraction P_N of the initial applied pressure. The uncertainty due to finite fracture boundary is shown by the shaded bands.

The single-fracture solutions, in particular the infinite-fracture solution, can be used as starting points for analyzing the pulse packer test. Early in the test, a general complex fracture system intersecting the wellbore will behave like a single infinite fracture with an effective conductance αk and an effective leaking capacity α. In general, α and k are two independent parameters. k depends only on the intrinsic fracture properties while α depends also on geometrical factors. Only for a known fracture-wellbore arrangement can α and k be interrelated. Possible changes of α due to geometry are discussed next.

B. Multiple Fractures and Tilted Fractures

The natural fractures in rock formations are usually in sets of parallel planes. When the packer separation is larger than the average fracture spacing, the wellbore space between the packers may intersect several fractures. In this case, the compressed water will flow into several fractures simultaneously, thus the pressure decline is faster than that due to a single fracture. The solution for n identical fractures can easily be obtained by generalization of the solution for single fractures through the replacement of the parameter α by nα. The parameter α appears only in the boundary condition at the wellbore radius. From the definition of α in equation (5) it is clear that the n-fold increase in the wellbore-fracture contact is equivalent to the n-fold increase in α.

The pressure declines for n identical infinite fractures are plotted in Figure 7. The corresponding single-fracture cases are also plotted for comparison. In the figures the notation $n(2b)_{V_F/V_W}$ is used to represent n fractures with aperture 2b and fracture-wellbore volume ratio V_F/V_W. For a given 2b, the n-fracture pressure decline rate is almost n times faster than the one-fracture rate; but the n-fracture curves are very similar in shape to the one-fracture curve. In principle one can distinguish whether a measured pressure change is due to n-fractures or 1-fracture by careful type-curve fitting, using Figure 4. From the independently-determined fitted values of nα and k, n can be determined after relating both α and k to 2b (equations (5) and (7)). However, due to the similarity in the shape of the type-curves (weak dependence on α) it is very likely that the pressure decline due to n-fractures is misinterpreted as a single-fracture decay. For example, the 10(1μm) curve in Figure 7 may be regarded as a (2.2μm) curve. The aperture is thus overestimated by a factor of $n^{1/3}$ ($= 2.2$ for $n = 10$). This $n^{1/3}$ factor originates from the approximate scaling of the pressure with t_{DF} which is proportional to nαk, or $n(2b)^3$ in this case.

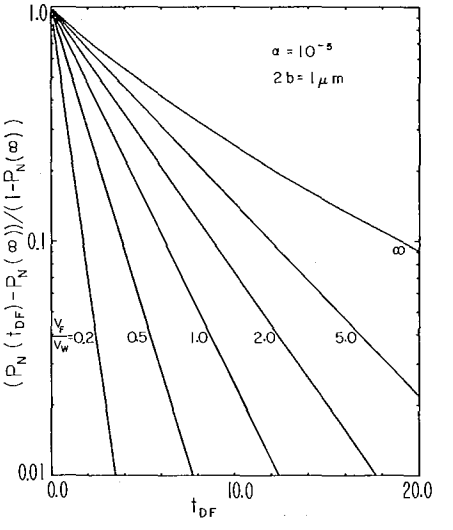

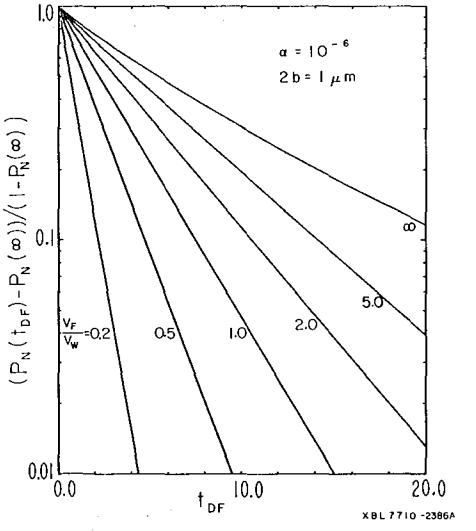

Figure 6(a), (b). Semi-log type curves of wellbore pressure change normalized to the asymptotic pressure change due to 10μm (a) and 1μm (b) fractures.

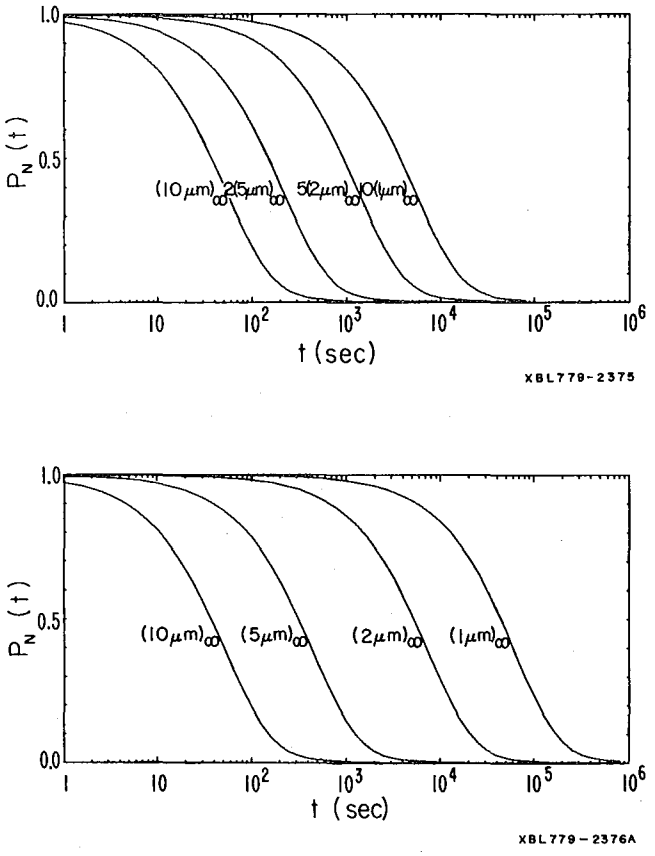

Figure 7(a), (b). Normalized pressure decay at a wellbore intersected by n identical infinite fractures. The four curves in (a) have the same wellbore-fracture contact n(2b) = 10μm but different multiplicity n and aperture 2b. The corresponding single-fracture (n = 1) curves are in (b).

It is also likely to overestimate the aperture of a tilted fracture. When the fracture plane intersects the wellbore at an angle other than 90°, the wellbore-fracture contact is an ellipse rather than a circle and has a longer contact length. Near the wellbore the flow pattern is also nearly elliptic in nature. Thus, at early time the pressure decline at the wellbore will be mainly affected by the increase of the contact length. Without knowing that the fracture is tilted, the aperture may be overestimated by the one-third power of the ratio of the ellipse's perimeter to the circle's circumference. In Figure 8 this overestimation factor is plotted as a function of the tilted angle. The deviation from the unity is not appreciable over large ranges of angles. Flow patterns change away from the wellbore and gravitational effects will further complicate the picture.

Both these possibilities of overestimation are due to the increase of the fracture-wellbore contact length above $2\pi r_w$. Since the circumference, $2\pi r_w$, is the shortest contact length between the wellbore and a fully intersected fracture, overestimating the aperture is much more likely than underestimating it in complicated geometry. Due to the one-third power of scaling, the degree of overestimation will not be serious in most situations. It should be emphasized that overestimation of the aperture is only a possibility. Careful type-curve fitting may distinguish the complex geometrical arrangements from the simple ones. In some cases the long-time pressure behavior will also be useful in the analysis.

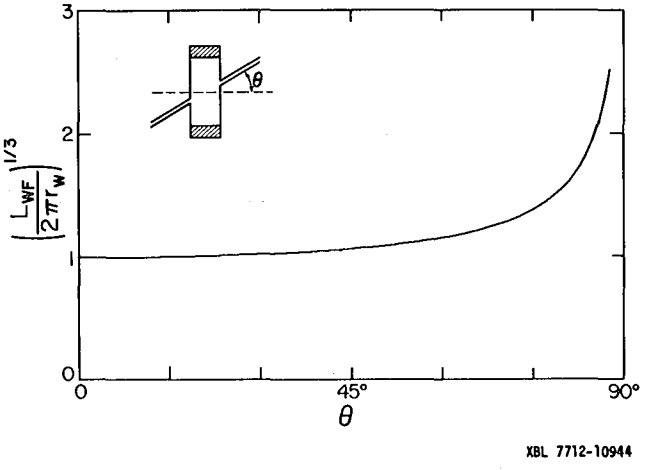

Figure 8. One-third power of the ratio of the wellbore-fracture contact length of a tilted fracture to the wellbore circumference as a function of the tilting angle θ.

C. Fractures in Series and in Parallel

In the above discussion, the early-time pressure decline has been emphasized for aperture estimation. At early times the pressure behavior is mainly determined by the near-wellbore flow and is insensitive to the fracture properties away from the wellbore. At large times the fracture geometry may profoundly affect the pressure changes. This is obvious for the single finite fracture shown in Figure 2. The deviations from the infinite-fracture curves due to no-flow or constant pressure fracture boundaries can be used to analyze the long-time pressure data. However there are more complicated pressure patterns than the single decay associated with single fractures. In the following, the less simple geometry of two fractures of different aperture in series or parallel to each other are considered (see the sketch in Figure 9a, b). The analytic solutions to these two fracture problems are given in the Appendix.

To demonstrate the effect of composite fractures on transient flow, the pressure declines due to a 10μm finite fracture with $V_F/V_w = 1$ in series or parallel to an infinite fracture ($V_F/V_w = \infty$) are plotted in Figure 9. For the in-series curves in Figure 9a, the early-time pressure decline is solely due to the finite fracture which intersects the wellbore. The long-time behavior depends on the aperture of the infinite-fracture. The smaller the aperture the longer it takes for the pressure

to decay to zero. The single-fracture solutions with no-flow or constant pressure boundary condition in Figure 2 are simply limiting cases of the two-fractures-in-series solutions shown in Figure 9a.

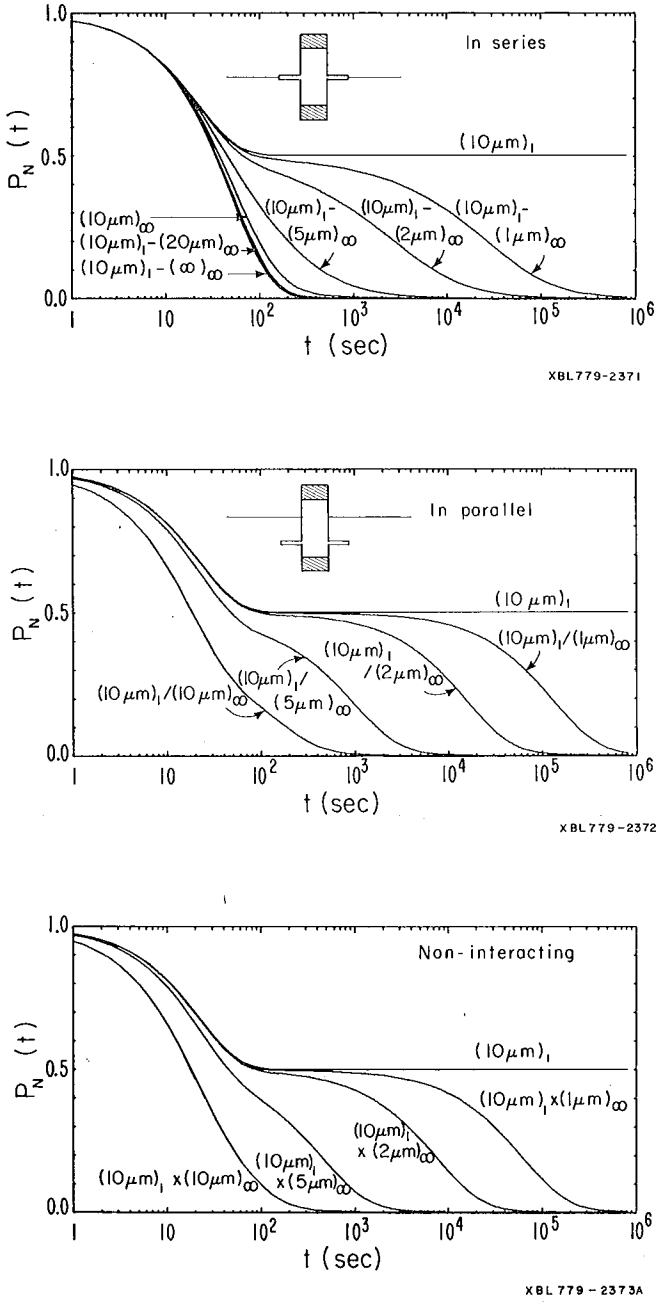

Figure 9(a), (b), (c). Normalized pressure decay at a wellbore intersected by a 10μm fracture with finite volume $V_F/V_W = 1$ in series (a), or in parallel (b) with an aperture 2b fracture with infinite volume. The product of single fracture solutions are presented in (c) for comparison.

With both the finite and infinite fractures intersecting the wellbore (in parallel, Fibure 9b), the water will flow into both fractures and the decay will be faster at early time. Between the two fractures with unequal apertures the flow into the fracture with the larger aperture will be faster and this large aperture will dominate the early-time pressure decline. If the fracture with the larger aperture has finite volume, the flow direction in this fracture will reverse at some later time in order to further release the pressure through the flow into the fracture with the smaller aperture.

It is interesting to compare the in-series and in-parallel curves of the same two fractures. The in-parallel pressure decays faster at early time due to the larger contact with the wellbore, at a later time the pressure decay is slower. The slowing of the pressure decay at the later time reflects the indirect connectivity of the two fractures in parallel. These two fractures communicate through the wellbore only, thus the compressed water, which at early time flows into the large-aperture-finite fracture has to flow back to the wellbore before flowing to the small-aperture-fracture. The finite resistance at the large-aperture fracture delays the final decay. In Figure 9c the product of the two single-fracture solutions are also plotted for comparison. These "nonintersecting" curves represent the approximation of decoupling of the transient flow in the two fractures. From the comparisons in Figures 9a, b, and c, it is clear that the interaction between the two fractures is significant at later time. In Figure 10 this comparison is summarized for one case. The dots are from numerical calculations.

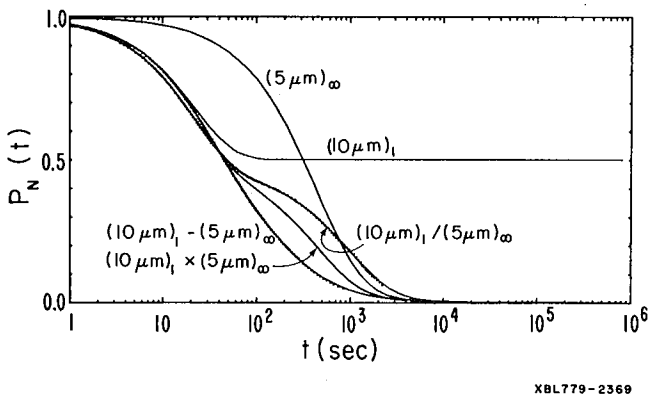

Figure 10. Normalized pressure decay at a wellbore intersected by a 10μm fracture with finite volume $V_F/V_W = 1$ in series (-) or in parallel (//) with a 5μm fracture with infinite volume. The single fracture solutions and their produce (x) are shown for comparison. Solid lines - analytic solutions. Dots = numerical results.

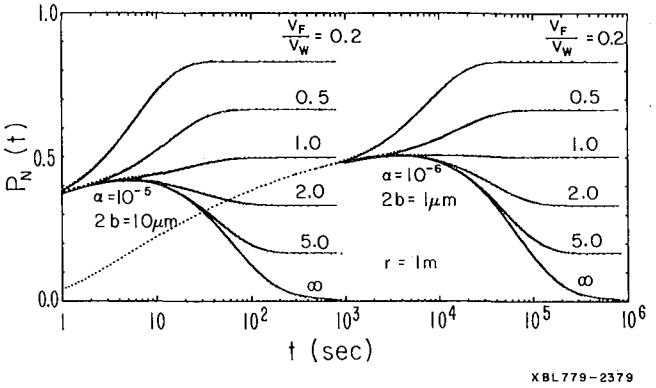

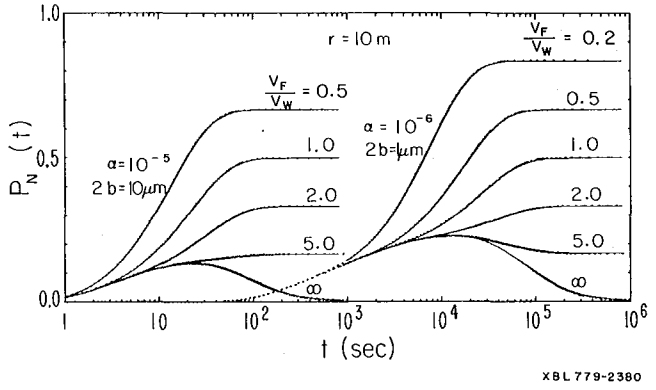

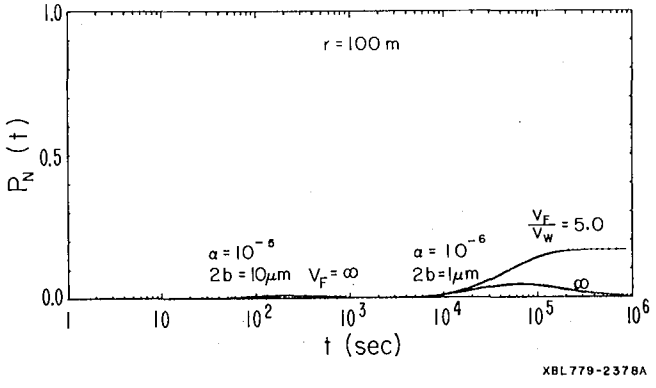

Figure 11(a), (b), (c). Normalized pressure changes in the single fracture at distance r = 1m (a), 10m (b), and 100m (c) from the wellbore. Solid lines = analytic solutions. Dots = numerical results.

D. Pressure Inside the Fracture

With only one well the wellbore is the only observation point in the test. The results discussed above are all on the pressure behavior at the wellbore. If several wells penetrate the fracture system, one can use an observation well to monitor the effects of the pressure pulse at other pulse wells. In Figure 11, the pressure changes at r = 1m, 10m, and 100m from the pulse well are plotted for the single-fracture cases. At a given r the pressure will first rise from the initial ambient pressure at early time and eventually approach the asymptotic pressure value. If the fracture volume is large, or r is far away from the fracture boundary, the pressure will reach maximum before decaying to $P_N(\infty)$. The curves at different r in Figure 11 should be compared with Figure 2a which are the corresponding curves at the wellbore. As noted earlier, the pressure changes at the wellbore are very similar in shape for different fracture apertures. Within the fractures at $r > r_w$ the difference in pressure changes are relatively more pronounced. The effect of the pressure pulse dissipates faster for larger-aperture fractures. This accounts for the differences in the peak pressure values between the two fractures in Figure 11. These single-fracture results at $r > r_w$ illustrate the possibility of increasing sensitivity in interference tests for studying fracture properties.

IV. DISCUSSIONS

In this study, pressure solutions pertinent to analyzing pulse packer tests are presented. This is a zero-flow-rate well testing scheme which is a variant of the slug test. It is a sensitive method for studying tight fractures in impermeable formations. The emphasis of the analysis is on the possibility of deducing fracture properties from the pressure changes due to transient flow into the fractures intersected by the wellbore. Some of the assumptions used in deriving the solutions will be discussed below.

Fracture aperture, or equivalently, fracture permeability is assumed to be independent of pressure. This should be a good approximation in deep formations where the applied pressure pulse is much less than the existing pressure in the fractures. Extrapolation of the laboratory study[7,8] of the pressure-induced aperture change in the hypothetical field condition of 1000m in saturated granite shows that the change in pressure of 20m of water will change the aperture by less than one percent. Even if the pressure range does induce aperture change, the simple solution for rigid fracture applies. The diffusivity equation is linear in pressure if the permeability is pressure-independent and the solutions are proportional to the applied pulse δP. By measuring the pressure responses with different δP's the nonlinear effect can be easily detected in the differences of normalized pressure plots. Thus repeat testing with different δP is desirable. The test with the smallest δP should be run first to avoid possible permanent aperture change in repeated loading. With the development of high-precision pressure guages it is now possible to make pressure

measurements without applying large perturbing pressure pulses. Since the primary interest is to study the intact fracture properties, the pressure perturbation should be minimized so long as the measurement accuracy is preserved.

Other parameters in the governing equations are also assumed to be independent of pressure. These include the fluid properties (μ, β) and the wellbore dimensions (r_w, D_w). The packer separation, D_w, may change slightly with the pressure if the packers are nonrigid. Laboratory studies of the pressure response of the packers may be required to isolate the packer effects.

The assumption of instantaneous pressure rise at initial time is valid if the rise time of the pulse is much shorter than the time required for appreciable pressure change. For the 1μm solutions in Figure 2 this is not a problem. For the 10μm solution, the rise time should be shorter than one second. The solutions presented in this study are applicable to any aperture fracture or porous reservoir as long as the assumption of instant pressure-rise is justified. For studying more permeable fractures or formations one needs a larger wellbore volume to delay the pressure decline. The time required for a given pressure drop is approximately proportional to the volume. In the slug test the whole well (without the packers) is the effective wellbore. The only limitation on the size of the wellbore volume is the requirement of negligible drag effect within the wellbore. The wellbore as a whole is assumed to have uniform pressure in deriving the solutions.

Immediately after the pressure pulse the pressure decline rate at the wellbore is very sensitive to the transmissivity of the fractures which intersect the wellbore. The transmissivity can be related to the aperture by the cubic law. From the single-fracture solutions a simple relation between the aperture and the time required for a given pressure drop has been deduced (Equations (21), (22)). With these equations the data can be easily analyzed for quick estimation of the aperture. Before the test these equations can also be used to help design the wellbore dimensions and packer separations, to assess the effects of different fluid properties, and to estimate the time required for a test.

The early-time pressure change depends not only on the intrinsic transmissivity of the fractures but also weakly on the geometrical factors of the wellbore-fracture contact. In principle, the intrinsic transmissivity and the geometrical factors can be determined separately by carefully fitting the data with the solutions. The insensitivity of the shape of the type curves on the multiplicity and orientation of the fractures may introduce ambiguity in the analysis of the data. Since the conventional downhole televiewer cannot resolve dimensions in the micron range, these aspects of fracture geometry are difficult to obtain directly. Without knowledge of fracture spacing and orientation, and using the single-fracture solutions to roughly analyse the data, the geometrical factors will slightly overestimate the aperture in most cases.

In addition to the aperture, other information about the fracture network properties away from the wellbore can be deduced from long-time pressure data. The transient flow in the fracture is very sensitive to the fracture boundaries. The width of the fracture may vary away from the wellbore. The effective aperture may increase at the intersection with other fractures. If the aperture is smaller at some distance from the wellbore, the flow will be slowed down and the pressure decline at the wellbore will be slowed down. In a completely-closed fracture, the pressure will not decay to the ambient pressure but will approach a higher pressure determined by the fracture volume. Thus the presence of a closed boundary fracture can be easily detected by long-time tests. On the other hand, if the fracture opens, the resistance to flow decreases and the pressure drop will be faster. In this case the decline rate is mainly controlled by the small near-wellbore aperture and the effect of aperture opening is relatively more difficult to detect. The small near-wellbore aperture could be caused by clogging during drilling. Every effort should be made to minimize wellbore damage to avoid the disconnection of the wellbore with the intact fractures.

Depending on the packer separation, the sealed wellbore may intersect more than one fracture and the pressure decline rate will be determined by the total transmissivity of the fractures. For fractures with identical aperture, the solutions can be easily obtained by generalization of the single-fracture solutions. For fractures with different aperture, the pressure changes are sensitive to the relative size of the fracture volume. The transient flows in different fractures can interact either directly with each other or indirectly through the wellbore. These multifracture effects have been modeled by two fractures with different apertures in series or in parallel with each other. The preliminary results presented in this study demonstrate the potential usage of the long-time data to deduce the fracture network properties.

Single-well single-packer wellbore testing concepts can be easily applied to interference well testing. The pressure pulse propagating into the fractures will induce pressure changes at observation wells or other packer-wellbores in the same well. These changes, if observable, will be more sensitive to the intrinsic fracture properties between the pulse and observation wellbores. With interference testing the transient flow is sensitive to the fracture boundaries and fracture connectivity in the formation, and the masking due to near-wellbore properties can be reduced. Other interference testing like simultaneous pulsing will undoubtedly provide further information about the fractures. In summary, pulse-packer transient well-testing can be developed into an effective method for in-situ study of the fracture properties in impermeable rock formations.

ACKNOWLEDGEMENTS

The authors would like to acknowledge the helpful discussions with Dr. J. E. Gale, Department of Earth Sciences, University of Waterloo, Waterloo. Ontario, Canada.

The work for this paper was supported by the U. S. Department of Energy, Division of Geothermal Energy through Lawrence Berkeley Laboratory.

NOMENCLATURE

A	area	$[L^2]$
$2b$	fracture aperture	$[L]$
$\bar{C}$	dimensionless wellbore storage constant	
D_w	packer separation	$[L]$
I_0, I_1	modified Bessel function of the first kind	
J_0, J_1	Bessel function of the first kind	
k	permeability	$[L^2]$
K_0, K_1	modified Bessel function of the second kind	
L_{wF}	well-bore fracture contact length	$[L]$
P	pressure	$[M/LT^2]$
$\bar{P}$	Laplace transformation of P	$[M/LT]$
P_N	normalized pressure - $P/\delta P$	
P_w	wellbore pressure	$[M/LT^2]$
$\delta P, P(0)$	applied pressure pulse	$[M/LT^2]$
q	$\sqrt{s/\kappa}$	$[1/L]$
r	radius	$[L]$
r_D	dimensionless radius = r/r_w	
r_F	fracture boundary radius	$[L]$
r_w	wellbore radius	$[L]$
$(Res)_n$	residues	
s	Laplace operator	$[1/T]$
t	time	$[T]$
t_D	dimensionless time of diffusivity equation (equation 11)	
t_{DF}	dimensionless time of wellbore storage (equation 14)	
u	flow velocity	$[L/T]$
u_w	flow velocity at the wellbore fracture contact	$[L/T]$
V	volume	$[L^3]$
V_F	fracture volume	$[L^3]$
V_w	wellbore volume	$[L^3]$
Y_0, Y_1	Bessel function of the second kind	
α	dimensionless leaking capacity (equation 5)	
β	compressibility of water	$[LT^2/M]$
β_n	positions of poles	
κ	hydraulic conductivity or diffusivity of fracture	$[L^2/T]$
μ	viscosity of water	$[M/LT]$
ρ	density	$[M/L^3]$
ρ_w	density at the wellbore	$[M/L^3]$
Θ	fracture tilting angle	

REFERENCES

1. Brace, W. F., J. B. Walsh, and W. T. Frangos, "Permeability of Granite under High Pressure" J. Geophysical Research 73, No. 6, pp.2225-2236, 1968.

2. van Everdingen, A. F. and W. Hurst, "The Application of the Laplace Transformation to Flow Problems in Reservoirs" Trans., AIME 186, pp.305-324, 1949

3. Papadopulos, I. S. and H. H. Cooper, Jr., "Drawdown in a Well of Large Diameter" Water Resources Research, 3, No.1, pp.241-244, 1967.

4. Agarwal, R. G., R. Al-Hussainy, and H. J. Ramey, Jr., "An Investigation of Wellbore Storage and Skin Effect in Unsteady Liquid Flow. I: Analytical Treatment." Soc. Pet. Eng. J., pp.279-290, September 1970.

5. Narasimhan, T. N. and P. A. Witherspoon, "Numerical Model for Saturated-Unsaturated Flow in Deformable Porous Media. I. Theory." Water Resources Research, 13, No.3., pp.657-664, 1977.

6. Iwai, K., "Fundamental Studies of Fluid Flow Through a Simple Fracture." Thesis, University of California, Berkeley, 1977.

7. Gale, J. E., "A Numerical, Field and Laboratory Study of Flow in Rocks with Deformable Fractures." Thesis, University of California, Berkeley, 1975.

8. Witherspoon, P. A., C. H. Amick, and J. E. Gale, "Stress Flow Behavior of a Fault Zone with Fluid Injection and Withdrawal." Report No. 77-1, Mineral Engineering, University of California, Berkeley, 1977.

9. Carslaw, H. S. and J. C. Jaeger, Conduction of Heat in Solids, Oxford at the Clarendon Press, 2nd ed., p.342, 1959.

10. Narasimhan, T. N. and P. A. Witherspoon, "An Integrated Finite Difference Method for Analyzing Fluid Flow in Porous Media." Water Resources Research, 2. No.1, pp.57-64, 1976.

11. Cooper, H. H., Jr., J. D. Bredehoeft, and I. S. Papadopulos, "Response of a Finite-Diameter Well to an Instantaneous Charge of Water." Water Resource Research, 3, No.1, pp.263-269, 1967.

12. Papadopulos, I. S., J. D. Bredehoeft, and H. H. Cooper, Jr., "On the Analysis of 'Slug Test' Data." Water Resource Research, 9, No.4, pp.1087-1089, 1973.

APPENDIX

SOLUTIONS OF THE DIFFUSIVITY EQUATION

The diffusivity equation to be solved is:

$$\frac{\partial^2 P}{\partial r^2} + \frac{1}{r}\frac{\partial P}{\partial r} = \frac{1}{\kappa}\frac{\partial P}{\partial t} \tag{8}$$

with boundary condition:

$$\alpha\kappa \frac{\partial P}{\partial r} = r_w \frac{\partial P}{\partial t} \qquad \text{at } r = r_w \tag{13}$$

and initial condition:

$$P = \begin{cases} P(0) & \text{for } r = r_w \\ 0 & \text{for } r > r_w \end{cases} \qquad \text{at } t = 0. \tag{16}$$

In terms of the Laplace transformation

$$\bar{P}_{(s)}(r) = \int_0^\infty e^{-st} P(r, t)\, dt, \tag{A1}$$

the time dependence of the diffusivity equation is removed:

$$\frac{d^2\bar{P}}{dr^2} + \frac{1}{r}\frac{d\bar{P}}{dr} = q^2\bar{P} \tag{A2}$$

where $q^2 = s/\kappa$. The initial condition and the boundary condition are combined

$$\alpha\kappa \frac{d\bar{P}}{dr} = r_w(s\bar{P} - P(0)) \qquad \text{at } r = r_w. \tag{A3}$$

The general solution of (A2) is the linear combination of the zeroth order modified Bessel functions

$$\bar{P} = C_1 K_0(qr) + C_2 I_0(qr). \tag{A4}$$

With (A3), the coefficients C_1 and C_2 are related by

$$C_1[qr_w K_0(qr_w) + \alpha K_1(qr_w)] + C_2[qr_w I_0(qr_w) - \alpha I_1(qr_w)] = \frac{r_w P(0)}{\kappa q} \tag{A5}$$

With an additional boundary condition at $r > r_w$, the C's can be determined. $\bar{P}$ is typically of the form

$$\bar{P} = \frac{r_w P(0) F(q, r)}{\kappa q \Delta(q)} \tag{A6}$$

The explicit expressions for F and Δ for the different cases will be described below. The solution is then obtained by inverse Laplace transformation.

$$P(r, t) = \frac{1}{2\pi i} \int_{-i\infty + 0^+}^{i\infty + 0^+} e^{st} \bar{P}_{(s)}(r)\, ds \tag{A7}$$

By contour integration, the line integral in (A7) may be replaced by integrals along branch cuts or around poles. If $\bar{P}$ is singular along $s = 0$ to $s = -\infty$ (and the small circle around the origin gives zero),

(A8)

$$P(r, t) = \frac{2P(0)}{\pi} \int_0^\infty \exp\left[\left(-\frac{\kappa t u^2}{r_w^2}\right) \times \mathrm{Re}\left(\frac{F(q, r)}{\Delta(q)}\right)_{qr_w \to -iu}\right] du$$

If $\bar{P}$ is singular at poles $s = 0$ and $s = -\kappa\beta_n^2$ (A9)

$$P(r, t) = P(0)(\mathrm{Res})_0 + P(0) \sum_{n=1}^{\infty} (\mathrm{Res})_n \exp(-\kappa\beta_n^2 t)$$

The residues can be determined by

$$(\mathrm{Res})_0 = \left(\frac{qr_w F(q, r)}{\Delta(q)}\right)_{q=0} \tag{A10}$$

$$(\mathrm{Res})_n = \left(\frac{2qr_w F(q, r)}{qd\Delta/dq}\right)_{q = i\beta_n} \tag{A11}$$

(A) SINGLE INFINITY FRACTURE

The boundary condition at $r = \infty$ is $\bar{P} = 0$. Therefore $C_2 = 0$ in (A5) and $\bar{P}$ is of the form of (A6) with

$$F(q, r) = K_0(qr) \tag{A12}$$

$$\Delta(q) = qr_w K_0(qr_w) + \alpha K_1(qr_w). \tag{A13}$$

With (A8),

$$P(r, t) = \frac{2P(0)}{\pi} \int_0^\infty \exp\left(-\frac{\kappa t u^2}{r_w^2}\right) \times \left\{ J_0\left(u\frac{r}{r_w}\right)[uY_0(u) - \alpha Y_1(u)] - Y_0\left(u\frac{r}{r_w}\right)[uJ_0(u) - \alpha J_1(u)] \right\} \frac{du}{\Delta(u)} \tag{A14}$$

where (A15)

$$\Delta(u) = [uJ_0(u) - \alpha J_1(u)]^2 + [uY_0(u) - \alpha Y_1(u)]^2$$

The pressure at the wellbore in $r < r_w$ is the value of (A13) with $r = r_w$.

$$P(t) = \frac{4\alpha P(0)}{\pi^2} \int_0^\infty \exp\left(-\frac{\kappa t u^2}{r_w^2}\right) \frac{du}{u\Delta(u)} \tag{18}$$

By changing the variable from u to $\sqrt{\alpha v}$, the exponential function in the integral is $\exp(-t_{DF} v)$.

(B) FINITE FRACTURE WITH NO-FLOW FRACTURE BOUNDARY

With the boundary condition $d\bar{P}/dr = 0$ at $r = r_F$,

$$-C_1 qK_1(qr_F) + C_2 qI_1(qr_F) = 0 \tag{A16}$$

With (A5), $\bar{P}$ is of the form of (A6) with

$$F(q, r) = K_0(qr)I_1(qr_F) + I_0(qr)K_1(qr_F) \tag{A17}$$

$$\Delta(q) = qr_w[K_0(qr_w)I_1(qr_F) + I_0(qr_w)K_1(qr_F)] + \alpha[K_1(qr_w)I_1(qr_F) - I_1(qr_w)K_1(qr_F)] \tag{A18}$$

The solution is an infinite series of the form (A9). Using the limiting forms for small arguments of the modified Bessel functions, the residue at $s = 0$ (A10) is:

$$(\text{Res})_0 = \frac{r_w/r_F}{r_w/r_F + 0.5\alpha(r_F/r_w - r_w/r_F)}$$

$$= \frac{V_w}{V_w + V_F} \qquad \text{(A19)}$$

with $0.5\alpha = (2b)/D_w$ and $V_F = \pi(2b)(r_F^2 - r_w^2)$.

Other roles are located at the zeros of $\Delta(q)$ at $s = -\kappa\beta_n^2$ with β_n's being the roots of

(A20)

$$\beta_n r_w[Y_0(\beta_n r_w)J_1(\beta_n r_F) - J_0(\beta_n r_w)Y_1(\beta_n r_F)] -$$

$$\alpha[Y_1(\beta_n r_w)J_1(\beta_n r_w) - J_1(\beta_n r_w)Y_1(\beta_n r_F)] = 0$$

To calculate the residues of (A11) one needs

$$\begin{aligned}\frac{d\Delta}{dq} = &- r_w[qr_wK_1(qr_w) + \alpha K_0(qr_w)]I_1(qr_F)\\ &+ r_w[qr_wI_1(qr_w) - \alpha I_0(qr_w)]K_1(qr_F)\\ &+ r_F[qr_wK_0(qr_w) + \alpha K_1(qr_w)]I_0(qr_F)\\ &- r_F[qr_wI_0(ar_w) - \alpha I_1(qr_w)]K_0(qr_F)\\ &- 2\alpha q^{-1}[K_1(qr_w)I_1(qr_F) - I_1(qr_w)K_1(qr_F)]\end{aligned} \qquad \text{(A21)}$$

When $q = i\beta_n$, $(\Delta(q) = 0)$,

$$\frac{qr_wK_0(qr_w) + \alpha K_1(qr_w)}{K_1(qr_F)} = \frac{-qr_wI_0(qr_w) + \alpha I_1(qr_w)}{I_1(qr_F)}$$

$$= \zeta, \text{ say.} \qquad \text{(A22)}$$

With (A22) and the Wronskian relations of K's and I's, (A21) is simplified:

$$\left(q\frac{d\Delta}{dq}\right)_{q=i\beta_n} = \frac{-\beta_n^2 r_w^2 - \alpha^2 + 2\alpha + \zeta^2}{\zeta}. \qquad \text{(A23)}$$

Together with

$$\left[qr_wF(q,r)\right]_{q=i\beta_n} =$$

$$\frac{\pi\beta_n r_w}{2}[Y_0(\beta_n r)J_1(\beta_n r_F) - J_0(\beta_n r)Y_1(\beta_n r_F)], \qquad \text{(A24)}$$

the residues of (A11) are:

$$(\text{Res})_n = \frac{\pi\beta_n r_w\zeta}{-\beta_n^2 r_w - \alpha^2 + 2\alpha + \zeta^2}$$

$$\times\ [Y_0(\beta_n r)J_1(\beta_n r_F) - J_0(\beta_n r)Y_1(\beta_n r_F)]$$

with

$$\zeta = \frac{-\beta_n r_w J_0(\beta_n r_w) + \alpha J_1(\beta_n r_w)}{J_1(\beta_n r_F)}. \qquad \text{(A25)}$$

The pressure solution is given by (A9), (A19), (A20), and (A25).

(C) FINITE FRACTURE WITH CONSTANT PRESSURE FRACTURE BOUNDARY

With the boundary condition $\bar{P} = 0$ at $r = r_F$, the expressions for F and Δ are similar to (A17) and (A18) with the replacements of $I_1(qr_F) \to I_0(qr_F)$ and $K_1(qr_F) \to -K_0(qr_F)$. There is no singularity at $s = 0$.

$$(\text{Res})_0 = 0 \qquad \text{(A26)}$$

The only contributions are from the poles at $s = -\kappa\beta_n^2$ with β_n the roots of

$$\beta_n r_w[Y_0(\beta_n r_w)J_0(\beta_n r_F) - J_0(\beta_n r_w)Y_0(\beta_n r_F)] -$$

$$\alpha[Y_1(\beta_n r_w)J_0(\beta_n r_F) - J_1(\beta_n r_w)Y_0(\beta_n r_F)] = 0 \qquad \text{(A27)}$$

The residues are:

$$(\text{Res})_n = \frac{\pi\beta_n r_w\zeta}{-\beta^2 r_w - \alpha^2 + 2\alpha + \zeta^2} +$$

$$x[Y_0(\beta_n r)J_0(\beta_n r_F) - J_0(\beta_n r)Y_0(\beta_n r_F)]$$

with

$$\zeta = \frac{-\beta_n r_w J_0(\beta_n r_w) + \alpha J_1(\beta_n r_w)}{J_0(\beta_n r_F)} \qquad \text{(A28)}$$

The only difference between the expressions (A27), (A28) and (A20), (A25) is the interchange of $J_1(\beta_n r_F) \leftrightarrow J_0(\beta_n r_F)$ and $Y_0(\beta_n r_F) \leftrightarrow Y_1(\beta_n r_F)$. The pressure solution is given by (A9), (A26)-(A28).

(D) FINITE FRACTURE IN SERIES WITH INFINITE FRACTURE

The diffusivity equations are:

$$\frac{\partial^2 P_1}{\partial r^2} + \frac{1}{r}\frac{\partial P_1}{\partial t} = \frac{1}{\kappa_1}\frac{\partial P_1}{\partial t} \qquad \text{for } r_w < r < r_F \qquad \text{(A29)}$$

$$\frac{\partial^2 P_1}{\partial r^2} + \frac{1}{r}\frac{\partial P_2}{\partial t} = \frac{1}{\kappa_2}\frac{\partial P_2}{\partial t} \qquad \text{for } r_F < r < \infty \qquad \text{(A30)}$$

The boundary conditions are:

$$\alpha_1\kappa_1\frac{\partial P_1}{\partial r} = r_w\frac{\partial P_i}{\partial t} \qquad \text{at } r = r_w \qquad \text{(A31)}$$

$$\alpha_1\kappa_1\frac{\partial P_1}{\partial r} = \alpha_2\kappa_2\frac{\partial P_2}{\partial r} \qquad \text{at } r = r_F \qquad \text{(A32)}$$

$$P_1 = P_2 \qquad \text{at } r = r_F \qquad \text{(A33)}$$

$$P_1 = 0 \qquad \text{at } r = \infty \qquad \text{(A34)}$$

The initial conditions are:

$$P_1 = \begin{cases} P(0) & \text{for } r = r_w \\ P_2 = 0 & \text{for } r > r_w \end{cases} \quad \text{at } t = 0 \qquad \text{(A35)}$$

The Laplace transformation solutions of (A29), (A30) are:

$$\bar{P}_1 = C_1K_0(q_1r) + C_2I_0(q_1r) \tag{A36}$$

$$\bar{P}_2 = C_3K_0(q_2r) + C_4I_0(q_2r) \tag{A37}$$

where

$$s = \kappa_1 q_1^2 = \kappa_2 q_2^2. \tag{A38}$$

With (A34), $C_4 = 0$. With (A32), (A33),

$$\frac{C_1}{C_3} = (\alpha_1\kappa_1)^{-1}[\alpha_1\kappa_1 q_1 r_F I_1(q_1r_F)K_0(q_2r_F) + \alpha_2\kappa_2 q_2 r_F K_1(q_2r_F)I_0(q_1r_F)] \equiv C_1' \tag{A39}$$

$$\frac{C_2}{C_3} = (\alpha_2\kappa_2)^{-1}[\alpha_1\kappa_1 q_1 r_F K_1(q_1r_F)K_0(q_2r_F) - \alpha_2\kappa_2 q_2 r_F K_1(q_2r_F)K_0(q_1r_F)] \equiv C_2' \tag{A40}$$

The wellbore boundary condition (A31) and the initial condition (A35) determine C_3:

$$C_3 = \frac{r_w P(0)}{\kappa_1 q_1 \Delta(q)} \tag{A41}$$

where

$$\Delta(q) = [q_1r_wK_0(q_1r_w) + \alpha_1K_1(q_1r_w)]C_1' + [q_1r_wI_0(q_1r_w) - \alpha_1I_1(q_1r_w)]C_2'. \tag{A42}$$

With (A39) - (A41) to (A36),

$$\bar{P}_1 = \frac{r_w P(0) F(q, r)}{\kappa_1 q_1 \Delta(q)} \tag{A43}$$

where

$$F(q, r) = C_1'K_0(q_1r) + C_2'I_0(q_1r). \tag{A44}$$

The pressure solution is of the form of (A8)

$$P_1(r, t) = \frac{2P(0)}{\pi}\int_0^\infty \exp\left(-\frac{\kappa_1 t u^2}{r_w^2}\right) \times \mathrm{Re}\left[\left(\frac{F(q, r)}{\Delta(q)}\right)_{q_1r_w \to -iu}\right] du \tag{A45}$$

with (A42) and (A44). In the limit of $\kappa_2 \ll \kappa_1$, the integrand of (A45) will be singular at $u = 0$ and the $u = \beta_n r_w$ of (A20). The two-fractures-in-series integral solution will reduce to the one-fracture-no-flow series solution of Appendix (B). Similarly in the limit of $\kappa_2 \gg \kappa_1$, the solution will reduce to the one-fracture-constant-pressure series solution in Appendix (C). In general, depending on the relative magnitude of κ_1 and κ_2, the integral of (A44) will have large values in the proximity of $u = 0$ and $u = \beta_n r_w$ of (A20) or (A27). The strongly varying integral can be properly integrated by subdividing the total integral into subintegrals between the $\beta_n r_w$'s.

(E) FINITE FRACTURE IN PARALLEL WITH INFINITE FRACTURE

The diffusivity equations are:

$$\frac{\partial^2 P_1}{\partial r^2} + \frac{1}{r}\frac{\partial P_1}{\partial r} = \frac{1}{\kappa_1}\frac{\partial P_1}{\partial t} \quad \text{for } r_w < r < r_F \tag{A46}$$

$$\frac{\partial^2 P_2}{\partial r^2} + \frac{1}{r}\frac{\partial P_2}{\partial r} = \frac{1}{\kappa_2}\frac{\partial P_2}{\partial t} \quad \text{for } r_w < r < \infty \tag{A47}$$

The boundary conditions are:

$$\alpha_1\kappa_1\frac{\partial P_1}{\partial r} + \alpha_2\kappa_2\frac{\partial P_2}{\partial r} = r_w\frac{\partial P_w}{\partial t} \quad \text{at } r = r_w \tag{A48}$$

$$P_1 = P_2 = P_w \quad \text{at } r = r_w \tag{A49}$$

$$\frac{\partial P_1}{\partial r} = 0 \quad \text{at } r = r_F \tag{A50}$$

$$P_2 = 0 \quad \text{at } r = \infty \tag{A51}$$

The initial conditions are:

$$P_1 = P_2 = \begin{cases} P(0) & \text{for } r = r_w \\ 0 & \text{for } r > r_w \end{cases} \quad \text{at } t = 0 \tag{A52}$$

The Laplace transformation solutions of (A46) and (A47) satisfying (A50) and (A51) are:

$$\bar{P}_1 = C_1[K_0(q_1r)I_1(q_1r_F) + I_0(q_1r)K_1(q_1r_F)] \tag{A53}$$

$$\bar{P}_2 = C_3K_0(q_2r) \tag{A54}$$

where q_1 and q_2 are related by (A38). With (A49),

$$\frac{C_1}{C_3} = \frac{K_0(q_2r_w)}{K_0(q_1r_w)I_1(q_1r_F) + I_0(q_1r_w)K_1(q_1r_F)} \equiv C_1' \tag{A55}$$

The wellbore condition (A48) and the initial condition (A52) determine C_3

$$C_3 = \frac{r_w P(0)}{\kappa_1 q_1 \Delta(q)} \tag{A56}$$

where

$$\Delta(q) = q_1r_wK_0(q_2r_w) + \alpha_2K_1(q_2r_w) - \alpha_1C_1'[I_1(q_1r_w)K_1(q_1r_F) - K_1(q_1r_w)I_1(q_1r_F)] \tag{A57}$$

With (A55), (A56)

$$\bar{P}_1 = \frac{r_w P(0) F(q, r)}{\kappa_1 q_1 \Delta(q)} \tag{A58}$$

where

$$F(q, r) = C_1'[K_0(q_1r)I_1(q_1r_F) + I_0(q_1r)K_1(q_1r_F)] \tag{A59}$$

$$\bar{P}_2 = \frac{r_w P(0) F(q, r)}{\kappa_1 q_1 \Delta(q)} \tag{A60}$$

where

$$F(q, r) = K_0(q_2r) \tag{A61}$$

The pressure solutions are of the form of (A45) with (A57), (A59), (A61). The integrals are also handled by subdividing into subintegrals between the $\beta_n r_w$'s of (A20) or (A27) as discussed in Appendix (D).

It is interesting to note that in the special case of $\kappa_1 = \kappa_2$, $\alpha_1 = \alpha_2$ and $r_F \to \infty$, (A57) becomes

$$\Delta(q) = qr_wK_0(qr_w) + (\alpha_1 + \alpha_2)K_1(qr_w). \tag{A62}$$

(A62) is similar to (A13) with $\alpha_1 + \alpha_2 = 2\alpha$ replacing α. In this special case, the two-fracture-in-parallel solution reduces to the $n = 2$ identical fracture solution discussed in Section IV-B. The solution for n identical fractures can be obtained by generalization of the solution of single fractures through the replacement of the parameter α by $n\alpha$.

PRESSURE BEHAVIOR OF WELLS INTERCEPTING FRACTURES

R. Raghavan
The University of Tulsa
Tulsa, Oklahoma

Abstract

The pressure behavior of wells intercepting fractures is of considerable interest to the petroleum industry due to the large number of wells that have been hydraulically fractured to improve well productivity. Hydraulic fracturing is recognized as one of the major developments in petroleum production technology within the last 30 years. As a result of extensive research to resolve differences between field results and expectations based on analytical studies, a considerable body of knowledge on the performance of fractured wells has been accumulated. This paper is a brief survey of the current level of understanding of this aspect of pressure transient analysis by petroleum engineers.

The topics considered here include the following: (i) the effect of vertical, horizontal, and inclined fractures on pressure behavior at the well, (ii) the influence of fracture flow capacity on pressure vs. time data, (iii) the effect of wellbore storage and damage on pressure response, (iv) the influence of closed (depletion or zero recharge) or constant pressure (complete recharge) boundaries. Both flowing and shut-in pressure behaviors are discussed.

This survey also indicates some of the problems that should be solved to improve our understanding of fractured well behavior.

Introduction

Virtually every commercial oil and gas well has been stimulated either at the start of production or during its productive life. The main objective of well stimulation is to bring productive capacity to commercial levels. Initially stimulation treatments consisted of acidizing wells being produced from limestone reservoirs. The first acid treatment job was performed on February 11, 1932. By 1934 acidizing had become an accepted practice for stimulating wells producing from intervals containing substantial amounts of acid-soluble components in the reservoir rock matter.[1] The acidizing process usually consists of injecting hydrochloric acid (normally 15 percent by weight) along with surface active agents and inhibitors (to protect casing and other equipment).

It was soon realized that pressure parting or formation lifting also played an important part in the ease with which the acidization is performed.[2] For example, at pressures below those required to lift the overburden, very little fluid could be injected; however, when the pressure became high enough to part or fracture the formation, the injection rate could be raised significantly with little or no additional increase in pressure. Similar observations were made by Dickey and Anderson[3] and Yuster and Calhoun[4] in their studies of injection rates in water injection wells. These authors concluded that formations could be parted by excessive injection pressures. Similar observations were reported by other investigators studying the use of squeeze cementing.[5-7] This process normally involves the injection of a slurry into a porous formation.

The realization that formations could be broken down or fractured during acidizing, squeeze cementing, and water injection operations, served as a precursor to hydraulic fracturing. Hydraulic fracturing was introduced to the petroleum industry in the Hugoton gas field in western Kansas. This method of increasing well productivity was conceived and patented by Farris of the Pan American Petroleum Corporation,[8] and has been defined as "the process of creating a fracture or fracture system in a porous medium by injecting a fluid under pressure through a wellbore in order to overcome native stresses and to cause material failure of the porous medium."[9]

The fluid used in hydraulic fracturing depends on the physical and chemical nature of the reservoir fluids and rock. Generally a proppant (Ottawa sand, glass beads, nutshells, or plastic particles) is also injected along with the fluid since hydraulically formed fractures tend to heal, that is, they lose their fluid carrying capacity after the parting pressure is released.[10]

Over the past twenty-eight years hydraulic fracturing has served as an inexpensive way of increasing the productive or injection capacity of wells. The success of many marginal wells and near-depleted fields can be directly attributed to this procedure. It is estimated that over 500,000 wells have been hydraulically fractured. The method has been used to accomplish four tasks: (i) to overcome wellbore damage, (ii) to improve well productivity by creating highly conductive paths to the wellbore, (iii) to aid in fluid injection operations and (iv) to assist in the disposal of brines and industrial waste material.

The principal objective of this paper is to provide a summary of the state of the art on the pressure analysis of wells intercepted by fractures. It shall examine wells that are intentionally fractured as well as those that intersect natural fractures. This paper is restricted only to the examination of a single fracture existing in a uniform, homogeneous porous formation; that is, naturally fractured reservoirs consisting of a

system of interconnected cracks or failure surfaces coupled to a matrix of different porosity and permeability in a random fashion are not examined.

This critique assumes that the reader is familiar with some of the developments in the petroleum engineering literature. Three developments which would be extremely useful for the reader to understand in following the subject matter of this paper are: (i) the concept of wellbore storage, (ii) the infinitesimally thin skin concept, and (iii) the pressure behavior of an unfractured well (plane radial flow) producing at a constant rate and located at the center of a square drainage region with the outer boundary closed (depletion or zero recharge) or at constant pressure (full recharge). Details regarding all of the above aspects are discussed in three monographs. Two of these have been published by the Society of Petroleum Engineers[11,12] and another by the American Gas Association.[13]

Prior to considering various aspects of fractured wells I shall enumerate the purposes of pressure transient testing and also provide a brief historical sketch of pressure transient analysis. Only those papers which have a direct bearing to this review are mentioned. This sketch is intended to provide those in the audience not familiar with the petroleum engineering literature some idea of the parallel developments that took place in the ground water hydrology and petroleum engineering literature pertaining to pressure transient behavior in the 1940's and 1950's.

Objectives of Pressure Transient Analysis

It is well established in the petroleum industry that pressure transient analysis is the most powerful tool existing to enable an engineer to determine the characteristics of a given reservoir, and then prepare a long-range forecast of production performance.

Questions which a petroleum engineer normally encounters include the following: (i) Is the low productivity of a well due to low formation flow capacity, to a low driving force for moving fluid to the wellbore or to well damage? (ii) Is it likely to be worthwhile to perform a stimulation treatment? and (iii) was a stimulation treatment, which was conducted to eliminate formation damage, successful? Answers to the above questions can enable an engineer to make decisions regarding operating practices and/or stimulation programs. Pressure transient tests can be used to provide these answers.

Today pressure transient tests are used for the following purposes: (i) A quantitative estimate of the formation flow capacity (permeability - thickness product) of the volume drained by a well, (ii) quantitative information on the shape and size of the drainage volume, (iii) an estimate of the mean or average reservoir pressure (this is necessary for material balance calculations), (iv) determination of reservoir heterogeneity, and (v) diagnosis of the well condition (whether the region near the sandface has been damaged or plugged, or whether it has been stimulated). It is not unusual to conduct a test for the sole purpose of determining the well condition.

Pressure Transient Analysis:

A Brief Historical Review

One of the earliest measurements of bottomhole pressures was for the estimate of the average or "static" reservoir pressure. This measurement is useful in material balance calculations to estimate the quantity of oil and/or gas in the reservoir. To obtain it a producing well was usually shut in for a period of 24 to 72 hours. The measured pressure after this period was assumed to be the static pressure. However, it was soon realized that estimates of static pressure were dependent on the time for which a well had been shut in and that the lower the permeability, the longer the time required for the well to be shut in. This immediately led to the important realization that the formation permeability can be determined from a well test. To my best knowledge the first determination of formation permeability via this method was presented by Moore, Schilthuis and Hurst[14] in 1933.

In 1935, Theis[15] presented a classic study on pump testing of water wells and discussed the analysis of pressure recovery data. Pressure recovery data are known as pressure build-up data in the petroleum engineering literature. The form of graphing and analysis suggested by Theis remains one of the basic techniques used in petroleum engineering today. In 1951, Horner[16] summarizing the important contributions of the research personnel of the Shell companies, presented the same method of analysis. (It should be mentioned that Horner and co-workers arrived at their approach independently.) At approximately the same time, Miller, Dyes and Hutchinson (MDH)[17] presented an alternate method of analysis. Although the methods of analysis of the Horner and MDH procedures were different, both methods reported that the formation permeability can be determined from wellbore pressures. The relationship between these two methods was shown only recently by Ramey and Cobb.[18]

In 1937, Muskat[19] presented a method for determining ultimate static pressure from pressure transient data. This method is especially useful in situations where early time data are unavailable or are dominated by wellbore storage effects.

Many studies appeared during the 1940's. Of note in the ground water literature were the works of Wenzel[20], Cooper and Jacob[21], and Jacob.[22] Jacob[23] was also the first to recommend semi-log graphical analysis for pressure draw-down data. In 1946, Elkins[24] presented graphs for analysis of interference test data. This information forms the basis for analyzing many of the interference tests conducted today. In 1949, van Everdingen and Hurst[25] presented a study on the application of Laplace Transforms to transient flow problems. Much of the work that has followed in the petroleum engineering literature is a direct

result of the van Everdingen-Hurst study.

All of the studies mentioned above concern pressure behavior when the well is flowing at a constant rate. Though studies of wells producing at a constant wellbore pressure have been examined (Hurst[26], Jacob and Lohman[27], van Everdingen and Hurst[25]) these solutions have not been used in well test analysis, probably due to the fact that it is not readily apparent how this condition would affect the important case of pressure build-up after the well had been shut-in at the sandface.

As mentioned earlier the results of two studies by Horner[16] and Miller, Dyes and Hutchinson[17] were presented in the early 1950's. These two methods formed the backbone of pressure transient analysis in the petroleum industry. As a result of the success of the above studies in describing pressure behavior of wells, a tremendous wealth of information pertaining to pressure behavior under a variety of conditions has been accumulated. These included studies on the effect of damage and stimulation (van Everdingen[28] and Hurst[29]), on the effect of partial penetration (Hantush[30], Nisle[31], Burns[32], and Prats[33])*, on wellbore storage phenomena (Agarwal, Al-Hussainy and Ramey[34], Ramey[35], Ramey and Agarwal[36], Ramey, Agarwal and Martin[37], and Cooper, Bredehoeft and Papadopulos[38]) and on the effect of heterogeneities.[11,12] Most of these studies are summarized in Refs. 11, 12, 13, and 39.

Flowing Pressure Behavior of Fractured Wells

With the advent of hydraulic fracturing as a stimulation technique in low permeability reservoirs, it soon became obvious that standard radial flow solutions considered by earlier works were inadequate for the analysis of fractured wells. The main problem was that a fracture is a plane of high conductivity extending into the formation for some distance and the radial flow idealization did not include this aspect.

Before proceeding further, a discussion of the azimuthul orientation of fractures intercepting wellbores is warranted. Howard and Fast state that the azimuthul orientation depends on whether the porous medium acts as an elastic, brittle, ductile or plastic material.[40] According to Hubbert and Willis[41], the general state of stress underground is one in which the three principal stresses are unequal and the plane of the hydraulic fracture would be perpendicular to the axis of the least stress. In tectonically relaxed areas the least stress is horizontal. Thus vertical fractures would result. But if orogenic forces are active, the direction of the least stress could be vertical (in this case it would equal the effective overburden stress) and could result in horizontal fractures. This then implies that, at least theoretically, the injection pressure during hydraulic fracturing must be equal to or greater than the effective overburden pressure for a horizontal fracture to result.

Today it is generally believed that hydraulic fracturing normally results in a single vertical fracture, the plane of which includes the wellbore.[42] But it is also agreed that if formations are shallow then horizontal fractures can result. The specific orientation of a fracture with respect to the vertical axis may be unidentifiable if it is a naturally occurring fracture. However, vertical fractures are by far the most common. Thus, most of the attention in the literature has been directed towards vertical fractures.

Much of the early work on fractured wells concerned the study of steady state behavior using potentiometric or analytical models (Muskat[43], Howard and Fast[44], McGuire and Sikora[45], Prats[46], van Poollen, Tinsley and Saunders[47], Craft, Holden and Graves[48], Dyes, Kemp and Caudle[49], Tinsley, Williams, Tiner and Malone[50]). Most of these papers were primarily interested in the productivity increase that would result due to a fracture treatment. Unfortunately, as shown in Fig. 1 the results are not in agreement.[51] Here J_{act} represents the productivity of the well following a fracture treatment, J_{theo} is the productivity prior to fracture treatment, k_f is the fracture permeability in md., and w is the fracture width in feet.

As far as pressure transient analysis is concerned Dyes, Kemp and Caudle[49] were the first to investigate the effect of a vertical fracture on the straight line that results on a Horner or Miller-Dyes-Hutchinson graph. In the limited number of cases they examined, they concluded that fractures which extend over 15 percent of the drainage radius alter the position and slope of the straight line on the pressure build-up curve. Others also studied the production response and pressure behavior of a closed cylindrical reservoir producing an incompressible[46] or a slightly compressible[52] fluid through a single, vertical fracture located at the center of the cylinder. They found that the production rate decline increases as the fracture length increases. Thus, they suggested that lateral extent of the fracture can be determined from a comparison of the production rate declines before and after fracturing, or it can be determined from the rate decline if the fluid and formation properties are known. Prats[46] also found that if the ratio of reservoir radius to fracture radius was greater than two, then the production behavior of such a fractured system can be represented by an equivalent radial-flow system having an effective well radius equal to one-fourth of the total fracture length. (Muskat[43] had arrived at a similar conclusion earlier when he examined a fractured well in an infinite reservoir.) In the petroleum engineering literature this observation is known as the "effective wellbore radius concept." Scott[53] developed curves of wellbore pressure versus time for a fractured well in a closed circular reservoir using this concept.

Russell and Truitt[54], in a comprehensive treatment of the subject, studied the pressure behavior of infinite-conductivity fractured wells in a square reservoir using a finite difference

*This list only includes those of direct consequence to this paper.

model. An infinite-conductivity fracture implies that there is no pressure drop along the fracture plane at any instant in time. They considered a homogeneous, isotropic reservoir in the form of a closed square completely filled with a slightly compressible liquid of constant viscosity. Pressure gradients were assumed to be small everywhere and gravity effects were neglected. The plane of the fracture was located symmetrically within the reservoir and parallel to one of the sides of the square boundary (Fig. 2). The fracture extended throughout the vertical extent of the formation and production at a constant rate was assumed to come only through the fracture. Russell and Truitt computed the pressure at the wellbore as a function of time and fracture penetration ratio. Here the term fracture penetration ratio will be defined as the ratio x_e/x_f and will be used consistently in all of the following. They demonstrated the effect of fracture length on the drawdown and build-up behavior of a vertically fractured well for a wide variety of conditions.

In 1974, Gringarten, Ramey and Raghavan[55] found it necessary to re-examine the solutions presented by Russell and Truitt as the Russell-Truitt study was not intended for short time analysis. They examined the problem analytically by the use of Green's functions[56] and the Newman[57] product method which had been discussed earlier by Gringarten and Ramey.[58] Gringarten, et al., were also the first to present a complete and comprehensive view of the pressure behavior of an infinite-conductivity vertical fracture. The work of Gringarten, et al., will serve as a starting point for our discussion.

The Infinite-Conductivity Vertical Fracture in a Closed Square Drainage Region

Gringarten, et al.[55], have presented drawdown data for an infinite-conductivity vertically fractured well located at the center of a closed square drainage region and producing a slightly compressible constant viscosity fluid at a constant rate (see Fig. 2). The solution for the producing pressure in psi, p_{wf}, at time, t, expressed in hours is

$$p_{wD}(t_{Dx_f}, x_e/x_f) = \frac{kh}{141.2\ qB\mu}(p_i - p_{wf}) \qquad (1)$$

where

$$t_{Dx_f} = \frac{0.000264kt}{\phi c_t \mu x_f^2} \qquad (2)^*$$

*In ground water hydrology $p_{wD} = 2\pi Ts/(q\mu)$ where s is the head draw-down and T is the transmissivity; dimensionless time $t_{Dx_f} = Tt/(\mu S x_f^2)$ where S is the storage coefficient.

Here, $p_{wD}(t_{Dx_f}, x_e/x_f)$ represents the dimensionless wellbore pressure drop for a particular fracture penetration ratio, x_e/x_f, and t_{Dx_f} is dimensionless time. The formation permeability is denoted by k in md., the thickness by h in feet, the porosity by ϕ, the system compressibility by c_t in psi^{-1} and the initial pressure by p_i. The flow rate is q, measured in Stock Tank Barrels/Day, the formation volume factor is B, which is Reservoir Barrels per Stock Tank Barrel, and the fluid viscosity in cp is μ. The distance from the center of the well to the external boundary is x_e feet, and the fracture length end-to-end is $2x_f$. All equations here are expressed in oil field engineering units. Figures 3 and 4 are graphs of p_{wD} vs. t_{Dx_f} for the system under examination on log-log and semi-log coordinates. The fracture penetration ratio, x_e/x_f, is the parameter of interest.

Prior to considering pressure behavior in the bounded system, let us for the present examine a vertically fractured well in an infinite reservoir. This corresponds to the $x_e/x_f = \infty$ line on Figs. 3 and 4. Note that we are examining a fractured well in an infinite reservoir and not an unfractured well in an infinite reservoir. For an infinite-conductivity fractured well in an infinite reservoir Gringarten, et al., have shown that the wellbore pressure drop is given by the following expression:

$$p_{wD}(t_{Dx_f}) = \frac{1}{2}\sqrt{\pi t_{Dx_f}}\left(\operatorname{erf}\frac{0.134}{\sqrt{t_{Dx_f}}} + \operatorname{erf}\frac{0.866}{\sqrt{t_{Dx_f}}}\right)$$

$$- 0.067\ \mathrm{Ei}\left(-\frac{0.018}{t_{Dx_f}}\right) - 0.433\ \mathrm{Ei}\left(-\frac{0.750}{t_{Dx_f}}\right) \qquad (3)$$

where erf (x) is the error function of x, and -Ei (-x) is the exponential integral.[59] At large values of time ($t_{Dx_f} \geq 3$) it can be shown that Eq. (3) can be written as

$$p_{wD}(t_{Dx_f}) = \frac{1}{2}\ln t_{Dx_f} + 1.100 \qquad (4)$$

where ln refers to natural logarithms. The above time limit of $t_{Dx_f} = 3$ was obtained empirically by examining the $x_e/x_f = \infty$ line on Fig. 4 and determining the time at which a straight line with a slope of $1.151/\log_{10}$ starts. This may be done by placing a triangle with the proper slope on Fig. 4 and checking the $x_e/x_f = \infty$ curve for the start of the straight line with the proper slope.

For small values of time ($t_{Dx_f} \leq 0.016$)

$$p_{wD}\,(t_{Dx_f}) = \sqrt{\pi t_{Dx_f}} \qquad (5)$$

This early time period is generally referred to as the linear flow period. As shown in Fig. 3 on log-log coordinates this period is characterized by a straight line of slope of 0.5. The reason for this may be seen if the logarithm of each side of Eq. 5 is considered. Taking these logarithms we obtain

$$\log\,[p_{wD}\,(t_{Dx_f})] = \log\sqrt{\pi} + \frac{1}{2}\log t_{Dx_f} \qquad (6)$$

Then the reason for the "half slope line" is clear. Here the abbreviation "log" refers to "logarithm to the base 10." The time limit of $t_{Dx_f} = 0.016$ was also obtained empirically. The log-log graph was used for this purpose and the end of the linear flow period was determined by placing a triangle with the correct slope on Fig. 3 and then searching for the end of the linear flow period.

From a practical viewpoint Eq. (4) implies that if data are obtained for a long enough period, then the permeability-thickness product may be calculated from the slope of the draw-down curve. The equation to be used would be the well known radial flow formula:

$$kh = \frac{162.6qB\mu}{m} \qquad (7)$$

where m is the slope of the straight line portion of the draw-down curve in psi/logν on semi-log paper. It is important to note, however, that the start of the semi-log straight line cannot be determined a priori. This can be a problem in analyzing pressure data by this approach.

Once the semi-log straight line has been identified and Eq. (7) has been used to estimate formation permeability the skin factor, s, can be determined from the expression[12]

$$s = 1.151\left[\frac{p_i - p_{1hr}}{m} - \log\frac{k}{\phi c_t \mu r_w^2} + 3.23\right] \qquad (8)$$

In Eq. (8), p_{1hr} is the pressure on the correct semi-log straight line at one hour or on the extrapolation of the correct semi-log straight line to one hour[12] and r_w is the wellbore radius in feet. Note that the skin factor, s, is related to the skin pressure drop, Δp_{skin}, by the expression:

$$s = \frac{kh}{141.2qB\mu}\,\Delta p_{skin} \qquad (9)$$

Equation (5) contains two unknowns, k and x_f. But if k can be determined then x_f can be calculated from a Cartesian graph of $\Delta p = (p_i - p_{wf})$ or p_{wf} vs. $\sqrt{\text{time}}$, since Eq. (5) indicates that

$$\Delta p \propto \sqrt{t} \qquad (10)$$

The relevant formula is

$$x_f = \frac{0.319}{m'}\sqrt{\frac{qBm}{\phi h c_t}} \qquad (11)$$

where m is the slope of the semi-log straight line and m' is the slope of the straight line on Cartesian coordinates in psi/$\sqrt{\text{hr}}$. The above represents the approach presented by Russell and Truitt[54] and Clark.[60]

Gringarten, et al., also proposed that log-log type curve matching (actually Ramey[35] suggested this approach in 1970) be used to calculate permeability and fracture length. The basis for the type curve matching procedure is well-known. It will be repeated here only for continuity. Taking the logarithm of both sides of Eqs. (1) and (2), respectively, we have:

$$\log\,[p_{wD}(t_{Dx_f}, x_e/x_f)] = \log\frac{kh}{141.2\ qB\mu} + \log\,(p_i - p_{wf}) \qquad (12)$$

$$\log t_{Dx_f} = \log\frac{0.000264\ k}{\phi c_t \mu x_f^2} + \log t \qquad (13)$$

If actual draw-down data are plotted as the logarithm of the absolute difference between initial pressure at the start of the test and pressure after the rate change versus the logarithm of time, the actual field data should be similar to a log-log graph of p_{wD} vs. t_{Dx_f}. The difference between the two graphs is only a linear translation of both coordinates, represented by the first terms on the right-hand side of Eqs. (12) and (13). If a proper match of the field curve with the dimensionless curve is obtained then kh/μ can be determined from the vertical displacement of the horizontal axes and $k/(\phi c_t \mu x_f^2)$ from the horizontal displacement of the vertical axes. Thus the permeability-thickness product and fracture half-length can be determined. The advantage of the type curve matching procedure is that the entire data obtained during a test can be used.

In addition it can be shown that the duration of testing can be greatly reduced if this procedure is followed.

All of the above discussion pertains to a fractured well in an infinite reservoir. Let us now consider the effect of outer boundaries. Returning to Fig. 3 we note that at early times the solutions for the bounded case are identical to that for a fractured well in an infinite reservoir. They possess an initial period controlled by linear flow to or from the vertical fracture surface. During this period, pressure is a function of the square root of time. On log-log coordinates the pressure behavior during this period is characterized by a straight line of slope of 0.5. Following the linear flow period a pseudo-radial flow period (slope = 1.151/log cycle on a semi-log graph) exists for fracture penetration ratios, x_e/x_f, greater than 5. The pseudo-radial flow period begins at $t_{Dx_f} = 3$. This can be demonstrated by plotting the graph of p_{wD} vs. t_{Dx_f} on semi-log coordinates (see Fig. 4). Finally, all solutions reach pseudo-steady state because fluid is produced at a constant rate from a closed system.[12] The advantages of identifying the various flow regimes are discussed later under "Some Practical Considerations." The time limits mentioned above can also be used in the design of field tests.

The Uniform-Flux Vertical Fracture in a Closed Square Drainage Region

During the course of their investigation on infinite-conductivity vertical fractures, Gringarten, et al., also arrived at another solution called the "uniform-flux" solution. This solution gave the appearance of a high, but not infinite, conductivity fracture. Thus unlike the infinite-conductivity case the pressure varies along the fracture length at any given instant in time. Application of these solutions to field data indicates that the uniform-flux solution matches wells intersecting naturally occurring fractures better than the infinite-conductivity solution. On the other hand the infinite-conductivity solution matches the pressure behavior of hydraulically fractured wells better than does the uniform-flux solution. More recent experience has indicated that the uniform-flux solution matches injection well pressure data, and wells that are acid-fractured much better than the infinite-conductivity solution. The exact nature of these solutions will be discussed in the section on finite-capacity fractures.

As already pointed out, the uniform-flux solution is useful in analyzing data obtained from wells intersecting natural fractures. For a well in an infinite reservoir it can be shown that the pressure drop at the wellbore is given by:

$$p_{wD}(t_{Dx_f}) = \sqrt{\pi t_{Dx_f}}\ \mathrm{erf}\left(\frac{1}{2\sqrt{t_{Dx_f}}}\right) - \frac{1}{2}\,\mathrm{Ei}\left(-\frac{1}{4t_{Dx_f}}\right) \qquad (14)$$

At long times, $t_{Dx_f} \gtrsim 2$, Eq. (14) may be written as

$$p_{wD}(t_{Dx_f}) = \frac{1}{2}(\ln t_{Dx_f} + 2.80907) \qquad (15)$$

This expression is similar to that for an unfractured well in an infinite reservoir. For small times, $t_{Dx_f} \lesssim 0.16$, Eq. (5) applies. The time limits mentioned above were obtained along the same lines as for the infinite-conductivity case.

On the basis of Eqs. (5) and (15), we can say that Eqs. (7) and (11) can be used to calculate formation permeability and fracture length, respectively provided that the test is run for a long enough period.

Figures (5) and (6) are log-log and semi-log graphs, respectively, for the pressure behavior at a fractured well for the uniform-flux case. Again three different flow periods can be characterized. A linear flow period occurs at early times. This corresponds to a straight line with a slope of one-half on log-log coordinates (Fig. 5). After a period of transition, there is a pseudo-radial flow period corresponding to the semi-log straight line (Fig. 6). After a second period of transition, pseudo-steady state flow occurs, which is characterized by an approximate unit slope straight line on log-log coordinates. This flow period results because fluid is produced at a constant rate from a closed reservoir. Depending upon x_e/x_f, one or more of these flow periods may be missing: in the total fracture penetration case ($x_e/x_f = 1$), for instance, the first transition period and the pseudo-radial period do not appear, whereas only the pseudo-radial period is missing for values of x_e/x_f between 1 and 3. Figures 3 and 5 can be used for type curve matching to obtain estimates of formation permeability fracture length, and distance to a drainage limit.[55]

The pressure response shown in Figs. 3 and 5 may also be displayed on a different type curve as p_{wD} vs. t_{DA} where t_{DA} is the dimensionless time based on the drainage area, A, and is given by

$$t_{DA} = \frac{0.000264kt}{\phi c_t \mu A} = t_{Dx_f}\left(\frac{x_f^2}{A}\right) \qquad (16)$$

Figure 7 displays the same information as that shown in Fig. 3 as p_{wD} vs. t_{DA}. It is convenient for long time analysis when bends due to the outer boundary become evident. As shown in Fig. 7, the time for the start of pseudo-steady state is approximately t_{DA} of 0.12 for all x_e/x_f. Thus the vertically-fractured well reaches pseudo-steady state in about the same time as an unfractured well in a closed square.[61] Figure 5 may also be

displayed in a similar manner.

In 1968, Earlougher, et al.,[61] showed that for an unfractured well in a closed square the time for onset of pseudo-steady state is greater for the well point than for any other point in the system. Thus pseudo-steady state flow at the well guarantees that all points in the drainage area are at pseudo-steady state. The same is also true for a vertically fractured well in a closed square drainage region.[62]

Comparison of Infinite-Conductivity and Uniform-Flux Solutions

Though the shapes of the infinite-conductivity and uniform-flux solutions are similar, some of the differences are worth mention. Comparison of the two solutions indicates that the pseudo-radial flow period begins somewhat earlier for the uniform-flux case ($t_{Dx_f} = 2$ for uniform-flux, $t_{Dx_f} = 3$ for infinite-conductivity). Furthermore, if $x_e/x_f \neq 1$, the linear flow period for a uniform-flux fracture exists for a much longer period than for the infinite-conductivity case ($t_{Dx_f} = 0.16$ for uniform-flux, $t_{Dx_f} = 0.016$ for infinite-conductivity). In conclusion, it should be noted that distinctions between the two cases vanish if $x_e/x_f = 1$.

The Vertically Fractured Well in a Constant Pressure (Full Recharge) Square

Recently Raghavan and Hadinoto[63] extended the solutions presented by Gringarten, et al.,[55] by considering that the pressure at the outer boundary was maintained at a constant value equal to the initial pressure (full recharge). Figures 8 and 9 are log-log graphs of p_{wD} vs. t_{Dx_f} for the infinite-conductivity and uniform-flux cases respectively. On both of these figures the results shown in Figs. 3 and 5 are also presented for purposes of comparison. Again the line corresponding to $x_e/x_f = \infty$ represents a vertically fractured well in an infinite reservoir.

The results in Figs. 8 and 9 indicate three characteristic flow periods. A linear flow period occurs at early times--the one-half slope line. After a period of transition a pseudo-radial flow period exists. Like the closed case this flow period exists only for certain values of x_e/x_f. After a second period of transition steady state flow conditions are reached for all x_e/x_f. This flow period is analogous to pseudo-steady state flow behavior for wells in closed systems. During steady state the pressure at each point within the drainage region is independent of time and there is no decline in pressure. Steady state conditions result when $t_{DA} = 0.4$ for all x_e/x_f.

For practical purposes, Figs. 8 and 9 may be used for type curve matching for the appropriate fracture type. If a drainage limit should become evident during the test, then data points would follow the appropriate x_e/x_f line. If the system under study is located in a constant pressure square then field data would fall below the $x_e/x_f = \infty$ curve, and follow the appropriate x_e/x_f line. On the other hand if the system boundaries are closed, then data would rise above the $x_e/x_f = \infty$ curve and follow the corresponding x_e/x_f line. Figures 7 and 8 may also be used for analyzing fall-off or build-up data. This aspect of pressure analysis will be considered in the section on "Shut-in Pressure Behavior."

For unfractured wells Hurst, Haynie and Walker[64], remarked that the system boundaries (closed or constant pressure) affect pressure behavior at the same time, i.e., curves influenced by outer boundary conditions will depart simultaneously from the infinite reservoir curve, regardless of the nature of the outer boundary. The results in Figs. 8 and 9 indicate that this observation also applies to fractured wells for all cases except $x_e/x_f = 1$. This then implies that a limiting statement can be made concerning the drainage volume for a fractured well which does not indicate a drainage boundary effect for both closed and constant pressure boundary cases provided $x_e/x_f \neq 1$; that is, if the fracture does not extend to the outer boundary.

Comparison of the results for $x_e/x_f = 1$ for the closed and constant pressure cases indicates one important difference. The pressure drops for the uniform-flux and infinite conductivity cases for the closed reservoir are identical, whereas for the constant pressure outer boundary case this is not so. This result is due to the influence of the outer boundary. For $x_e/x_f = 1$ in a closed reservoir, no gradients parallel to the fracture exist; in the constant pressure reservoir this is not so.

From the viewpoint of field applications, the pressure behavior for vertically fractured wells located in other drainage shapes is also needed. These may be found in Ref. 65.

Some Practical Considerations

As mentioned earlier one of the problems in analyzing pressure data by the semi-log approach is that it is difficult to locate the beginning of the pseudo-radial flow period. Inspection of the theoretical solutions, however, indicates that if the one-half slope line can be identified then the correct semi-log line should start approximately two cycles from the time of the end of the one-half slope line for an infinite-conductivity fracture. For a uniform-flux fracture the time for start of the correct straight line is one cycle from the end of the one-half slope line. In general, data over a one-half cycle time period would be required to form a well-defined semi-log line. Only thus can the proper straight line be identified and if early time data are analyzed at

the test site then the total time of testing can be readily determined.

A second rule, which is probably more useful than the one stated above, is the "double-Δp rule." In examining vertically fractured gas wells, Wattenbarger[66] noticed that the dimensionless pressure drop at the start of the semi-log straight line is twice that of the dimensionless pressure at the top of the one-half slope line. This result, strictly true only for the uniform-flux case, is the "double Δp rule." For the infinite-conductivity vertical fracture the pressure change between the end of the one-half slope line and the beginning of the semi-log straight line is approximately 8. In any event it is clear that the ratio of the pressure change must be at least 2. This rule is particularly useful in those cases where pressure behavior at an unfractured well dominated by wellbore storage is wrongly identified as a fractured well (see Ramey[67] for further discussion).

The Effective Wellbore Radius Concept

As mentioned earlier, Prats[46] has shown that an infinite-conductivity vertical fracture, producing an incompressible fluid from a closed circular reservoir, was equivalent to an unfractured well with an effective radius equal to a quarter of the total fracture length for ratios of the reservoir radius to the fracture half-length greater than 2. The same is true for a well producing a slightly compressible fluid under pseudo-steady state conditions.[52] We can see that these results also apply to a vertically fractured well in an infinite reservoir during the pseudo-radial period, because Eq. (4) can be written as

$$p_{wD}(t_{Dx_f}) = \frac{1}{2}\left\{\ln\left[\frac{0.000264kt}{\phi c_t \mu \left(\frac{x_f}{2}\right)^2}\right] + 0.80907\right\} \qquad (17)$$

The effective well radius for an infinite-conductivity vertical fracture in an infinite reservoir is thus exactly one fourth of the total fracture length. This, of course, is only valid for the pressure drop on the fracture during the pseudo-radial period, and must not be used for other conditions.

The effective wellbore radii for the results discussed in Figs. 8 and 9 are shown in Fig. 10. Here x_f/x_e rather than x_e/x_f is used for convenience. The symbol r_w' represents the effective wellbore radius of a vertically fractured well and equals the product $r_w \exp(-s)$.[12] The results are applicable for pseudo-steady state flow (closed) and steady state flow (full recharge) conditions. Examination of the data in Fig. 10 indicates that the effective wellbore radius for the uniform-flux case is smaller than that for the infinite-conductivity case. Furthermore, the value of the effective wellbore radius is essentially constant for fracture penetration ratios, $x_e/x_f > 2$. It is also evident that the outer boundary conditions must be considered if this concept is to be used to describe pressure behavior at the well.

Determination of the Fracture Length from the Effective Wellbore Radius

Gringarten, et al.[55], have shown that the effective wellbore radius can be used to calculate fracture length if x_e/x_f is known or if it is large. This procedure is simple if one notes that for large penetration ratios values of x_f/r_w' are essentially constant. From Fig. 10 we see that for $x_e/x_f > 2$, $x_f/r_w' \approx 2$ for an infinite-conductivity fracture, and $x_f/r_w' \approx e = 2.71828$ for a uniform-flux fracture. The first step is to estimate the skin factor, s. The second step involves determining x_f/r_w' from Fig. 10. As $r_w' = r_w \exp(-s)$ an estimate of x_f can now be obtained. For example consider a uniform-flux fracture where $x_e/x_f > 2$. Noting that $x_f/r_w' \approx e = 2.71828$ the fracture half-length is given by

$$r_w' \approx \frac{x_f}{e} = r_w e^{-s} \qquad (18)$$

Approximate Determination of Formation Permeability and Fracture Half-Length

There are a number of instances, particularly in tight reservoirs, in which the linear flow period lasts for several hundred hours. Under these conditions neither the type curve nor the conventional approach may be applicable. However, the last point on the half slope line may be used to estimate an upper limit of the permeability-thickness product. Using the resultant value of permeability, a corresponding fracture length may also be calculated. The appropriate expressions to be used are:

$$\frac{kh}{141.2qB\mu}\Delta p = 0.215 \qquad (19)$$

and

$$\frac{0.000264kt}{\phi c_t \mu x_f^2} = 0.016 \qquad (20)$$

where Δp, and t are the pressure change and time corresponding to the last available point on the half slope line. Equations (19) and (20) are applicable for penetration ratios $x_e/x_f >> 1$. Equations (19) and (20) may also be used if data beyond the half slope line are available but are not sufficient to perform a type curve match or to use the semi-log graph. If natural fractures are to be analyzed in this fashion, then the right-hand sides of Eqs. (19) and (20) should be replaced by 0.76 and 0.16, respectively.

A Finite-Capacity Vertically-Fractured Well in an Infinite Reservoir

Application of the Gringarten, et al., type curves to hydraulically fractured wells in many instances produces results that are compatible with reservoir performance and design calculations prior to treatment. But in some instances the results are not compatible with design calculations or production performance even though field data matched the type curve very well. In many instances when data following large volume fracture treatments (injection of several thousand gallons of fluid and several hundred thousand pounds of proppant) were analyzed, then computed effective fracture lengths were small--of the order of a few feet. One of the potential reasons for this anomaly appears to be the finite flow capacity of the vertical fracture. To date three groups have published results on the effect of finite fracture capacity on pressure behavior.[51,68,69] A summary of the work of the three groups follows. Let the reader be cautioned that most of the results presented here represent only the beginning of the work which needs to be done to understand the pressure behavior of finite-capacity fractures.

Before proceeding to document the results in Refs. 51, 68, and 69, let us refer back to the study of Prats[46] which was published almost fifteen years ago. It appears that the results of this paper have been virtually ignored. (Surprisingly this paper appeared in the Society of Petroleum Engineers Journal and not in the Journal of Petroleum Technology - only a small fraction of the SPE membership subscribes to this journal.) The effect of finite fracture capacity defined as "the product of fracture permeability and fracture width" was demonstrated in this paper. Prats showed that three parameters controlled the pressure distribution around a fractured well. They are, (i) the ratio of the fracture length to the well radius, (ii) the ratio of the reservoir drainage radius to the well radius, and (iii) the dimensionless fracture flow capacity, F'_{cD} defined by:

$$F'_{cD} = \frac{\pi k(2x_f)}{4k_f w} \tag{21}$$

The first two parameters describe the geometry of the system and the third is the measure of the ability of the formation to carry fluids into the fracture relative to the ability of the fracture to carry fluids into the well. For a very effective fracture, that is one which has a great ability to carry fluids, F'_{cD} is small and approaches the limiting value of zero for infinite fracture permeability. Likewise, for a very ineffective fracture, F'_{cD} would be large and approaches infinity for the limiting case of an unfractured well.

The effect of fracture capacity on the pressure distribution around a fractured well is shown in Fig. 11. It shows that the pressure distribution for $F'_{cD} = 0$ is given by confocal ellipses. For $F'_{cD} = \infty$ the pressure distribution is given by circles concentric with the well axis. Prats noted that for $F'_{cD} = 100$ the pressure distribution was essentially the same as that for an unfractured well (radial flow). For intermediate values of F'_{cD} the pressure distribution lies in between the two extremes. As the pressure draw-down or build-up curve is essentially the reflection of pressure distribution in the reservoir, it is clear that finite fracture capacity can drastically influence the pressure draw-down or build-up trace.

Figure 12 presents the effect of fracture capacity on the effective wellbore radius. Three observations are evident: (i) If $F'_{cD} > 28$ then any increase in the fracture length would be totally ineffective, (ii) for F'_{cD} between 1 and 28 increases in productivity may be significant if the fracture length is increased and, (iii) since the formation flow capacity is fixed, the fracture capacity would have to be increased if production increases are to be significant.

The most important message of Prats' paper, however, is the following: The dimensionless fracture flow capacity, F'_{cD}, determines well performance and productivity increases--not fracture length; that is, for a long fracture to be as effective as a short one, the fracture flow capacity would have to be much higher for the longer one. Fracture capacity dictates optimum fracture length. Unfortunately this has not been recognized by reservoir or production engineers.

Let us now return to the discussion of the effect of dimensionless fracture flow capacity on pressure transient behavior. Before proceeding further it should be noted that the various research groups mentioned earlier have defined dimensionless fracture capacity somewhat differently from Prats' definition. The Agarwal, et al.[69] definition is

$$F_{cD} = \frac{k_f w}{k x_f} = \frac{\pi}{2F'_{cD}} \tag{22}$$

Cinco, et al.[68], define dimensionless fracture capacity as

$$C_r = \frac{k_f w}{\pi k x_f} = \frac{F_{cD}}{\pi} \tag{23}$$

Ramey, et al.[51], define dimensionless fracture capacity as

$$\frac{1}{(k_f w)_D} = \frac{k x_f}{k_f w} = \frac{1}{F_{cD}} \tag{24}$$

Clearly some consistency in the nomenclature is called for. Personally, I prefer the definition of Agarwal, et al.

Figure 13 demonstrates the effect of dimensionless fracture capacity, F_{cD}, on the pressure behavior at the well, when all other parameters are constant. The dimensionless fracture capacity ranges from 10^{-1} to 500. Agarwal, et al., report that for practical purposes the infinite-conductivity solution obtained by Gringarten, et al.,[55] can be used if $F_{cD} \geq 500$.

The most important point to note in Fig. 13 is that for small values of time the shape of the curves for various F_{cD} do not possess distinctive characteristics. Furthermore, there is a wide separation between the various curves at small times. Thus fracture capacity strongly influences pressure behavior at early times. However, this separation diminishes as t_{Dx_f} increases.

Figure 13 may be used for type curve matching to estimate k, x_f and F_{cD}. The pressure match should provide an estimate of the formation permeability, k, the time match for the value of the fracture half-length, x_f, and the appropriate F_{cD} curve for the value of fracture flow capacity, $k_f w$. At the present time no method is available to estimate k_f and w separately. From a practical viewpoint, however, the shapes of the curves are so similar that the probability of matching data with an erroneous value of F_{cD} is high. If type curve matching is attempted, care and diligence are needed. If the formation flow capacity is known, the matching procedure is simplified and more importantly becomes more reliable since values of p_{wD} may be computed prior to matching. In this event the tracing paper needs to be moved in only the horizontal direction during the matching process. Matching, even along these lines, can be difficult. Agarwal, et al.[69], strongly recommend that pre-fracture pressure data be measured whenever possible. In extreme cases a numerical model may be needed to match field data adequately. The need of the hour is to be able to devise a procedure for analyzing field data conveniently and correctly.

The results in Fig. 13 also agree with the speculation by some that fracture capacity can be one potential reason leading to apparent short vertical fracture lengths that are calculated from well tests when the solutions of Gringarten, et al.[55], are used. For example, data obtained for $F_{cD} = 2$ can be matched with the similar parameter value $F_{cD} = 500$ by moving to the right on the time scale. If this is done, an erroneous value of t_{Dx_f} would be obtained, which in turn would result in a low estimate of x_f.

Figure 14 presents the data shown in Fig. 13 on a semi-log graph (p_{wD} vs. log t_{Dx_f}). The straight line shown in Fig. 14 corresponds to the slope of the straight line that would be obtained for plane radial flow. All of the curves in Fig. 14 show a much shallower slope than 1.151 per log cycle. Since the time range of $10^{-5} \leq t_{Dx_f} \leq 1$ covers most of the times for which testing would be carried out in low permeability reservoirs, it is doubtful that the radial flow response will be seen. If data were graphed on semi-log graph paper to compute permeability from an apparent straight line an optimistic estimate of formation permeability would result. The error in the estimate would depend on the producing time.

Actually, for data beyond $t_{Dx_f} \geq 1$, a semi-log straight line with the proper slope eventually results (see Fig. 15). This straight line may be used to determine formation permeability. For $F_{cD} = 10^{-1}$ the semi-log straight line begins at $t_{Dx_f} \approx 1$. The time for onset of pseudo-radial flow is dependent on F_{cD} and increases as F_{cD} increases. From the earlier discussion this result should be expected. Cinco, et al.[68], and Ramey, et al.[51], point out that for times $t_{Dx_f} \geq 5$ pseudo-radial flow prevails for all values of F_{cD} of interest. (Note that this assumes no boundary effects.)

Figure 15 also demonstrates the behavior of the uniform-flux fracture with respect to F_{cD}. For small times ($t_{Dx_f} \leq 0.16$) the dimensionless fracture capacity of the uniform-flux fracture is 500; for times greater than the time for the onset of pseudo-radial flow ($t_{Dx_f} \geq 2$) it follows the curve corresponding to $F_{cD} \approx 4.4$. For intermediate times, the uniform-flux solution changes from $F_{cD} = 500$ to $F_{cD} = 4.4$. Thus the uniform-flux solution is essentially a variable fracture capacity solution.

Agarwal, et al.[69], suggest that a graph of p_{wD} vs. $\sqrt{t_{Dx_f}}$ is also useful in analyzing data when fracture capacity is important. Figure 16 presents a replot of the data shown in Fig. 13 along these lines. On a graph such as Fig. 16 early time data for the infinite-conductivity or infinite-capacity fracture will fall on a straight line passing through the origin with a slope equal to $\sqrt{\pi}$ [see Eq. (5)]. As F_{cD} decreases straight lines with the same slope can be seen, however they do not pass through the origin. Agarwal, et al.[69], have empirically correlated the p_{wD} intercept as a function of F_{cD} (see Fig. 9 of Ref. 69). This correlation may be used to determine F_{cD}. But it should be noted that as F_{cD} decreases then the length of the straight line segment decreases--and disappears for $F_{cD} = 1$.

For practical applications the difficulties involved in using this graph are essentially the same as those for the log-log or semi-log graphs; that is, that the shape of the curves are not distinct enough to permit any identification of the correct fracture solution or the appropriate straight line.

Although it will not be considered here in detail, some information is available on the effect of the closed outer boundary. Ramey, et al.[51], report that for values of $F_{cD} \geq 300$

solutions obtained were very close to those of Gringarten, et al.[55], for all values of x_e/x_f. Note that the Ramey, et al., criterion for specifying a finite-capacity fracture to be an infinite-conductivity fracture is somewhat different from the Agarwal, et al.[69], value of 500. This difference is mainly due to the precision used in comparing the solutions and should not be construed as an error on the part of either of the two research groups.

Finally it should be noted that there are a number of other factors which can give an appearance of a small fracture capacity. These include the effect of producing time on build-up data, non-Darcy flow[70,71,72], confining pressure[69], and damage, to name only a few. Much work remains to be done, particularly in improving the ability to analyze field data. Let us now return to the consideration of other aspects of fractured well behavior.

The Skin Effect in Fractured Wells (Uniform-Flux or Infinite-Conductivity)

In many instances, particularly in injection wells, there is skin damage associated with the fractured systems. Interpretation of data from these wells can be difficult. A typical pressure trace on log-log graph paper is shown as Curve A, in Figure 17. If pressure data, plotted on log-log graph paper, approach the half slope line from above one may be reasonably certain that skin damage exists. If the skin effect is fairly large, then no one-half slope line may be evident (Curve B). In that event it would be difficult to identify a vertical fracture using log-log graph paper. This flat data on log-log paper, however, will graph as a straight line on Cartesian graph paper (Δp or p_{wf} is plotted versus $\sqrt{t}$). It should also be noted that it is possible to mistake the skin effect for a finite-capacity fracture.

The basis for the above discussion is evident if the skin effect is included in the solutions for fractured well behavior. Analogous to the procedure for radial flow, the solution for the producing pressure at small times for a fractured well with a skin effect may be written as:

$$p_{wD}(t_{Dx_f}) = \sqrt{\pi t_{Dx_f}} + s \qquad (25)$$

where s is the skin factor. Equation (25) indicates that for small times the first term would be small and thus the one-half slope line would be obscured. Therefore, a graph of $(p_i - p_{wf})$ vs. t on log-log coordinate paper would be flat. However, a graph of p_{wf} vs. $\sqrt{t}$ would be a straight line on Cartesian graph paper.

The use of log-log and Cartesian graphs to identify a resistance to flow in a fractured well has been discussed only recently[73], though Ramey[35] makes passing reference to this possibility.

This visualization of the skin effect makes no mention of the exact nature of the skin except that it is an infinitesimally thin steady state resistance to flow. The impediment may exist within the fracture, on the fracture surface or extend some distance into the formation. It is again emphasized that Eq. (25) is not intended to describe pressure behavior of wells intersecting finite flow capacity fractures.

Wellbore Storage in Fractured Wells

As fractured wells normally have high productive capacities wellbore storage should not be important. However, Ramey[35] has shown that wellbore storage effects can be important in some cases. Theoretical studies of the wellbore storage effect in fractured wells have been presented by Wattenbarger and Ramey[74], and Ramey and Gringarten[75] (for the infinite-conductivity vertically fractured well), and by Raghavan[73] (for the uniform-flux case).

Figure 18 is a log-log graph depicting the pressure behavior of a well producing via a uniform-flux fracture which is controlled at early times by wellbore storage. The well is assumed to be located in an infinite reservoir. The parameter of interest in Fig. 18 is the wellbore storage constant defined by the relation:

$$C_{Dx_f} = \frac{c}{2\pi\phi c_t h x_f^2} \qquad (26)$$

where c is the unit storage factor and is identical to that defined in Ref. 34. The $C_{Dx_f} = 0$ curve corresponds to a fractured well with no wellbore storage (uniform flux) in an infinite reservoir.[55] For large values of C_{Dx_f} a line of unit slope similar to that for unfractured systems is obtained.* However for small values of C_{Dx_f} no unit slope line is evident for times of interest. (Actually a unit slope line does exist for dimensionless times smaller than that considered here.) As time increases, all curves become asymptotic to the $C_{Dx_f} = 0$ line. Figure 18 also demonstrates that if wellbore storage is large then the presence of the fracture would be obscured. Then the fracture would have to be detected by comparing storage volume calculations with wellbore completion data.[35] All of the above observations are also applicable to the infinite-conductivity case.[74,75]

In practical applications, the most important point to be noted about Figure 18 is that a transition region exists between the unit slope and the half slope lines. In some cases when field data are plotted on log-log coordinates no transition is evident. In such cases it is probable that the value of Δp may be in error. A detailed

*A unit slope line on log-log graph implies that wellbore storage is dominant. Data during the unit slope period cannot be used to estimate formation properties.

discussion of this aspect may be found in Refs. 67 and 73.

Preliminary results on the effect of fracture capacity on wellbore storage have been reported by Cinco, et al.[68] They pointed out that for small times, $t_{Dx_f} \leq 10^{-5}$ the porosity and compressibility of the fracture system also influence the pressure behavior. They demonstrated that for small times two dimensionless groups control wellbore pressures. These dimensionless groups are defined as follows:

$$A = \frac{w\phi_f c_{ft}}{\pi x_f \phi c_t} \tag{27}$$

and

$$B = \frac{k_f \phi c_t}{k \phi_f c_{ft}} \tag{28}$$

where ϕ_f and c_{ft} are the porosity and effective compressibility of the fracture, respectively. Note that the product AB is equal to F_{cD}/π and $A \equiv C_{Dx_f}$ since $c = (2\phi_f c_{ft} h x_f w)$. Figure 19 is a graph of p_{wD} vs t_{Dx_f} for a finite-capacity fracture with $A = 10^{-1}$ and $B = 10^{7}$. Also shown are the results obtained by Ramey and Gringarten[75] for $C_{Dx_f} = 10^{-1}$. The results are in good agreement. More work needs to be done in this area of pressure analysis.

Wellbore Storage and Skin Effect in a Vertically-Fractured Well (Uniform-Flux)

Figure 20 is a log-log graph of p_{wD} vs. t_{Dx_f} for a vertically fractured well (uniform-flux) including the wellbore storage and skin effects. All lines start out with a line of unit slope and for each value of C_{Dx_f} are independent of s for small times. Thus, at early times fractured well behavior is similar to that of an unfractured well (see Agarwal, et al.[34]).

Figure 20 demonstrates several interesting and instructive features. For example, if the wellbore storage period is followed by a half slope period and data do not approach the half slope line from above, then damage is negligible. The solutions shown here also indicate that if wellbore storage and skin are negligible, then the half slope line will be observed. Raghavan[73] has discussed application of the theoretical results shown in Fig. 20 to field data.

A Horizontally-Fractured Well in an Infinite Reservoir

An analytical solution[76] for a well with a single horizontal, uniform-flux fracture located at the center of the formation with impermeable upper and lower boundaries in an infinite reservoir was presented in 1973. The main objective of this work was to determine if the early time pressure behavior of a horizontally fractured well is distinctly different from that of either a vertical fracture, or plane radial flow. The results obtained in Ref. 76 were used to prepare the curves shown in Fig. 21 where the dimensionless wellbore pressure drop per unit of dimensionless reservoir thickness is graphed as a function of dimensionless time. The dimensionless thickness is the parameter of interest. For purposes of this discussion the dimensionless time and dimensionless thickness groups are defined, respectively, as follows:

$$t_{Dr_f} = \frac{0.000264kt}{\phi c_t \mu r_f^2} \tag{29}$$

$$h_{Dr_f} = \frac{h}{r_f}\sqrt{\frac{k}{k_z}} \tag{30}$$

In Eqs. (29) and (30) r_f is the fracture radius, k is the horizontal permeability, and k_z is the is the vertical permeability (see inset Fig. 21).

Fig. 22 is a semi-log graph of the same data presented in Fig. 21 in terms of p_{wD} vs. t_{Dr_f}. As shown in Fig. 22, at long times the dimensionless pressure drop is a linear function of the logarithm of time with a characteristic slope of $1.151/\log\vee$. Thus a semi-log graph of Δp or p_{w_f} vs. t may be used to estimate horizontal permeability if the test is run for a long enough period. Fig. 21 is easy to use for type-curve matching purposes because all curves have in common an initial one-half slope straight line, corresponding to early time vertical linear flow (instead of horizontal linear flow, as for the vertical fracture case). Also, a single curve is obtained for $h_{Dr_f} \geq 100$. For practical purposes this curve represents the situation in which fluid is withdrawn via a single plane horizontal fracture in a reservoir of infinite extent in all directions.

The curves corresponding to $h_{Dr_f} > 3$ in Fig. 22, and $h_{Dr_f} < 1$ in Fig. 21 have shapes which are different from those of the vertical fracture cases (see Fig. 3 and Fig. 5). Furthermore if $h_{Dr_f} < 0.7$ then there is an increase in slope from one-half towards unity that has no counterpart in the vertical fracture case. Thus it may be possible to distinguish between the two types of fracture from a well test. If $1 \leq h_{Dr_f} \leq 3$, however, there is a possibility that horizontal and vertical fracture behavior will be confused: The line for a uniform-flux vertical fracture in an infinite reservoir was found to match the horizontal fracture case of h_{Dr_f} of

about 2.4 in Fig. 21 reasonably well. However, the dimensionless pressure scales are basically different in nature and in magnitude, and it is likely that results would appear questionable, should the wrong fracture type be selected.

A few expressions useful in well test analysis are summarized from Ref. 76. The initial vertical linear flow period (one-half slope on log-log coordinates) is represented by:

$$\frac{p_{wD}}{h_{Dr_f}} = 2\sqrt{\frac{t_{Dr_f}}{\pi}} \tag{31}$$

which may be rearranged to the dimensional form:

$$\frac{(k_z)^{1/2} r_f^2 (p_i - p_{wf})}{141.2qB\mu} = 2\left(\frac{0.000264}{\pi\phi\mu c_t}\right)^{1/2} \tag{32}$$

At long times, the flow is the same as that created by an unfractured well, with an additional pressure drop which is referred to in the petroleum engineering literature as the pseudo-skin effect. A long time approximation for $h_{Dr_f} < 1$ can be written as:

$$p_i - p_{wf} = \frac{70.6qB\mu}{kh}\left(\ln\frac{0.000264kt}{\phi\mu c_t r_f^2} + 1.80907 + \frac{h^2k}{6r_f^2k_z}\right) \tag{33}$$

The proper time limits for the application of either Eqs. (32) or (33) depend upon h_{Dr_f}. The pseudo-skin factor which is the quantitative measure of the pseudo-skin effect during the pseudo-radial flow period may be obtained from Eq. (33) by subtracting the pressure drop due to an unfractured well. Further details are given in Ref. 76. Application of the results presented here may be found in Ref. 77.

Wells Intercepting an Inclined Fracture in an Infinite Reservoir

The dimensionless wellbore pressure drop for an inclined fracture is shown in Fig. 23 for several values of the inclination of the fracture, θ_w,[78] (see Fig. 24 for a description of the geometry of the system). The results shown here are probably most useful in analyzing pressure behavior at fractured wells in steeply dipping reservoirs. The fracture conductivity is assumed to be infinite and the fracture extends over the entire thickness of the formation. The symbol h_{Dx_f} represents the dimensionless thickness of the formation and is defined by the expression:

$$h_{Dx_f} = \frac{h}{x_f}\sqrt{\frac{k}{k_z}} \tag{34}$$

For large values of dimensionless time, t_{Dx_f}, the dimensionless wellbore pressure drop, p_{wD}, is a linear function of the logarithm of dimensionless time with a characteristic slope equal to 1.151. Thus long time data can be analyzed using conventional semi-logarithmic techniques. The time for the start of the pseudo-radial flow period is a function of θ_w and h_{Dx_f}. For the case shown here pseudo-radial flow prevails for dimensionless times, $t_{Dx_f} \geq 8$. Cinco, et al.[78], have also mentioned that at early times linear flow (perpendicular to the fracture surface) prevails. Thus the transient flow behavior of a well intercepting an inclined fracture in an infinite reservoir includes a linear flow period, a transition region, and a pseudo-radial flow period. Qualitatively the above description also holds for other values of h_{Dx_f}. The duration of the various flow regimes depends on h_{Dx_f} and θ_w. It can also be seen that the dimensionless wellbore pressure drop for an inclined fracture is always less than that for a vertical fracture. As the inclination of the fracture, θ_w, increases, the dimensionless pressure drops are smaller. At long times (pseudo-radial flow) the difference in the pressure drop between the inclined fracture case and the vertical fracture case becomes constant. This difference can be handled as a pseudo-skin factor, s, defined by[78]

$$s = p_{wD}(t_{Dx_f}, h_{Dx_f}, \theta_w) - p_{wD}(t_{Dx_f}; \theta_w = 0) \tag{35}$$

The pseudo-skin factor is a function of θ_w and h_{Dx_f}. Figure 25 presents the pseudo-skin factor as a function of dimensionless thickness, h_{Dx_f}, and angle of inclination, θ_w. If θ_w and h_{Dx_f} are small, then s is small. As h_{Dx_f} increases the pseudo-skin factor, s, increases. This implies that well productivity is affected considerably by the angle of inclination, θ_w, when the fracture half-length, x_f, is much smaller than the thickness, h.

A Limited Entry Vertical Fracture in an Infinite Reservoir

In this section we shall briefly discuss the effect of limited entry on the pressure behavior of vertically-fractured wells. For brevity only the uniform-flux case will be considered. Here we shall use the term "limited entry" to describe situations where the vertical fracture height, h_f, is less than the formation thickness, h.

Figure 26 is a graph of p_{wD} vs. t_{Dx_f} for a uniform-flux fracture located at the center of the formation.[79] Fig. 27 presents the details regarding the geometry of the system. The dimensionless thickness, h_{Dx_f}, is 5. The term b, which is the ratio of the fracture height, h_f, to the thickness h, is the parameter of interest. In this paper this ratio will be described as the entry ratio. The case b = 1 corresponds to the complete entry (or $h_{Dx_f} = \infty$) case--the Gringarten, et al., solution.[55] As can be seen from Fig. 26, all straight lines start out with a slope of one-half which corresponds to the linear flow period. (For b = 0.1 this period occurs earlier and is not shown.) The duration of the linear flow period is a function of the entry ratio and increases as the entry ratio increases. This is to be expected since larger values of b correspond to a greater fracture area. Following the linear flow period there is a transition region and finally there is a pseudo-radial flow period. It can be shown that pressure data in this region will graph as a straight line with a slope of 1.151 per log cycle on semi-log paper.[79] As shown in Fig. 26 the start of the semi-log straight line for b < 1 occurs much later than that for b = 1. Thus if conventional semi-log methods are used to analyze pressure data this observation indicates that tests should be run for a much longer period than for the complete entry case. In some instances all of the data obtained during a test may correspond only to times prior to the onset of pseudo-radial flow.

The displacement of the curves shown in Fig. 26 is a result of the additional pressure drop caused by the convergence of flow into the open interval. The magnitude of this additional pressure drop changes with time until the pseudo-radial flow period. During pseudo-radial flow the magnitude of this additional pressure drop is constant. This stabilized additional pressure drop, which is a result of the fracture height being less than the formation thickness, can be quantitatively described by the pseudo-skin factor. It is a function of h_{Dx_f} and b. Pseudo-skin factors for systems of interest are presented in Ref. 79.

Figure 28 is a log-log graph of the same data shown in Fig. 26. However, in this graph the ordinate is the product of the dimensionless pressure drop and the entry ratio. Plotting the results in this manner results in the curves for entry ratios, b < 1, merging into the b = 1 curve at early times. Therefore all curves start out from the one-half slope line corresponding to b = 1. As the vertical component of flow begins to affect pressure behavior the limited entry curves leave the curve for b = 1. Ultimately pseudo-radial flow develops and the pressure drop is a linear function of the logarithm of flow time.

From a practical point of view, however, graphs such as Fig. 29 are more useful than those considered so far. Fig. 29 is similar to Fig. 28 except that in this case the dimensionless fracture height, h_{fD}, is the parameter of interest. This dimensionless fracture height is defined as

$$h_{fD} = \frac{h_f}{x_f}\sqrt{\frac{k}{k_z}} \tag{36}$$

The advantage of this procedure is that it gives more order to the graph. For example, in this instance all curves merge at early times into the complete entry curve just as for the case shown in Fig. 28. But Fig. 29 also permits display of data for several values of b and h_{fD} on the same graph without expanding the scale. This may be more clearly seen in Fig. 30 where the dimensionless pressure drop for $h_{fD} = 5$ and two values of b are presented. The first deviation from the b = 1 curve is independent of b and depends only on h_{fD}. After a period of transition, the effect of b can be seen. Finally there is a pseudo-radial flow period corresponding to the semi-log straight line. The beginning of the pseudo-radial flow period is a function of h_{Dx_f} (or h_{fD} and b). Figure 29 may be used to obtain system parameters. If the test is run for a long enough period then the permeability-thickness product, kh, the fracture half-length, x_f, the vertical permeability, k_z, and the entry ratio, b, can be determined by type curve matching. This, of course, assumes that x_e/x_f is large. Further details may be found in Ref. 79. Type curves for other cases such as the pressure behavior for a limited entry infinite-conductivity vertical fracture are also presented in Ref. 79.

From the above discussion it can be concluded that as h_{Dx_f} or h_{fD} increases, that is, as stratification becomes more severe, the pressure response for the limited entry fracture is delayed in time. Furthermore, for any dimensionless time beyond the linear flow period the dimensionless pressure drop is higher for larger values of h_{fD} or h_D. Thus, in terms of real variables it can be concluded that as the vertical permeability decreases the pressure drops are larger and the pressure response is slower.

Raghavan, et al.[79], also examined the effect of fracture location within the producing interval. After examining various fracture locations within the producing interval, Raghavan, et al., concluded that the productivity for a given set of conditions decreases as the fracture position departs from the center of the producing interval.

Raghavan, et al.[79], also delineated conditions under which it would be possible to recognize that the fracture height is less than the formation thickness. They concluded that it would be difficult to identify this condition from pressure versus time data if $h_{fD} > 5$. They also found that the position of the fracture within the producing interval was unimportant if $b > 0.7$.

Vertically Fractured Wells Producing at Constant Wellbore Pressure

As mentioned earlier, the constant terminal pressure case has not attracted attention--mainly because it is not readily apparent how this condition might affect pressure build-up after the well is shut in at the sand face. Nevertheless, results for this wellbore condition are useful. If the formation permeability is low, then it may not be possible to hold the rate constant for long periods of time.

If the well is produced at a constant rate then the wellbore pressure changes with time. However, if the pressure is held constant then the rate would vary as a function of time. Locke and Sawyer[80] have examined the change in rate versus time for an infinite-conductivity vertical fracture in an infinite reservoir and in a closed square drainage region. The results are shown in Fig. 31. Here the reciprocal dimensionless rate, $1/q_D$, has been graphed vs. dimensionless time, t_{Dx_f}, and x_e/x_f is the parameter of interest. The reciprocal dimensionless rate for the constant terminal pressure case is analogous to the dimensionless wellbore pressure drop, p_{wD}, for the constant terminal rate case and is defined as

$$\frac{1}{q_D} = \frac{kh\Delta p}{141.2qB\mu} \tag{37}$$

Here $\Delta p = p_i - p_{wf}$ = a constant, and all other symbols have the same meaning as before.

At small values of time it can be shown that the following relationship holds

$$\frac{1}{q_D} = \frac{\pi^{3/2}}{2}\sqrt{t_{Dx_f}} \tag{38}$$

Thus if we graph 1/q vs. t on log-log paper one should obtain a straight line with a slope equal to 0.5. This observation can be used to identify a fractured well producing at a constant wellbore pressure. Figure 31 can be examined along the same lines as Fig. 3; however, since the characteristics of the $1/q_D$ vs. t_{Dx_f} curves are similar to those of p_{wD} vs. t_{Dx_f} for the constant rate case, we will not examine these results in detail.

The effect of fracture capacity on the dimensionless rate has also been investigated. Figure 32 presents $1/q_D$ vs. t_{Dx_f} for a finite capacity vertical fracture in an infinite reservoir.[69] The parameter is F_{cD}. As in the constant rate case, the curves for various values of F_{cD} do not possess distinctive characteristics. At early times there is a wide separation between different F_{cD} curves. As t_{Dx_f} increases, the separation between the curves decreases. Agarwal, et al.[69], have also shown that if $F_{cD} \geq 500$, then the finite capacity curves merge into the infinite-conductivity curves of Locke and Sawyer.

Figure 32 may be used to estimate formation permeability, k, fracture half-length, x_f, and fracture capacity, k_fw, by type curve matching. If the fracture capacity can be considered to be infinite then the curves of Locke and Sawyer may be used. The procedure is essentially the same as that for the constant rate curves. The only difference is that in the present instance the ordinate is 1/q rather than Δp.

It is obvious that care and diligence should be exercised in analyzing data by the type curve method (or any other approach) if the fracture capacity is important. The curves shown in Fig. 32 have no distinct characteristics and the probability of obtaining a match with the wrong value of F_{cD} is high. If an estimate of the formation flow capacity is available then the type curve matching procedure is simplified and would be more reliable. Since various aspects of analyzing data for finite-capacity vertically fractured wells have been discussed already at length, further discussion is not warranted here.

Pressure Transient Analysis for Steam Wells

Virtually all of the results discussed so far are strictly applicable to fluids of constant compressibility and viscosity. The theoretical justification for the application of these solutions to the analysis of gas well test data is based on the work of Aronofsky and Jenkins[81] and Al-Hussainy, Ramey and Crawford.[82] In applying these results to the flow of steam (gas) only, the definitions of the dimensionless pressure drop and dimensionless time need to be modified. For application to steam (gas) wells the right hand side of the definition of dimensionless pressure drop, p_{wD}, is modified as follows:

$$p_{wD} = \frac{19.87 \times 10^{-6}\ kh\ T_{sc}}{p_{sc}qT}\left[m(p_i) - m(p_{wf})\right] \tag{39}$$

where q is the flow rate, measured in thousands of cubic feet per day, and T is the reservoir temperature in °R. The subscript, sc, refers to standard conditions of pressure and temperature, and m(p) is the pseudo pressure function defined

by:[82]

$$m(p) = 2\int_{p_b}^{p} \frac{p'}{\mu Z}\, dp' \qquad (40)^*$$

Here p_b refers to a base pressure and Z is the compressibility factor. The viscosity and compressibility terms in the definition of dimensionless time should be evaluated at the initial pressure, p_i. Thus the equation for the definition of dimensionless time, t_{Dx_f}, is

$$t_{Dx_f} = \frac{0.000264kt}{\phi c_{ti}\mu_i x_f^2} \qquad (41)$$

Other expressions for dimensionless time should be modified appropriately.

Shut-in Pressure Behavior of Vertically Fractured Wells

As mentioned earlier, Russell and Truitt[54] were the first to present detailed information on the transient pressure behavior of a vertically fractured well. They also analyzed a limited number of pressure build-up cases and found that the straight-line slope on a Horner[16] build-up graph required significant correction as the fracture length increased. They also recommended the Muskat[19] semi-log graph for estimation of static formation pressure.

In 1968, Clark[60] suggested a method for calculating fracture length using the results of the Russell and Truitt study. In 1972, Raghavan, Cady and Ramey[86] further extended the Russell and Truitt study by examining an extreme variety of semi-log build-up methods (Horner,[16] Miller-Dyes-Hutchinson[17] and Muskat[19]). Raghavan, et al.[86], and Raghavan and Hadinoto[63] have pointed out that the determination of the permeability-thickness product by semi-log build-up methods is a trial-and-error process, as the slope of the build-up curve is influenced by both the fracture penetration ratio (ratio of drainage length to fracture length) and the formation permeability. Also in Ref 86, the durations of producing time and shut-in time were found to have significant influence on pressure behavior and the authors state that care should be taken to insure that data are selected properly to estimate formation properties and fracture length.

Recently, the type curve matching technique has been proposed to analyze pressure data in fractured wells.[55] This method involves plotting the pressure change versus shut-in time [$(p_{ws} - p_{wf,s})$ vs. Δt] on log-log graph paper. Here p_{ws} is the shut-in pressure, $p_{wf,s}$ is the pressure at the time of shut-in, and Δt is the shut-in time. The principal advantage of the type curve approach is that the trial and error procedure inherent in the semi-log methods can be avoided. The log-log method is also useful to insure that proper straight lines are chosen when data are analyzed by semi-log techniques.

Here both the type curve and the conventional methods will be presented. The advantages and disadvantages of both of these methods will be discussed.

The Type Curve Approach for the Analysis of Build-up Data

Recent papers by Gringarten, et al.[55,77], have demonstrated the usefulness of the type curve method to interpret pressure data obtained at fractured wells. The basis for the type curve approach for analyzing build-up data is identical to that for draw-down.

Pressure Build-up Equations for Type Curve Analysis. Shut-in pressures for a fractured well producing at a constant rate, q, for a time, t, can be determined by superimposing an injection well starting at time, t, with the injection rate being equal to the production rate prior to shut-in. This results in a zero rate for times $t + \Delta t$. Using the draw-down equation and applying the above principle the basic equation for the analysis of build-up data by the type curve method is given by:[34,86]

$$\tilde{p}_{Ds} = \frac{kh}{141.2qB\mu}\,[p_{ws}(t+\Delta t) - p_{wf}(t)] =$$

$$p_{wD}(t_{Dx_f}, x_e/x_f) - p_{wD}[(t+\Delta t)_{Dx_f}, x_e/x_f]$$

$$+ p_{wD}(\Delta t_{Dx_f}, x_e/x_f) \qquad (42)$$

where

$$t_{Dx_f} = \frac{0.000264kt}{\phi c_t \mu x_f^2} \qquad (2)$$

*The pseudo pressure function is essentially a transformation which accounts for the variation in fluid properties. This transformation is known as the Kirchoff Transformation[83] in the heat conduction literature, as the Leibenzon Transformation in the Russian literature, and as the Matrix Flux Potential in the soil mechanics literature. For hydrocarbon gases at low pressures (<3000 psi) it has been observed that the product (μZ) is essentially constant. Thus in this region $m(p) \propto p^2$. In the high pressure region ($p > 3000$ psi) it can be shown that ($p/\mu Z$) is reasonably constant. Thus in the high pressure range $m(p) \propto p$.

and $$\Delta t_{Dx_f} = \frac{0.000264k\Delta t}{\phi c_t \mu x_f^2} \quad (43)$$

In Eqs. (42) and (43), t is the producing time and Δt is the shut-in time. If now $(t + \Delta t) \simeq t$, we then have:

$$\frac{kh}{141.2qB\mu}\,[p_{ws}(t+\Delta t) - p_{wf}(t)] = p_{wD}\,(\Delta t_{Dx_f}, x_e/x_f) \quad (44)$$

Taking logarithms of both sides of Eqs. (44) and (43), respectively, we obtain:

$$\log\,[\,p_{wD}\,(\Delta t_{Dx_f}, x_e/x_f)\,] \quad (45)$$

$$= \log\frac{kh}{141.2qB\mu} + \log[p_{ws}(t+\Delta t) - p_{wf}(t)]$$

and

$$\log \Delta t_{Dx_f} = \log\frac{0.000264k}{\phi c_t \mu x_f^2} + \log \Delta t \quad (46)$$

If actual build-up data are plotted as the logarithm of the absolute difference between flowing pressure at the start of build-up and pressure after the change vs. the logarithm of shut-in time then the actual field data should be similar to a log-log graph on which p_{wD} vs. t_{Dx_f} have been plotted. The difference between the two graphs is only a linear translation of both coordinates, represented by the first terms on the right-hand sides of Eqs. (45) and (46). If a proper match is obtained, then the formation permeability and fracture length can be estimated from the type curve match. Both uniform-flux and infinite-conductivity fractures can be analyzed by this approach. Though the above derivation has specifically assumed a vertically fractured well in a square drainage region it is applicable to any of the systems considered here.

The importance of Eq. (44) deserves emphasis. Equation (44) states that if $t \gg \Delta t$, that is, the duration of the shut-in period is much smaller than the producing period prior to shut-in, then the pressure changes which form the build-up trace after the well is shut in are identical to the draw-down trace. This then implies that all of the characteristics discussed in the section on pressure draw-down behavior for the various systems examined here are applicable to the respective build-up case.

The Semi-Log Approach: An Infinite-Conductivity Vertically Fractured Well in a Closed Square

In the following we shall take the approach suggested by Raghavan, et al.[86], and explore the characteristics of common build-up methods of analysis along the lines of the pressure build-up theory suggested by Ramey and Cobb.[18] Our attention will be restricted to the Miller, Dyes, and Hutchinson and Horner methods.

Pressure Build-up Equations for Semi-Log Analysis. Shut-in pressures for a fractured well producing at a constant rate, q, for a time, t, can be determined by superimposing an injection well starting at time t; the injection rate being equal to the production rate before shut-in. This then results in a zero production rate after time t, and thus at the well location we have:[18]

$$p_{Ds} = \frac{kh}{141.2qB\mu}\,(p_i - p_{ws}) = p_{wD}[(t+\Delta t)_{Dx_f}, x_e/x_f] - p_{wD}(\Delta t_{Dx_f}, x_e/x_f) \quad (47)$$

Equation (47) serves as the basis for the Horner analysis.

For a well located in a closed reservoir the Miller-Dyes-Hutchinson graph requires the pressure difference $(\bar{p} - p_{ws})$. This difference can be determined from the following:

$$\bar{p}_{Ds} = \frac{kh}{141.2qB\mu}\,(\bar{p} - p_{ws}) = p_{wD}[(t+\Delta t)_{Dx_f}, x_e/x_f] - p_{wD}[\Delta t_{Dx_f}, x_e/x_f] - 2\pi t_{DA} \quad (48)$$

The volumetric average pressure, $\bar{p}$, is of interest for two reasons. The average pressure in the reservoir is a direct reflection of the quantity of fluids in place and is necessary to perform material balance calculations. Also, in a closed, bounded system the average pressure, $\bar{p}$, is the limit of the shut-in pressure, p_{ws}, as build-up time approaches infinity.

The Miller-Dyes-Hutchinson Method. This method requires that build-up pressures be plotted as a function of the logarithm of shut-in time. Perrine[87] first presented a dimensionless form of the Miller-Dyes-Hutchinson build-up curve in which the pressure difference was $(\bar{p} - p_{ws})$. For unfractured wells in closed drainage systems, this

graph offers a direct and simple extrapolation from shut-in pressures, p_{ws}, to the fully static pressure, $\bar{p}$.

Figure 33 presents a Miller-Dyes-Hutchinson graph for a vertically fractured well, for the fracture penetration ratio, $x_e/x_f = 10$. The producing time prior to shut-in is the parameter of interest. As in the unfractured well case, a single curve results for pseudo-steady state production prior to shut-in.

In the conventional Miller-Dyes-Hutchinson graph for an unfractured well, a linear portion is evident for early shut-in times. This linear portion possesses a slope of 1.151 per log cycle and is inversely proportional to the permeability-thickness product. But Fig. 33 exhibits some surprising differences from unfractured well behavior. The maximum slope to be found on any of the curves on Fig. 33 is 0.90--much less than the expected value of 1.151. Furthermore, there are no well-defined straight lines evident, and the maximum slope for each producing time decreases as producing time decreases.

Figure 34 presents build-up curves (pseudo-steady production) for all fracture penetration values x_e/x_f, discussed in Ref. 86. The build-up behavior for an unfractured well is also shown for purposes of comparison. The maximum slope of the build-up curves decreases as fracture penetration ratio decreases. It is also evident that the maximum slope is significantly less than that for the unfractured case for all fracture penetration ratios.

Russell and Truitt[54] described a similar effect for the Horner[16] graph for vertically-fractured well data. This will be discussed in a following section. But Russell and Truitt did point out clearly that the reduced slope for a Horner graph could lead an analyst to compute a permeability-thickness value which could be too large. They pointed out that this could explain the apparent opening of "new sand" after fracturing.

At this stage is should be emphasized that the slope of a pressure build-up graph is not necessarily related to the slope of a draw-down graph. A straight line with the correct slope may appear in a draw-down test, but not on any of the conventional build-up graphs.

As pointed out by Raghavan, et al.[86], Figs. 33 and 34 raise serious questions concerning appropriate interpretation measures for use with Miller-Dyes-Hutchinson graphs of vertically-fractured well data. In order to apply the Miller-Dyes-Hutchinson method to fractured well build-up data Raghavan, et al., followed the suggestion Russell and Truitt had proposed for the Horner build-up graph. Russell and Truitt had suggested that the maximum slope be read for the fractured well build-up data, and then the permeability corrected to the true value. Figure 35 presents the permeability-thickness correction factors for the Miller-Dyes-Hutchinson form of plotting for an infinite-conductivity vertical fracture in a closed square reservoir as a family of dashed lines (x_f/x_e rather than x_e/x_f is used here for convenience). The correction factor was obtained from graphs similar to Fig. 33 by dividing the actual maximum slope by 1.151. The solid line represents a similar correction factor for a Horner-type build-up graph, and will be discussed later. All of the Miller-Dyes-Hutchinson graph correction factors are considerably smaller than those for the Horner graph. This means that the apparent permeability-thickness found via the Miller-Dyes-Hutchinson graph could contain a much greater error than that from a Horner graph.

One appealing feature of the Miller-Dyes-Hutchinson graph is that knowledge of the producing time is not required to prepare the graph.[17,87] But it should be clear that this advantage is more apparent than real. It is necessary to know the producing time to be able to complete a Miller-Dyes-Hutchinson analysis properly. Production time would be required to enable selection of the proper line on Fig. 35 for permeability correction. This operation would require trial-and-error and the following procedure is recommended:

1. From Fig. 35 determine permeability using the pseudo-steady state line.
2. Calculate dimensionless producing time to check on the permeability correction factor.
3. Repeat the above procedure until the proper value of permeability is determined.

If producing times were long enough that pseudo-steady production could be assumed safely, the above procedure would be simplified.

The Horner Method. The Horner method requires a graph of the shut-in pressures versus the logarithm of $(t + \Delta t)/\Delta t$; where t represents the producing time prior to shut-in and Δt represents the shut-in time. The dimensionless Horner graph can be prepared by means of Eq. (47).

Figure 36 presents a Horner-type build-up graph for a vertically-fractured well with a fracture-penetration ratio of 10. Producing time prior to shut-in is shown as a parameter. As in the case of the Miller-Dyes-Hutchinson graph, no extensive linear portion is evident in the build-up for any of the curves of Fig. 36. But all curves do appear to approach a common value of maximum slope at long build-up times. The maximum slope is indicated by the dashed line in Fig. 36. Thus the duration of the production period does not appear to affect the maximum slope over the range of producing times considered. Inspection of graphs similar to Fig. 36, but for other fracture-penetration ratios, indicated that the maximum slope was affected by the fracture penetration ratio, but not by the producing time.

As mentioned earlier permeability-thickness correction factors have been prepared by Raghavan, et al., for the Horner graph. The results for all fracture-penetration ratios are shown as the heavy line on Fig. 35. Again, the correction

factors for a Horner-type graph are not functions of the duration of the production period. Thus a single line is shown on Fig. 35.

The Semi-Log Approach: An Infinite-Conductivity Vertically Fractured Well in a Constant Pressure Square

As the constant pressure square case is of interest in geothermal reservoir engineering we shall briefly examine the characteristics of the MDH and Horner methods for this case.

The Miller-Dyes-Hutchinson Method. Figure 37 presents a typical Miller-Dyes-Hutchinson graph for a vertically-fractured well in a constant pressure square. The producing time is the parameter of interest, and the fracture penetration ratio, $x_e/x_f = 15$. Equation (47) was used for preparing the results displayed in Fig. 37. The rationale for using Eq. (47) is discussed in Ref. 88. As in the case of the closed square drainage region the maximum slope for any of the curves in Fig. 37 is 0.965--much less than the expected value of 1.151. This maximum slope decreases as the producing time decreases and as x_e/x_f decreases.

An important difference between the results shown here and that shown in Fig. 33 must be noted. Unlike the closed case, the shut-in wellbore pressure eventually reaches p_i for all producing times. This is due to fluid recharge across the constant pressure boundary. Following the procedure suggested by Raghavan, et al.[86], correction factors can be prepared for this case also. These are shown in Fig. 38. They are a function of producing time for times prior to steady state and the fracture penetration ratio, x_e/x_f.

The Horner Method. Figure 39 presents a typical Horner graph for a vertically fractured well in a constant pressure square ($x_e/x_f = 15$). Unlike the closed square, the shut-in wellbore pressure reaches p_i for all producing times due to fluid recharge. Again as in the case of the Miller-Dyer-Hutchinson graph, no extensive linear portion is evident. Correction factors necessary to use the Horner method to estimate the permeability-thickness product are presented in Fig. 38. For this case the correction factors are a function of producing time for $x_e/x_f > 1.5$.

A comparison of the shape of the build-up curves shown in Fig. 39 with that for an unfractured well in a constant pressure square shows an important difference. Kumar and Ramey[88] showed that as producing time increases, the curves move to the right, and suggested that a system under recharge could be identified by this property. In the present instance, however, the curves move to the left for small producing times before moving back to the right. Thus, the suggestion of Kumar and Ramey to identify a constant pressure boundary system from pressure data is not applicable to vertically fractured wells unless producing times are very large.

The Uniform-Flux Fracture

Because of the obvious difficulties involved in graphical differentiation of the Horner and MDH graphs and associated problems involved in determining correct slopes, the uniform-flux case has not been examined in detail. Furthermore, the type curve approach is more advantageous to determine permeability-thickness and fracture length.

Pressure Build-up Analysis for Finite-Capacity Fractures

The basis for the type curve approach for finite-capacity fractures is identical to that discussed earlier. The draw-down type curves are applicable if the producing time, t_{Dx_f}, is much greater than the largest build-up time. This is a critical assumption and has not been explored fully in the literature. The effect of small producing time on build-up data is to give an appearance of a small fracture capacity. This point is demonstrated in Fig. 40 where the effect of producing time on build-up data for an infinite-conductivity vertical fracture is displayed.[89] The shape of the curves shown here is similar to those shown in Fig. 13. For example, the curve for $t_{Dx_f} = 10^{-1}$ may be matched with many of the F_{cD} curves shown in Fig. 13. This, in addition to the difficulties mentioned earlier, indicates that analysis of build-up data for fractured wells of finite-capacity is a formidable challenge.

To my knowledge the applicability of semi-log methods to the finite fracture capacity system has not been investigated in any detail. However, considering the results that have been obtained so far, work along these lines may not be fruitful.

Determination of Static or Average Reservoir Pressure

As mentioned in the section titled "Uses of Pressure Transient Data" one of the objectives of a pressure test is to determine average reservoir pressure for material balance calculations. For the case of an unfractured well this may be estimated by extrapolating the proper straight line on a Horner or MDH graph to an appropriate shut-in time. However, for the case of a vertically fractured well no simple method of extrapolation exists since a linear portion is not evident on the semi-log graphs. A thorough discussion of this aspect is beyond the scope of this paper. Pertinent information on this subject may be found in Refs. 54, 63 and 86.

Application to Injection Wells

The preceding discussion also forms the basis for the analysis of the shut-in pressure behavior in injection wells. For type curve analysis the ordinate of the log-log graph should be $(p_{wf,s} - p_{ws})$ rather than $(p_{ws} - p_{wf,s})$. If the

semi-log approach is used than the results presented in the section titled "The Semi-log Approach: An Infinite-Conductivity Vertically Fractured Well in a Constant Pressure Square" should be used.

Shut-in Pressure Behavior for other Fractured Systems

The shut-in pressure behavior for wells intercepting horizontal or inclined fractures has not been examined in the petroleum engineering literature. The principal reason for this appears to be the limited application of these solutions. It should be noted that the basis for analyzing data by the type curve approach is identical to that for a vertically-fractured well. Applicability of the semi-log techniques can also be investigated along the lines presented here.

Discussion and Summary

The main object of this survey is to document most of the recent work that has been conducted and which is available in the open literature (until Oct. 8, 1977). In doing so I have labored under one important restriction. I am aware that several research groups (universities and industrial laboratories) are actively working in this area. Thus, it is possible that some of the problems I have outlined here have been solved. Hopefully the results of any such investigations will be presented shortly.

Judging from the work that has been presented in the past few years, it is probable that new solutions which include the effects of non-Darcy flow (within the fracture, on the fracture surface, or both), wellbore storage and skin damage, and confining pressure will be discussed in the open literature shortly. Furthermore, it is clear that the effect of fracture height on the pressure behavior of finite flow capacity fractures will be available in the near future. Another problem which needs consideration is the effect of the variation in fracture capacity with distance on pressure response and deliverability. Undoubtedly solutions to most of these problems will be obtained via the digital computer.

The availability of solutions for specific cases, however, does not necessarily imply that it would be possible to analyze field data conveniently. In some instances consideration of one of the effects mentioned above would provide answers which are compatible with production performance. In other instances a combination of factors would have to be taken into account. In such an event simple graphical techniques would be inadequate and one would have to resort to parameter estimation techniques[90-94] (automatic history matching, inverse problem solving).

In summary, it appears that two avenues are available for us to increase our understanding of fractured well pressure behavior. The first is to investigate each parameter that affects pressure behavior individually and obtain the necessary solutions. This catalogue would be useful in identifying the potential characteristics for each specific circumstance. It would also be useful in reducing the range of variables that need to be considered in analyzing field data. The second avenue is to develop techniques whereby field data can be analyzed conveniently and at the same time insure that the description of the fracture and reservoir are realistic and compatible with production performance.

Nomenclature

A = drainage area, sq. ft.
A = constant defined by Eq. (27)
b = entry ratio
B = formation volume factor, RB/STB
B = constant defined by Eq. (28)
c = unit storage factor, RB/psi
c_{ft} = fracture compressibility, psi^{-1}
c_t = system compressibility, psi^{-1}
C_{Dx_f} = dimensionless storage constant based on fracture half-length
c_r = relative fracture capacity defined by Cinco, et al., dimensionless
F_{CD} = dimensionless fracture capacity defined by Agarwal, et al.
F'_{CD} = dimensionless fracture capacity defined by Prats
h = formation thickness, feet
h_f = fracture height, feet
h_{Dr_f} = dimensionless thickness based on fracture radius
h_{Dx_f} = dimensionless thickness based on fracture half-length
h_{fD} = dimensionless fracture height
h_w = edge length of an inclined fracture
h_{wD} = dimensionless edge length of an inclined fracture
k = horizontal permeability, md
k_f = fracture permeability, md
k_z = vertical permeability, md
$m(p)$ = real gas pseudo pressure, psi^2/cp
$\Delta[m(p)]$ = difference in real gas pseudo pressures, psi^2/cp
m = slope of semi-log straight line, psi/logν, psi^2/logν, or $psi^2/cp/\log\nu$
m' = slope in psi/$\sqrt{hour}$ or, $psi^2/\sqrt{hour}$, psi/cp/$\sqrt{hour}$
p = fluid pressure, psi
p_D = dimensionless pressure drop
p_{Ds} = dimensionless shut-in wellbore pressure drop
p_i = initial pressure in the system, psi
p_{sc} = standard pressure, psi
p_{wD} = dimensionless wellbore pressure drop
p_{wf} = wellbore flowing pressure, psi
$p_{wf,s}$ = wellbore pressure at instant of shut-in, psi
p_{ws} = wellbore shut-in pressure, psi

$\bar{p}$ = average reservoir pressure, psi
$\bar{p}_{Ds}$ = MDH dimensionless wellbore pressure drop
q = surface flow rate, STB/D, Mcf/D
q_D = dimensionless flowrate
r = radius, feet
r_f = horizontal fracture radius, feet
r_w = radius of well, feet
r'_w = effective wellbore radius, feet
s = skin factor, dimensionless
t_{Dr_f} = dimensionless time based on horizontal fracture radius
t_{Dx_f} = dimensionless time based on fracture half-length
Δt = shut-in time, hours
T = temperature, °R
T_{sc} = standard temperature, °R
w = fracture width, feet
x_e = drainage length, feet
x_f = fracture half-length, feet
Z = compressibility factor
ϕ = porosity
μ = viscosity, cp
θ = angle of inclination of the fracture from the vertical

Subscripts

CD = dimensionless capacity
D = dimensionless
e = external boundary
Dx_f = dimensionless variable based on fracture half-length
f = fracture
i = initial
w = wellbore

ACKNOWLEDGEMENTS

The financial support of the Department of Petroleum Engineering at the University of Tulsa is acknowledged with deep gratitude. I am also indebted to Dr. Ram G. Agarwal of Amoco Production Company, Tulsa, Oklahoma, for the stimulating discussions we have had on the subject of finite flow capacity fractures during 1972-1975. I am thankful to the Geothermal Program at the Lawrence Berkley Laboratory, University of California, for the invitation to present this paper.

References

1. Howard, G. C. and Fast, C. R.: Hydraulic Fracturing, Monograph Series, Society of Petroleum Engineers of AIME, Dallas (1970), 2, p. 2.
2. Clark, J. B.: "A Hydraulic Process for Increasing the Productivity of Wells," Trans., AIME (1949), 186, 1-8.
3. Dickey, P. A. and Andersen, K. H.: "Behavior of Water Input Wells--Part 4," Oil Weekly (Dec. 10, 1945).
4. Yuster, S. T. and Calhoun, J. C., Jr.: "Pressure Parting of Formations in Water Flood Operations--Part I," Oil Weekly (March 12, 1945) and Part II," Oil Weekly (March 19, 1945).
5. Torrey, P. D.: "Progress in Squeeze Cementing Application and Technique," Oil Weekly (July 29, 1940).
6. Teplitz, A. J. and Hassebroek, W. E.: "An Investigation of Oil Well Cementing," Drill. and Prod. Prac., API (1946), 76.
7. Howard, G. C. and Fast, C. R.: "Squeeze Cementing Operations," Trans., AIME (1950), 189, 53-64.
8. Howard, G. C. and Fast, C. R.: Hydraulic Fracturing, Monograph Series, Society of Petroleum Engineers of AIME, Dallas (1970), 2, p. 1.
9. Howard, G. C. and Fast, C. R.: Hydraulic Fracturing, Monograph Series, Society of Petroleum Engineers of AIME, Dallas (1970), 2, p. 11.
10. Howard, G. C. and Fast, C. R.: Hydraulic Fracturing, Monograph Series, Society of Petroleum Engineers of AIME, Dallas (1970), 2, p. 59.
11. Earlougher, R. C., Jr.: Advances in Well Test Analysis, Monograph Series, Society of Petroleum Engineers of AIME, Dallas (1977), 5.
12. Matthews, C. S. and Russell, D. G.: Pressure Buildup and Flow Tests in Wells, Monograph Series, Society of Petroleum Engineers of AIME, Dallas (1967), 1.
13. Ramey, Henry J., Jr., Kumar, Anil, and Gulati, Mohinder S.: Gas Well Test Analysis Under Water-Drive Conditions, AGA, Arlington, VA. (1973).
14. Moore, T. V., Schilthuis, R., and Hurst, W: "The Determination of Permeability from Field Data," Proc., API Bull. 211 (1933), 4.
15. Theis, Charles V.: "The Relation Between the Lowering of the Piezometric Surface and the Rate and Duration of Discharge of a Well Using Ground-Water Storage," Trans., AGU (1935), 519-524.
16. Horner, D. R.: "Pressure Build-Up in Wells," Proc., Third World Pet. Cong., The Hague (1951), Sec. II, 503-523.
17. Miller, C. C., Dyes, A. B., and Hutchinson, C. A., Jr.: "The Estimation of Permeability and Reservoir Pressure From Bottom Hole Pressure Build-Up Characteristics," Trans., AIME (1950), 189, 91-104.
18. Ramey, H. J., Jr., and Cobb, William M.: "A General Buildup Theory for a Well in a Closed Drainage Area," J. Pet. Tech. (Dec. 1971), 1493-1505.
19. Muskat, Morris: "Use of Data on the Build-Up of Bottom-Hole Pressures," Trans., AIME (1937), 123, 44-28.
20. Wenzel, L. K.: "Methods of Determining Permeability of Water-Bearing Materials with Special Reference to Discharging Well Methods," U.S. Geol. Survey W.S.P. 887, 1942.
21. Cooper, H. H., Jr., and Jacob, C. E.: "A Generalized Graphical Method for Evaluating Formation Constants and Summarizing Well Field History," Trans. Am. Geophys. Union (1986), 27, 526-534.
22. Jacob, C. E.: "Flow of Water in Elastic Artesian Aquifer", Trans., AGU (1940), II, 574.
23. Jacob, C. E.: "Flow of Groundwater," Engineering Hydraulics, by Rouse and Hunter, John Wiley & Sons, New York (1950), Ch. 5.

24. Elkins, L. R.: "Reservoir Performance and Well Spacing--Silica Arguckle Pool," Drill. and Prod. Prac., API (1946), 109.
25. van Everdingen, A. F. and Hurst, W.: "The Application of the Laplace Transformation to Flow Problems in Reservoirs," Trans., AIME (1949), 186, 305-324.
26. Hurst, W.: "Unsteady Flow of Fluids in Oil Reservoirs," Physics (Jan. 1934), 5.
27. Jacob, C. E. and Lohman, S. W.: "Nonsteady Flow to a Well of Constant Drawdown in an Extensive Aquifer," Trans., AGU (Aug. 1952), 559-569.
28. van Everdingen, A. F.: "The Skin Effect and Its Influence on the Productive Capacity of a Well," Trans., AIME (1953), 198, 171-176.
29. Hurst, W.: "Establishment of the Skin Effect and Its Impediment to Fluid-Flow Into a Well Bore," Pet. Eng. (Oct., 1953), B-6.
30. Hantush, M. S.: "Nonsteady Flow to a Well Partially Penetrating an Infinite Leaky Aquifer," Proceedings, Iraq Scientific Society (1957).
31. Nisle, R. G.: "The Effect of Partial Penetration on Pressure Buildup in Oil Wells," Trans., AIME (1958), 213, 85.
32. Burns, William A., Jr.: "New Single-Well Test for Determining Vertical Permeability." J. Pet. Tech. (June 1969), 743-752.
33. Prats, Michael: "A Method for Determining the Net Vertical Permeability Near a Well From In-Situ Measurements," J. Pet. Tech. (May 1970), 637-643.
34. Agarwal, Ram G., Al-Hussainy, Rafi, and Ramey, H. J., Jr.: "An Investigation of Wellbore Storage and Skin Effect in Unsteady Liquid Flow: I. Analytical Treatment," Soc. Pet. Eng. J. (Sept. 1970), 279-290.
35. Ramey, H. J., Jr.: "Short-Time Well Test Data Interpretation in the Presence of Skin Effect and Wellbore Storage," J. Pet. Tech. (Jan. 1970), 97-104.
36. Ramey, Henry J., Jr., and Agarwal, Ram G.: "Annulus Unloading Rates as Influenced by Wellbore Storage and Skin Effect," Soc. Pet. Eng. J. (Oct. 1972), 453-462.
37. Ramey, Henry J., Jr., Agarwal, Ram G., and Martin, Ian: "Analysis of 'Slug Test' or DST Flow Period Data," J. Cdn. Pet. Tech. (July-Sept. 1975), 37-47.
38. Cooper, Hilton, H., Jr., Bredehoeft, John D., and Papadopulos, Istavros S.: "Response of a Finite-Diameter Well to an Instantaneous Charge of Water," Water Resources Res. (1967), 3, No. 1, 263-269.
39. Witherspoon, P. A., Javandel, I., Neuman, S.P., and Freeze, R. A.: Interpretation of Aquifer Gas Storage Conditions from Water Pumping Tests, Monograph on Project NS-38, American Gas Association, Inc., New York, 1967.
40. Howard, C. C. and Fast, C. R.: Hydraulic Fracturing, Monograph Series, Society of Petroleum Engineers of AIME, Dallas (1970), 2, p. 22.
41. Hubbert, M. K. and Willis, D. G.: "Mechanics of Hydraulic Fracturing," Trans., AIME (1957), 210, 153-166.
42. Zemanek, J., Caldwell, R. L., Glenn, E. E., Jr., Holcomb, S. V., Norton, L. J., and Strauss, A. J. D.: "The Borehole Televiewer --A New Logging Concept for Fracture Location and Other types of Borehole Inspection," J. Pet. Tech. (June 1969), 762-774.
43. Muskat, M.: Flow of Homogeneous Fluids Through Porous Media, McGraw-Hill Book Co., Inc., New York (1937), p. 409.
44. Howard, G. C. and Fast, C. R.: "Optimum Fluid Characteristics for Fracture Extension," Drill. and Prod. Prac., API (1957), 261.
45. McGuire, W. J. and Sikora, V. J.: "The Effect of Vertical Fractures on Well Productivity," Trans., AIME (1960), 219, 401-403.
46. Prats, M.: "Effect of Vertical Fractures on Reservoir Behavior--Incompressible Fluid Case," Soc. Pet. Eng. J. (June, 1961), 105-118.
47. van Poollen, H. K., Tinsley, John M. and Saunders, Calvin D.: "Hydraulic Fracturing: Fracture Flow Capacity vs. Well Productivity," Trans., AIME (1958), 213, 91-95.
48. Craft, B. C., Holden, W. R. and Graves, E. D., Jr.: Well Design: Drilling and Production, Prentice-Hall, Inc., Englewood, Cliffs, N.J. (1962), p. 494.
49. Dyes, A. B., Kemp, C. E. and Caudle, B. H.: "Effect of Fractures on Sweep-Out Pattern," Trans., AIME (1958), 213, 245-249.
50. Tinsley, J. M., Williams, J. R., Jr., Tiner, R. L. and Malone, W. T.: "Vertical Fracture Height--Its Effect on Steady-State Production Increase," J. Pet. Tech. (May 1969), 633-638.
51. Ramey, H. J., Jr., Barker, B., Ariharaz, N. Mao, M. L. and Marquis, J. K.: "Pressure Transient Testing of Hydraulically-Fractured Wells," presented at the spring meeting of the American Nuclear Soc., 1972.
52. Prats, M., Hazebroek, P. and Strickler, W. R.: "Effect of Vertical Fractures on Reservoir Behavior--Compressible-Fluid Case," Soc. Pet. Eng. J. (June, 1962), 87-94.
53. Scott, J. O.: "The Effect of Vertical Fractures on Transient Pressure Behavior of Wells," J. Pet. Tech. (Dec., 1963), 1365-1369.
54. Russell, D. G. and Truitt, N. E.: "Transient Pressure Behavior in Vertically Fractured Reservoirs," J. Pet. Tech. (Oct., 1964), 1159-1170.
55. Gringarten, Alain C., Ramey, Henry J., Jr., and Raghavan, R.: "Unsteady-State Pressure Distributions Created by a Well With a Single Infinite-Conductivity Vertical Fracture," Soc. Pet. Eng. J. (Aug. 1974), 347-360.
56. Carslaw, H. S. and Jaeger, J. C.: Conduction of Heat in Solids, Oxford at the Clarendon Press (1959), p. 353-386.
57. Newman, A. B.: "Heating and Cooling Rectangular and Cylindrical Solids," Ind. and Eng. Chem. (1936), Vol. 28, 545.
58. Gringarten, A. C., and Ramey, H. J., Jr.: "The Use of Source and Green's Functions in Solving Unsteady Flow Problems in Reservoirs," Soc. Pet. Eng. J. (Oct. 1973), 285-296.

59. Abramowitz, Milton and Stegun, Irene A. (ed.): Handbook of Mathematical Functions With Formulas, Graphs and Mathematical Tables, National Bureau of Standards Applied Mathematics Series-55 (June 1964), 227-253, 295-330.
60. Clark, K. K.: "Transient Pressure Testing of Fractured Water Injection Wells," J. Pet. Tech. (June 1968), 639-643.
61. Earlougher, R. C., Jr., Ramey, H. J., Jr., Miller, F. G. and Mueller, T. D.: "Pressure Distributions in Rectangular Reservoirs," J. Pet. Tech. (Feb. 1968), 199-208.
62. Simon, L. G.: "Effect of Compass Orientation of a Vertical Fracture on Pressure Behavior in Closed Rectangular Reservoirs," Master of Science Thesis, University of Tulsa, Tulsa, OK, 1976.
63. Raghavan, R. and Hadinoto, Nico: "Analysis of Pressure Data for Fractured Wells: The Constant Pressure Outer Boundary," paper SPE 6015 presented at the SPE-AIME 51st Annual Fall Technical Conference and Exhibition, New Orleans, Oct. 3-6, 1976.
64. Hurst, William, Haynie, Orville K., and Walker, Richard N.: "New Concept Extends Pressure Buildup Analysis," Pet. Eng. (Aug. 1962), 65-72.
65. Khan A.: "Pressure Distributers in Rectangular Reservoirs Drained by Vertically-Fractured Well," Master of Science Thesis, University of Tulsa, to appear.
66. Wattembarger, Robert A.: "Effects of Turbulence, Wellbore Damage, Wellbore Storage, and Vertical Fractures on Gas Well Testing," PhD Dissertation, Stanford U., Stanford, Calif. (1967).
67. Ramey, H. J., Jr., "Practical Use of Modern Well Test Analysis," paper SPE 5878 presented at the SPE-AIME 46th Annual Calif. Regional Meeting, Long Beach, April 8-9, 1976.
68. Cinco-L., Heber, Samaniego-V., F., and Dominguez-A., N.: "Transient Pressure Behavior for a Well With a Finite Conductivity Vertical Fracture," paper SPE 6014 presented at the SPE-AIME 51st Annual Fall Technical Conference and Exhibition, New Orleans, Oct. 3-6, 1976.
69. Agarwal, Ram. G., Carter, R. D. and Pollock, C. B.: "Evaluation and Prediction of Performance of Low Permeability Gas Wells Stimulated by Massive Hydraulic Fracturing," SPE 6838, presented at the 52nd Annual Fall Technical Conference, Denver, Colorado, Oct. 9-12, 1977. Also see Agarwal, Ram G.: "Evaluation of Fracturing Results in Conventional and MHG Applications," SPE Mid-Continent Section, Continuing Education Course on Well Completion and Stimulation, Feb. 1977.
70. Swift, G. W. and Kiel, O. G.: "The Prediction of Performance Including the Effect of Non-Darcy Flow," J. Pet. Tech. (July, 1962), 791-798.
71. Smith, R. V. (1961). Unsteady-State Gas Flow into Gas Wells, J. Pet. Tech., 13, 1151-1159.
72. Holditch, S. A. and Morse, R. A.: "The Effects of Non-Darcy Flow on the Behavior of Hydraulically Fractured Gas Wells," J. Pet. Tech. (Oct. 1976), 1169-1179.
73. Raghavan, R.: "Some Practical Considerations in the Analysis of Pressure Data," J. Pet. Tech., (Oct., 1976), 1256-1268.
74. Wattenbarger, Robert A. and Ramey, H. J., Jr.: "Gas Well Testing With Turbulence, Damage and Wellbore Storage," J. Pet. Tech. (Aug. 1968), 877-887.
75. Ramey, H. J., Jr. and Gringarten, A. C.: "Effect of High Volume Vertical Fractures on Geothermal Steam Well Behavior," paper presented at the second United Nations Symposium on the Use and Development of Geothermal Energy, San Francisco, May 20-29, 1975.
76. Gringarten, Alain C. and Ramey, Henry J., Jr.: "Unsteady-State Pressure Distributions Created by a Well With a Single Horizontal Fracture, Partial Penetration, or Restricted Entry," Soc. Pet. Eng. J. (Aug. 1974), 413-426.
77. Graingarten, A. C., Ramey, H. J., Jr., and Raghavan, R.: "Applied Pressure Analysis for Fractured Wells," J. Pet. Tech. (July 1975), 887-892.
78. Cinco-Ley, Heber, Ramey, Henry J., Jr., and Miller, Frank G.: "Unsteady-State Pressure Distribution Created by a Well With an Inclined Fracture," paper SPE 5591 presented at the SPE-AIME 50th Annual Fall Technical Conference and Exhibition, Dallas, Sept. 28-Oct. 1, 1975.
79. Raghavan, R., Uraiet, A., and Thomas, G. W.: "Vertical Fracture Height: Effect on Transient Flow Behavior," paper SPE 6016 presented at the SPE-AIME 51st Annual Fall Technical Conference and Exhibition, New Orleans, Oct. 3-6, 1976.
80. Locke, C. D. and Sawyer, W. K.: "Constant Pressure Injection Test in a Fractured Reservoir-History Match Using Numerical Simulation and Type Curve Analysis," paper SPE 5594 presented at SPE-AIME 50th Annual Fall Meeting, Dallas, Sept. 28-Oct. 1, 1975.
81. Aronofsky, J. S. and Jenkins, R.: "A Simplified Analysis of Unsteady Radial Gas Flow," Trans., AIME (1954), 201, 149-154.
82. Al-Hussainy, R., Ramey, H. J., Jr., and Crawford, P. B.: "The Flow of Real Gases Through Porous Media," J. Pet. Tech. (May 1966), 624-636.
83. Carslaw, H. S. and Jaeger, J. C.: Conduction of Heat in Solids, 2nd Ed., Oxford at the Clarendon Press (1959), p. 11.
84. Leibenzon, L. S.: "Subsurface Hydraulics of Water, Oil and Gas," Publ. Acad. Sci., collected works, U.S.S.R. (1953), 2.
85. Raats, P.A.C., Steady infiltration from line sources and furrows. Soil Sci. Soc. Amer. Proc. 34 (1970), 709-714.
86. Raghavan. R., Cady, Gilbert V., and Ramey, Henry J., Jr.: "Well-Test Analysis for Vertically Fractured Wells," J. Pet. Tech. (Aug. 1972), 1014-1020.
87. Perrine, R. L.: "Analysis of Pressure Buildup Curves," Drill. and Prod. Prac., API (1956), 482-509.

88. Kumar, Anil and Ramey, Henry J., Jr.: "Well-Test Analysis for a Well in a Constant-Pressure Square," Soc. Pet. Eng. J. (April 1974), 107-116.

89. Raghavan, R.: "The Effect of Producing Time on Type Curve Analysis," submitted to SPE of AIME.

90. Wasserman, M. L. and Emanuel, A. S.: "History Matching Three-Dimensional Models Using Optimal Control Theory," J. Can. Pet. Tech. (Oct.-Dec. 1976), 70-77.

91. Carter, R. D., Kemp, L. F., Jr., Pierce, A. C. and Williams, D. L.: "Performance Matching with Constraints," Soc. Pet. Eng. J. (April 1974) 187-196.

92. Chavent, C., Dupuy, M. and Lemonier, P.: "History Matching by Use of Optimal Control Theory," Soc. Pet. Eng. J. (Feb. 1975), 74-86.

93. Chen, W. H., Gavalas, G. R. and Seinfeld, J. H.: "A New Algorithm for Automatic History Matching," Soc. Pet. Eng. J. (Dec. 1974) 593-608.

94. Wasserman, M. L., Emanuel, A. S. and Seinfeld, J. H.: "Practical Application of Optimal-Control Theory to History-Matching Multiphase Simulator Models," Soc. Pet. Eng. J. (Aug. 1975), 347-355.

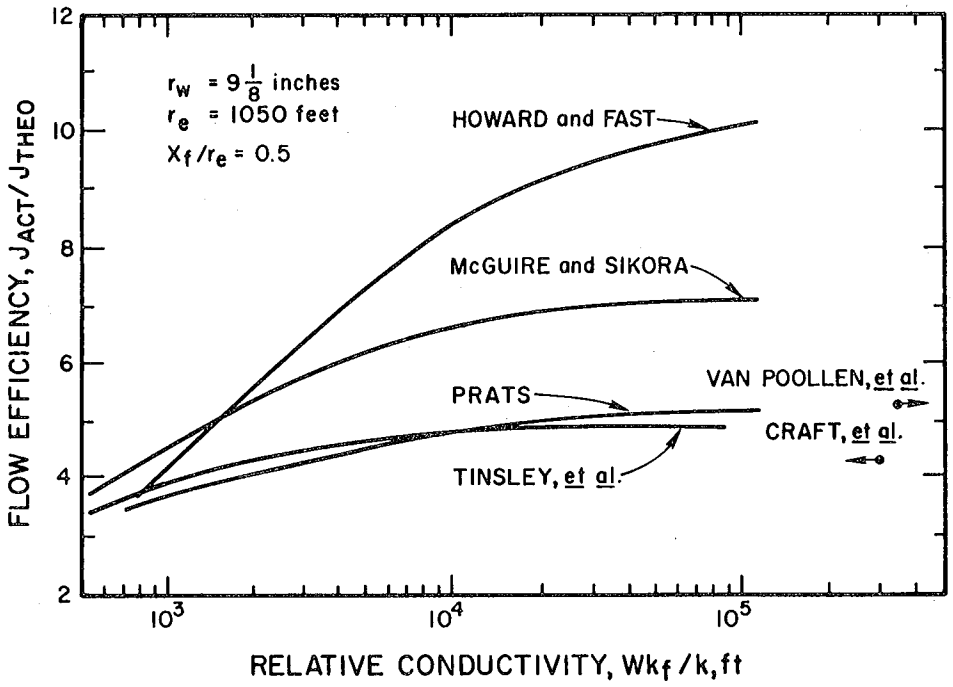

Fig. 1. Flow efficiency vs. relative conductivity for a vertically fractured well.

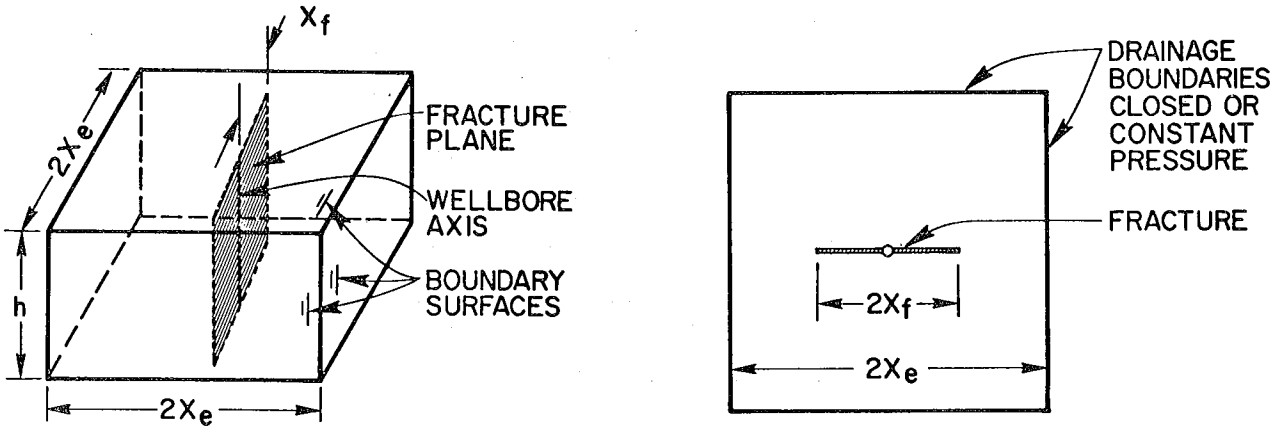

Fig. 2. Schematic diagram for a vertically fractured system.

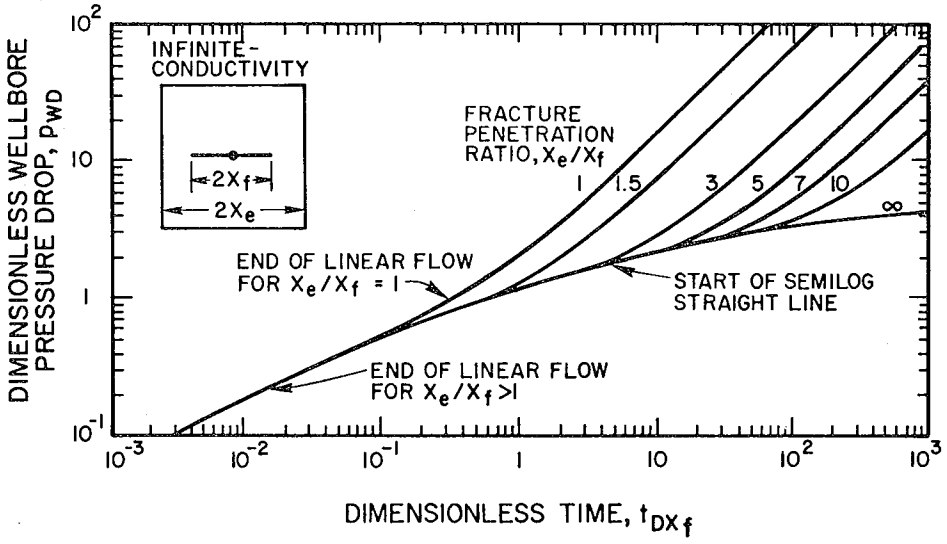

Fig. 3. Dimensionless wellbore pressure drop vs. dimensionless time for an infinite-conductivity vertically fractured well in a closed square drainage region.

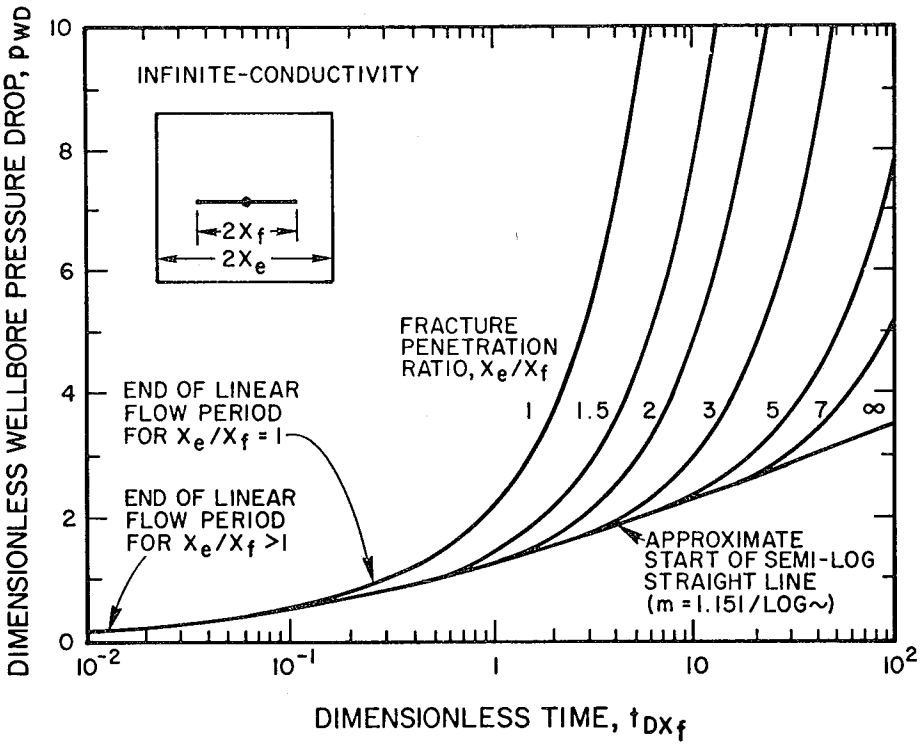

Fig. 4. Dimensionless wellbore pressure drop vs. dimensionless time for an infinite-conductivity vertically fractured well in a closed square drainage region.

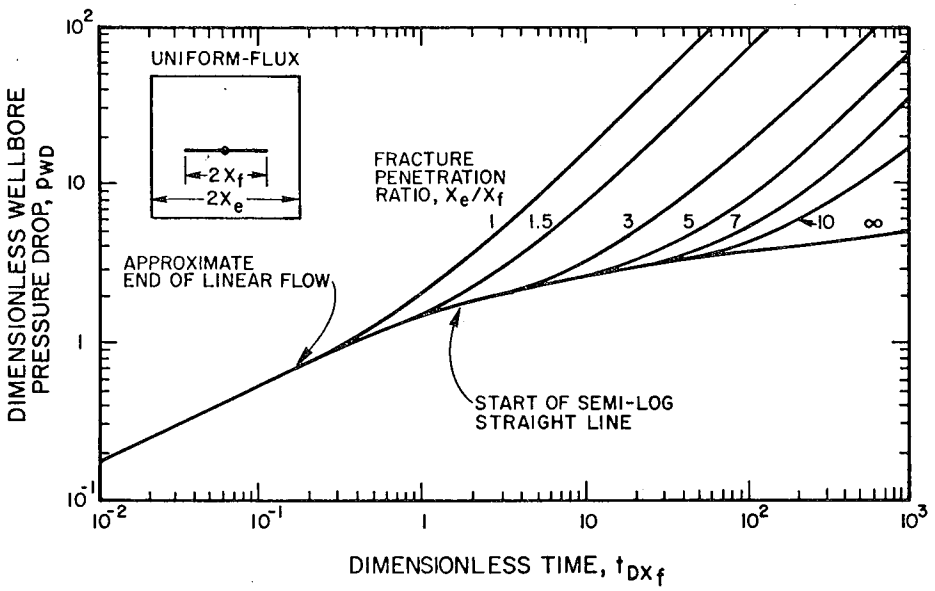

Fig. 5. Dimensionless wellbore pressure drop vs. dimensionless time for an uniform-flux vertically fractured well in a closed square drainage region.

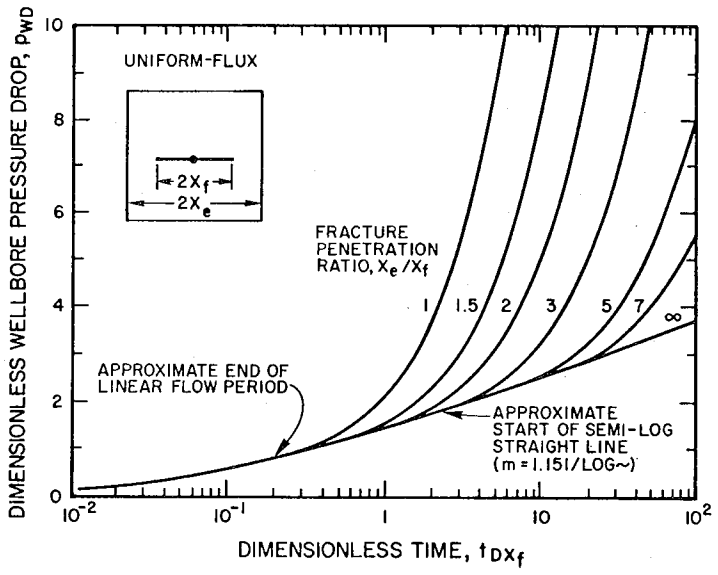

Fig. 6. Dimensionless wellbore pressure drop vs. dimensionless time for an uniform-flux vertically fractured well in a closed square drainage region.

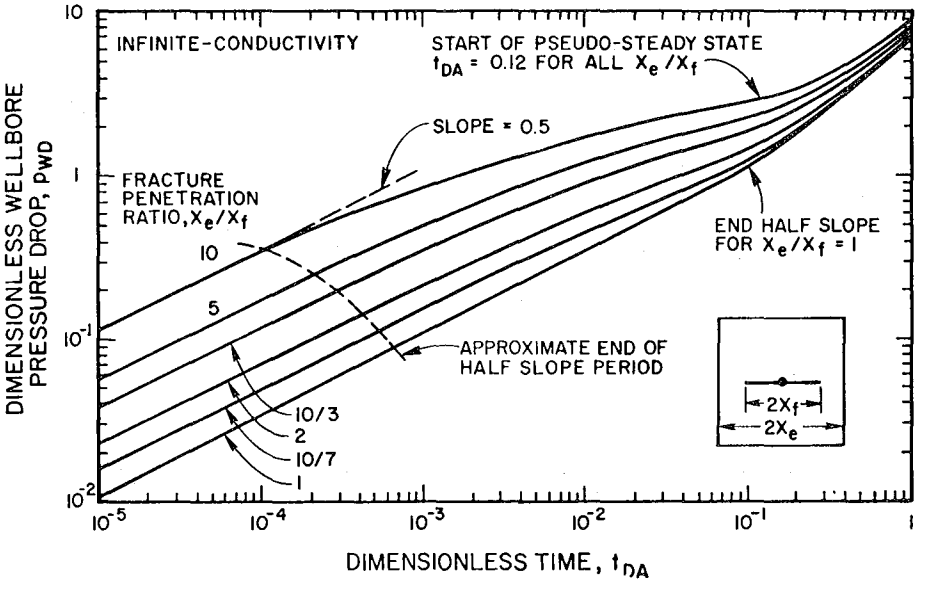

Fig. 7. Dimensionless wellbore pressure drop vs. dimensionless time for an infinite-conductivity vertically fractured well in a closed square drainage region.

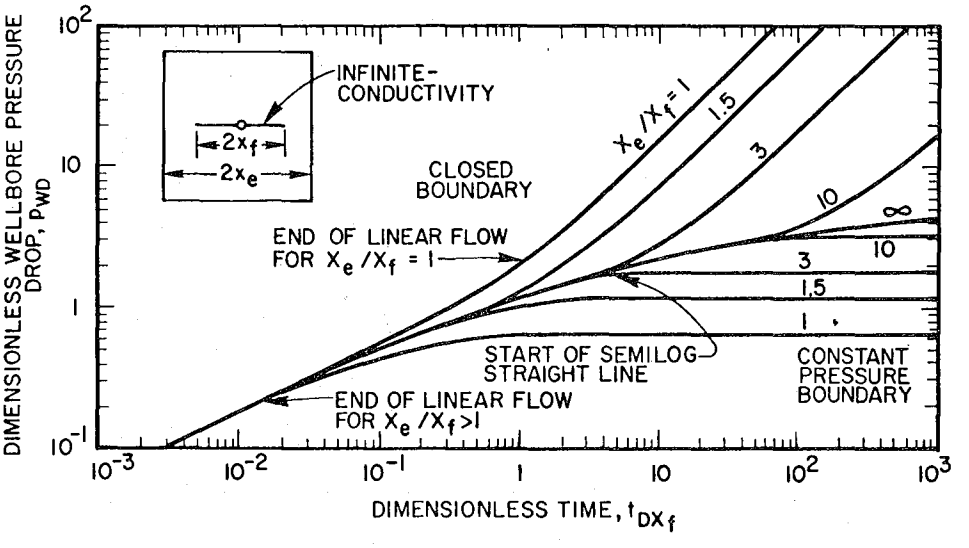

Fig. 8. Dimensionless wellbore pressure drop vs. dimensionless time for an infinite-conductivity vertically fractured well in a square drainage region.

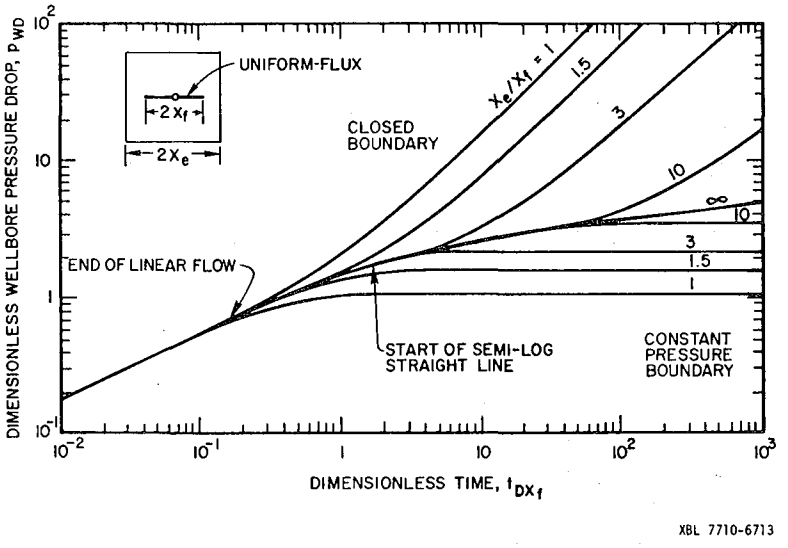

Fig. 9. Dimensionless wellbore pressure drop vs. dimensionless time for an uniform-flux vertically fractured well in a square drainage region.

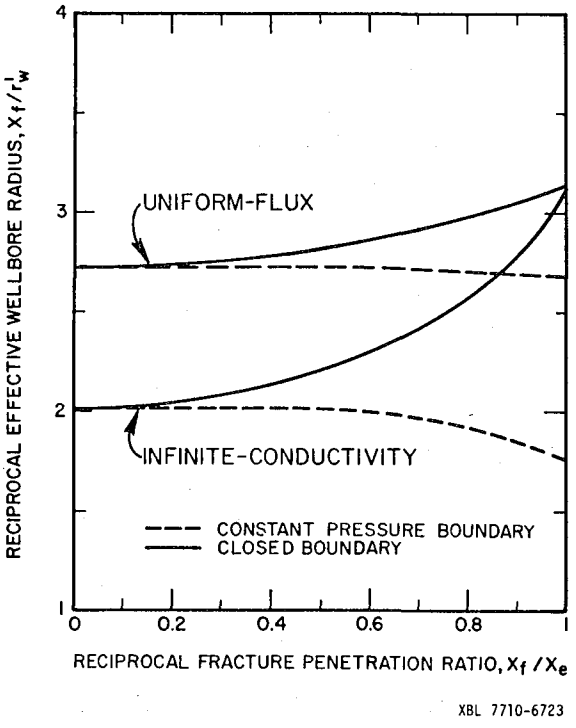

Fig. 10. Effective wellbore radius for a vertically fractured well in a square drainage region.

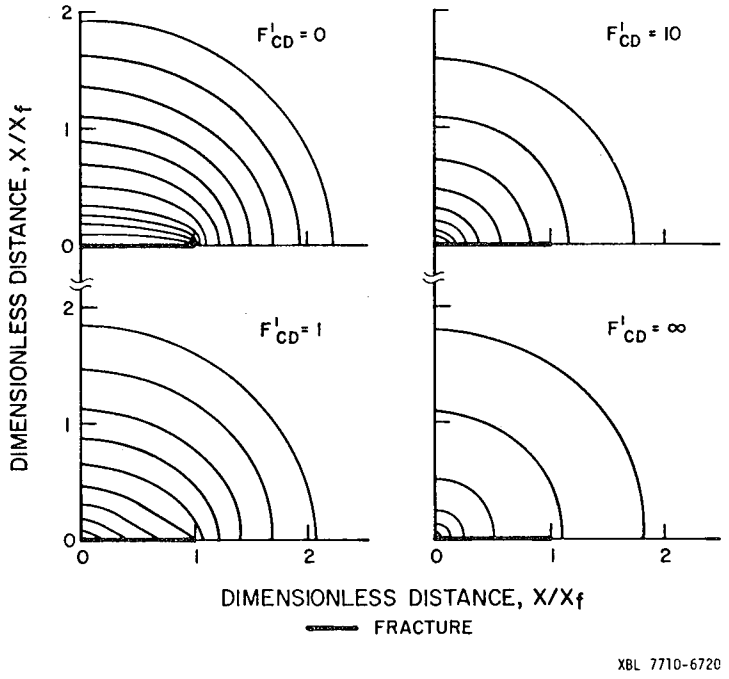

Fig. 11. Effect of fracture capacity on the pressure distribution around a fractured well.

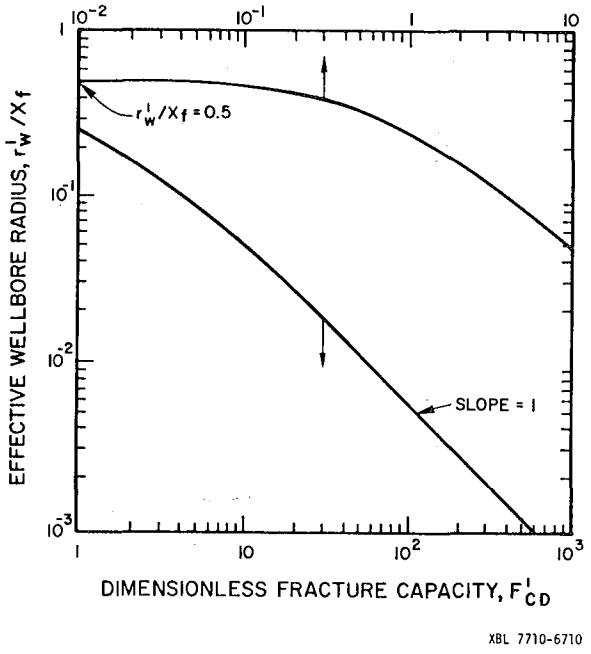

Fig. 12. Effective wellbore radius vs. dimensionless fracture capacity.

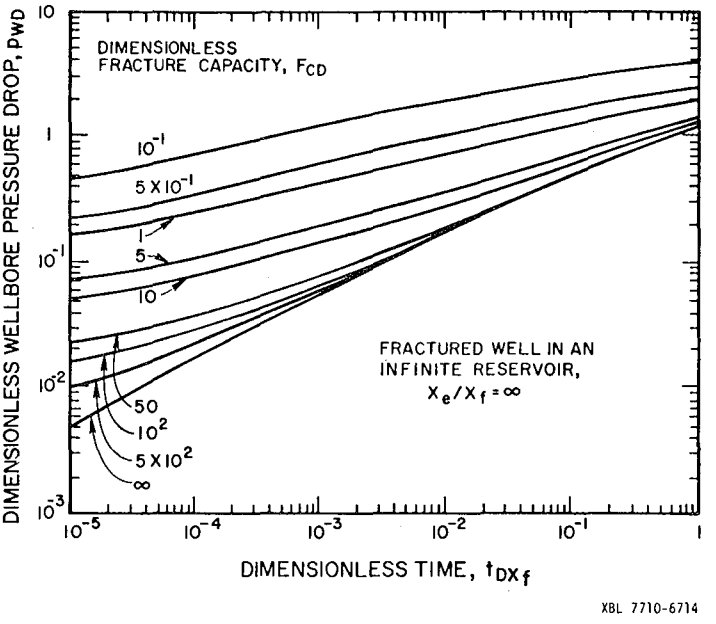

Fig. 13. Dimensionless wellbore pressure drop vs. dimensionless time for a finite-capacity vertically-fractured well in an infinite reservoir.

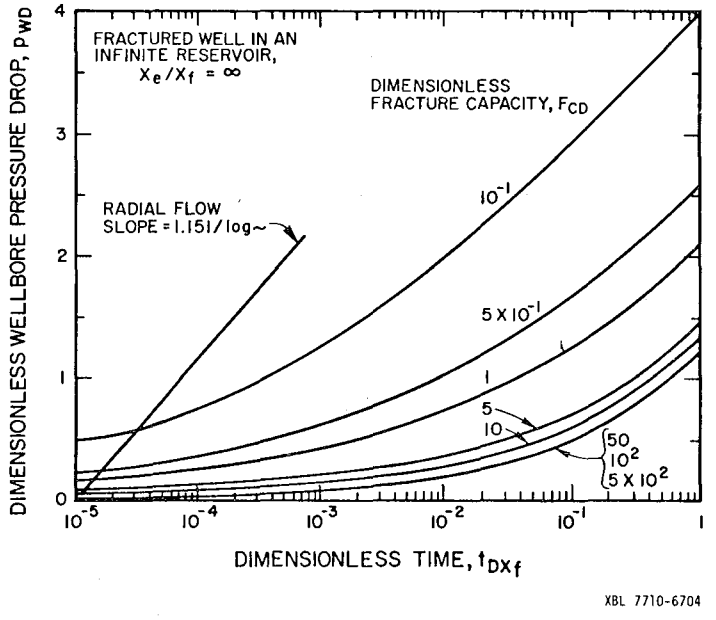

Fig. 14. Dimensionless wellbore pressure drop vs. dimensionless time for a finite-capacity vertically-fractured well in an infinite reservoir.

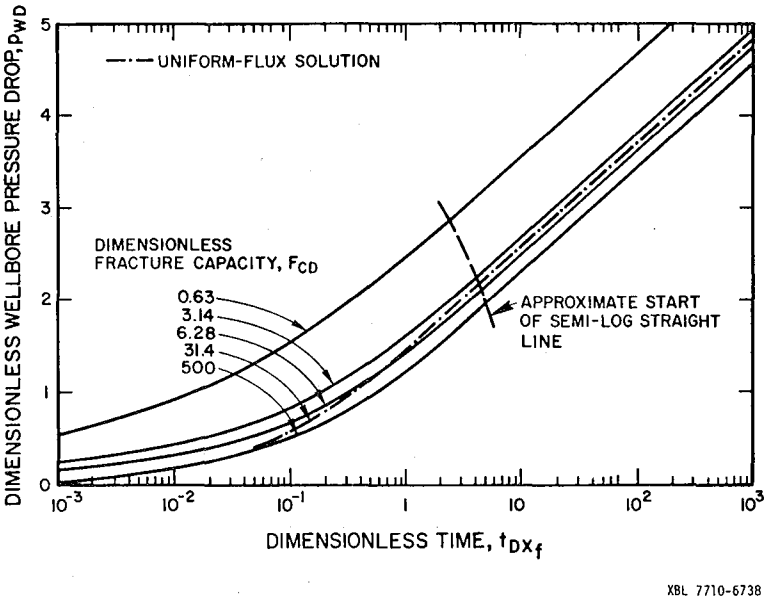

Fig. 15. Late time draw-down data for a finite fracture capacity vertically fractured well in an infinite reservoir.

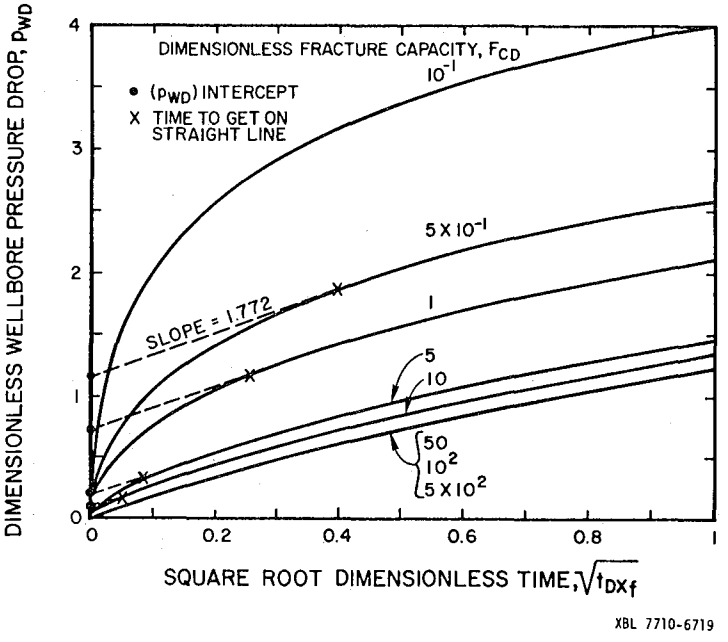

Fig. 16. Dimensionless wellbore pressure drop vs. square root dimensionless time for a finite-capacity vertical fracture.

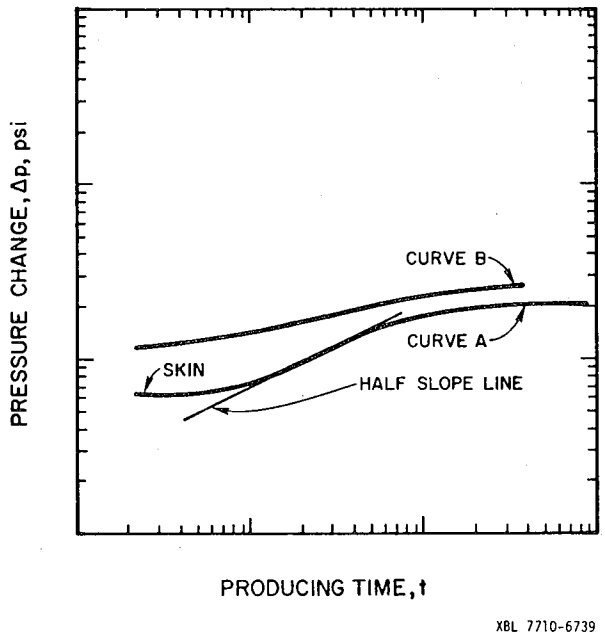

Fig. 17. Effect of skin on fractured well behavior.

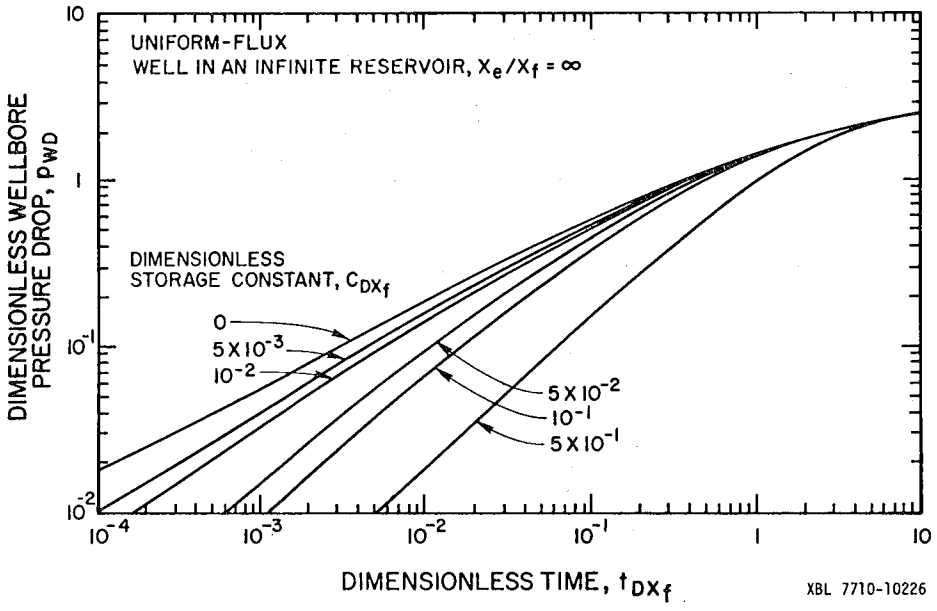

Fig. 18. Dimensionless wellbore pressure drop vs. dimensionless time for a uniform-flux vertical fracture with wellbore storage.

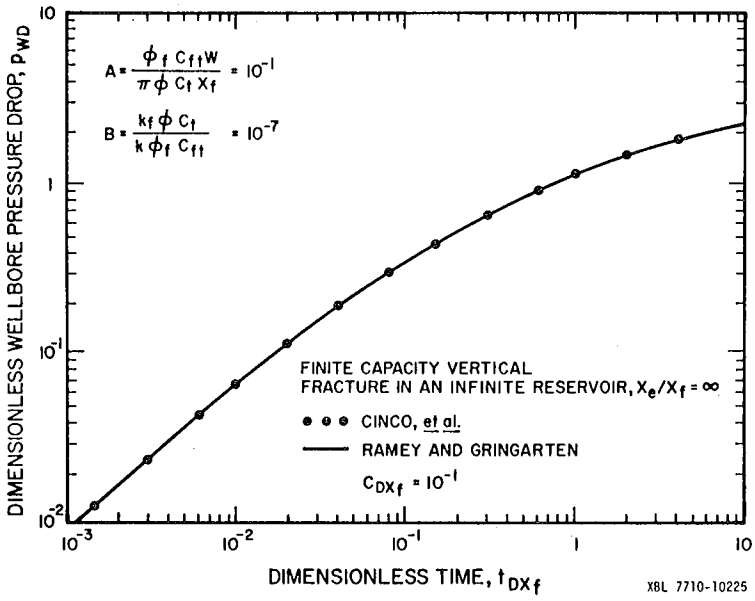

Fig. 19. Dimensionless wellbore pressure drop vs. dimensionless time for a finite-capacity vertical fracture with wellbore storage.

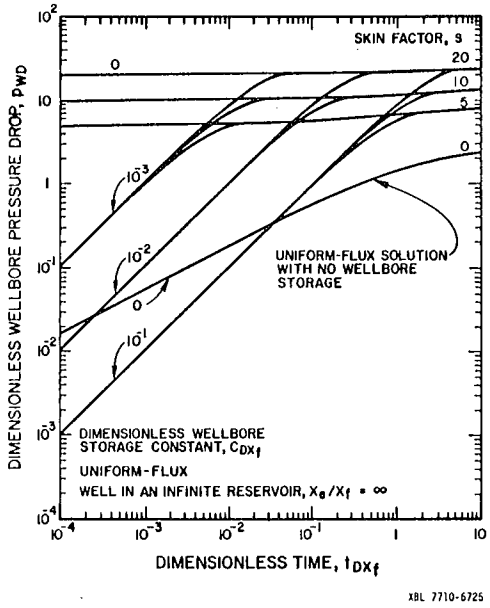

Fig. 20. Dimensionless pressure drop vs. dimensionless time for a vertically fractured well with skin and wellbore storage.

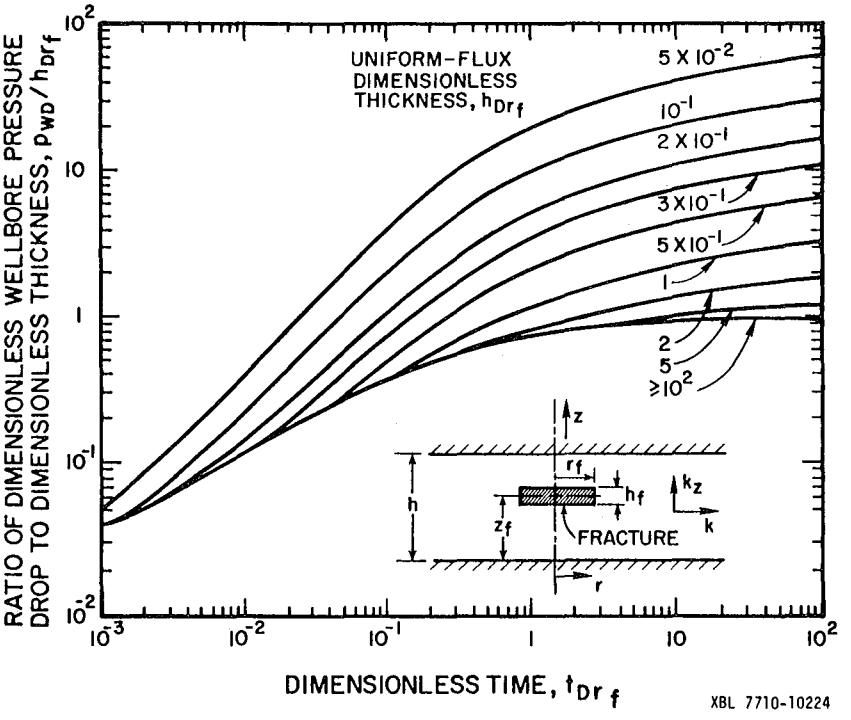

Fig. 21. Dimensionless wellbore pressure drop vs. dimensionless time for a uniform-flux horizontal fracture in an infinite reservoir.

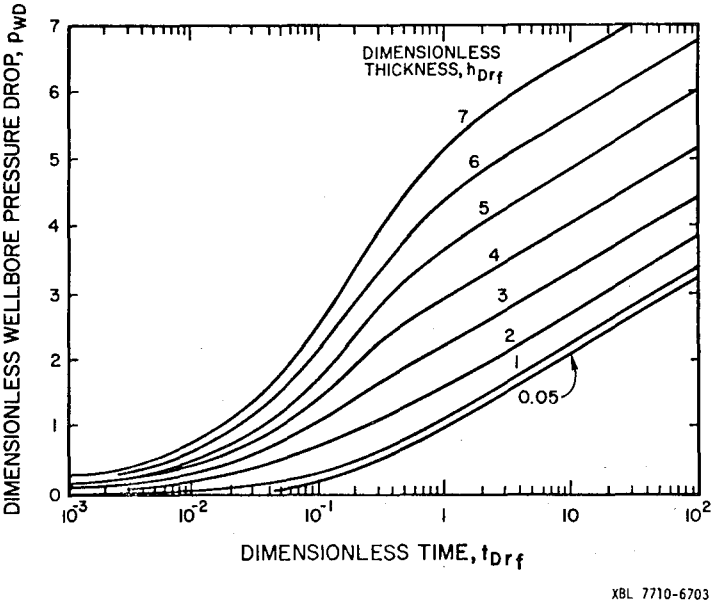

Fig. 22. Dimensionless wellbore pressure drop vs. dimensionless time for a uniform-flux horizontal fracture in an infinite reservoir.

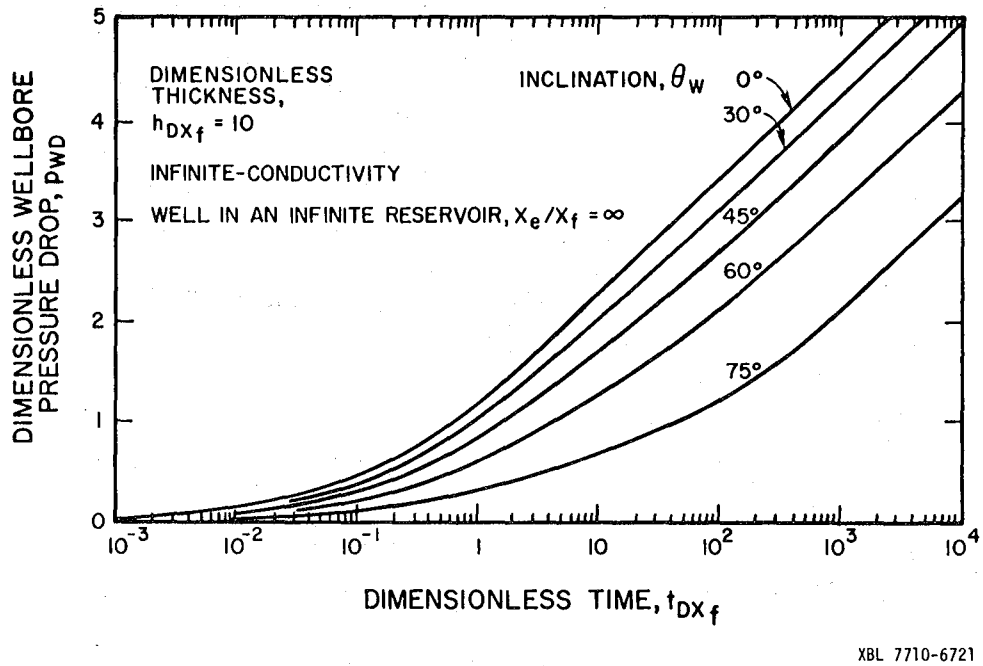

Fig. 23. Dimensionless wellbore pressure drop vs. dimensionless time for an infinite-conductivity inclined fracture in an infinite reservoir.

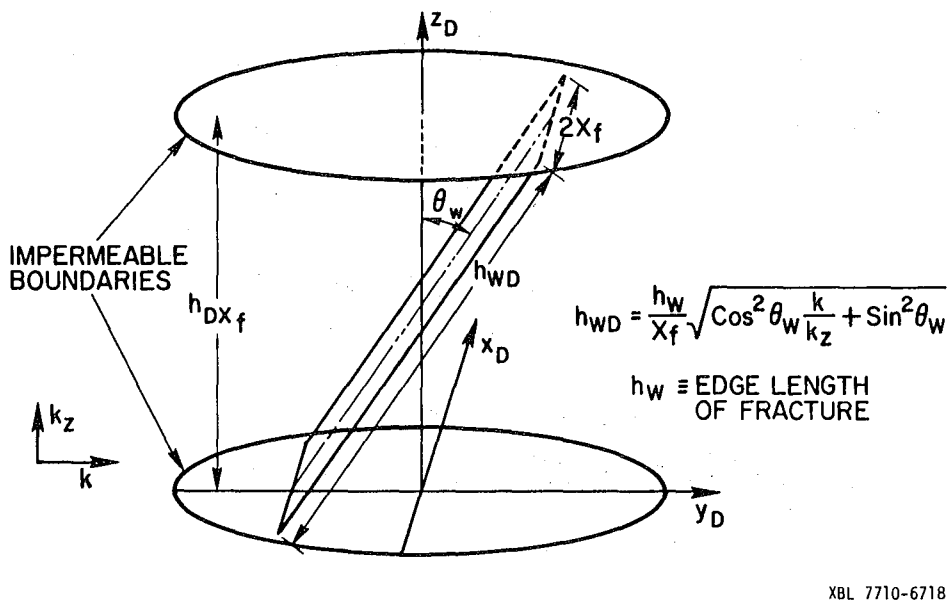

Fig. 24. Schematic diagram for an inclined fracture.

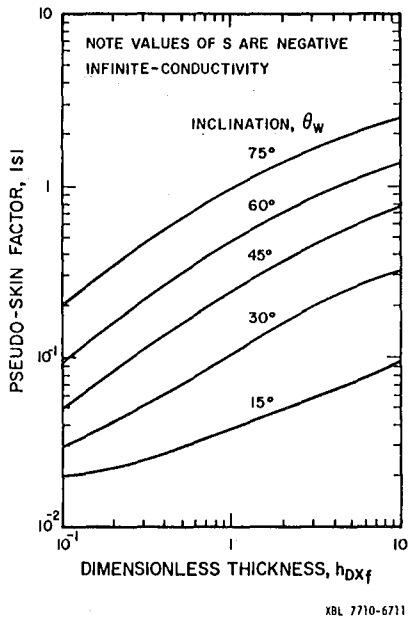

Fig. 25. Pseudo-skin factor vs. dimensionless thickness for an inclined fracture.

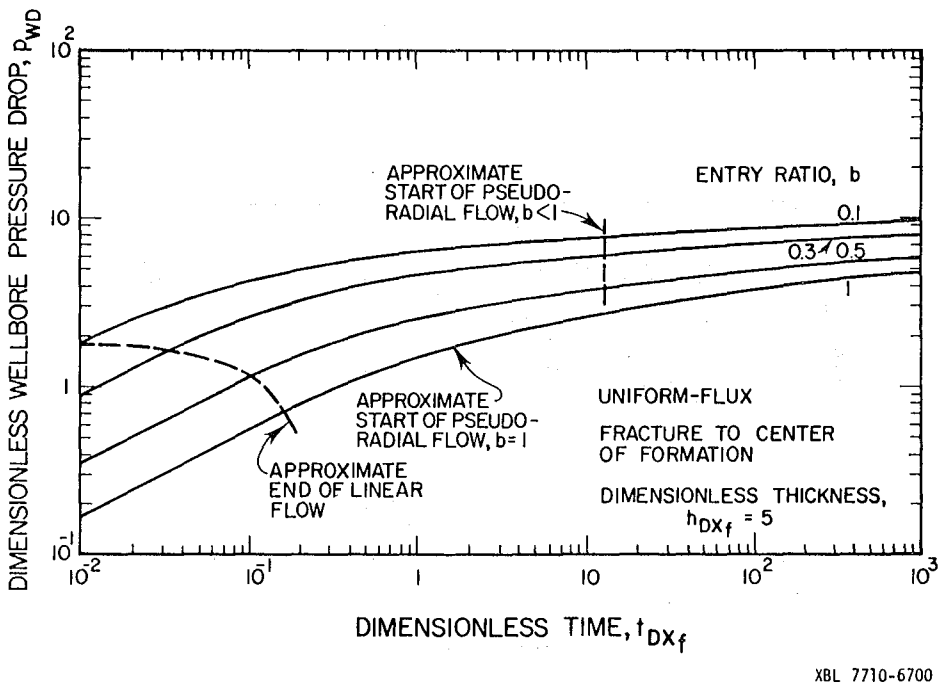

Fig. 26. Dimensionless wellbore pressure drop vs. dimensionless time for a limited entry uniform-flux vertical fracture located at the center of the formation.

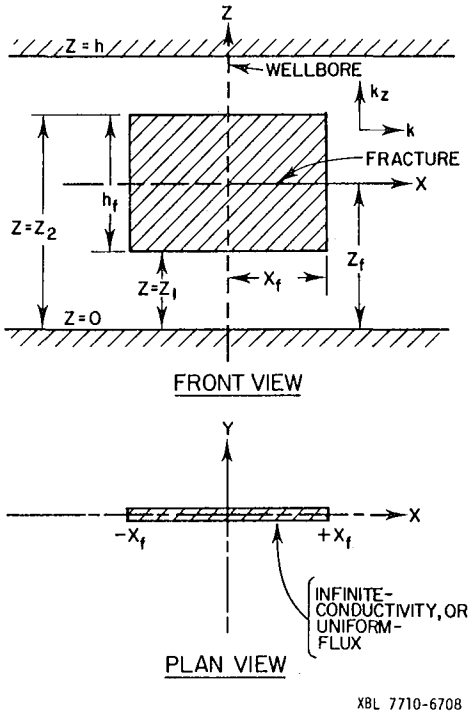

Fig. 27. Schematic diagram: a limited entry vertical fracture.

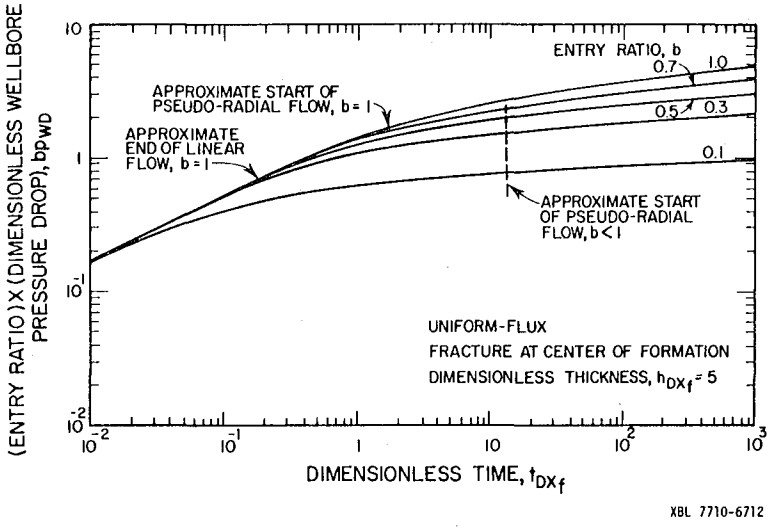

Fig. 28. Draw-down data for a limited entry uniform-flux vertical fracture in an infinite reservoir.

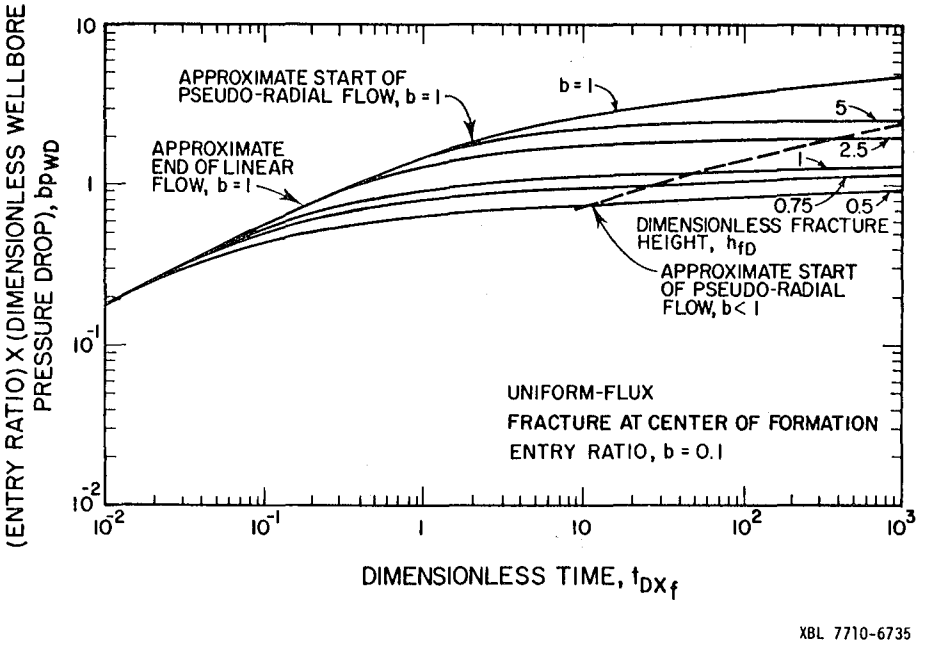

Fig. 29. Draw-down data for a limited entry uniform-flux vertical fracture in an infinite reservoir.

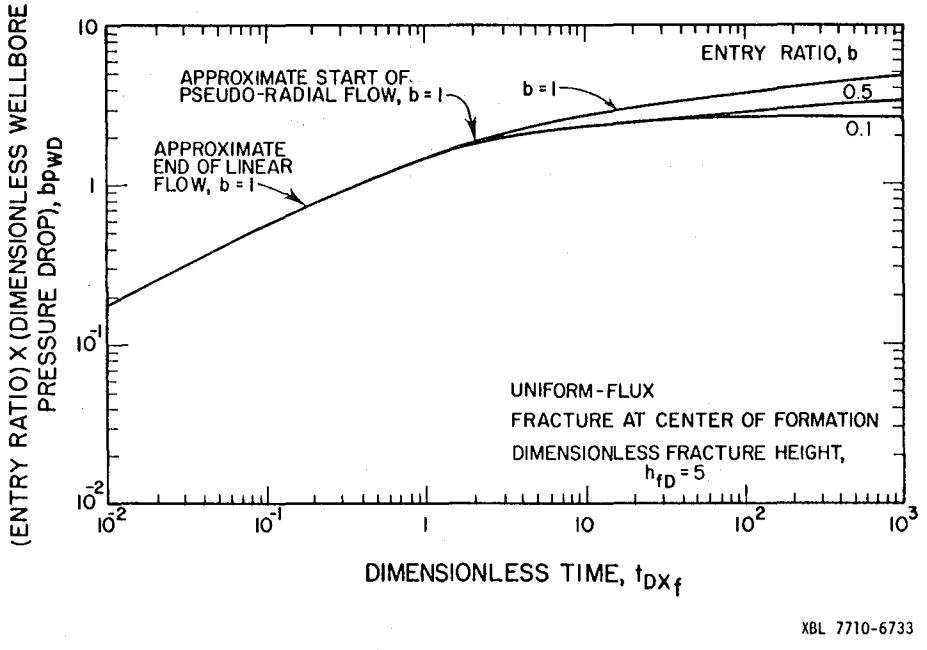

Fig. 30. Draw-down data for a limited entry uniform-flux vertical fracture.

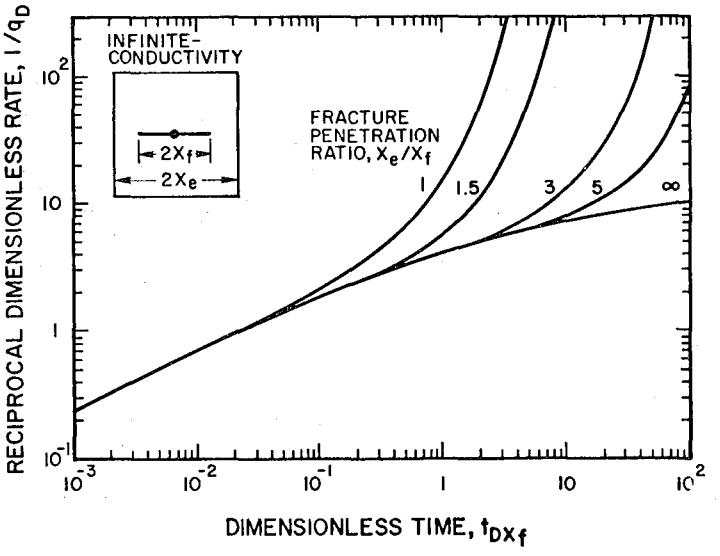

Fig. 31. Reciprocal dimensionless rate vs. dimensionless time for an infinite-conductivity vertical fracture in a closed square reservoir.

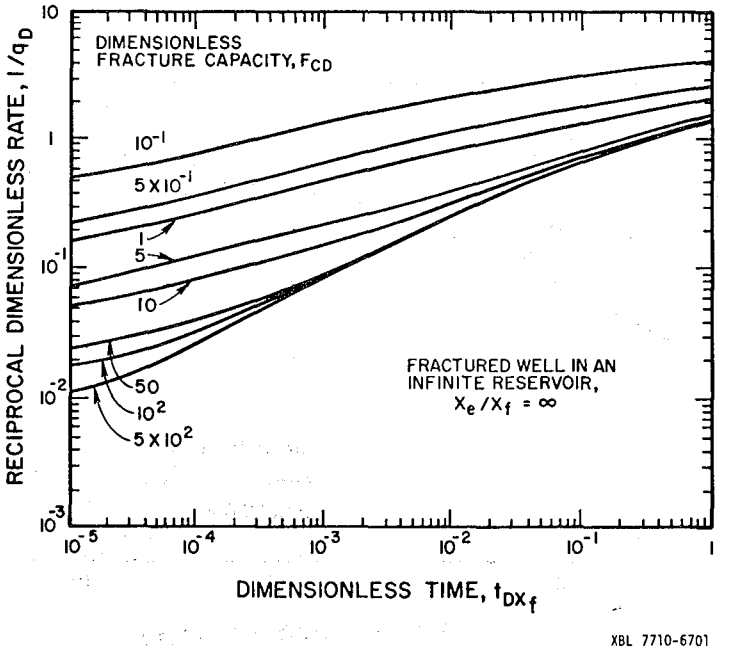

Fig. 32. Reciprocal dimensionless rate vs. dimensionless time for a finite-capacity vertical fracture producing at a constant terminal pressure.

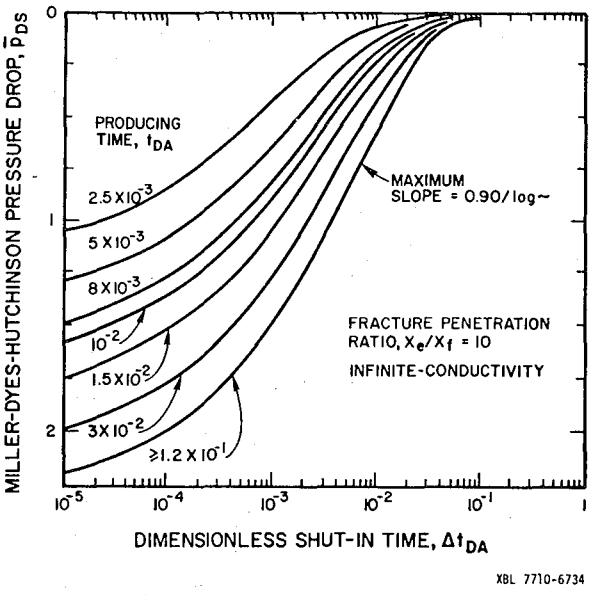

Fig. 33. Miller-Dyes-Hutchinson build-up graph for an infinite-conductivity vertically fractured well in a closed square.

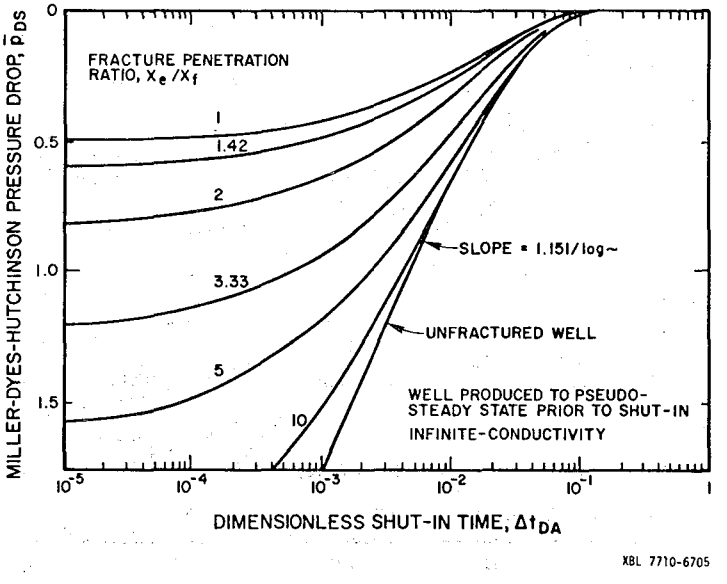

Fig. 34. Miller-Dyes-Hutchinson build-up graph for a vertically fractured well in a closed square--effect of fracture penetration ratio.

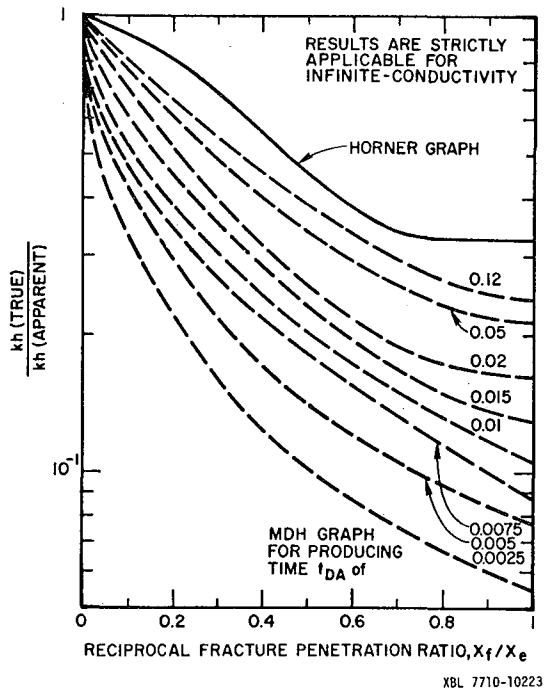

Fig. 35. Permeability-thickness correction for a vertically fractured well at the center of a closed square.

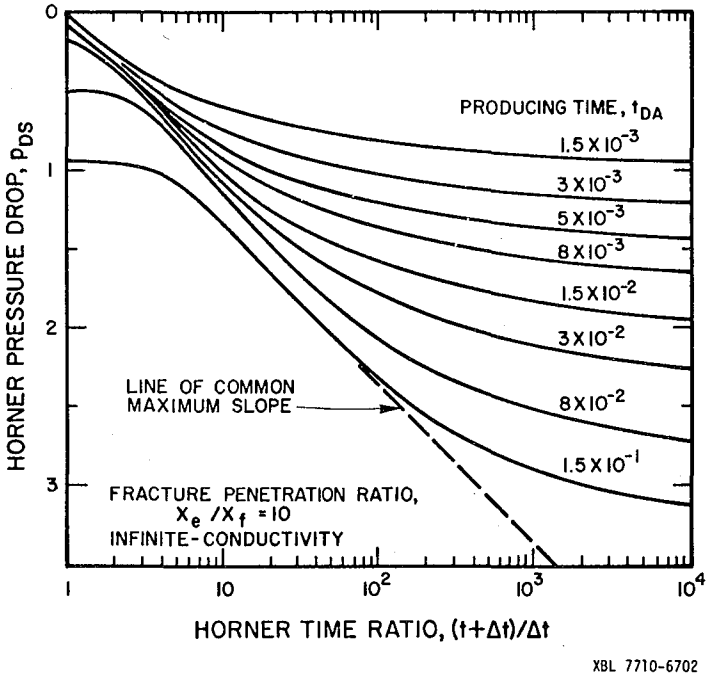

Fig. 36. Horner build-up graph for a vertically fractured well in a closed square.

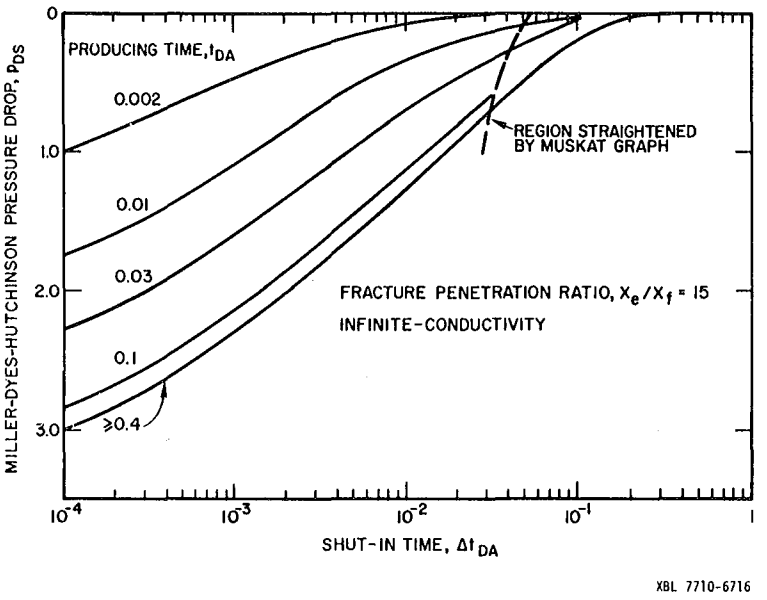

Fig. 37. Miller-Dyes-Hutchinson build-up graph for a vertically-fractured well in a constant pressure square.

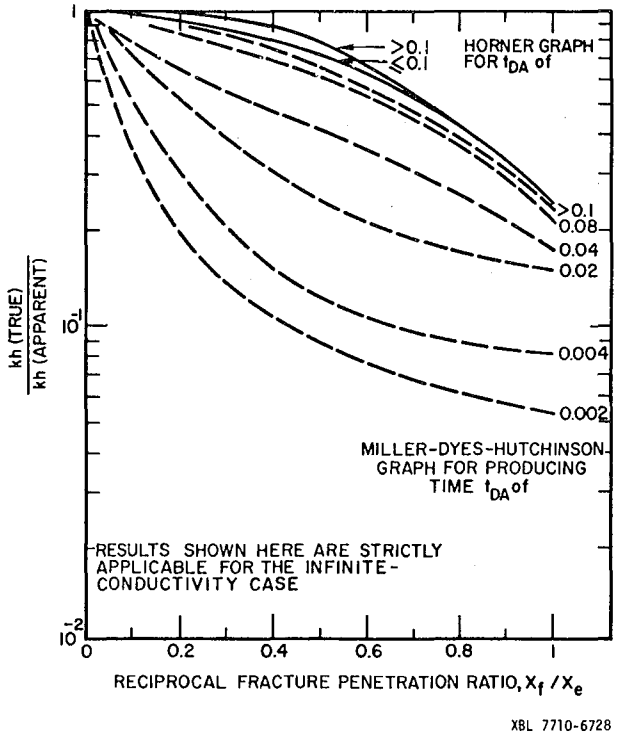

Fig. 38. Permeability-thickness correction for a vertically fractured well at the center of a constant pressure square.

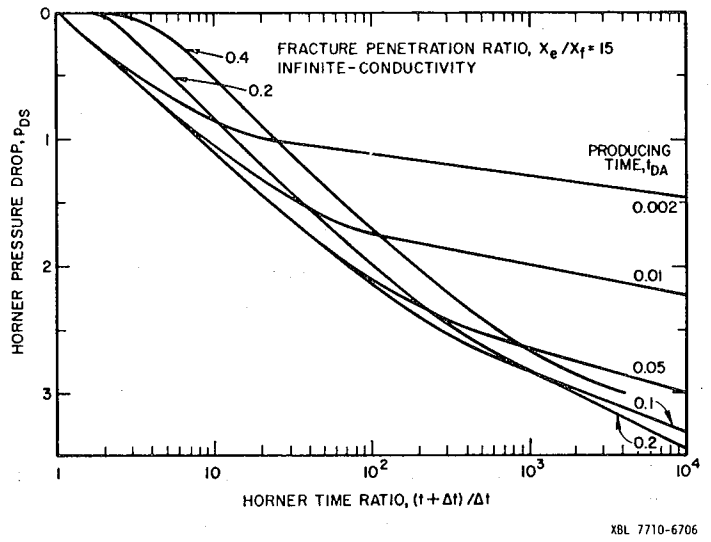

Fig. 39. Horner build-up graph for a vertically fractured well in a constant pressure square.

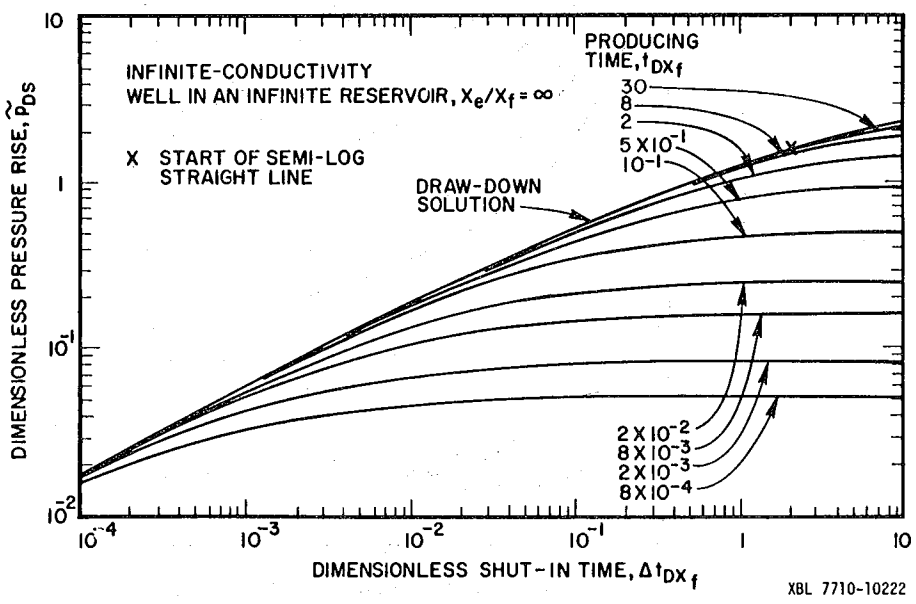

Fig. 40. Effect of producing time on build-up data.

APPLICATION AND INTERPRETATION OF DRILL STEM TEST

Merlin Anderson
Halliburton Services
Duncan,Oklahoma

INTRODUCTION

The Drill Stem Test is an analysis tool for evaluating potentially productive formation. A properly conducted test can yield information as to production rate, transmissibility, flow capacity, relative permeability, damage and possibly indicate if a limited reservoir has been encountered. The Drill Stem Test provides this information at a time when the least expenditure has been made,i.e. before the well has been completed and often before casing has been set. Knowledge of the original reservoir conditions can be important both in designing the well completion and in the reservoir engineering work performed later in the life of the well. Technology available today has provided the tools and equipment to safely evaluate almost any formation being encountered.

TESTING ON LAND

SURFACE EQUIPMENT

The surface control head equipment provides control of the well at the surface during the test. Careful thought needs to be given to the selection of this equipment to see that it adequately fulfills the requirements of the test. Questions that need to be considered are: What surface pressures are expected? Are multiple choke changes required? Will high flow rates for extended periods of time be encountered? Will the formation be treated during the test? Will wire line equipment be run through the string? Is a kill line to be connected to the test tree? Can sour gas be expected? Will chemical injection be required? The integrity of the test tree should not be compromised.

UNITEST TREE surface control equipment SYSTEM: The Unitest Tree surface control equipment System provides a series of components such that by proper selection, the control head can be custom built for the individual test requirements. A description of the components available are described below. Figure I shows two possible test tree designs.

THE LIFT NIPPLE provides a means of latching the elevators to the control head to handle the string of pipe at the surface. Often a joint of drill pipe is used for this purpose.

THE QUICK DISCONNECT provides a means of quickly altering the form of the control head. It is located in the test tree at the place it is to be changed. The portion of the test tree to be added (a lubricator for example) is preassembled to a top half of a Quick Disconnect. When it becomes desirable to change the tree design, the Master Valve is closed, the Quick Disconnect is knocked loose, the portion of the tree above the Disconnect removed and the new portion installed.

TWO TYPICAL SYSTEMS OF SURFACE EQUIPMENT FOR AN OPEN HOLE LAND TEST

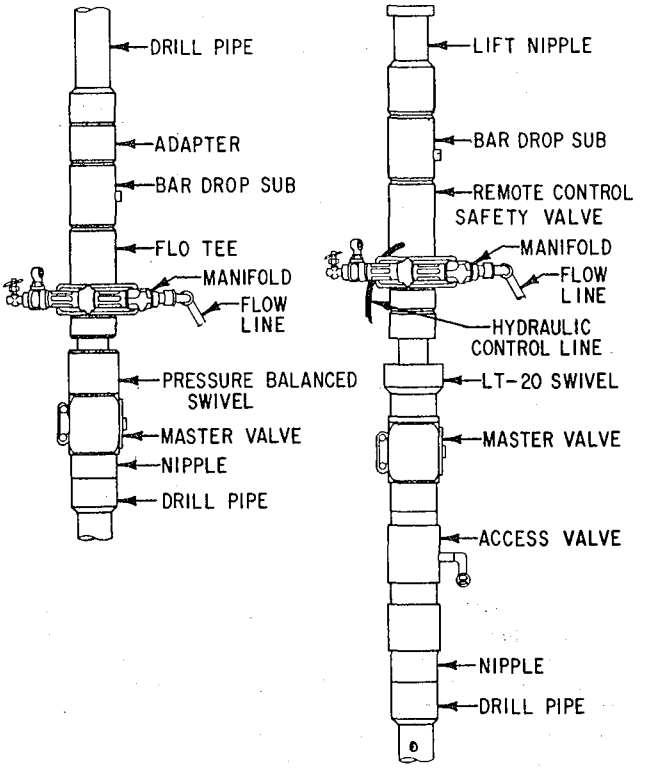

Figure I

THE BAR DROP SUB contains the brass bar that is released at the end of the test, allowed to fall to bottom, break the pin in the Impact Reversing Sub, and permit the recovery to be reversed. The Bar Drop Sub allows the bar to be installed in the control head, out of the flow stream, before the start of the test. The bar may be released with pressure on the control head. It is always recommended that, for safety reasons, the recovery be reverse circulated.

THE FLOW-TEE provides ports for the production to exit from the test tree into the manifold or the flow line. Dual ported Flow-Tee's are available when extreme flow rates for extended periods are expected. A plug is available which will close the bore at the top of the tool. The plug can be removed if other equipment is to be run above or can be replaced with a back pressure valve which will permit fluid movement down through the Flow-Tee but prevent any fluid movement in the reverse direction.

THE REMOTE CONTROL SAFETY VALVE is run in place of the Flow-Tee to provide an exit for the flow into the Manifold or flow line. As its name implies it provides additional safety by allowing the well to be shut in at the surface from a remote position. The remote Control Safety Valve contains an internal spring loaded sleeve valve. The valve normally is in the closed position. Prior to the start of the test, pressure applied through a high pressure rubber hose (run from the valve to a remote position) opens the valve. As long as the pressure is maintained, the valve will stay open. If it should become desirable to close the valve, all that is required is to release the pressure from the line. The spring, aided by the well head pressure, will close the valve. The valve may be reopened at any time by applying enough pressure to overcome the valve spring plus the well head pressure time a small differential area. The remote control valve provides an easy method of taking surface closures when the control head is positioned some distance up in the derrick. Using the safety valve for surface closures also prevents wear and possible damage to the master valve maintaining its integrity for emergency situations. The remote control valve is very desirable when testing offshore or in an area where hydrogen sulfide might be encountered.

A SWIVEL provides the ability to rotate the pipe to operate down hole tools without having to close the master valve and release the surface flow lines. If the test is conducted with rotational tools and a swivel is not used, all bottom hole closures will be preceded by a surface closure. This may be detrimental to the information being obtained.

THE MASTER VALVE is the main valve in the Control Head System and provides a means of shutting the well in at the surface. If surface closures are to be taken, it may be desirable to take these with the Remote Control Safety Valve or the manifold valves. This prevents possible wear on the Master Valve maintaining its integrity for possible emergency situations. A second Master Valve can be added if redundancy is desired.

THE ACCESS VALVE provides a means of having access into the flow stream at the Control Head. It may be necessary to inject chemicals into the flow stream to prevent a freezing action from occurring at the chokes or retard hydrate forming in the surface equipment. The Access Valve has also been used as a tap for measuring surface pressures. The Access Valve may be opened or closed by rotation of a sleeve located on the valve.

THE MANIFOLD has the valve, chokes and pressure gauges necessary for monitoring the up stream flowing pressure and controlling the flow rate. The double wing construction (two identical halves connected together) allows the well to be flowed through multiple choke sizes without ever having to shut the well in. This is accomplished by closing two valves which isolate one half of the manifold and forces the flow through the choke on the open wing. If it should become desirable to flow through a second choke size, this choke is placed in the isolated wing. The two valves controlling this wing are opened and the two valves controlling the side containing the original choke are closed, diverting the flow through the second choke. This process may be continued to flow through as many chokes as desired. The Manifold is usually fastened directly to the Flow-Tee or Remote Control Safety Valve. However, it can be placed on the rig floor with a high pressure steel hose connecting it to the Control Head.

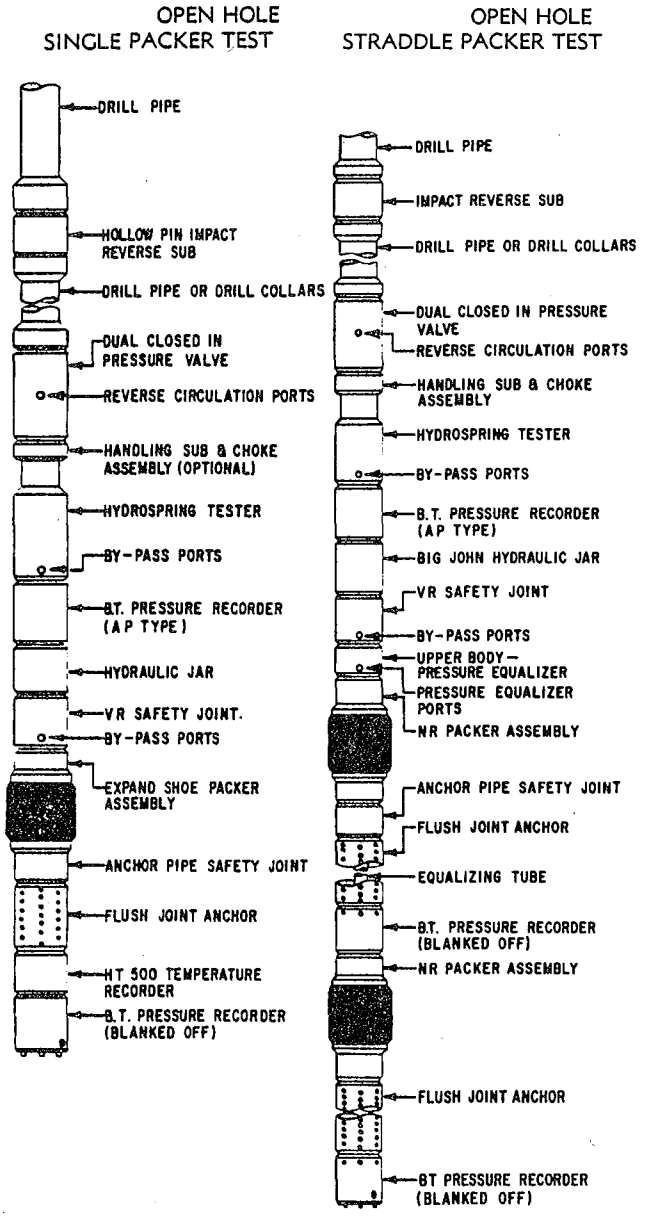

Figure 2

ROTATIONALLY OPERATED TOOLS FOR OPEN HOLE TESTING

Figure 2 illustrates a typical string of open hole and open hole straddle testing tools.

THE IMPACT REVERSING SUB provides a means of reverse circulating the recovery from the drill pipe at the conclusion of the test. The sub has a hollow brass pin that protrudes to the inside of the bore of the tool. The inside of the hollow

pin is exposed to the annulus. At the conclusion of the test a brass bar is released from the surface and allowed to fall through the drill pipe to the reversing sub, striking the hollowpin, breaking it off and opening a port from the inside of the drill pipe to the outside. The recovery may then be reverse circulated from the hole.

THE PUMP OUT SUB offers a means of reverse circulating the recovery from the drill pipe. A brass disc seals the port leading from the bore of the tool to the annulus. At the conclusion of the test, an approximate 1200 psi differential pressure applied inside the sub will shear the disc and allow the well to be reverse circulated. The disc is so constructed that it will withstand 10,000 psi differential pressure from the annulus.

THE HANDLING SUB AND CHOKE ASSEMBLY provides a means of latching the elevators on the tool string at the surface facilitating making up the tools for running in the well. There is a provision for placing a choke inside the tool if a down hole choke is required. A metal screen is placed ahead of the choke to help filter out solids in the flow stream which might tend to plug the choke. The tool is so constructed that if it should become desirable to pump fluids down through the tools, the choke and screen are by-passed removing the restriction to flow in the reverse direction.

THE DUAL CIP VALVE provides bottom hole valve for taking flow and closed in pressure periods. The Valve is initially in the open position so that when the main tester valve (Hydrospring Tester) opens, the test begins. After the desired amount of time has been given to the initial flow period, the valve may be closed by rotating the Drill Pipe to the right. The flow, closed in pressure sequence, may be repeated by further right hand pipe rotation giving a total of two flow and closed in pressure periods. After the Valve has been rotated to the final closed in pressure position, continued rotation will open reverse circulation ports allowing the recovery to reverse circulate during the final closed in pressure period. Reverse circulating through the Dual C.I.P. Valve is not normally attempted when testing open hole.

THE HYDROSPRING tester is the main valve in the tool string and is run in the hole in the closed position. A by-pass port located in the lower portion of the tool allows the well bore fluid to by-pass the packers through the inside of the tool string. This aids in reducing the pressure surges as the tools are lowered in the hole. When the tools are on bottom and pipe weight is applied to expand the packer elements, the weight activates a hydraulic metering system which controls the opening of the tester valve. After a time delay of approximately 3-5 minutes, the metering system releases allowing free fall for the last inch of valve travel. The free fall closes the by-pass port, opens the valve and provides a surface indication that the test has started. At the conclusion of the test, upward movement of the drill pipe closes the tester valve and opens the by-pass placing annulus hydrostatic pressure across the formation and terminating the test.

THE AP CASE is used to hold the flowstream pressure recorder. The pressure recorder is positioned in the center of the case with flow passage provided around the outside of the gauge.

THE HYDRAULIC JARS are used to provide an upward flow to help release the tools if they should become stuck during the test. A hydraulic metering system in the jar prevents any relative travel in the jar so a pull can be taken to stretch the drill pipe. After a short time delay, the hydraulic system releases allowing rapid upward movement of the jar mandrel which delivers an upward impact to help knock the tools loose. The jar does not meter on the downward stroke so it can be recocked rapidly to permit the maximum number of blows per unit time.

THE V.R. (VERTICAL-ROTATION) SAFETY JOINT provides a place to back-off and release the tools above the packer if packer becomes stuck and is unable to be jarred loose. This is accomplished by raising the drill pipe, applying right hand torque and lowering the pipe. This process is repeated a total of 39 times to release the safety joint. There is also a by-pass built in the Safety Joint to aid the well bore fluid in by-passing the packers. A telescoping action closes the by-pass when weight is applied to the packers.

THE OPEN HOLE PACKER affects a seal between the tool string and the wall of the hole isolating the formation to be tested from the fluid in the annulus. The packers are designed to allow the metal supports on either end and the packer elements to be changed readily so the O.D. of the packer can be sized to the diameter of the hole. A small hard rubber element below the main packer is expanded by controlled travel. It does not seal but partially bridges the gap between the metal shoes and the hole reducing the clearance and providing additional support for the main packer. All exterior metal parts are locked to the inside mandrel preventing any free rotation if it should ever become necessary to remove the packers with a wash over tool.

THE DISTRIBUTOR VALVE allows you to control the pressure in the annulus between two packers when more than one packer is run. When two packers are set in tandem the annulus fluid trapped between the two packers is compressed creating a pressure build-up ranging from 1200 psi to more than 2000 psi. The pressure increase may be sufficient to break down a weak or naturally vertical fractured formation allowing the annulus hydrostatic pressure to communicate through the formation to the tested interval. The Distributor Valve permits the annulus pressure between the two packers to be maintained at a preset valve. This progressively drops the pressure differential across the packers subjecting the formation to the least stress possible. The valve is designed such that if during the test the top packer should lose its seat dropping the total hydrostatic pressure on the bottom packer, the valve will not reopen. If the bottom packer holds, the test can be completed.

THE ANCHOR PIPE SAFETY JOINT is run below the bottom packer. This permits the string to be released below the bottom packer if the anchor pipe

becomes stuck and can not be jarred loose. It is important to back-off below the packers if possible.

This leaves a relatively simple fishing job of just having to fish for the anchor and not having to cut over the packers. A very high percentage of the time it is the anchor that becomes stuck and not the packer.

THE ANCHOR PIPE is very heavy wall pipe with a multitude of small holes through it to provide access for the well production to enter the drill pipe. The length of the anchor is varied to space the packer(s) the proper distance above the bottom of the hole. The Anchor Pipe has to be of high strength because the entire weight of the annulus column of fluid is transferred through the anchor to the bottom of the hole.

THE BLANKED OFF RUNNING CASE carries the blanked-off pressure recorder in the hole. This gauge can not sense pressure in the flow stream. It only has access to pressure from the annulus in the tested interval.

STRADDLE TESTING

Sometimes it is desirable to test a formation that had been previously penetrated and is above the bottom of the hole. Straddle Testing provides a means of isolating the formation to be tested from other potentially productive formations in the well. The Pressure Equalizing tube provides a means of maintaining annulus hydrostatic pressure below the bottom packer while preventing it from being placed across the tested interval. See Figure 2.

THE SIDE WALL ANCHOR provides a means of supporting the weight necessary to expand the packer on a straddle test when it is not practical to run anchor pipe to bottom. The tool consists of large slips which can be expanded against the bore of the hole to support the tools. The equalizing tube run when straddle testing maintains hydrostatic pressure below the bottom packer eliminating the need for the side wall anchor to support the annulus hydrostatic pressure. The drag spring assembly which provides the resistance required to expand the slips will not rotate as the tools are removed from the hole. This allows the Drill Pipe to be rotated out without the drag springs damaging the filter cake.

RECIPROCAL TESTING

The Drill Stem Test tools can also be controlled by reciprocating the drill pipe. To conduct the test with up and down pipe movement, all of the previously described tools are used with the exception of the Dual C.I.P. Valve. The tools listed below are added or modified as described.

THE MODIFIED HYDROSPRING TESTER is a conventional hydrospring that has been modified to permit taking closed in pressures. The bypass is removed from the bottom of the tool and an indexing 'J' slot added at the top. The tool is run in the closed position. When weight is set through the Hydrospring tester to expand the packers, a hydraulic metering system is activated in the tool. After a 3 to 5 minute time delay the Hydrospring tester opens starting the test. A free fall travel of approximately one inch at the time the tool opens, jars the drill pipe, giving a surface indication that the test has started. When it becomes desirable to close the Hydrospring tester for a bottom hole closed in pressure, the drill pipe is picked up until the Hydrospring tester closes. The 'J' slot at the top of the tool indexes allowing weight to be reapplied to the tools without the valve reopening. To open the valve for subsequent flow, the drill pipe is again raised to a neutral position and weight applied to the tool. The 'J' slot indexes and the Hydrospring tester opens after the 3-5 minute time delay caused by the hydraulic metering system. This process may be repeated to permit as many flow and closed in pressure periods as desired.

THE L.O.C. (LOCKED OPEN CLOSED) BY-PASS is run in conjunction with the modified Hydrospring tester to provide the fluid by-pass that was removed from the bottom of the Hydrospring tester. The By-Pass is open going in the hole and does not close until just before the Hydrospring opens. After the by-pass has closed, it remains closed until returned to the surface.

THE EXTENSION JOINT provides the free travel necessary to close the Hydrospring tester without unseating the packer. After the Hydrospring tester closes the additional upward travel of the Extension Joint can be taken before the packer releases. Each Extension Joint provides 30 inches of free travel. As many Extension Joints as required can be run to provide the free travel necessary to conduct the test.

TESTING INSIDE CASING

The tools required for testing inside casing are the same as described for open hole testing with the exception that the open hole packers are replaced with a casing hookwall packer and the flush joint anchor is replaced with perforated tail pipe.

Additional tools for testing in casing are described in the section under Floating Vessel Testing.

THE SAMPLER is a modification of the tester valve to allow it to catch a sample under final flowing conditions. Samplers are available for rotational or reciprocal testing. The size of the trapped sample ranges from 2100 to 2750 cc depending on the Sampler used. The sample from a drill stem test is taken at final flowing conditions where phase separation may have occurred and therefore should not be considered a P.V.T. sample. The following information is available from the sample: Recovery volumes, amounts of gas, oil, water, mud, API gravity of the oil, specific gravity of the water, chloride content of the water, resistivity of the water, and the gas oil ratio in the Sampler.

If there is water in the drill pipe recovery and no water in the Sampler, then the final fluids flowing contained no water and this is a good in-

dication that the water in the Drill Pipe is infiltrate loss and not formation production. This is an additional check in conjunction with the chlorides, and the resistivity as to where the water came from.

If a larger sample is required, then one to three drill collars can be run between the Dual C.I.P. Valve and the Hydrospring tester. A drain valve is run above and below the collars. A drop and seat, to prevent fluids in the sample from draining to bottom during the closed in pressure periods, is run below the lower drain valve. The sample will be trapped at final closed in pressure. The gas is removed from the sample chamber through top drain valve. The liquids are then drained from the lower drain valve.

MECHANICS OF TESTING

Preplanning and the use of proper procedures will greatly aid in safely obtaining the objectives of the test. Selection of the equipment will have to be based on the type of test to be conducted and the hole conditions that exist. Consideration should be given to the size and type of tools required, the pressure gauge range, length of the gauge clocks, bottom hole temperature, whether the well is being drilled underbalanced, whether H_2S is to be expected. All these factors will have an effect on the success of the test.

If it is to be open hole test, conditioning the hole prior to the test will do more to insure a mechanically successful test than any other single factor. More misruns are caused by anchor perforation and/or tool plugging than any other reason.

As the tools are made up on location, the proper amount of flush joint anchor is placed in the tail pipe to space the packer(s) the desired distance from bottom. If the available flush joint anchor, usually about 40 feet, does not provide the desired length, then drill collars can be added to achieve the proper interval. When drill collars are run in the anchor, they are normally placed above the perforated anchor. This is because the O.D. of the collars is usually larger than the perforated anchor and would, if run on bottom, expose an upward step at the transition between the collars and the anchor. This step would be a good place for any solids settling out of the flow stream to bridge and possibly stick the tail pipe. If the perforations are run on bottom, any small solids in the annulus would be carried through the anchor into the flowstream. Drill Pipe should never be used as tail pipe. It does not have the strength to withstand the tremendous loads that can be applied to the anchor during the test.

It is common to place drill collars on top of the string of test tools to help provide the rigidity and weight required at the tools to set the packers. In some areas "weight pipe" is used for this purpose. Weight pipe is Drill Pipe with a second piece of pipe fitted lengthwise providing additional weight and rigidity. Weight pipe can not be distinguished from Drill Pipe by outward appearance. If weight pipe is used, it should be made certain that the length and I.D. is correctly reported; otherwise, an erroneous liquid production rate calculation could result.

The hole should be full at the time the tools are started. If water cushion is to be run, either for protecting the drill pipe from collapse pressure, or for placing a back pressure against the formation, a heavy gel should be mixed and poured in the first few joints of pipe run on top of the tools. This will hold in suspension any scale, dried mud, etc., that may be washed out of the drill pipe and prevent it from settling inside and plugging the tools.

Water cushion should be added approximately every 10 stands. This will help prevent large air pockets from accumulating in the cushion.

The rise in the level of the mud pit should be monitored as the drill pipe is run. The increase should be equal to the volume of mud being displaced by the pipe. If it is less than the volume being displaced, then fluid is being lost in the hole. A formation may be taking fluid or the drill pipe may be leaking. If the increase is greater than the volume being displaced, then some formation is producing into the well. If this is occurring, the well is underbalanced and the threat of a kick is very real.

The drill pipe should not be run at an exceedingly high rate. The piston effect could create pressure surges great enough to exceed the fracture gradient of the formation. A rate of approximately 1 foot per second is about right.Periodically, the drill pipe should be checked for leaks. A very slight blow from the drill pipe should not create concern, as this may be caused by expansion of air from the increase in temperature. However, if a drill pipe leak develops, it should be discovered and corrected or a mis-run will result.

As the tools approach packer depth, the rate should be slowed down to watch for bottom. If the pipe tally is in error, the tools could hit bottom before expected and possibly damage the pipe or tool string. The Control Head equipment is made up on the last joint and the pipe slowly worked up and down observing the indicator coming up and going down. A 5 minute wait with the pipe hanging stationary prior to setting weight on the packer should yield a clean place on the charts for reading initial hydrostatic pressure.

After it has been observed that the hole is full, the desired weight, usually 20-40,000 lb, is placed on the packer. The height of the Control Head above the rotary table should be observed. If it is higher in the derrick than it should be,this is an indication of fill on bottom. The cuttings and cavings creating the false bottom will usually explode up around the tail pipe when the tester valve opens causing the packers to start sliding to bottom, picking up additional mud in the recovery, creating situations conducive to anchor perforation plugging, and also possibly sticking the anchor pipe.

Someone should be assigned to observe the

annulus from the time the tester valve opens until the packer is unseated. If the fluid in the annulus drops, the pipe should be picked up immediately to close the tester valve and prevent the mud from u-tubing. A second attempt may be made to obtain a test by setting more weight on the packers than was applied in the first attempt. If the packer does not seat after 2 or 3 tries, the tools should be removed and the hole conditioned or another packer seat selected.

The recommended testing procedures for obtaining good reservoir information are discussed under the chart interpretation section. However, it is felt the test should be conducted based on the well's performance and not restricted to some preset inflexible plan.

If the test is being conducted inside casing, the drill pipe recovery may be reverse circulated during the final closed in pressure. However, it is usually unacceptable to reverse in open hole while the packers are still seated.

At the conclusion of the final C.I.P., the pipe is raised to terminate the test.
The by-pass opens placing hydrostatic pressure across the tested interval and equalizing pressure around the packers. Continued upward movement unseats the packers. The packers should be given a few minutes after releasing to give them time to return to their original diameter. If the pipe is started out of the hole immediately, the packers may not have returned to size and cause a problem in swabbing the well. After the packers have been unseated and the tools free, one of the reverse circulating subs should be activated and the recovery reverse circulated from the drill pipe. The constituents in the recovery can be fairly accurately determined by observing the returns, catching samples and counting the pump strokes. There will be a fluid sample below the reversing sub, and a sample between the Dual C.I.P. valve and the Hydrospring tester. Also, a sampler may be run if desired.

The trip out of the hole is probably the most dangerous time during a drill stem test. This is when everyone feels the test is concluded and lets their guard down. As the pipe is removed from the hole, the annulus should be filled approximately every 10 stands. The amount of mud required to fill the annulus should be measured. If this is less than the volume of the pipe removed, then some formation is feeding into the annulus. This may be caused by the packer swabbing the well. The rate the tools are being pulled should be reduced. If the amount to fill the annulus continues to be less than the volume of the drill pipe removed, consideration should be given to going back to bottom and conditioning the mud. If the trip out of the hole is continued with the formation coming in, the well may become underbalanced and the threat of a blow out exists.

Another hazard is present when hydrocarbons have been recovered and not reverse circulated. The pipe is pulled wet. The agitation of the recovery as the pipe is removed often causes gas to come out of solution resulting in a spray of oil blowing out the top of the pipe. Anytime the rig is showered with oil, there is a threat of fire. The fire will not last long, but the toll in human resources and equipment can be great. Wet plugs (plugs designed to blank off the top joint of a stand of drill pipe to prevent the pipe from unloading as it is raised in the derrick) are sometimes used when pulling a set string. However, the tendency of the plug to get loose and fall from the elevators as they are lowered for the next stand seems to present a greater threat to the crew than the risk of fire. Both threats are removed if the recovery is reverse circulated.

When the tools reach the surface, the pressure recordings should be inspected for a visual interpretation of the test. This will indicate if the test is a mechanical test as well as giving an immediate indication of permeability (low, medium, high), well bore damage (none, low,medium, high), possibly depletion,etc. The first pressure recording recovered will be from the flow stream gauge. A decision on the test should not be based on analysis of this gauge alone. The blanked off pressure recording should also be inspected and compared to the flow stream gauge. If they do not look alike, an explanation as to why they don't should be obtained.

TESTING FROM FLOATING VESSELS

Figure 3 illustrates a Drill Stem Test being conducted from a floating vessel(next page).

SURFACE EQUIPMENT

The Unitest Tree surface control equipment system as described for land testing is applicable for the offshore testing. The componentized approach allows the control head to be configured in the manner required for a particular test. Often two master valves are run for redundancy. A master valve and flow-tee may be placed on top of the test tree to permit a kill line to be installed throughout the test.

SUBSURFACE EQUIPMENT

THE SUB-SEA TEST TREE (SSTT) increases the safety of an offshore test by providing an ocean floor test tree. The SSTT is run as a part of the test string and is spaced out such that it is landed in the blow-out preventer (BOP) stack when the tools are on bottom. The Test Tree is sized to the stack so the pipe rams may be closed against the SSTT. Two ball valves in the SSTT are in the normally closed position. A dual conduit hydraulic line is run from the SSTT, strapped to the side of pipe, to the surface. Pressure applied through the hydraulic line to the SSTT rotates the ball valves to the open position. The valves will remain open as long as the pressure is maintained. Anytime the pressure is released, either on purpose or through an accident such as the line being severed by the vessel being blown off location,the ball valves automatically close shutting the well in at the ocean floor. The valves may be reopened by again applying pressure to the lines.

A quick disconnect allows the pipe above the SSTT to be released from the SSTT if it should become desirable to do so. This is accomplished

either hydraulically applying pressure through the second conduit of line running to the surface or by rotation of the pipe. The geometry of many of the BOP Stack will permit the blind rams to be closed above the SSTT after the pipe is released. The pipe from the surface can be run and re-engaged in the SSTT whenever desired.

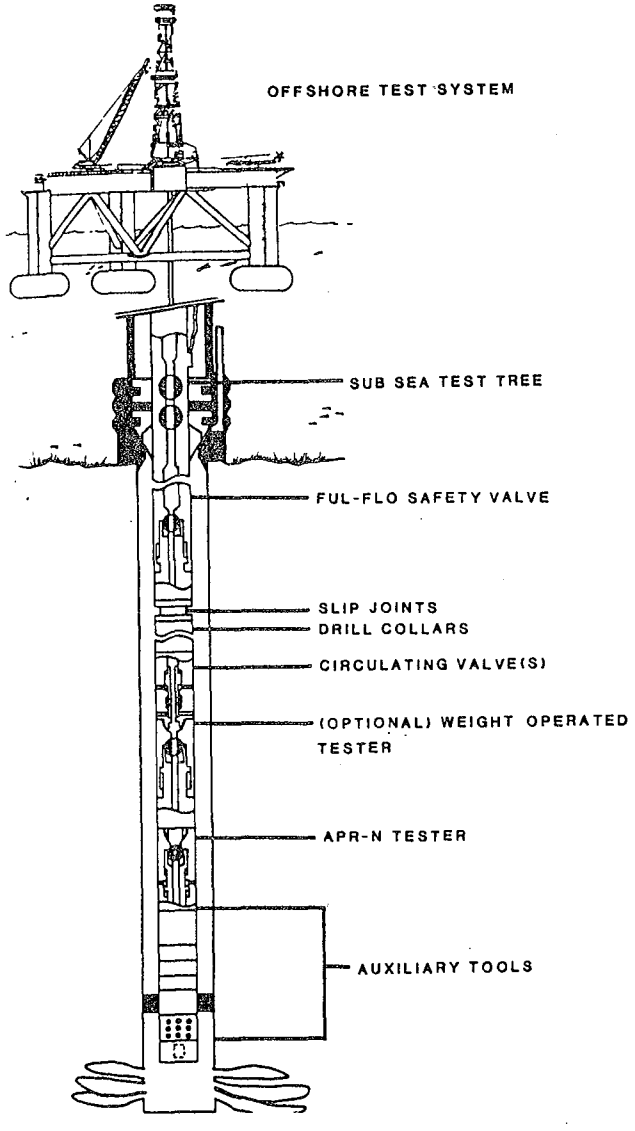

Figure 3

THE FUL-FLO SAFETY VALVE TESTING TOOL is designed to provide additional safety by automatically shutting the well in if the pipe should part near the ocean floor but below the Sub-Sea Test Tree. The valve is placed in the string the appropriate distance above the upper slip joints. It consists of a ball valve which is held open as long as the valve is in tension. If the pipe parts the falling action of the pipe will telescope the valve to the closed position. A pressure build-up in the pipe below the valve will not pump the valve back to the open position.

The valve has also found an application for open hole tests in areas where Hydrogen Sulfide may be encountered. It is run just high enough in the string to remain in tension when the packer is set. If the pipe should part during the test, the valve will close shutting in the well and possibly preventing a blowout.

THE SLIP JOINTS are free travel joints designed to counteract the effect of pipe movement while operating down hole tools and to provide a means of accurately placing the desired weight on the down hole packers. After the amount of weight to be placed on the down hole tools has been run, the Slip Joints are inserted in the string. When the packer is set and the pipe landed at the ocean floor, the Slip Joints will be in the neutral position with the weight below resting on the tools. In areas where the vessel movement is minimal, these Slip Joints are sometimes omitted from the string. Slip Joints are also used for free travel joints below the weight operated tester valves to aid in their operation.

THE TYPE 'A' REVERSE CIRCULATING VALVE provides a dependable means of reverse circulating the recovery from the pipe. The valve is set, prior to going in the hole, to open when the desired pressure is applied to the casing. This permits the recovery to be reverse circulated without any mechanical manipulation. Usually either the pump out or impact reverse circulating sub (described in open hole testing) is run to provide redundancy.

THE ANNULUS PRESSURE RESPONSIVE (APR) TESTER VALVE was designed to permit a test to be conducted inside casing without any manipulation of the pipe. This greatly simplified testing from floating vessels where the constant motion of the rig made the operation of the tool by pipe movement difficult. The valve is controlled by the application and release of pressure applied to the casing. After the packer has been set, the valve is opened by applying the appropriate pressure to the casing. The valve is closed by releasing the casing pressure. The tester valve can be opened and closed as many times as necessary. If the casing pressure should exceed a pre-determined amount, the valve automatically closes and can not be re-opened until it is returned to the surface. This is a safety feature which will shut the well in, if a leak should develop in the drill pipe, before a dangerously high pressure could be applied to the casing.

PROCEDURE FOR TESTING FROM FLOATING VESSELS

The testing tools are made up and run in the hole until the weight indicator shows the desired amount of weight, usually about 25,000 lb, to be above the tools. The upper slip joints are installed in the string and the pipe from the slip joints to the ocean floor run. The Sub-Sea Test Tree placed in the string and the remainder of the pipe run. The surface test tree is installed and pressure tested. If a full string of water cushion is run, the entire pipe string from the surface to the tester valve can be tested. The packer is then set and the pipe lowered until the Sub-Sea Test Tree is landed in the B.O.P. stack. This places the upper Slip Joints in the neutral position with the pipe weight above supported by the fluted hanger. The weight below the Slip Joints is resting on the tools and packer.

If the weight actuated tools are run, the tester valve will open after a short time delay. The remainder of the test is conducted by reciprocating the pipe when it is desired to open or close the tester valve.

If the Annulus Pressure Responsive tools are run, the pipe rams are closed against the Sub-Sea Test Tree and the casing pressured to the predetermined amount. This opens the tester valve. The remainder of the test is conducted by release and reapplication of the casing pressure. No pipe movement is required.

During the final bottom hole closure, or after the packer has been unseated, one of the reverse circulating valves is opened and the recovery is reverse circulated from the pipe. The tools are then returned to the surface.

HIGH VOLUME TESTING

Some of the offshore wells being encountered were capable of producing at extremely high rates. These wells needed to be adequately defined during the test so the proper drilling and producing platforms could be designed. The extreme cost of these facilities left little room for error. The restricted bore through conventional tool did not permit the highly prolific wells to be drawn down sufficiently to allow the reservoir's characteristics to be accurately determined. To obtain the formation parameters from these wells, a full opening string of test tools and related surface equipment was developed. These tools permit a well to be flowed at high rates for extended periods of time. See Figure 3.

THE SURFACE CONTROL HEAD equipment was modified to permit the flow to exit from both sides of the Remote Control Safety Valve. All right angle turns are replaced with large radius sweeps to help prevent fluid cutting. A bypass floor choke manifold allowed the flow to be diverted through the manifold when desired and bypass the manifold the remainder of the time.

THE TESTER VALVES, the Ful-Flo Hydrospring tester which is a weight actuated valve, and the full opening APR tester valve were designed with full openings to permit unrestricted flow.

THE BUNDLE CARRIER was designed to carry two pressure recorders and two temperature recorders without restricting the bore through the case. The recorders are carried in pockets milled in the outside of the case. The pressure gauges have ports leading from the bore of the case to the gauge. This allows the gauges to be run above the packers as flow stream gauges or they may be run as blanked off gauges below the packers.

THE FULL OPENING TESTING TOOLS designed for high volume testing had several other advantages which became apparent. The full opening permitted the formation to be perforated through the tool after they were in place and the packer set. This allows the well to be perforated in an underbalanced condition (formation pressure greater than tubing hydrostatic) helping prevent the well from becoming damaged by producing back crushed formation particles and debris from shooting. If the bundle carrier is used, the gauges are already in place, the perforating gun is removed and the test started. If the bundle carrier is not used, the perforating gun is removed and the gauges run in on wire line and landed in a seating nipple positioned below the packer. The wire line is then removed and the test run.

The full opening tools also permit the formation to be stimulated through the tools. When the formation is to be treated during the test, the reverse circulating valves are often replaced with tubing operated circulating valves. The pumping equipment is connected to the Test Tree through a kill line. The well is tested in the conventional manner taking the desired flow and closed in periods. The well can then be stimulated through the test tools. The top circulating valve is opened, the recovery reverse circulated and the treating fluid circulated to bottom. The tester valve is opened, and the formation treated. After the treatment, the formation is again tested to evaluate the treatment.

If difficulty is encountered in breaking down the formation, the test can be terminated or special procedures may be followed. One procedure would be to kill the well through the circulating valve, pull the test string and remove the Sub-Sea Test Tree. Install a back pressure valve and run the string back down until the upper circulating valve is below the perforations. Acid is spotted across the perforations and the string pulled to remove the back pressure valve. The Sub-Sea Test Tree is reinstalled and the test string run back to the original packer depth. The formation is broken down, treated and the testing resumed.

CHART INTERPRETATION

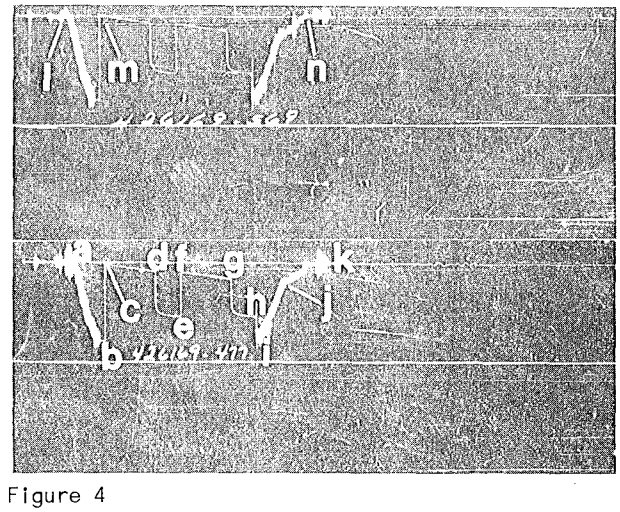

Figure 4

The Charts shown in Figure 4 are typical Bourdon Tube (BT) type pressure recordings of a dual closed in drill stem test. The top chart is the flow stream gauge and the bottom chart is the blanked off gauge. Time on a B.T. chart starts at the left and increases from left to right. The time represented in the time axis is dependent upon the clock being used in the gauge. Clocks of 12, 24, 48, 72 and 120 are available. Pressure

starts at the zero pressure line or "base line" and increases in the down direction. The base line is scribed on the chart by the gauge at the surface prior to running in the well. The other horizontal line on the charts are placed on the chart at the time it is read. Each of these lines represent 1000 psi unless another value is written on the lines. The vibrations at the start 4-a and at the end 4-k of the test represent vibration of the stylus at the time the gauges are made up and removed from the running case. These vibrations should be on the charts and indicate the stylus assembly is free. The vibration excursions should be centered on the base line with approximately one half above and one half below. The line extending diagonally down is the recording of the tools being run in the hole. The width of the line is actually drawn by vertical stylus movement caused by pressure surges due to the piston effect of the tools being lowered in the hole.

Visual observation of this line will indicate hole conditions and/or the speed the tools were run in the hole. Running the tools at excessive speeds can cause pressure surges sufficient to possibly break down a formation. The short horizontal line at 4-b represents the initial hydrostatic pressure. At 4-c, the test valve has opened and the pressure dropped to the hydrostatic head above the gauges. When no water cushion is run, the pressure will be close to zero. The portion of the chart from 4-c to 4-d represents the initial flow period. The rise in pressure is due to the increase in hydrostatic pressure from the formation flowing into the drill pipe. At point 4-d, the tester valve is closed and the formation allowed to regenerate its pressure in the drawn down area, from 4-d to 4-e. The valve is again opened at point 4-e. The pressure at the start of the second flow period on a liquid production test should be close to the same as the pressure at the end of the initial flow period. This is because there should be the same hydrostatic head on the gauge at the start of the second flow as was there when the valve was closed for the initial C.I.P. If the pressure is less than the final of the initial flow, then this indicates the drill pipe is unloading at the surface during the closed in pressure. If the second flow starts at a distinct higher pressure than the end of the initial flow, this is a strong indication of possible drill pipe leakage. The well is open to flow from 4-f to 4-g. At point 4-g, the valve is closed for the final closed in pressure. At point 4-h, the drill pipe is raised opening the by-pass and dropping the hydrostatic pressure across the formation. The final hydrostatic pressure is read at 4-i. At 4-j, the rate the tools are being pulled is slowed down. The recovery has been reached and the string is pulled wet. At 4-k, the gauge has been returned to the surface.

When looking at a B.T. pressure chart, the first observation that should be made is if the base line is good. Does the gauge start and end on the base line? If the gauge starts and ends on the base line, then the information recorded can be considered to be true. If it does not start and/or end on the base line, a gauge problem may be indicated. The flow stream gauge starts above the base line 4-l and returns to the surface above the base line 4-n. The initial flow pressure also extends above the base line 4-m, indicating a vacuum was drawn against the gauge. Of course, this did not occur. The base line on a B.T. chart has to be drawn with the gauge in the vertical position. If the base line is drawn with the gauge laying down, the weight of the stylus assembly will cause the Bourdon Tube to rotate slightly causing the base line to be drawn in error. When the gauge is returned to the vertical position, the stylus assembly rotates back to the true zero. This is an example of an improperly drawn base line.

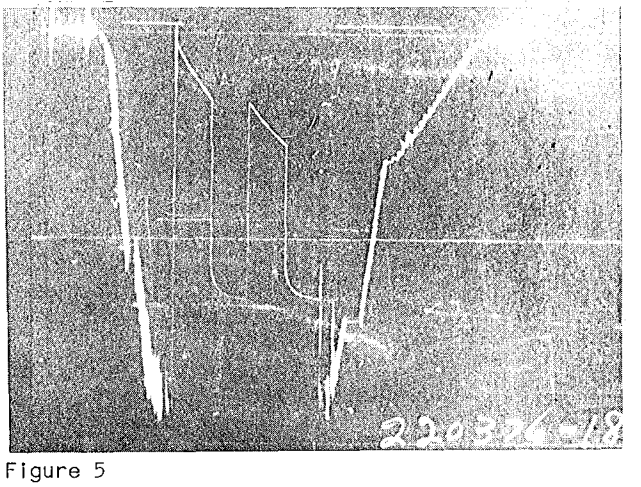

Figure 5

Figure 5 is an example of a properly conducted test. Two good flow periods are taken with one half of the total flow time given to each flow. Production calculation can be made from each flow period. Two good closed in pressures are recorded both with sufficient closure for reliable Horner extrapolation. The closed in pressure periods are equal in duration to the flows. This is sufficient for a well with this permeability but is not necessarily the correct procedure for other wells. More will be discussed on this later. With the ability to make production calculations from the flow periods and to extrapolate the closed in pressures, the reservoir parameters may be calculated from both build-ups. The drill pipe was not reverse circulated and the string was pulled wet.

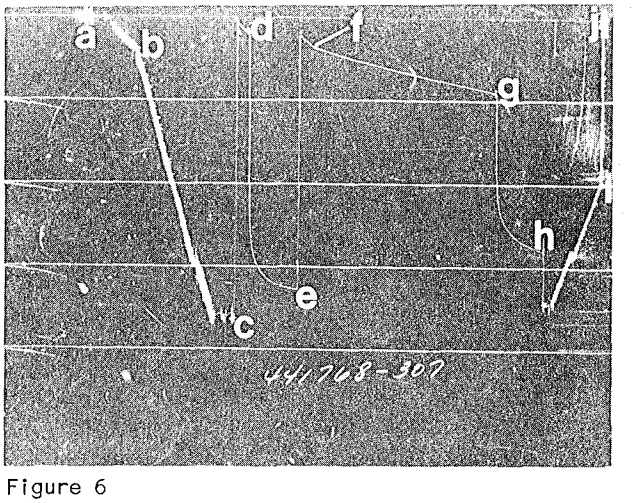

Figure 6

The test in Figure 6 is a good test mechanically. The gauge starts on the base line 6-a. At point 6-b, the rate the tools are being run in the hole is increased. The reason for the slower rate to this point is that drill collars are being run until this time. At 6-c, the tester valve is opened and the initial flow is started. At 6-d, the valve is closed for the initial closed in pressure. At 6-e, the valve is reopened for the final flow. At point 6-f, there is a direct angular break recorded in the flow period. It gives the appearance of a sudden reduction in rate when such is not the case. It is caused by the transition of production from the small capacity of the drill collars into the large capacity of the drill pipe. At 6-g, the valve is closed and the final closed in pressure period taken until the test is terminated at point 6-h. The trip out of the hole is recorded until 6-i, at which the chart time expired. It is not necessary for the trip out of the hole to be on the chart. The vibration that occurs when the gauge is removed 6-j indicates the gauge did return to the base line. The obvious question that arises from this test is, is the well depleting? A comparison of the two closed in pressures gives a strong indication of reservoir pressure caused by the production during the second flow period. If that is the case, then the well should not be completed based on this zone. However, there is a second possible cause for the discrepancy between the two closed in pressures: Super Charge. Super Charge is a term that is used to describe the over pressured zone adjacent to the well bore and caused by infiltrate loss into the formation. This is referred to as the flush zone or invaded zone on the logs. There is a pressure gradient starting at hydrostatic pressure at the well bore and extending to true reservoir pressure some distance back in the formation. The depth of the pressure invasion is primarily a function of permeability. The lower the permeability, the deeper the invasion. If the well is not produced for a sufficient length of time during the initial flow period to remove this invaded pressure, the initial build up will reflect the invaded pressure and record a false closed in pressure. The problems involved in interpreting this test would be removed if sufficient time to positively remove Super Charge had been given to the initial flow. It is recommended that a minimum of 30 minutes and preferably half the total flow time be given to the initial flow period. If the possibility of Super Charge does exist, the one clue which can help determine if it is depletion or Super Charge is the second flow period. If the well is producing at a constant rate, approximately equal increases in flow pressure for incremental time, then the reservoir can not be losing energy. This test does indicate a relative constant rate of production from 6-f to 6-g; therefore depletion is not occurring and the initial closed in pressure is Super Charged. The time spent during the initial C.I.P. 6-d to 6-e is actually a waste of rig time.

The test shown in Figure 7 is similar in appearance to the preceding test with a short initial and long final flow. The final closed in pressure will never reach the valve recorded on the initial C.I.P. Again the question, is this Super Charge or is it depletion? Looking at the

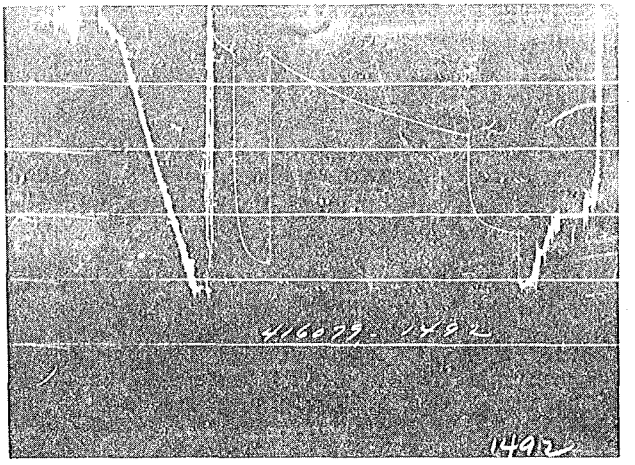

Figure 7

second flow period, it can be seen that the production rate is continually declining from start to finish. This is a very strong indication that depletion is occurring. If it is felt that this is not conclusive enough evidence, then the well should be retested. On the second test sufficient time should be given to the initial flow period to positively remove Super Charge forces. Again a long second flow should be taken. A comparison of the two closed in pressures on this test with each other and with the pressures recorded on the previous test should give a conclusive answer.

There is one other phenomena that causes a declining rate during the flow period back pressure. The back pressure due to the increase in hydrostatic head inside the drill pipe will eventually cause a decline in production rate. A 'rule of thumb' from the observation of many tests is that the declining rate will start to become readily apparent when the back pressure is approximately equal to half of the formation pressure.

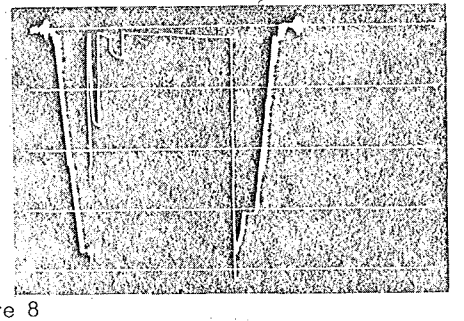

Figure 8

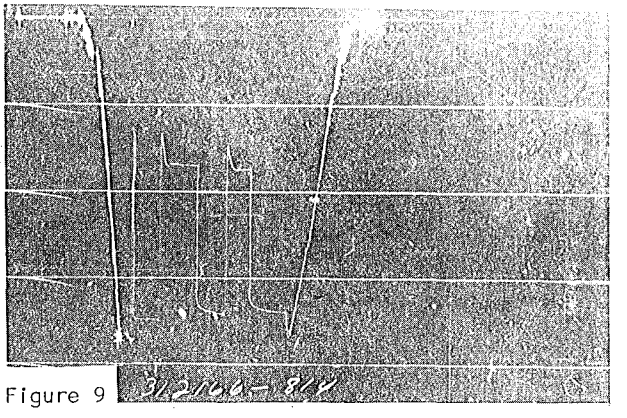

Figure 9

Figure 8 shows a test with three flows and closed in pressures. The reason usually given for taking three flows and closed in pressures is to check for depletion. On this test the reservoir pressure is almost completely depleted at the conclusion of the final flow. However, what we most often see with three flows and closed in pressures is indicated in Figure 9. On this test, due to the short first flow, the initial closed in pressure is still under the influence of Super Charge and will extrapolate to a higher value than the second and third C.I.P. The second and third closed in pressures are good. It is felt that many times two properly conducted flows and closed in periods will yield better information than three or more. Often there is only a certain amount of time permitted on bottom. If this time is divided into three or more flow and closed in periods, there is not sufficient time in any of the periods to obtain good information.

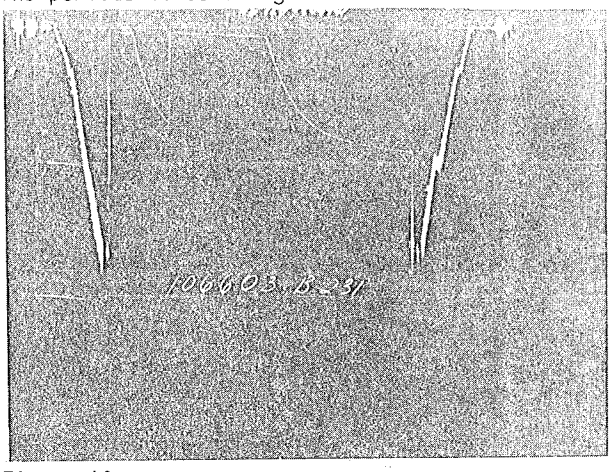

Figure 10

Figure 10 is a test where the surface reaction (very little indicated production) is saying low permeability. If the formation has low permeability, then it takes longer to get good reservoir information. More time is required to remove Super Charge and it will take longer for the closed in pressures to develop. On this test the initial flow period may or may not have been long enough to remove Super Charge. Insufficient time was given the initial C.I.P. It does not have enough closure for a reliable Horner extrapolation and provides very little information. The second closed in pressure was given enough time to develop a good build up from which reservoir parameter can be determined. The initial C.I.P. could be considered a waste of rig time.

Figure 11 illustrates a test where again the reaction at the surface indicated low permeability. This suggested an extended time would be required to obtain good closed in pressures. However, the buildups developed very rapidly with short radius of curvature and yielded two good closed in pressures. The fast build up is not compatible with low permeability. The reason for the discrepancy is high well bore damage. The quick buildup results because the formation is capable of producing at a much greater rate than the restricted permeability at the well bore will allow. Consequently there is little draw down and when the tester valve is closed, the formation quickly regenerate pressure. With a little practice, a visual interpretation will give an indication of damage. The indicated permeability needs to be weighed against how rapidly the build up occurs. Figure 12 shows a test indicating high permeability and no damage. The visual interpretation of damage on gas wells can be a little more difficult.

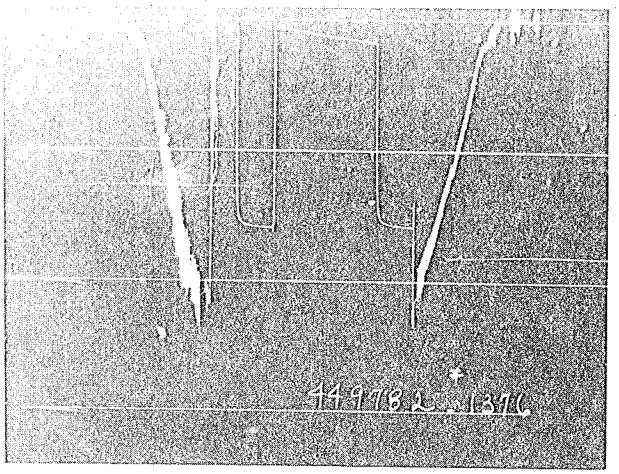

Figure 11

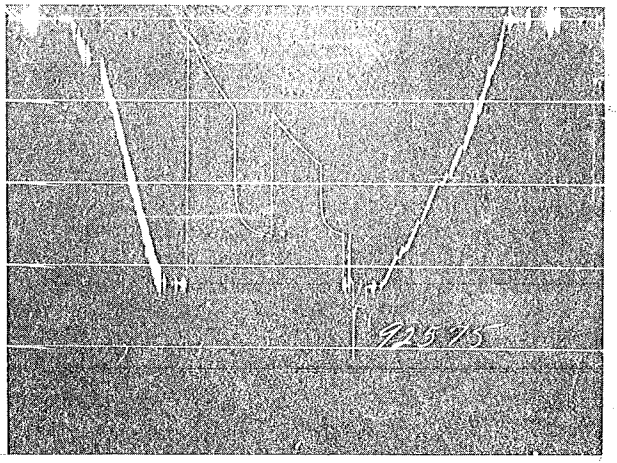

Figure 12

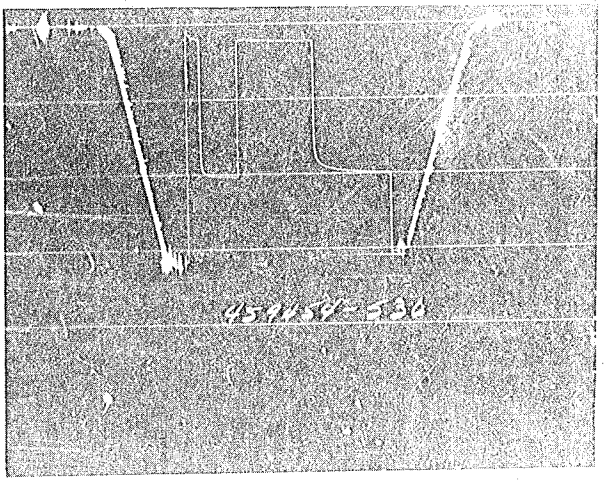

Figure 13

Figure 13 illustrates a gas producing well.

There is one procedure difference be[illegible]ring a gas well and a liquid well. The pr[illegible]on rate on a liquid test can be gauged if it [illegible] to the surface or can be calculated from the [illegible]wing pressure on the chart if it does not. [illegible]e rate on a gas well has to be measured at the surface. Due to the short duration of the initial flow period on this test, the rate was not measured and therefore no reservoir calculations can be made from the initial C.I.P. A near stabilized rate was obtained during the final flow period. The final C.I.P. could be extrapolated and reservoir calculations made.

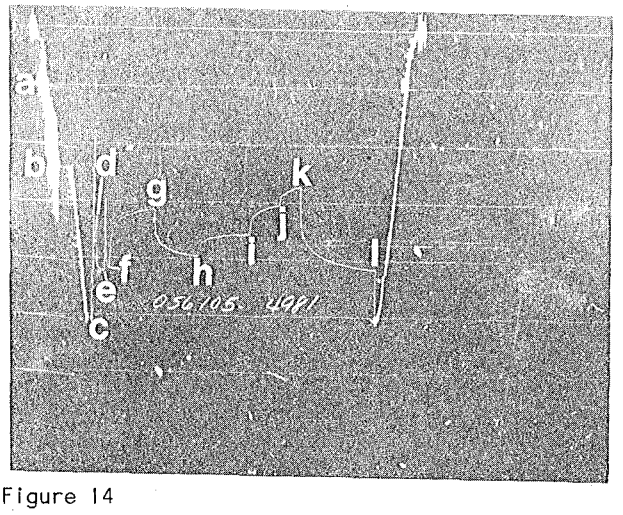

Figure 14

Figure 14 illustrates a mechanically successful gas well test. The test starts and ends on the base line. Stops were made at 14-a and 14-b to add water cushion. The tester valve was opened at 14-c for a short initial flow. At 14-d the tester valve was closed and a build up recorded. At 14-e the tester valve was opened and the surface valve closed. The surface valve was opened at 14-f and the well flowed for a clean up period to 14-g. At 14-g the well was placed on a small choke and produced against the small choke until 14-h. At 14-h the well was placed on a larger choke. At 14-i the choke was changed to a still larger choke. At 14-j the final choke change was made. At 14-k the tester valve was closed and a bottom hole closed in pressure taken. At 14-l the bypass was opened and the hydrostatic pressure dropped across the formation. If the well is to be flowed through a series of chokes, the proper sequence is to start with the smallest choke and progressively change to larger ones. This extends the radius of investigation further into the reservoir and increases the radius of curvature in the closed in pressures making them easier to interpret. If the well is flowing against a small choke at the time it is closed in, the back pressure may be so great that the closed in pressure will build so quickly that it is difficult to obtain enough reading in the curved portion to make a Horner Plot.

Flowing the well against increasingly larger choke sizes, however, can also create problems. If the well is not allowed to stabilize during the flow periods, it can be exceedingly difficult to obtain accurate information from the test. On this test the bottom hole charts indicate the sand face flowing pressure was never allowed to stabilize during the test.

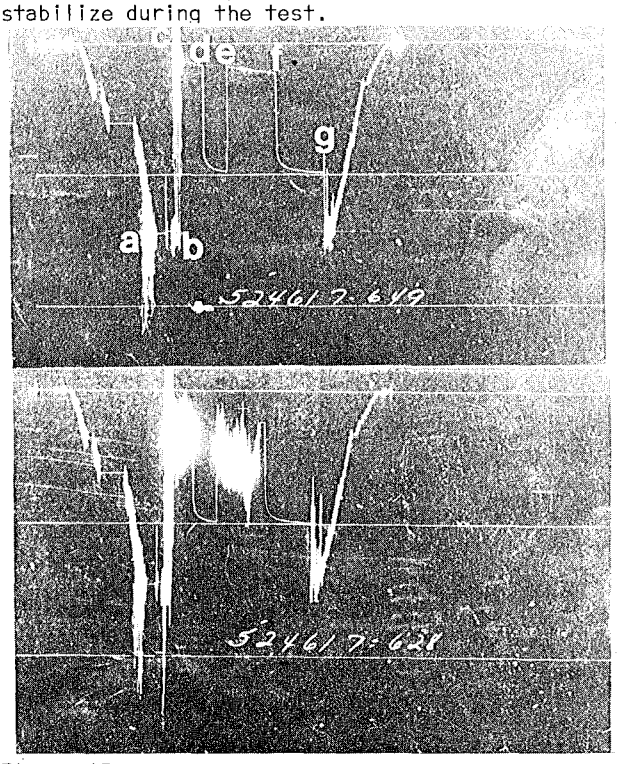

Figure 15

A decision on a test should not be made on the basis of the flow stream gauge alone. It should always be compared to the blank-off gauge. Figure 15 shows the flow stream and blanked off gauge. The charts indicate severe hole conditions exist near the bottom 15-a. The extreme shake of the opening line 15-b to 15-c is an indication of the tools sliding to bottom. The height of the control head above the rotary should have been a clue that the tools were resting on fill and not on bottom. The flow periods from the flow stream gauge 15-c to 15-d and 15-e to 15-f indicate low permeability. Close examination does show a little roughness during the flows. The flow periods on the blanked off gauge show a completely different picture. Severe anchor perforations plugging is occurring. When all of the anchor perforations plug, it is the same as closing a valve on the blanked off gauge; and it starts a pressure buildup. Then a perforation breaks free and the pressure released. The continual plugging and releasing creates the appearance of the flow periods shown on the blanked off chart. The bypass is opened at 15-g. The pressure surges at the start of the trip out indicate the jars had to be tripped to drive the tools out of the cuttings and cavings on bottom. It should have been expected that plugging and possible sticking the tools would occur because of the difficulty in reaching bottom. The conditions encountered at 15-a should have been sufficient cause to remove the tools and make a bit trip to clean the hole. This test was a complete waste of rig time. Plugging due to cuttings and cavings left on bottom are the single largest cause of misruns.

Figure 16 shows a test where the plugging action is shown on both the flow stream and the

blanked off charts. This indicates the plugging is occurring above the flow stream gauge, and therefore it is the tools that are plugging.

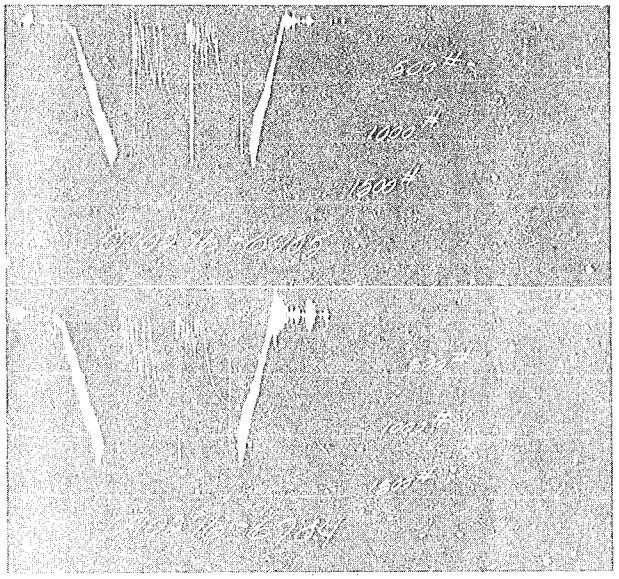

Figure 16

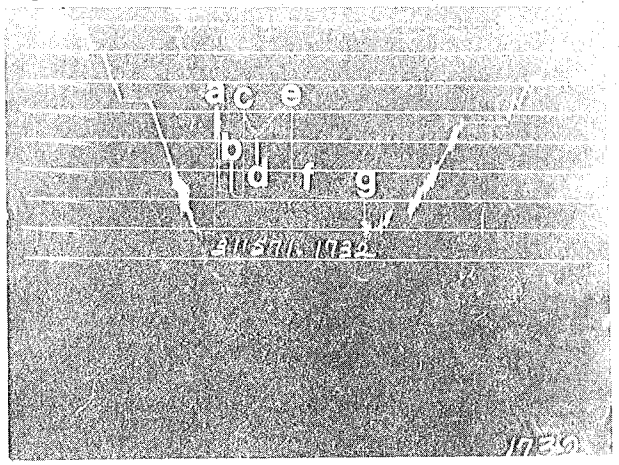

Figure 17

Figure 17 illustrates a problem that can occur when long intervals are tested. The trip in the hole indicates stops were made periodically to add water cushion. The tester valve was opened at 17-a with the gauges recording the back pressure of the water cushion. After an extremely short initial flow period, the tester valve was closed and the initial shut in pressure taken. Observing the initial C.I.P. at 17-b, it can be seen that a second buildup is imposed on the early buildup. The tester valve was opened at 17-c for a second flow. The portion of the second flow from 17-c to 17-d indicates a rise in hydrostatic due to production into the drill pipe. At 17-d the water cushion surfaces and the decline in flowing pressure for the remainder of the period is caused by the water cushion being produced from the pipe and being replaced by a lighter oil. At 17-e the tester valve is closed for the final closed in pressure. Again at 17-f a second buildup is imposed on the early buildup. At 17-g the bypass is opened and the test terminated. The buildup on a buildup is an indication that two distinct zones of different permeability and pressure are open in the tested interval. This makes it very difficult to arrive at the individual reservoir properties. To evaluate these zones, they should be isolated and tested separately.

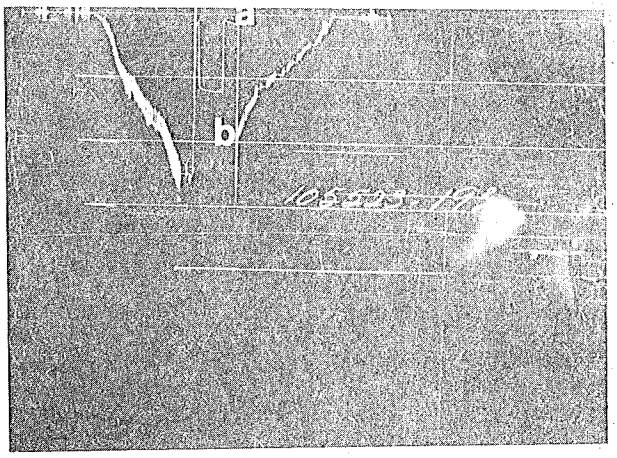

Figure 18

Figure 18 indicates a test where there was a gauge malfunction. The chart shows the initial flow and closed in periods. The test appears to have terminated at 18-a. However, the second flow was longer than shown and there was a final closed in pressure taken. The clock in the pressure gauge stopped at 18-a and the remainder of the flow and the C.I.P. was recorded as a vertical line. The clock remained stopped until the vibration of the gauge on the trip out of the hole started the clock running again at 18-b and the rest of the trip from the hole was recorded.

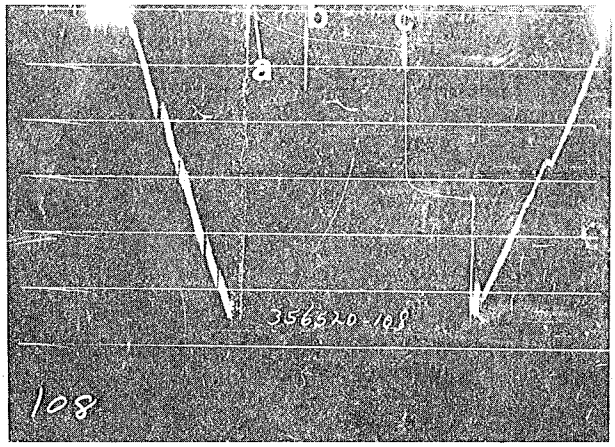

Figure 19

Figure 19 shows a test which has one flow and closed in pressure. However, the operator attempted to close the valve at 19-a for an initial closed in pressure. The valve was not successfully operated and remained open. At 19-b the operator thinking the valve was closed attempted to open it for a second flow. Again the valve remained open. At 19-c the operator successfully closed the valve and a closed in pressure was recorded.

Figure 20 represents an unsuccessful test. The tester valve was opened at 20-a and an initial flow period recorded from 20-a to 20-b. The valve was closed at 20-b for an initial closed in

pressure. The tester valve was leaking and no C.I.P. was recorded. The valve was again opened at 20-c and a second flow taken from 20-c to 20-d. The tester valve was closed at 20-d for the final C.I.P. Again the tester valve was leaking and the pressure buildup was not recorded. At 20-e the bypass was opened ending the test.

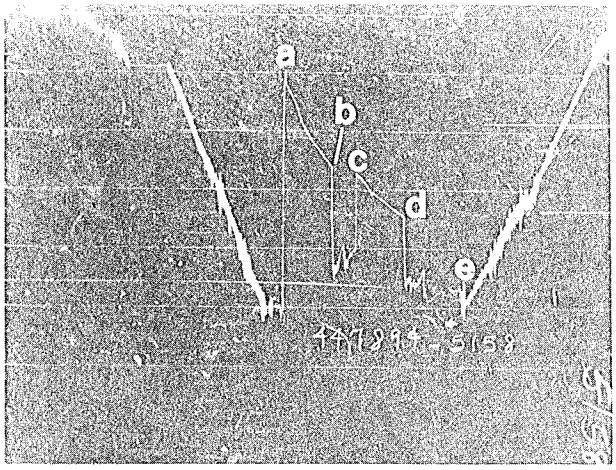

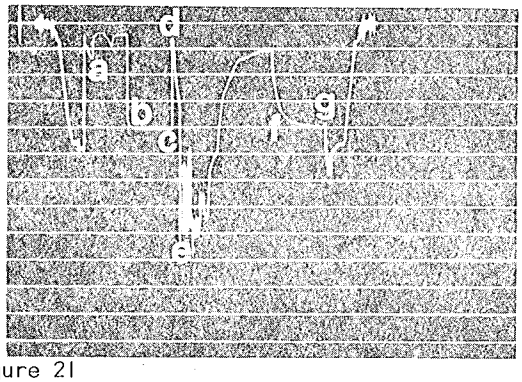

Figure 21

Figure 21 shows a Drill Stem Test where the formation was tested, then treated through test tools and retested to evaluate the treatment. This test was conducted in the North Sea through full opening tools. The tester valve was opened and after 25 minutes the water cushion flowed to the surface 21-a. At the end of the flow period the rate had stabilized at 1500 MCF/D with a surface pressure of 136 PSI. The tester valve was closed and an initial C.I.P. reached 4048 PSI, 21-c. The physical appearance of this buildup (a relatively low flowing back pressure followed by a very rapid short radius buildup 21-b is an indication of well bore damage. The damage ratio for this buildup was calculated to be 9.3. The tester valve was reopened 21-d and the well stimulated with acid 21-e. The well was then opened for a second flow and produced at a rate in excess of 7200 MCF/D at a surface pressure of 180 PSI. This is an increase of 4.8 fold over the initial rate. The valve was closed and a final closed in pressure of 3975 PSI recorded 21-g. The appearance of the final C.I.P. 21-f differs in appearance from the initial closed in pressure. The final C.I.P. has a more gradual rate of closure indicating little well bore damage and a greater radius of investigation.

CONCLUSION

Modern equipment and techniques offer the versatility to test a well in the manner best suited for that particular well. The test can be conducted by or without pipe movement. The full opening test tools permit the extreme flow necessary to evaluate prolific wells, allows the formation to be perforated with the tools already in place and permits the formation to be tested, treated and retested all on one trip in the hole.

There is a need to have real time pressure information available at the surface during the test. This can be accomplished currently with wire line run through the test string to bottom. However, the objections to the wire line have been sufficient that very few people have been willing to test in this manner. Telemetry (which has received considerable attention but no workable solution for testing) would be extremely beneficial on Drill Stem Test.

ABSTRACT

WELL-TESTING PRACTICE AND ANALYSIS IN FISSURED AQUIFERS

A. C. Gringarten
Bureau de Recherches Geologiques et Minieres

A new method for interpreting pump test data in fissured aquifers is discussed. The pumped well behavior is analysed in terms of an equivalent anisotropic porous medium, with a single fracture intersecting the well-bore. By means of type curves, it is possible to calculate the directional permeabilities of the aquifer, and the direction and volume of the "equivalent single fracture," which provides a measurement of the fissure density. Field data are presented, which indicate that accurate very early time measurements (of the order of a few seconds) are required in many cases for the method to be applicable.

CONVERSION TABLES

Table 1.

PERMEABILITY

ρ_ω = 1 viscosity = 1 centipoise

	cm^2	m^2	ft^2	Darcy	cm/sec	ft/sec	ft/year	litres/ $sec \cdot m^2$	gpd[U.S.]/ft^2 (Meinzer)	Ebhlm*
cm^2	1	10^{-4}	1.076×10^{-3}	1.014×10^{8}	9.804×10^{4}	3.216×10^{3}	1.015×10^{11}	8.698×10^{5}	1.845×10^{9}	0.9
m^2	10^{4}	1	1.076×10^{1}	1.014×10^{12}	9.804×10^{8}	3.216×10^{7}	1.015×10^{15}	8.697×10^{9}	1.845×10^{13}	0.8
ft^2	9.294×10^{2}	9.294×10^{-2}	1	9.417×10^{10}	9.109×10^{7}	2.988×10^{6}	9.430×10^{13}	8.080×10^{8}	1.714×10^{12}	0.7
Darcy	9.862×10^{-9}	9.862×10^{-13}	1.062×10^{-11}	1	9.66×10^{-4}	3.173×10^{-5}	1.001×10^{3}	8.58×10^{-3}	1.82×10^{1}	0.6
cm/sec	1.020×10^{-5}	1.020×10^{-9}	1.097×10^{-8}	1.035×10^{3}	1	3.281×10^{-2}	1.035×10^{6}	9.985×10^{0}	2.118×10^{4}	0.5
ft/sec	3.109×10^{-4}	3.109×10^{-8}	3.347×10^{-7}	3.152×10^{4}	3.048×10^{1}	1	3.156×10^{7}	2.704×10^{2}	5.736×10^{5}	0.4
ft/year	9.852×10^{-12}	9.852×10^{-16}	1.060×10^{-14}	9.990×10^{-4}	9.662×10^{-7}	3.169×10^{-8}	1	8.570×10^{-6}	1.818×10^{-2}	0.3
litres/$sec \cdot m^2$	1.150×10^{-6}	1.150×10^{-10}	1.238×10^{-9}	1.166×10^{2}	1.001×10^{-1}	3.698×10^{-3}	1.167×10^{5}	1	2.121×10^{3}	0.2
gpd[U.S.]/ft^2 (Meinzer)	5.420×10^{-10}	5.420×10^{-14}	5.834×10^{-13}	5.494×10^{-2}	4.721×10^{-5}	1.743×10^{-6}	5.500×10^{1}	4.714×10^{-4}	1	0.1
Ebhlm*	0.9	0.8	0.7	0.6	0.5	0.4	0.3	0.2	0.1	1

*Standard Ethiopian buckets per hectare per lunar month.

Dimensions: k, Absolute Permeability [L^2]

K, Hydraulic Conductivity [L/t]

k/μ, Mobility [L^3t/M]

Table 2.

COMPRESSIBILITY

[Lt^2/M]

	m^2/N (Pascals)$^{-1}$	m^2/kg_f	in^2/lb_f (psi)$^{-1}$	Bars^{-1}	Atm^{-1}	(ft of water)$^{-1}$ at 68°F	(m of water)$^{-1}$ at 68°F
m^2/N (Pascals)$^{-1}$	1	9.807	6.897×10^{3}	10^{5}	1.0133×10^{5}	2.984×10^{3}	9.794×10^{3}
m^2/kg_f	1.020×10^{-1}	1	7.031×10^{2}	1.0197×10^{4}	1.0332×10^{4}	3.042×10^{2}	9.980×10^{2}
$in.^2/lb_f$ (psi)$^{-1}$	1.450×10^{-4}	1.4223×10^{-3}	1	14.504	14.696	0.4327	1.419
Bars^{-1}	10^{-5}	9.8068×10^{-5}	6.895×10^{-2}	1	1.01325	2.984×10^{-2}	9.790×10^{-2}
Atm^{-1}	9.8692×10^{-6}	9.6787×10^{-5}	6.805×10^{-2}	0.98692	1	2.945×10^{-2}	9.662×10^{-2}
(ft of water)$^{-1}$ at 68°F	3.351×10^{-4}	3.287×10^{-3}	2.311	33.512	33.956	1	3.281
(m of water)$^{-1}$ at 68°F	$1.021\ 10^{-4}$	$1.002\ 10^{-3}$	.7044	10.214	10.349	0.3048	1

Table 3.

TEMPERATURE

°C to °F

°C	°F	°C	°F	°C	°F	°C	°F	°C	°F
0	32	100	212	200	392	300	572	400	752
5	41	105	221	205	401	305	581	405	761
10	50	110	230	210	410	310	590	410	770
15	59	115	239	215	419	315	599	415	779
20	68	120	248	220	428	320	608	420	788
25	77	125	257	225	437	325	617	425	797
30	86	130	266	230	446	330	626	430	806
35	95	135	275	235	455	335	635	435	815
40	104	140	284	240	464	340	644	440	824
45	113	145	293	245	473	345	653	445	833
50	122	150	302	250	482	350	662	450	842
55	131	155	311	255	491	355	671	455	851
60	140	160	320	260	500	360	680	460	860
65	149	165	329	265	509	365	689	465	869
70	158	170	338	270	518	370	698	470	878
75	167	175	347	275	527	375	707	475	887
80	176	180	356	280	536	380	716	480	896
85	185	185	365	285	545	385	725	485	905
90	194	190	374	290	554	390	734	490	914
95	203	195	383	295	563	395	743	495	923

Table 4.

VOLUME

$[L^3]$

	m^3	litre	bbl	Gallon (U.S.)	Gallon (Imp.)	ft^3
m^3	1	10^3	6.289	2.642×10^2	2.20×10^2	35.315
litre	10^{-3}	1	6.289×10^{-3}	0.2642	0.220	3.5315×10^{-2}
bbl	.1590	1.590×10^2	1	42.0	34.97	5.6146
gallons (U.S.)	3.7854×10^{-3}	3.7854	2.381×10^{-2}	1	0.8327	0.13368
gallons (IMP)	4.546×10^{-3}	4.546	2.860×10^{-2}	1.2009	1	0.16054
ft^3	2.832×10^{-2}	28.32	0.178	7.481	6.229	1

Table 5.

FLOW RATE $[L^3/t]$ or $[M/t]$

	m^3/sec	litres/min	bbl/day	gallons/min (U.S.)	gallons/min (Imp.)	ft^3/sec	klb/hr (ρ_w=1.0)	klb/hr (ρ_w=.9)
m^3/sec	1	6×10^{4}	5.434×10^{5}	1.585×10^{4}	1.320×10^{4}	35.315	7.94×10^{3}	7.15×10^{3}
litres/min	1.667×10^{-5}	1	9.058	0.2642	0.220	5.885×10^{-4}	1.32×10^{-1}	1.19×10^{-1}
bbl/day	1.840×10^{-6}	1.10×10^{-1}	1	2.917×10^{-2}	2.428×10^{-2}	6.498×10^{-5}	1.46×10^{-2}	1.31×10^{-2}
gallons/min (U.S.)	6.31×10^{-5}	3.785	34.28	1	0.8327	2.2280×10^{-3}	0.50	0.45
gallons/min (Imp.)	7.58×10^{-5}	4.546	41.19	1.2009	1	2.676×10^{-3}	0.601	0.541
ft^3/sec	2.8317×10^{-2}	1.699×10^{3}	1.539×10^{4}	4.488×10^{2}	3.737×10^{2}	1	2.25×10^{2}	2.03×10^{2}
klb/hr ρ_w=1.0	1.26×10^{-4}	7.56	68.5	2.00	1.66	4.45×10^{-3}	1	0.900
klb/hr ρ_w=0.9	1.40×10^{-4}	8.42	76.2	2.22	1.85	4.93×10^{-3}	1.11	1

Table 6.

PRESSURE
$[M/Lt^2]$

	N/m^2 (Pascals)	kg_f/m^2	lb_f/in^2 (psi)	Bars	Atm	ft of water (at 68°F)	m of water (at 68°F)
N/m^2 (Pascals)	1	1.020×10^{-1}	1.450×10^{-4}	10^{-5}	9.8692×10^{-6}	3.351×10^{-4}	1.021×10^{-4}
kg_f/m^2	9.804	1	1.4223×10^{-3}	9.8068×10^{-5}	9.6787×10^{-5}	3.287×10^{-3}	1.002×10^{-3}
lb_f/in^2 (psi)	6.895×10^{3}	7.031×10^{2}	1	6.895×10^{-2}	6.805×10^{-2}	2.311	0.7042
Bars	10^{5}	1.0197×10^{4}	14.504	1	0.98692	33.512	10.214
Atm	1.0133×10^{5}	1.0332×10^{4}	14.696	1.01325	1	33.956	10.349
ft of water (at 68°F)	2.984×10^{3}	3.042×10^{2}	0.4328	2.984×10^{-2}	2.945×10^{-2}	1	0.3048
m of water (at 68°F)	9.794×10^{3}	9.980×10^{2}	1.419	9.790×10^{-2}	9.662×10^{-2}	3.281	1

Table 7: Viscosity (dynamic)

Pa·s	lbf·s/in^2	lbf·s/ft^2	kgf·s/m^2	lbm/ft·s	dyne·s/cm^2	cP	lbm/ft·h
Pa·s	6.894 757 E+03	4.788 026 E+01	9.806 650*E+00	1.488 164 E+00	1.0* E-01	1.0* E-03	4.133 789 E-04

Table 8: Viscosity (kinematic)

m^2/s	ft^2/s	in^2/s	m^2/h	cm^2/s	ft^2/h	cSt
m^2/s	9.290 304*E+04	6.451 6* E+02	2.777 778 E+02	1.0* E+02	2.580 64* E+01	1

Table 9: Diffusivity

m^2/s	ft^2/s	cm^2/s	ft^2/h
m^2/s	9.290 304*E+04	1.0* E+02	2.580 64* E+01

Table 10: Thermal Conductivity

W/m·K	cal/s·cm^2·°C/cm	Btu/h·ft^2·°F/ft	kcal/h·m^2·°C/m	Btu/h·ft^2·°F/in	cal/h·cm^2·°C/cm
W/m·K	4.184* E+02	1.730 735 E+00	1.162 222 E+00	1.442 279 E-01	1.162 222 E-01

Table 11: Density (liquids)

kg/m^3	lbm/U.S. gal	lbm/U.K. gal	lbm/ft^3	g/cm^3	°API
kg/m^3	1.198 264 E+02 1.198 264 E-01	9.977 633 E+01 9.977 633 E-02	1.601 846 E+01 1.601 846 E-02	1.0* E+03 1	

Table 12: Specific Heat Capacity (mass basis)

J/kg·K	kW·h/kg·°C	Btu/lbm·°F	kcal/kg·°C
J/Kg·K	3.6* E+03	4.186 8* E+00	4.184* E+00

Table 13: Enthalpy Calorific Value on (mass basis)

J/kg	Btu/lbm	cal/g	cal/lbm
J/kg	2.326 000 E-03 2.325 000 E+00 6.461 112 E-04	4.184* E+00	9.224 141 E+00

Table 14.

COMPARISON OF UNITS AND EQUATIONS IN VARIOUS UNIT SYSTEMS.*

Oilfield Units	SI Units	Preferred API Standard SI Units	cgs Units*	Groundwater Units
q — production rate, STB/D	m^3/s	dm^3/s	cm^3/s	Q — production rate, gal/min
h — formation thickness, ft	m	m	cm	m — formation thickness, ft
k — permeability, md	m^2	μm^2	darcy	—
μ — viscosity, cp	$Pa \cdot s$	$Pa \cdot s$	cp	—
k/μ — mobility, md/cp	$m^2/(Pa \cdot s)$	$\mu m^2/(Pa \cdot s)$	darcy/cp	P or K — coefficient of permeability, gal/day ft^{2}**
kh/μ — mobility-thickness product, md ft/cp	$m^3/(Pa \cdot s)$	$m(\mu m^2)/(Pa \cdot s)$	darcy · cm/cp	T — coefficient of transmissivity, gal/(day ft)**
Δp — pressure difference, psi	Pa	kPa	atm	s — drawdown, ft of water, >0 for pressure drawdown**
p — pressure, psi	Pa	kPa	atm	h — head of water, ft of water
r — radius, ft	m	m	cm	r — radius, ft
t — time, hours	s	h	s	t — time, days
ϕ — porosity, fraction				—
c_t — total system compressibility, psi^{-1}	Pa^{-1}	kPa^{-1}	atm^{-1}	—
$\phi c_t h$ — porosity-compressibility-thickness product, ft psi^{-1}	$m \cdot Pa^{-1}$	$m \cdot kPa^{-1}$	$cm \cdot atm^{-1}$	S — coefficient of storage, fraction**
DIMENSIONLESS TIME				
$t_D = \dfrac{0.000263679\,kt}{\phi\mu c_t r_w^2}$	$t_D = \dfrac{kt}{\phi\mu c_t r_w^2}$	$t_D = 3.6 \times 10^{-4}\,\dfrac{kt}{\phi\mu c_t r_w^2}$	$t_D = \dfrac{kt}{\phi\mu c_t r_w^2}$	$\alpha = 0.1336805\,\dfrac{Tt}{Sr_w^2}$
DARCY'S LAW FOR INCOMPRESSIBLE, RADIAL FLOW				
$q = \dfrac{0.00708188\,kh(p_e - p_w)}{B\mu \ln(r_e/r_w)}$	$q = 2\pi\,\dfrac{kh(p_e - p_w)}{B\mu \ln(r_e/r_w)}$	$q = \dfrac{2\pi \times 10^{-4}\,kh(p_e - p_w)}{B\mu \ln(r_e/r_w)}$	$q = 2\pi\,\dfrac{kh(p_e - p_w)}{B\mu \ln(r_e/r_w)}$	$Q = \dfrac{0.00436332\,T(h_e - h_w)}{\ln(r_e/r_w)}$
DIFFUSIVITY EQUATION				
$\dfrac{\partial^2 p}{\partial r^2} + \dfrac{1}{r}\dfrac{\partial p}{\partial r} = \dfrac{1}{0.000263679}\dfrac{\phi\mu c_t}{k}\dfrac{\partial p}{\partial t}$	$\dfrac{\partial^2 p}{\partial r^2} + \dfrac{1}{r}\dfrac{\partial p}{\partial r} = \dfrac{\phi\mu c_t}{k}\dfrac{\partial p}{\partial t}$	$\dfrac{\partial^2 p}{\partial r^2} + \dfrac{1}{r}\dfrac{\partial p}{\partial r} = \dfrac{1}{3.6 \times 10^{-4}}\dfrac{\phi\mu c_t}{k}\dfrac{\partial p}{\partial t}$	$\dfrac{\partial^2 p}{\partial r^2} + \dfrac{1}{r}\dfrac{\partial p}{\partial r} = \dfrac{\phi\mu c_t}{k}\dfrac{\partial p}{\partial t}$	$\dfrac{\partial^2 h}{\partial r^2} + \dfrac{1}{r}\dfrac{\partial h}{\partial r} = \dfrac{1}{0.1336805}\dfrac{S}{T}\dfrac{\partial h}{\partial t}$
GENERALIZED TRANSIENT FLOW EQUATION				
$\Delta p = \dfrac{141.205\,qB\mu\,p_D(t_D)}{kh}$	$\Delta p = \dfrac{qB\mu\,p_D(t_D)}{2\pi kh}$	$\Delta p = 10^{6}\,\dfrac{qB\mu\,p_D(t_D)}{2\pi kh}$	$\Delta p = \dfrac{1}{2\pi}\,\dfrac{qB\mu}{kh}\,p_D(t_D)$	$s = 229.183\,\dfrac{Q}{T}\,p_D(\alpha)$
SLOPE OF SEMILOG STRAIGHT LINE				
$m = 162.568\,\dfrac{qB\mu}{kh}$	$m = 0.183234\,\dfrac{qB\mu}{kh}$	$m = 1.83234 \times 10^{5}\,\dfrac{qB\mu}{kh}$	$m = 0.183234\,\dfrac{qB\mu}{kh}$	$M = 263.857\,\dfrac{Q}{T}$
GENERALIZED SKIN-FACTOR EQUATION				
$s = 1.15129\left[\dfrac{p_{1hr} - p(\Delta t = 0)}{m} - \log\left(\dfrac{k}{\phi\mu c_t r_w^2}\right) + 3.227546\right]$	$s = 1.15129\left[\dfrac{p_{1hr} - p(\Delta t = 0)}{m} - \log\left(\dfrac{k}{\phi\mu c_t r_w^2}\right) - 0.351378\right]$	$s = 1.15129\left[\dfrac{p_{1hr} - p(\Delta t = 0)}{m} - \log\left(\dfrac{k}{\phi\mu c_t r_w^2}\right) + 5.092319\right]$	$s = 1.15129\left[\dfrac{p_{1hr} - p(\Delta t = 0)}{m} - \log\left(\dfrac{k}{\phi\mu c_t r_w^2}\right) - 0.351378\right]$	$\text{skin} = 1.15129\left[\dfrac{s_{1hr} - s(\Delta t = 0)}{M} - \log\left(\dfrac{T}{Sr_w^2}\right) + 0.522555\right]$

SOURCE: Robert C. Earlougher, Jr., *Advances in Well Test Analysis*, Monograph Volume 5: Henry L. Doherty Series, Henry L. Doherty Memorial Fund of AIME, Society of Petroleum Engineers of AIME (New York, Dallas: 1977).

*The cgs system is considered to be obsolete and is replaced by SI; cgs units are included only for comparison with published material. SI is a coherent system, so equations do not contain units conversion factors.

**See Table A.8.

GLOSSARY OF TERMS

GW: Terms commonly used in Hydrogeology

PE: Terms commonly used in Petroleum Engineering

AFTER FLOW, (PE) See "Wellbore Storage".

AFTER INJECTION, (PE) See "Wellbore Storage".

AFTER PRODUCTION, (PE) See "Wellbore Storage".

ANNULUS UNLOADING, (PE) The unloading of fluid stored between tubing and casing. See "Wellbore Storage".

ANISOTROPY, Term used to denote the dependence of properties such as permeability on spacial orientation. Anisotropy is usually expressed as a tensor. When the principal axes are perpendicular to each other, the material is said to be orthotropic.

AQUICLUDE, (GW) A body of saturated but relatively impermeable material that does not yield appreciable amounts of water to wells. Characterized by very low "leakance" (the ratio of vertical hydraulic conductivity to thickness) and very low rates of yield from compressible storage.

AQUIFER SYSTEM, (GW) A heterogeneous body consisting of two or more permeable beds separated at least locally by aquitards that impede groundwater movement but do not greatly affect the regional hydraulic continuity of the system.

AQUITARD, (GW) A saturated, but poorly permeable, bed that impedes groundwater movement and does not yield water freely to wells, but which may transmit water between aquifers and may constitute an important storage unit. Leakance values can range from relatively low to relatively high. When low, an aquitard may function as a boundry to an aquifer flow system.

AREA OF INFLUENCE, (GW) Defined by Meinzer to be the land area of the same horizontal extent as the portion of the potentiometric surface that is perceptibly lowered due to withdrawal of water by a production well.

BANK STORAGE, (GW) The change in storage in an aquifer resulting from a change in stage of an adjacent surface water body.

BAROMETRIC EFFICIENCY OF A WELL, The ratio of water-level changes in the well to the water-level changes in a water barometer.

BOUNDARY PRESSURE, (PE) Pressure at boundary of drainage area.

CAPILLARY FRINGE, (GW) A zone whose lower part is completely saturated, but with water under less than atmospheric pressure. May range in thickness from a small fraction of an inch in gravel to more than 5 feet in silt. The water table forms its lower boundary.

CAPTURE, (GW) The decrease in discharge plus the increase in recharge of an aquifer. A term usually used in reference to the aftereffects of artificial withdrawal of water from an aquifer.

COEFFICIENT OF PERMEABILITY, (GW) See "Hydraulic Conductivity".

COEFFICIENT OF SPECIFIC STORAGE, (GW) See "Specific Storage".

COEFFICIENT OF STORAGE, (GW) See "Storage Coefficient".

COEFFICIENT OF TRANSMISSIBILITY, (GW) See "Transmissibility".

COEFFICIENT OF VOLUME COMPRESSIBILITY, (GW) The compression of a lithologic unit, per unit of original thickness, per unit increase of effective stress, in the load range exceeding preconsolidation stress.

COMMINGLED SYSTEMS, (PE) Two-layered or multiple layer reservoirs with communication taking place between layers, either through the wellbore alone or directly across the layer interface. (cf: "multi-aquifer well)

COMPACTION, (GW) Decrease in volume of sediments, as a result of compressive stress, usually resulting from continued deposition of them. Also called "one-dimensional consolidation".

COMPACTION, RESIDUAL, (GW) The difference between 1) the amount of compaction that will occur ultimately for a given increase in applied stress, once steady-state pore pressures are achieved, and 2) that which has occurred so far as of a specified time.

COMPACTION, SPECIFIC, (GW) The decrease in thickness of deposits, per unit increase in applied stress, during a specific time period.

COMPACTION, SPECIFIC UNIT, (GW) The compaction of deposits, per unit thickness, per unit increase in applied stress, during a specific time period.

COMPACTION, UNIT, (GW) The compaction per unit thickness of the deposit.

COMPOSITE SYSTEM, (PE) An injection well where the injected fluid bank is surrounded by an oil bank, and in which the locations of the fluid banks move.

COMPRESSIBILITY, TOTAL SYSTEM, (PE) A term representing the combined compressibility of all the elements in an aquifer system. Accounts for the compressibilities of the oil phase, water phase, gas phase, and of the rock formation itself, according to the relative fraction of the total system volume occupied by each.

CONDITION RATIO, (PE) Also called flow efficiency, indicates approximate fraction of a well's undamaged producing capacity. Ratio of actual productivity index to the productivity index if there were no skin (ideal conditions).

CONFINING BED, (GW) A body of relatively impermeable material stratigraphically adjacent to one or more aquifers. Can be either an "aquitard" or an "aquiclude".

CONSOLIDATION, (GW) See "Compaction".

CONSTANT DRAWDOWN TEST, (GW) Also known as constant pressure test in petroleum engineering. A test in which flow rate is gradually varied in time to maintain a constant drawdown (or constant pressure) in the producing well.

CONSTANT PRESSURE TESTING, (PE) Also known as constant drawdown test in groundwater hydrology. Involves recording change in flow rate with time while bottom-hole pressure is held constant.

CRITICAL FLOW, (PE) Occurs in high-permeability zones; the rate of flow into the drill pipe is independent of drawdown during a drill-stem test.

CRITICAL FLOW PROVER, (PE) Device that measures flow rate of a gas through an orifice under critical conditions (velocity is constant at a maximum value despite downstream pressure variations).

DAMAGE FACTOR, A measure of wellbore damage obtained by subtracting the condition ratio from 1.

DAMAGE RATIO, (PE) Inverse of condition ratio. Indicates wellbore condition.

DELAYED DRAINAGE, (GW) Term used to identify the slow release of water from the unsaturated zone in an unconfined aquifer.

DELIVERABILITY TESTING OF OIL WELLS, (PE) Determines capability of a well to deliver against a specific flowing bottom-hole pressure. Two main types: 1) flow-after-flow test; flowing pressure is recorded for three or more successive flow rates. Each flow rate is held constant until pressure has stabilized. 2) modified isochronal flow test; used for systems where stabilization time is too long for flow-after-flow test. For each flow rate, the well is shut-in after pressure transience is recorded, but before stabilization occurs. At each step the final flowing pressure and then the final shut-in pressure are observed. At the final flow rate, the well is allowed to produce until the pressure stabilizes, and this pressure is recorded.

DIMENSIONLESS PRESSURE, (PE) A dimensionless solution to the diffusivity equation. Directly proportional to physical pressure, where the scaling factor is dependent on flow rate and reservoir properties. Usually denoted by $P_D = \frac{2\pi kH\Delta P}{q\mu}$

DIMENSIONLESS TIME, (PE) A scaled version of real time. Scaling factor depends on reservoir properties and distance to point of observation $t_D = \frac{kt}{\phi\mu cr^2}$, where k is intrinsic permeability; t is time; ϕ is porosity; μ is viscosity; c is total compressibility; r is distance to point of observation.

DRAWDOWN, (GW) Difference in water level (or pressure) between the static condition and that at any given instant during discharge.

DRAWDOWN TESTING, (PE) Involves recording the lowering of bottom-hole pressure when a shut-in production well is switched to production at constant flow rate.

DRILLSTEM TESTING - DST, (PE) Used in testing uncompleted wells. An arrangement of packers seals off the interval to be tested, allowing a pressure to be built up as formation fluid flows into the drillstem and surface-actuated valves are closed. Pressure changes are observed by a pressure gauge located in the test interval. See "Single Packer Test", "Straddle Packer Test".

DYNAMIC PRESSURE, (PE) The pressure at a given time and location in a reservoir during a period of transient pressure distribution, such as during a build-up or drawdown test.

EFFECTIVE WELL RADIUS, (GW) The radius of an imaginary cylinder centered at the wellbore in which the permeability is much higher than in the reservoir. In a gravel-packed well it may often denote the probable radius of the gravel pack.

EQUIVALENT INJECTION TIME, (PE) In a fall-off test on an injection well where the injection rate before shut-in varies, this is equivalent to the length of time it would have taken to inject the same volume of fluid at constant flow rate as was injected at a variable flow rate since the last pressure equalization.

EXCESS PORE PRESSURE, (GW) Transient pore pressure at any point in an aquitard or aquiclude in excess of the pressure that would exist under steady-flow condition.

EXPANSION, SPECIFIC, (GW) The increase in thickness of deposits per unit decrease in applied stress.

EXPANSION, SPECIFIC UNIT, The expansion (increase in volume) of deposits, per unit thickness, per unit decrease in applied stress.

EXPONENTIAL INTEGRAL, (PE) See "Theis Solution".

FALLOFF TESTING, (PE) Involves shutting in an injection well and observing the decrease in bottom-hole pressure with time.

FALSE PRESSURE, (PE) Obtained by extrapolating the straight-line section of a Horner plot of pressure build-up data to infinite shut-in time. Approximates average reservoir pressure in an infinite system and can be used to estimate average drainage region pressure in a bounded system.

FIVE-SPOT PATTERN, (PE) An arrangement of production and injection wells with four production wells at the corners of a square and one injection well in the center.

FLOW-AFTER-FLOW TESTING, (PE) See "Deliverability Testing of Oil Wells".

FLOW EFFICIENCY, (PE) See "Condition Ratio".

FLUID POTENTIAL, (GW) The mechanical energy per unit mass of a fluid at any given point in space and time with respect to an arbitrary state and datum.

FORMATION VOLUME FACTOR, (PE) A factor to account for changes in volume in each phase upon transition from reservoir to standard surface conditions. The ratio of the volume at reservoir conditions to the volume at standard surface conditions.

GROUNDWATER, PERCHED, (GW) Confined groundwater seperated from an underlying body of groundwater by an unsaturated zone. It is held up by a "perching bed" of low permeability, and its water table is a "perched water table".

HEAD, STATIC, (GW) The height (above a datum) of a column of water that can be supported by the static pressure at a given point. The sum of the "elevation head" and the "pressure head". See "Head, Total".

HEAD, TOTAL, (GW) The sum of three components: 1) "elevation head", which is the elevation of the point above a datum; 2) "pressure head", the height of a column of static water that can be supported by the static pressure at the point; 3) "velocity head", the height the kinetic energy of the liquid is capable of lifting the liquid.

HORNER PLOT, (PE) A plot of pressure build-up versus log $\frac{t+\Delta t}{t}$ where t is time since production and Δt is time since shut-in. A similar plot was proposed in groudwater hydrology by Theis to analyze recovery data.

HYDRAULIC CONDUCTIVITY (K), (GW) Has dimensions of length per unit time. A medium has a hydraulic conductivity of unit length per unit time if it will transmit in unit time a unit volume of groundwater at the prevailing viscosity through a cross-section of unit area, measured at right angles to the direction of flow, under a hydraulic gradient of unit change in head through unit length of flow. Replaces the term "coefficient of permeability".

HYDRAULIC CONDUCTIVITY, EFFECTIVE, (GW) The rate of flow of water through a porous medium that contains more than one fluid.

HYDRAULIC DIFFUSIVITY, (GW) The ratio between hydraulic conductivity and specific storage.

HYDRAULIC GRADIENT, (GW) The change in static head per unit of distance in a given direction.

HYDROCOMPACTION, (GW) The process of volume decrease and density increase that occurs when moisture-deficient deposits are wetted for the first time.

IMAGE METHOD (METHOD OF IMAGES), (PE) The technique of using image wells to generate no-flow and constant pressure boundaries in an infinite system.

IMAGE WELL, (GW) An imaginary well which effectively produces the same drawdown (or recovery) as a linear boundary limiting the aquifer. See "Image Method".

INFLOW PERFORMANCE RELATIONSHIP, (PE) Used to predict a well's deliverability when deliverability test data is not available. A relationship between flow-rate, bottom-hole pressure, average reservoir pressure, and a productivity index.

INFLUENCE REGION, (PE) The region surrounding a well or wells whose properties influence transient tests performed on those wells. (Not to be confused with Meinzer's "area of influence".)

INJECTIVITY TESTING (INJECTION WELL TESTING), (PE) Pressure transient testing during injection into a well. Bottom-hole pressure is recorded while injection rate is held constant.

INTERFERENCE TESTING, (PE) A multiple-well transient test which involves the production of an active well (injection) and observing the resulting pressure changes in an observation well.

INTERPOROSITY FLOW PARAMETER, (PE) A dimensionless property of a fractured system. Dependent on the well radius, a matrix-to-fracture geometric factor, and the ratio of the formation matrix permeability to the effective fracture permeability.

ISOCHRONAL TESTING, (PE) See "Deliverability Testing of Oil Wells".

JACOB'S METHOD, (GW) Also known as asymptotic solution. Involves a semi-logarithmic plot of drawdown as a function of the log of time.

LEAKANCE, (GW) The ratio of vertical hydraulic conductivity to thickness of aquiclude.

LEAKY AQUIFER, (GW) An aquifer into which overlying and/or underlying aquitards discharge water as the potentiometric head in the aquifer is lowered.

MEINZER UNIT, (GW) A unit of hydraulic conductivity defined as the flow of water in gallons per day through a cross-sectional area of 1 square foot under a hydraulic gradient of 1 at a temperature of 60°F.

MOBILITY, (PE) The ratio of absolute permeability to viscosity.

MOBILITY RATIO, The ratio of the mobility of the injected fluid to that of the in-situ fluid.

MULTI-AQUIFER WELL, (GW) A well which is screened to produce fluids from more than one aquifer, seperated by aquicludes. (cf: "commingled systems")

MULTIFLOW EVALUATOR, (PE) A tool used in drillstem testing which allows unlimited sequences of production and shut-in. Includes a fluid chamber to recover an uncontaminated formation-fluid sample under pressure at the end of the flow period.

MULTIPLE RATE TESTING, (PE) Tests involving a variable flow-rate. Testing at a series of constant flow-rates, or testing at constant bottom-hole pressure with continuously changing flow-rate.

ORTHOTROPY, (GW) See "Anisotropy".

PERMEABILITY, EFFECTIVE, (GW) See. "Hyraulic Conductivity, Effective".

PERMEABILITY, INTRINSIC, Same as "Permeability". Term adopted by U. S. Geological Survey to indicate that it is a property of the medium alone, independent of the fluid properties. Has dimensions of L^2. Also called "Absolute Permeability".

PIEZOMETRIC SURFACE, (GW) See "Potentiometric Surface".

POROSITY, (GW) The property of a rock or soil of containing interstices. Expressed as the ratio of the volume of interstices to the total volume.

POROSITY, EFFECTIVE, (GW) Refers to the amount of interconnected pore space available for fluid transmission. Expressed as the percentage of total volume occupied by interconnecting interstices.

POTENTIOMETRIC SURFACE, A surface which represents the static head. An imaginary surface connecting points to which water would rise in tightly cased wells from a specified surface or stratum in the aquifer.

PRESSURE, AVERAGE RESERVOIR, The pressure a reservoir would attain if all wells were shut in for infinite time, assuming no natural influx of fluid.

PRESSURE BUILDUP TESTING, (PE) Involves shutting in a producing well and analyzing the resultant pressure buildup curve for reservoir properties and wellbore condition

PRESSURE, INITIAL RESERVOIR, (PE) Stabilized pressure of a shut-in well.

PRESSURE, INTERWELL, (PE) The pressure halfway between an injection well and a production well. Sometimes used to approximate average reservoir pressure.

PRESSURE, PSEUDOCRITICAL, For a mixture of gases, calculated from relative amounts and critical pressures of the components.

PRESSURE, PSEUDOREDUCED, (PE) The ratio of the pressure of interest to the pseudocritical pressure.

PRODUCTIVITY INDEX, (PE) Also known as the specific capacity of a well. Denotes, in petroleum engineering, the productivity of a well per unit drawdown.

PSEUDO SKIN FACTOR, (PE) The apparent skin factor in a well which has no true physical damage (or improvement) but is not drilled completely through the formation thickness or is only partially completed, thus appearing damaged.

PSEUDO STEADY STATE, (PE) A transient flow regime in which the rate of pressure change with time is constant at all points in the reservoir.

PULSE TESTING, (PE) A multiple-well transient test, in which flow rate pulses are produced in an active well and the resulting pressure changes are recorded in an observation well. Provides reservoir information for the region around and between the two wells. (Because of the shorter time intervals, the influence region for a pulse test is less than that for an interference test, and thus information is gained about a smaller portion of the reservoir.)

RADIUS OF DRAINAGE, (PE) Defines a circular system around a well in which a pseudo steady state pressure distribution exists.

RECOVERY TEST, (GW) Also known as build-up test in petroleum engineering. Denotes a test which involves the measurement of recovery in a well after the well is shut in following a known period of production.

RELATIVE PERMEABILITY, (PE) Also called effective permeability in groundwater hydrology. Denotes the permeability of the porous medium to a particular fluid when more than one fluid is present.

RESIDUAL DRAWDOWN, (GW) During recovery, the difference between the static water level and the water level at any instant during recovery.

SAFE YIELD , (GW) Given a variety of meanings, but originally defined (by Meinzer) as the rate at which groundwater can be withdrawn year after year from a given aquifer system without depleting the supply to the point where withdrawal at this rate is no longer economically feasible.

SEEPAGE FACE, (GW) For a well piercing an unconfined aquifer, seepage face denotes that segment of the well screen over which the total head equals elevation above datum and water flows from the aquifer into the well.

SEEPAGE FORCE, See "Stress, Seepage".

SHAPE FACTOR, (PE) A geometric factor, characteristic of the system shape and well location.

SLUG METHOD, (GW) Used to determine transmissivity of an aquifer. A known volume or "slug" of water is suddenly injected into or removed from a well and the decline or recovery of the water level is measured at closely spaced time intervals during the ensuing minute or two.

SINGLE-PACKER TEST, (PE) A drillstem test utilizing one packer in which fluid flows through the perforated anchor pipe into the drillstring.

SKIN, (PE) A zone of decreased permeability near the wellbore created by drilling and completion practices.

SKIN FACTOR, (PE) A constant which relates the pressure drop across the skin to the dimensionless rate of flow. A measure of wellbore damage.

SPECIFIC CAPACITY, (GW) The rate of discharge of water from a well divided by the drawdown of water level within the well. Varies slowly with duration of discharge. Also called Productivity Index in Petroleum Engineering.

SPECIFIC DISCHARGE or SPECIFIC FLUX, (GW) The rate of discharge of groundwater per unit area measured at right angles to the direction of flow.

SPECIFIC RETENTION, (GW) The ratio of the volume of water a saturated rock or soil will retain against the pull of gravity to its own volume.

SPECIFIC STORAGE, (GW) The volume of water released from or taken into storage per unit volume of the porous medium per unit change in head.

SPECIFIC YIELD, (GW) The water yielded by water-bearing material by gravity drainage, as occurs when the water table declines. The ratio of the volume of water a saturated rock or soil will yield by gravity to its own volume.

STABILIZATION TIME, (PE) The time corresponding to the start of the pseudo steady state period.

STATIC WATER LEVEL, (GW) The static position of the potentiometric surface in a well prior to the commencement of discharge. (cf: Initial reservoir pressure in petroleum engineering.)

STEADY STATE, Pressure is constant at all points in the reservoir.

STEP DRAWDOWN TEST, (GW) Also known as productivity index test or step-rate test in petroleum engineering. Involves producing a well at different rates for predetermined periods of time and monitoring drawdown.

STEP-RATE TESTING, (PE) A multiple-rate injection well test in which fluid is injected at a series of increasing rates, each rate lasting an equal amount of time. Injection pressure at the end of each rate is plotted versus injection rate.

STORAGE COEFFICIENT, The volume of water an aquifer releases from or takes into storage per unit surface area of the aquifer per unit change in head.

STRADDLE-PACKER TEST, (PE) A drillstem test in which the tested interval lies between two packers.

STRESS, APPLIED, The downward stress imposed at the aquifer boundary by 1) the weight (per unit area) of sediments and moisture above the water table, 2) the submerged weight of the saturated sediments overlying the boundary, and 3) the net seepage stress due to flow within the saturated sediments above the boundary .

STRESS, EFFECTIVE, Stress that is borne by and transmitted through the grain to grain contacts of a deposit. The effective stress at a point in an aquifer differs from the applied stress at the aquifer boundary by the submerged weight (per unit area) of the intervening sediments and the net seepage stress due to flow within the intervening sediments.

STRESS, SEEPAGE, Stress created by the seepage force, which is transferred from the water to the porous medium by viscous friction. Seepage force is exerted in direction of flow.

SUBSIDENCE, Sinking or settlement of the land surfaces, due to any of several processes, but most importantly due to artificial withdrawal of sub-surface fluids.

TEMPERATURE: PSEUDOCRITICAL; PSEUDOREDUCED, (PE)
Pseudocritical Temperature: For a mixture of gases, calculated from the relative amounts and critical temperatures of the components.
Pseudoreduced Temperature: The ratio of the temperature of interest to the pseudocritical temperature.

THEIM EQUATION, (GW) Represents steady-state radial flow solution to a well in the center of a circular, homogeneous, horizontal aquifer with prescribed potential at the circular boundary.

THEIS SOLUTION, (GW) Represents the solution to a continuous line source in a homogeneous, horizontal, infinite, isotropic aquifer. (Also known as exponential intergral in petroleum engineering.)

TIDAL EFFICIENCY, A measure of the response of the water level in a well to changes in ocean level. Equal to the barometric efficiency subtracted from 1.

TRANSIENT TESTING, The study of pressure variation with time in an active well (production or injection) under a variety of conditions and possible operating procedures.

TRANSMISSIVITY (T), (GW) The rate at which water of the prevailing kinematic viscosity is transmitted through a unit width of the aquifer under a unit hydraulic gradient.

TWO-RATE TESTING, (PE) A multiple-rate test on a production well using only two different flow-rates.

TWO-ZONE SYSTEMS, See "Composite Systems".

U, (GW) Dimensionless quantity related to the reciprocal of dimensionless time, t_D, used in petroleum engineering.

$$u = \frac{r^2 s}{4Tt} = \frac{1}{4t_D}$$

UNCONFINED AQUIFER, (GW) Also called water table aquifer. An aquifer which contains a water table, at which it is in direct contact with the atmosphere.

UNIFORM-FLUX FRACTURE, (PE) One in which fluid enters at a uniform flow-rate per unit area. A first approximation to the behavior of a vertically fractured well.

VERTICAL PULSE TESTING, (PE) Used to determine vertical permeability of a formation. Fluid is injected in pulses above a packer, escapes the wellbore through flow perforations and re-enters below the packer through observation perforations where pressure changes are observed with a pressure gauge.

VOID RATIO, (GW) The ratio of the volume of the interstices in a rock or soil to the volume of its mineral particles.

WATER DRIVE RESERVOIRS, (PE) Reservoirs in direct communication with an active aquifer.

WELLBORE STORAGE, (PE) Fluid stored in the wellbore above reservoir level. Usually occurs when a production well is shut-in without packers used to maintain fluid level. Affects pressure build-up data at early time as fluid continues to flow into the wellbore after shut-in.

WELL FUNCTION OF U, (GW) Equal to twice the value of P_D, dimensionless pressure, which denotes the value of the exponential integral.

WELL LOSSES, (GW) Denotes drawdowns at the well in excess of the theoretical capability of the reservoir. Such well losses may be due to poor development of the well, excessive entrance velocities and casing damages due to skin, scaling, or corrosion.

WIRELINE FORMATION TESTING, (PE) A tool is lowered into the well on a logging cable. The mechanism establishes communication with formation fluid and measures pressure response. Slightly more qualitative than a DST.

LIST OF PARTICIPANTS

ABRIL, Alejandro
C.F.E.
Mexico

ACHARYA, K.
University of California
Berkeley, California

ADAM, Monique
Lawrence Berkeley Laboratory
Berkeley, California

ADDUCI, Anthony
Department of Energy
San Francisco, California

AGRAWAL, R. G.
Amoco Research Center
Tulsa, Oklahoma

AMICK, C. H.
Lawrence Berkeley Laboratory
Berkeley, California

AMMORTIA, A.
University of California
Berkeley, California

ANDERSON, Merlin F.
Halliburton Services
Duncan, Oklahoma

ANDERSON, T. O.
Halliburton Services
Duncan, Oklahoma

ANGEVINE, Jack
Lawrence Berkeley Laboratory
Berkeley, California

ARRIAGA, C. C.
Comision Federal de Electricidad
Calexico, California

ASHBY, Ted
Sperry-Sun
Denver, Colorado

ASSENS, Guy
Lawrence Berkeley Laboratory
Berkeley, California

AYATOLLAHI
University of California
Berkeley, California

BASHAM, Ed
Go Wireline Service
Fort Worth, Texas

BENSON, Sally
Lawrence Berkeley Laboratory
Berkeley, California

BERMEJO, Ing. Roberto
Instituto Envestigaciones Electricas
Calexico, California

BINNALL, Eugene
Lawrence Berkeley Laboratory
Berkeley, California

BLAIR, Allen
Los Alamos Laboratory
Los Alamos, New Mexico

BLANKENNAGEL, R. K.
U. S. Geological Survey
Denver, Colorado

BODVARSSON, B.
Lawrence Berkeley Laboratory
Berkeley, California

BODVARSSON, Gunnar
Oregon State University
Corvallis, Oregon

BOYD, W. E.
University of Texas
Austin, Texas

BRIGHAM, W. E.
Stanford University
Stanford, California

BROWN, Choate
Lawrence Berkeley Laboratory
Berkeley, California

BUSCHECK, Tom
Lawrence Berkeley Laboratory
Berkeley, California

BUTZ, Jim
Denver Institute
Denver, Colorado

CAMPBELL, Don
Republic Geothermal, Inc.
Santa Fe Springs, California

CANNON, Jim
Sperry-Sun
Houston, Texas

CARTWRIGHT, Keros
Illinois Geological Survey
Illinois

CASTOR, Trevor P.
University of California
Berkeley, California

CATARINO, Ing.
GCIA
Mexico

CHAN, Tin
Lawrence Berkeley Laboratory
Berkeley, California

CHEN, Bill H.
University of Hawaii
Honolulu, Hawaii

CHEN, Jay C.
University of Hawaii
Honolulu, Hawaii

CHENG, Ping
University of Hawaii
Honolulu, Hawaii

CHERRY, J. A.
University of Waterloo
Ontario, Canada

CINCO, Herber
Stanford University
Stanford, California

COATS, Owen
C.E.R. Corporation
Las Vegas, Nevada

COQUAT, Joe
Sandia Laboratories
Albuquerque, New Mexico

DAVIS, Robert
Lawrence Berkeley Laboratory
Berkeley, California

DINWIDDIE, George
U. S. Geological Survey
Denver, Colorado

DORFMAN, Myron
University of Texas
Austin, Texas

DOTY, Ben
Lawrence Berkeley Laboratory
Berkeley, California

DOTY, Sandra
Lawrence Berkeley Laboratory
Berkeley, California

DYKSTRA, Herman
Petroleum Engineer
Concord, California

ERSHAGHI, Iraj
University of Southern California
Los Angeles, California

FAUST, Charles
U. S. Geological Survey
Reston, Virginia

FISHER, Henry
Los Alamos Laboratory
Los Alamos, New Mexico

FRYE, George A.
Aminoil U. S. A., Inc.
Santa Rosa, California

GASPAR, A. A.
Comision Federal de Electricidad
Calexico, California

GEPHART, R. E.
Rockwell
Richfield, California

GORANSON, Colin
Lawrence Berkeley Laboratory
Berkeley, California

GOLDMAN, Dennis
University of Idaho
Moscow, Idaho

GRAF, Alex
Lawrence Berkeley Laboratory
Berkeley, California

GREIDER, Robert
Larkspur, California

GRINGARTEN, Alain C.
B.R.G.M.
Orleans, France

GULATI, M. S.
Union Oil Company
Santa Rosa, California

HAWS, G. W.
Marathon Oil Company
Littleton, Colorado

HELLIER, Bruce H.
U. S. Geological Survey
Denver, Colorado

HERKELRATH, William
U. S. Geological Survey
Menlo Park, California

HOWARD, John H.
Lawrence Berkeley Laboratory
Berkeley, California

HSU, S.
Halliburton Services
Duncan, Oklahoma

HYDE, E. K.
Deputy Director
Lawrence Berkeley Laboratory
Berkeley, California

JACOBSON, J. J.
Battelle N. W. Laboratory
Richland, Washington

JAFFEE, L.
California Institute of Technology
Pasadena, California

JAMISON, D.
Lawrence Berkeley Laboratory
Berkeley, California

KAMAL, Med
Amoco Production Co.
Tulsa, Oklahoma

KANEHIRO, B.
Lawrence Berkeley Laboratory
Berkeley, California

KELLY, Ronald D.
Mechanics Research, Inc.
Santa Monica, California

KENYON, W. E.
Schlumberger-Doll
Ridgefield, Connecticut

KIHARA,
University of Hawaii
Honolulu, Hawaii

KINTZINGER, Paul
University of California
Los Alamos, New Mexico

KUMATAKA, Mark
Aminoil U. S. A.
Santa Rosa, California

KUNZE, Jay
Idaho National Engineering Lab.
Idaho Falls, Idaho

LAMERS, Mike
Measurement Analysis Corporation
Palos Verdes, California

LANGE, A.
Amax Corporation
Denver, Colorado

LIPPERT, Donald R.
Lawrence Berkeley Laboratory
Berkeley, California

LIPPMANN, Marcelo
Lawrence Berkeley Laboratory
Berkeley, California

LONG, Jane
University of California
Berkeley, California

LOVE, Robert
Halliburton Services
Duncan, Oklahoma

MAGNANI, Charles F.
Chevron Oil Field Research
La Habra, California

MALLOY, Martin W.
Department of Energy
San Francisco, California

MANN, Robert L.
C.E.R. Corporation
Las Vegas, Nevada

MANETTI, Grazano
Enel Dsr
Pisa, Italy

MATHIAS, Ken
Bureau of Reclamation
Boulder City, Nevada

McCONNELL, T. D.
Sandia Laboratories
Albuquerque, New Mexico

McDONALD, W. J.
Maurer Engineering
Houston, Texas

McEDWARDS, Donald
Lawrence Berkeley Laboratory
Berkeley, California

McELWRATH, Bob
Go Wireline Service
Bakersfield, California

McFARLANE, James D.
Westbay Instruments Ltd.
West Vancouver
British Columbia, Canada

McSPADDEN, William
Battelle N. W. Laboratory
Richland, Washington

MERCER, James
U. S. Geological Survey
Reston, Virginia

MILLER, Constance
Lawrence Berkeley Laboratory
Berkeley, California

MILLER, George
Occidental Research Corporation
La Verne, California

MILLER, W. C.
Shell Oil Company
Houston, Texas

MINK, Leland L.
Department of Energy
Washington, D. C.

MIRK, Kenneth F.
Lawrence Berkeley Laboratory
Berkeley, California

MOEBUS, Milton
Lawrence Berkeley Laboratory
Berkeley, California

MOENCH, Allen
U. S. Geological Survey
Menlo Park, California

MORSE, John
Lawrence Livermore Laboratory
Livermore, California

NARASIMHAN, T. N.
Lawrence Berkeley Laboratory
Berkeley, California

NATHENSON, Manuel
U. S. Geological Survey
Menlo Park, California

NELSON, Garn
Hewlett Packard
Palo Alto, California

NELSON, Philip
Lawrence Berkeley Laboratory
Berkeley, California

NEUMAN, Shlomo P.
University of Arizona
Tucson, Arizona

NOBLE, John
Lawrence Berkeley Laboratory
Berkeley, California

O'BRIEN, Maura
Lawrence Berkeley Laboratory
Berkeley, California

PALEN, Walt
Lawrence Berkeley Laboratory
Berkeley, California

PAPAZIAN, Harold
Lawrence Berkeley Laboratory
Berkeley, California

PAROS, Jerome
Paroscientific, Inc.
Redmond, Washington

PATTON, Frank
Patton Consultants
West Vancouver, Canada

PERKINS, Gerald S.
Jet Propulsion Laboratory
Pasadena, California

PICKENS, John
University of Waterloo
Waterloo, Ontario, Canada

PRICKETT, Tom
Camp, Dresser & McKee
Champaign, Illinois

RAGHAVAN, Raj
University of Tulsa
Tulsa, Oklahoma

RAMEY, Henry J., Jr.
Stanford University
Stanford, California

RUDISILLI, Jacob
Thermal Power Company
San Francisco, California

RILEY, Francis
U. S. Geological Survey
Denver, Colorado

RINEY, David
Systems, Science & Software
San Diego, California

RIVEROS, Carlos
Lawrence Berkeley Laboratory
Berkeley, California

ROGERS, Phila
Lawrence Berkeley Laboratory
Berkeley, California

RUBIN, L. A.
Ensco, Inc.
Springfield, Virginia

SANYAL, Subir
Supri
Stanford, California

SAUTY, Jean Pierre
Brgm Bp
Orleans, France

SCHIANKER, Bob
System Control, Inc.
Palo Alto, California

SCHROEDER, Ron
Lawrence Berkeley Laboratory
Berkeley, California

SCHWARZ, Werner
Lawrence Berkeley Laboratory
Berkeley, California

SMITH, H. Rodney
Patton Consultants
West Vancouver, Canada

STAFFORD, Glen
Department of Energy
Washington, D. C.

STILL, W. L.
Ensco, Inc.
Springfield, Virginia

STOKER, Roger
Eg&g - Inel
Idaho Falls, Idaho

STOLLER, H. M.
Sandia Laboratory
Albuquerque, New Mexico

STROBEL, Calvin
Union Oil Company
Santa Rosa, California

STROMDAHL, William
Lawrence Berkeley Laboratory
Berkeley, California

SOLBAU, Ray
Lawrence Berkeley Laboratory
Berkeley, California

THORPE, Richard J.
Lawrence Berkeley Laboratory
Berkeley, California

THORSON, Lewis
Lawrence Livermore Laboratory
Livermore, California

TONN, E. G.
Crown Zellerbach
San Francisco, California

TSANG, Chin-Fu
Lawrence Berkeley Laboratory
Berkeley, California

UPTON, Joseph
Battelle N. W. Laboratory
Richland, Washington

van POOLLEN, Hank K.
van Poollen & Associates
Littleton, Colorado

VENERUSO, Anthony A.
Sandia Laboratory
Albuquerque, New Mexico

WALTON, William C.
Upper Mississippi River Basin Commission
Twin Cities, Minnesota

WANG, Joseph
Lawrence Berkeley Laboratory
Berkeley, California

WEEKS, Edward
U. S. Geological Survey
Lubbock, Texas

WETZEL, John
Hewlett Packard
Palo Alto, California

WILBUR, Arthur C.
Department of Energy
San Francisco, California

WITHERSPOON, Paul A.
Lawrence Berkeley Laboratory
Berkeley, California

YOUMANS, A. H.
Dresser Atlas
Houston, Texas

YUEN, Paul C.
University of Hawaii
Honolulu, Hawaii

ZAIS, Elliot
Elliot Zais & Associates
Albany, Oregon

NAME INDEX

C = Committee
P = Panelist
A = Author
Ch = Chairman

GPO 794-326/224

0 0 3 0 4 9 0 4 4 0 6

This report was done with support from the Department of Energy. Any conclusions or opinions expressed in this report represent solely those of the author(s) and not necessarily those of The Regents of the University of California, the Lawrence Berkeley Laboratory or the Department of Energy.

TECHNICAL INFORMATION DEPARTMENT
LAWRENCE BERKELEY LABORATORY
UNIVERSITY OF CALIFORNIA
BERKELEY, CALIFORNIA 94720